December 1981
Final Report

DOT HS-806 279

US Department
of Transportation

National Highway
Traffic Safety
Administration

VALIDATION OF THE CRASH VICTIM SIMULATOR
Volume I: Engineering Manual
Part I: Analytical Formulation

John T. Fleck
Frank E. Butler

Calspan Corporation
Advanced Technology Center
4455 Genesee Street
Buffalo, N.Y.   14225

TECHNICAL REPORT STANDARD TITLE PAGE

1. Report No. DOT-HS-806 279	2. Government Accession No.	3. Recipient's Catalog No.
4. Title and Subtitle Validation of the Crash Victim Simulator Volume 1, Engineering Manual - Part I: Analytical Formulation		5. Report Date December, 1981
		6. Performing Organization Code W69
7. Author(s) John T. Fleck and Frank E. Butler		8. Performing Organization Report No. ZS-5881-V-1
9. Performing Organization Name and Address Calspan Corporation Advanced Technology Center 4455 Genesee Street Buffalo, NY 14225		10. Work Unit No.
		11. Contract or Grant No. DOT-HS-6-01300
12. Sponsoring Agency Name and Address U. S. Department of Transportation National Highway Traffic Safety Administration 400 Seventh Street, S.W. Washington, DC 20590		13. Type of Report and Period Covered Final Report January 1976 - December 1981
		14. Sponsoring Agency Code

15. Supplementary Notes

16. Abstract

A combined analytical and experimental research project was carried out to develop and examine the validity of an improved version of the computer program used to simulate the three-dimensional dynamic gross motion responses of motor vehicle crash victims. Among the improvements incorporated in the new (CVS-IV) version of the program are a more efficient integration technique, a routine to automatically position a seated occupant in equilibrium, and modifications of the input and output control routines that make it easier to use the program. Measurements of a Part 572 50th percentile male anthropomorphic dummy were made to define an input data set for a simulation model of the dummy. Dynamic pendulum impact tests of dummy sub-assemblies were performed and modeled with the computer program. Detailed comparisons of predicted system responses with those measured in special impact sled tests of the dummy restrained by a three-point restraint belt and by a pre-inflated air bag are also presented.

Results of the project are documented in four manuals as follows:

Volume 1 - Engineering Manual - Part I: Analytical Formulation
Volume 2 - Engineering Manual - Part II: Validation Effort
Volume 3 - User's Manual
Volume 4 - Programmer's Manual

17. Key Words Computer Simulation Three-Dimensional Dynamics Mathematical Models Crash Victim Simulation Rigid Body Dynamics	18. Distribution Statement Document is available to the U. S. public through the National Technical Information Service, Springfield, Virginia 22161	
19. Security Classif. (of this report) Unclassified	20. Security Classif. (of this page) Unclassified	21. No. of Pages 272	22. Price

Form DOT F 1700.7 (8-69)

i

METRIC CONVERSION FACTORS

Approximate Conversions to Metric Measures

Symbol	When You Know	Multiply by	To Find	Symbol

LENGTH

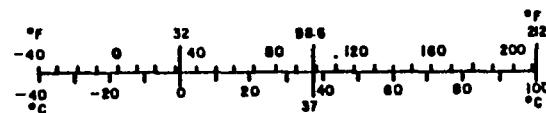| Symbol	When You Know	Multiply by	To Find	Symbol
in	inches	*2.5	centimeters	cm
ft	feet	30	centimeters	cm
yd	yards	0.9	meters	m
mi	miles	1.6	kilometers	km

AREA

Symbol	When You Know	Multiply by	To Find	Symbol
in^2	square inches	6.5	square centimeters	cm^2
ft^2	square feet	0.09	square meters	m^2
yd^2	square yards	0.8	square meters	m^2
mi^2	square miles	2.6	square kilometers	km^2
	acres	0.4	hectares	ha

MASS (weight)

Symbol	When You Know	Multiply by	To Find	Symbol
oz	ounces	28	grams	g
lb	pounds	0.45	kilograms	kg
	short tons (2000 lb)	0.9	tonnes	t

VOLUME

Symbol	When You Know	Multiply by	To Find	Symbol
tsp	teaspoons	5	milliliters	ml
Tbsp	tablespoons	15	milliliters	ml
fl oz	fluid ounces	30	milliliters	ml
c	cups	0.24	liters	l
pt	pints	0.47	liters	l
qt	quarts	0.95	liters	l
gal	gallons	3.8	liters	l
ft^3	cubic feet	0.03	cubic meters	m^3
yd^3	cubic yards	0.76	cubic meters	m^3

TEMPERATURE (exact)

Symbol	When You Know	Multiply by	To Find	Symbol
°F	Fahrenheit temperature	5/9 (after subtracting 32)	Celsius temperature	°C

*1 in = 2.54 (exactly). For other exact conversions and more detailed tables, see NBS Misc. Publ. 286, Units of Weights and Measures, Price $2.25, SD Catalog No. C13.10.286.

Approximate Conversions from Metric Measures

LENGTH

Symbol	When You Know	Multiply by	To Find	Symbol
mm	millimeters	0.04	inches	in
cm	centimeters	0.4	inches	in
m	meters	3.3	feet	ft
m	meters	1.1	yards	yd
km	kilometers	0.6	miles	mi

AREA

Symbol	When You Know	Multiply by	To Find	Symbol
cm^2	square centimeters	0.16	square inches	in^2
m^2	square meters	1.2	square yards	yd^2
km^2	square kilometers	0.4	square miles	mi^2
ha	hectares (10,000 m^2)	2.5	acres	

MASS (weight)

Symbol	When You Know	Multiply by	To Find	Symbol
g	grams	0.035	ounces	oz
kg	kilograms	2.2	pounds	lb
t	tonnes (1000 kg)	1.1	short tons	

VOLUME

Symbol	When You Know	Multiply by	To Find	Symbol
ml	milliliters	0.03	fluid ounces	fl oz
l	liters	2.1	pints	pt
l	liters	1.06	quarts	qt
l	liters	0.26	gallons	gal
m^3	cubic meters	35	cubic feet	ft^3
m^3	cubic meters	1.3	cubic yards	yd^3

TEMPERATURE (exact)

Symbol	When You Know	Multiply by	To Find	Symbol
°C	Celsius temperature	9/5 (then add 32)	Fahrenheit temperature	°F

°F -40   0   32   40   80   98.6 120   160   200   212
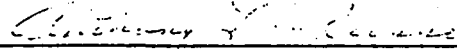°C -40 -20   0   20   37   40   60   80   100

FOREWORD

This document is one of four manuals that constitute the final report of the research project conducted under Contract No. DOT-HS-6-01300 for the National Highway Traffic Safety Administration. Dr. John T. Fleck and Mr. Frank E. Butler of J & J Technologies, Inc. served as Principal Investigator and Project Engineer, respectively, during their earlier tenure as members of the Calspan Transportation Research Department. Subsequently, Mr. Norman J. DeLeys coordinated the efforts of Calspan and J & J Technologies, Inc., who was retained as a subcontractor to maintain the continuity necessary to preparation of the report.

The Contract Technical Monitor for this project was Dr. Lee Ovenshire of the National Highway Traffic Safety Administration.

This report has been reviewed and approved by:

Anthony L. Russo, Head
Transportation Research Department

TABLE OF CONTENTS

TABLE OF CONTENTS (cont'd)

LIST OF FIGURES

LIST OF FIGURES (cont'd)

LIST OF TABLES

General Notation

Due to the large number of variables used to develop and derive relationships in this volume specific notation is defined in the section where it is used. In many cases, variables which are defined in one section may have a different definition in another section. For example, the symbol ρ is used for the shortest vector from origin to the plane, it is also a vector defining the specified fixed distance in the fixed distance constraint, and it is also used as the friction coefficient for the sliding constraint. The following is a list of nomenclature which is used extensively throughout Volume I.

A	Ellipsoid matrix
D_n	Direction cosine matrix for the nth segment
f_{nj}	Constraint force on the nth segment applied at joint j
I	Identity matrix
$\hat{i}, \hat{j}, \hat{k}$	Unit vectors defining orthonormal inertial reference system
M_n	Mass matrix of the nth segment
N	Total number segments
n	Subscript used to define the nth arbitrary segment
$\mathcal{g}$	Constraint force (position, sliding and rolling)
r	Vector from ellipsoid center to ellipsoid surface
r_{nj}	Location of joint j in the local system of segment n.
t	Unit vector normal to a plane

t Independent variable of integration

X_n Vector position of the c.g. of segment n in inertial reference

ϕ_n Inertia matrix for the nth segment

ω_n Angular velocity vector for the nth segment in n's local coordinate system

SECTION 1

INTRODUCTION

In 1970 Calspan Corporation (formerly Cornell Aeronautical Laboratory, Inc.) began development of a mathematical model for simulating the three-dimensional dynamic responses of a motor vehicle crash victim. Under the joint sponsorship of the Motor Vehicle Manufacturers Association (MVMA) and the National Highway Traffic Safety Administration (NHTSA), the original development and validation of the program was accomplished in two phases (Ref. 1 and 2). Except for a special version of the Phase II crash victim simulation (CVS) program created for the MVMA (Ref. 3), the next major developmental effort was accomplished for the NHTSA and resulted in what was designated as the CVS-III computer program (Ref. 4).

Recognizing the CVS-III as a potentially valuable tool for aiding studies of crew member dynamics during ejection from high-speed aircraft, the Air Force Aerospace Medical Research Laboratory (AFAMRL) sponsored the development of a special version of the program that formed the basis of the AFAMRL "Articulated Total Body" model or ATB (Ref. 5). Later, the ATB model was updated and some new features were added under another contract with the AFAMRL (Ref. 6).

This report documents work performed in the research project entitled "Validation of the Crash Victim Simulator" under Contract No. DOT-HS-6-01300 with the NHTSA which states the general objective as "the development of the CVS to a level that it can be used for a variety of rulemaking activities." A significant goal was "to conduct studies that specifically, quantitatively and validly pertain to the Part 572 dummy in several realistic crash safety compliance test situations." The project consisted of two principal areas of effort: (1) further development, improvement and refinement of the computer program, culminating in a version designated as the CVS-IV, and (2) the performance of detailed measurements and tests to define inputs for modeling the 50th percentile male dummy conforming to government specifications (Ref. 7) and executing computer simulations of experiments performed with the dummy to examine the validity of the model results.

1

The CVS-IV version of the computer program incorporates many modifications and features developed in this project as well as in conjunction with other closely related research studies (e.g., Ref. 5, 6 and 8). Among the improvements implemented in the CVS-IV are the following:

- a new, more efficient integration technique.
- a routine to automatically position a seated occupant in equilibrium.
- an advanced harness belt formulation that treats interaction of belts connected at a common junction point, belt slippage on deformable segments, and allows use of rate-dependent functions for calculation of belt forces.
- simulation of aerodynamic forces acting on body segments that may be partially shielded.
- improved routines for calculating joint torques.
- use of the main program integrator for computing vehicle and air bag motions.
- the ability to specify the motion of as many as six segments.
- a provision to account for segment principal axes that are not coincident with geometric axes, thereby allowing use of any convenient geometric axis system as the reference for segment input data.
- generality in specifying axes about which segments are rotated, and the sequence of rotations, to achieve a desired initial orientation.
- elimination of the need for multiple output units.
- routines for computing injury criteria values (HIC, HSI, and CSI) and for plotting any output variable(s) against any other variable or time.

During the course of the present study, several interim verions of the computer program were distributed to numerous users throughout the world. However, it should be noted that the modifications of each version were incorporated in such a way that, in most instances, input data decks remained upward compatible and useable with successive versions of the program.

2

The final report of this project is composed of four volumes:

Volume 1 - Engineering Manual - Part I: Analytical Formulation
Volume 2 - Engineering Manual - Part II: Validation Effort
Volume 3 - User's Manual
Volume 4 - Programmer's Manual

Volume 1 describes the analytical formulations, assumptions and the detailed development of the mathematical equations and relations used in the program.* Volume 2 documents the measurement of the dummy geometric, inertial and joint characteristics and experiments performed to validate computer models of the physical systems tested. The experiments simulated include static tests of an ellipsoidal air bag to check the validity of the idealized bag shape and force algorithms, dynamic pendulum impact tests of dummy component sub-assemblies, and impact sled tests in which the dummy was restrained by an air bag and a three-point belt restraint system (Ref. 9). The third volume provides instruction on how to use the program. Besides giving a detailed description of all data furnished on each input card, it explains the special input and output features and provides examples of program applications along with the Job Control Language needed to execute a simulation run. Volume 4 is intended primarily for use by programmers interested in the detailed structure of the program. Included in Volume 4 are descriptions of each subroutine, cross reference charts showing the subroutines called by other subroutines, labeled common blocks used by each subroutine and usage of each variable in the labeled common blocks in every subprogram, and a complete listing of the computer Fortran source deck.

_____

* See also Reference 5 and 6 which document the analytical formulation of some
  algorithms and features not decribed in detail herein.

SECTION 2

GENERAL MATH AND GEOMETRY RELATIONSHIPS

In order to assist the reader in understanding the theoretical development of the equations used in the program, a description of general mathematical notation and basic geometrical relationships is presented. This includes discussions of the coordinates and vector/matrix notation adopted, basic equations for defining planes and ellipsoids and the relationship between rotations, quaternions and direction cosine matrices. Finally, this section concludes with a discussion of a method for determining yaw, pitch and roll angles from the direction cosine matrix.

2.1 COORDINATES AND VECTOR/MATRIX NOTATION

In the development of the program, it was convenient to use a matrix notation because it bears a one to one correspondence with the coding. For example, consider figure 2.1 below
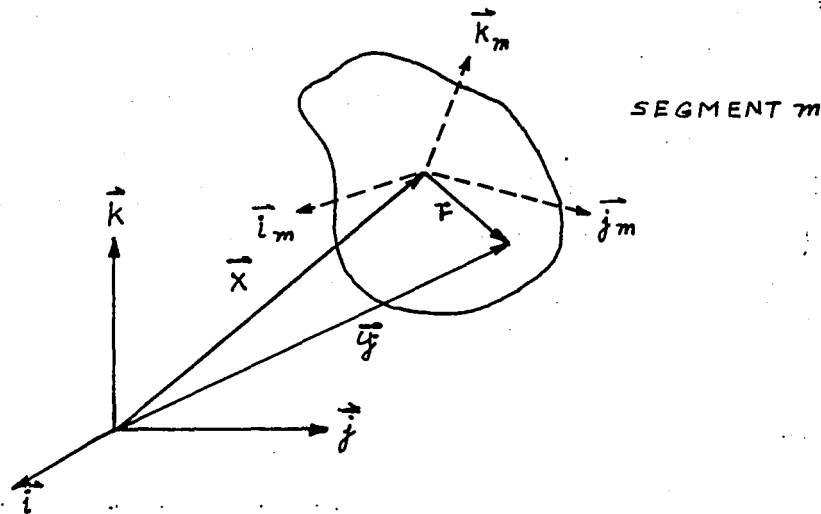
Figure 2.1 BASIC COORDINATE SYSTEMS

$\vec{x}$ - location of c.g. as measured in the inertial reference
$\vec{r}$ - location of a point in segment m in m's local reference
$\vec{y}$ - location of the same point in inertial reference

Each of the quantities $\vec{x}, \vec{r}, \vec{y}$ have three components and are considered as column vectors (a 3 x 1 matrix) thus (the bars are deleted.)

$$x = \begin{pmatrix} x_1 \\ x_2 \\ x_3 \end{pmatrix} \qquad r = \begin{pmatrix} r_1 \\ r_2 \\ r_3 \end{pmatrix} \qquad y = \begin{pmatrix} y_1 \\ y_2 \\ y_3 \end{pmatrix} \qquad (2.1)$$

In standard vector notation write the following:

$$\vec{X} = X_1 \vec{i} + X_2 \vec{j} + X_3 \vec{k}$$

$$\vec{r} = r_1 \vec{i}_m + r_2 \vec{j}_m + r_3 \vec{k}_m$$

$$\vec{Y} = Y_1 \vec{i} + Y_2 \vec{j} + Y_3 \vec{k}$$

$$(2.2)$$

where $\vec{i}, \vec{j}, \vec{k}$ are unit vectors along the axes 1, 2, 3 of the inertial reference and $\vec{i}_m, \vec{j}_m, \vec{k}_m$ are unit vectors along the axes 1, 2, 3 of the local reference.*
Unless otherwise stated we assume all references systems are right handed orthonormal systems. That is

$$\vec{i} \cdot \vec{i} = \vec{j} \cdot \vec{j} = \vec{k} \cdot \vec{k} = 1$$

$$\vec{i} \cdot \vec{j} = \vec{j} \cdot \vec{k} = \vec{i} \cdot \vec{k} = 0$$

$$(2.3)$$

where " $\cdot$ " represents the dot (scalar) product, and that

$$\vec{i} \otimes \vec{j} = \vec{k} , \quad \vec{j} \otimes \vec{k} = \vec{i} , \quad \vec{k} \otimes \vec{i} = \vec{j}$$

$$\vec{i} \otimes \vec{i} = \vec{j} \otimes \vec{j} = \vec{k} \otimes \vec{k} = 0$$

$$(2.4)$$

where " $\otimes$ " designates the cross (vector) product.

The direction cosine matrix, D, is the 3 x 3 matrix which converts the components of a vector as measured in the inertial reference to its components in the local system, thus the 3 x 1 matrix resulting from the multiplication operation Dx would be the components of x as given in the local system.

---

* Alternate notation which is often used is the expression of a vector in terms of the unit basis vectors $\vec{x}_1, \vec{x}_2, \vec{x}_3$ or $\hat{e}_1, \hat{e}_2, \hat{e}_3$. Then a compact notation for the vector, $\vec{X} = \sum_{P=1}^{3} x_P \vec{x}_P$ or $\vec{r} = \sum_{P=1}^{3} r_P \hat{e}_P$

Note that the unit vectors are related by

$$\begin{pmatrix} \vec{i}_m \\ \vec{j}_m \\ \vec{k}_m \end{pmatrix} = D_m \begin{pmatrix} \vec{i} \\ \vec{j} \\ \vec{k} \end{pmatrix} \qquad (2.5)$$

Explicitly writing D in terms of its components yields

$$D_m = \begin{pmatrix} d_{11} & d_{12} & d_{13} \\ d_{21} & d_{22} & d_{23} \\ d_{31} & d_{32} & d_{33} \end{pmatrix}_m \qquad (2.6)$$

Note also that,

$$D_m = \begin{pmatrix} \vec{i} \cdot \vec{i}_m & \vec{j} \cdot \vec{i}_m & \vec{K} \cdot \vec{i}_m \\ \vec{i} \cdot \vec{j}_m & \vec{j} \cdot \vec{j}_m & \vec{K} \cdot \vec{j}_m \\ \vec{i} \cdot \vec{k}_m & \vec{j} \cdot \vec{k}_m & \vec{K} \cdot \vec{K}_m \end{pmatrix} \qquad (2.7)$$

Since the dot product of two vectors is the product of the magnitudes times the cosine of the angle between them, the dot product $\vec{i} \cdot \vec{i}_m$ is the cosine of the angle between the vector $\vec{i}_m$ and the vector $\vec{i}$. Thus each of the components of D is the cosine of the angle between the respective unit vectors, hence the name direction cosine matrix. Since the direction cosine matrix is orthogonal, the inverse of D, D^{-1}, is the transpose of D, D^T.

$$\text{i.e.} \quad D^{-1} = D^T$$

hence $DD^T = D^T D = I$, the identity matrix. $\qquad (2.8)$

To obtain the transpose of a matrix interchange the rows and columns: if d_{mn} are the elements of D and a_{mn} are the elements of D transpose,

$$d_{mn} = a_{nm} \qquad (2.9)$$

6

In vector notation, it is permissible to write the expression

$$\vec{X} + \vec{r} = \vec{Y}$$

(2.10)

but in matrix notation it is not permissible to write

$$X + r = Y$$

(2.11)

because this would imply that

$$X_1 + r_1 = Y_1$$
$$X_2 + r_2 = Y_2$$
$$X_3 + r_3 = Y_3$$

(2.12)

which is true only if all three quantities have been expressed in the same reference system.

The proper relation is

$$X + D^{-1} r = Y$$

(2.13)

or equivalently

$$X + D^{T} r = Y$$

or in the local reference systems

$$DX + r = DY$$

(2.14)

For example, substituting equation (2.2) into (2.10) yields,

$$X_1 \vec{i} + X_2 \vec{j} + X_3 \vec{k} + r_1 \vec{i}_m + r_2 \vec{j}_m + r_3 \vec{k}_m$$
$$= Y_1 \vec{i} + Y_2 \vec{j} + Y_3 \vec{k}$$

(2.15)

Examining (2.15) shows that it is incorrect to say $x_1 + r_1 = y_1$ since x_1 and y_1 multiply $\vec{i}$, and r_1 multiplies $\vec{i}_m$, and $\vec{i}$ is not necessarily equal to $\vec{i}_m$.

But from 2.5 we get

$$\vec{i}_m = d_{11}\,\vec{i} + d_{12}\,\vec{i} + d_{13}\,\vec{k}$$
$$\vec{j}_m = d_{21}\,\vec{i} + d_{22}\,\vec{j} + d_{23}\,\vec{k}$$
$$\vec{k}_m = d_{31}\,\vec{i} + d_{32}\,\vec{j} + d_{23}\,\vec{k}$$

$$(2.16)$$

hence

$$r_1\,\vec{i}_m + r_2\,\vec{j}_m + r_3\,\vec{k}_m = (d_{11}\,r_1 + d_{21}\,r_2 + d_{31}\,r_3)\,\vec{i}$$
$$+ (d_{12}\,r_1 + d_{22}\,r_2 + d_{32}\,r_3)\,\vec{j}$$
$$+ (d_{13}\,r_1 + d_{23}\,r_2 + d_{33}\,r_3)\,\vec{k}$$

$$(2.17)$$

It can now be recognized that the quantities multiplying i, j, k are the quantities obtained from the matrix operation

$$D^T r = \begin{pmatrix} d_{11} & d_{21} & d_{31} \\ d_{12} & d_{22} & d_{32} \\ d_{13} & d_{23} & d_{33} \end{pmatrix} \begin{pmatrix} r_1 \\ r_2 \\ r_3 \end{pmatrix}$$

$$(2.18)$$

Hence the validity of equation (2.13) is established.

Dot Product

In matrix notation the dot product of x and y is the sum of the products of the respective components when given in the same coordinate system, hence

$$X \cdot Y = X_1\,Y_1 + X_2\,Y_2 + X_3\,Y_3$$

Note that

$$X \cdot Y = X^T Y = Y \cdot X = Y^T X \qquad (2.19)$$

since

$$X^T = (X_1, X_2, X_3) \qquad (2.20)$$

and

$$X^T Y = (X_1\;\;X_2\;\;X_3) \begin{pmatrix} Y_1 \\ Y_2 \\ Y_3 \end{pmatrix} = X_1\,Y_1 + X_2\,Y_2 + X_3\,Y_3$$

$$(2.21)$$

8

In vector notation

$\vec{X} \cdot \vec{r}$ is a valid expression, but in matrix notation

$X \cdot r$ is invalid and must be written as

$$X \cdot D^{-1} r \text{ or } X^T D^{-1} r$$

$$\vec{X} \cdot \vec{r} = X \cdot (D^{-1} r) = X^T D^{-1} r = X^T D^T r = (DX)^T r = (DX) \cdot r \qquad (2.22)$$

here use the matrix identity

$$(AB)^T = B^T A^T \qquad (2.23)$$

Note that in 2.22 parentheses have been used to avoid confusion on the order of operation.

Also note that the notation x_* is equivalent to x^T, hence, it would make sense to write $A \cdot B$ for $A^T B$, where A and B are matrices for which the product $A^T B$ is defined.

Since $X \cdot X = X_1^2 + X_2^2 + X_3^2$ the magnitude of x is defined as

$$|x| = \sqrt{(x \cdot x)} \qquad (2.24)$$

Cross Product

The cross product of two vectors x, y is designated by $\vec{x} \otimes \vec{y}$ and may be obtained from 2.2 and 2.4, thus

$$
\begin{aligned}
\vec{X} \otimes \vec{Y} &= (X_1 \vec{i} + X_2 \vec{j} + X_3 \vec{k}) \otimes (Y_1 \vec{i} + Y_2 \vec{j} + Y_3 \vec{k}) \\
&= X_1 Y_1 \vec{i} \otimes \vec{i} + X_1 Y_2 \vec{i} \otimes \vec{j} + X_1 Y_3 \vec{i} \otimes \vec{k} \\
&\quad + X_2 Y_1 \vec{j} \otimes \vec{i} + X_2 Y_2 \vec{j} \otimes \vec{j} + X_2 Y_3 \vec{j} \otimes \vec{k} \\
&\quad + X_3 Y_1 \vec{k} \otimes \vec{i} + X_3 Y_2 \vec{k} \otimes \vec{j} + X_3 Y_3 \vec{k} \otimes \vec{k} \\
&= (X_2 Y_3 - X_3 Y_2) \vec{i} + (X_3 Y_1 - X_1 Y_3) \vec{j} + (X_1 Y_2 - X_2 Y_1) \vec{k}
\end{aligned}
$$

$$(2.25)$$

where the fact that $a \otimes b = -b \otimes a$ has been used.

Note that the final result in 2.25 is the expansion of the determinant

$$\begin{vmatrix} \vec{i} & \vec{j} & \vec{k} \\ X_1 & X_2 & X_3 \\ Y_1 & Y_2 & Y_3 \end{vmatrix} \qquad (2.26)$$

The components of x and y must be expressed in the same coordinate system. In matrix notation the cross product is

$$X \otimes Y \qquad (2.27)$$

with the same meaning. That is if

$$X = \begin{pmatrix} X_1 \\ X_2 \\ X_3 \end{pmatrix} \quad , \quad Y = \begin{pmatrix} Y_1 \\ Y_2 \\ Y_3 \end{pmatrix}$$

then

$$X \otimes Y = \begin{pmatrix} X_2 Y_3 - X_3 Y_2 \\ X_3 Y_1 - X_1 Y_3 \\ X_1 Y_2 - X_2 Y_1 \end{pmatrix} \qquad (2.28)$$

Note that $X \otimes$ may be defined as the matrix

$$X \otimes = \begin{pmatrix} 0 & -X_3 & X_2 \\ X_3 & 0 & -X_1 \\ -X_2 & X_1 & 0 \end{pmatrix} \qquad (2.29)$$

since

$$X \otimes Y = \begin{pmatrix} 0 & -X_3 & X_2 \\ X_3 & 0 & -X_1 \\ -X_2 & X_1 & 0 \end{pmatrix} \begin{pmatrix} Y_1 \\ Y_2 \\ Y_3 \end{pmatrix} = \begin{pmatrix} X_2 Y_3 - X_3 Y_2 \\ X_3 Y_1 - X_2 Y_3 \\ X_1 Y_2 - X_2 Y_1 \end{pmatrix}$$

This is analgous to our use of $X \cdot$ as X^T

$$\text{i.e.} \quad X \cdot = (X_1, X_2, X_3) = \begin{pmatrix} X_1 \\ X_2 \\ X_3 \end{pmatrix}^T = X^T$$

Also note that

$$Y \otimes X = -X \otimes Y = (X \otimes)^T Y \qquad (2.30)$$

10

Matrix notation permits the assignment of a definition to the operator $X \otimes$, (i.e. the matrix as defined in 2.29) whereas in ordinary vector analysis $X \otimes$ has no meaning by itself.

This is useful in later work where it is convenient to consider an expression like

$$- h \otimes (h \otimes$$

$$h = \begin{pmatrix} h_1 \\ h_2 \\ h_3 \end{pmatrix} \qquad (2.31)$$

where

and $h \otimes$ is defined by 2.29.

To make sense of expression 2.31 consider the following identity

$$a \otimes (b \otimes c) = (a \cdot c) b - (a \cdot b) c$$

Then if $a = b = h$ and $c = y$, the following results

$$- h \otimes (h \otimes y) = (h \cdot h) y - h (h \cdot y)$$

which can be written as

$$- h \otimes (h \times y) = (h^T h \ I - h h^T) y$$

Thus $- h \otimes (h \otimes = h^T h \ I - h h^T$ is a matrix

If $h^T h = 1$ (a unit vector) then

$$- h \otimes (h \otimes \quad = I - h h^T \qquad (2.32)$$

and

$$- h \otimes (h \otimes y) = y - h \ h \cdot y$$

This may be recognized as a projection of y on a plane perpendicular to h, thus $I - h h^T$ is a projection operator (matrix).
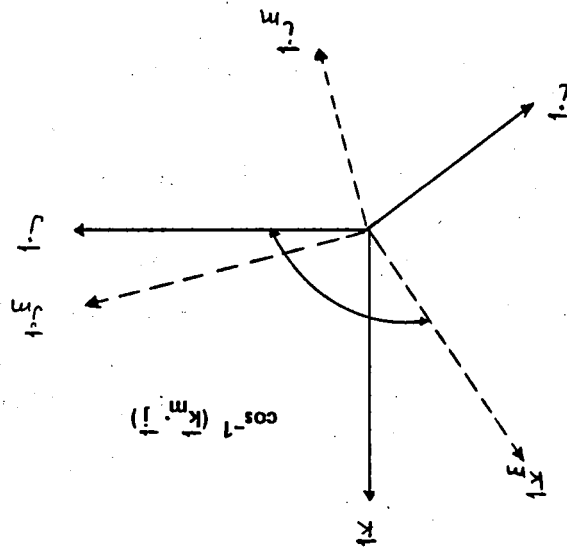
PLANES.   Planes are used extensively in the program for modeling various surfaces in or on the vehicle.
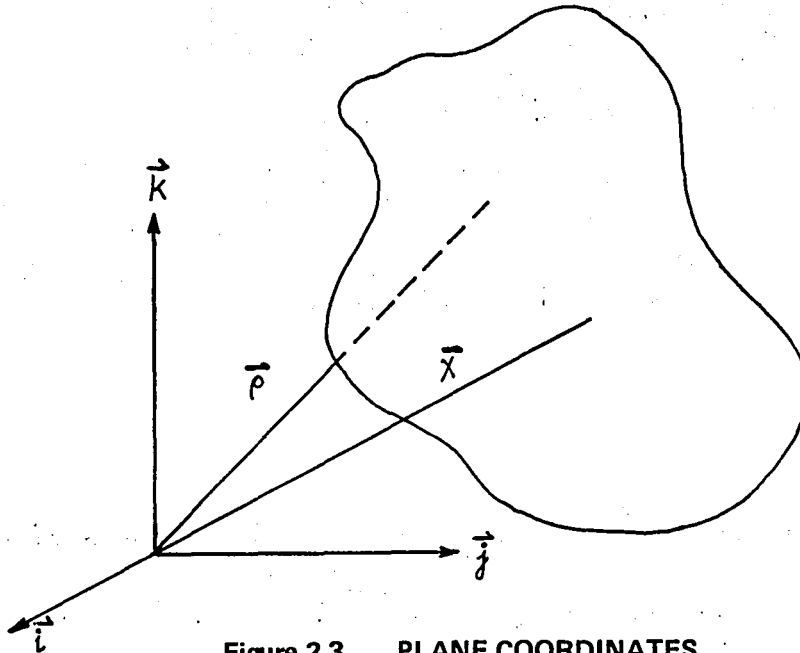
Figure 2.3   PLANE COORDINATES

Points which lie in a plane satisfy the linear relation

$$a x_1 + b x_2 + c x_3 = d$$

<div align="right">(2.33)</div>

where a, b, c, d are constants and x_1, x_2, x_3 are components of the vector x which is defined from the origin to the point in the plane.

Let $\vec{p}$ be the vector which locates the point in the plane which is nearest to the origin; hence $\vec{p}$ must be perpendicular to the plane and $|\vec{p}|$ is the distance of the plane from the origin.

It is convenient to define the plane by the unit vector

$$\vec{t} = \vec{\rho}/|\vec{\rho}| \qquad \text{and the distance} \quad \beta = |\vec{\rho}| \qquad (2.34)$$

Therefore

$$\vec{t} = \frac{a}{\sqrt{a^2+b^2+c^2}}\, \vec{i} + \frac{b}{\sqrt{a^2+b^2+c^2}}\, \vec{j} + \frac{c}{\sqrt{a^2+b^2+c^2}}\, \vec{k}$$

$$(2.35)$$

The equation of the plane may then be written as

$$\vec{t} \cdot \vec{X} = \beta \quad , \quad \vec{t} \cdot \vec{t} = 1 \qquad (2.36)$$

or

$$t \cdot X = t^T x = \beta \qquad \text{in matrix notation.}$$

Note that a vector which is parallel to the plane satisfies $\quad t \cdot X = 0$

Contact Planes
Contact planes in the program are defined as follows.
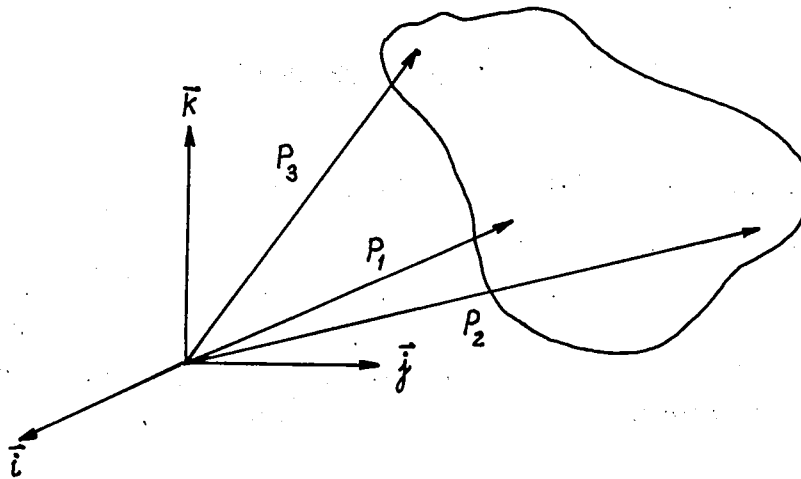
Figure 2.4   DEFINITION OF PLANE SPECIFICATION

The user inputs the coordinates of three points P_1, P_2, P_3 which lie in the plane $(P_i^T = (x_i, y_i, z_i),\ i=1,3)$.

The program computes the unit vectors (this is done in subroutine SINPUT)

$$q_1 = \frac{(p_2-p_1) \otimes (p_3-p_1)}{|(p_2-p_1) \otimes (p_3-p_1)|}$$

$$q_2 = \frac{(p_3-p_1) \otimes q_1}{|(p_3-p_1) \otimes q_1|}$$

$$q_3 = \frac{q_1 \times (p_2-p_1)}{|q_1 \times (p_2-p_1)|}$$

(Note - these are matrix equations)

Since q_2 and q_3 lie in the plane, q_1 is a unit vector normal (perpendicular) to the plane.

It also computes

$$q_1 \cdot P_1 = \beta_1$$
$$q_2 \cdot P_1 = \beta_2$$
$$q_3 \cdot P_1 = \beta_3$$

The equation of the plane is also given by q_1 and β_1; that is, a point x lies in the plane if

$$q_1 \cdot x = \beta_1$$

To establish contact, it is important to establish whether a point has penetrated the plane (in back of the plane) or if a point has not penetrated the plane (in front of the plane.)

The direction of q_1 is used to define the front surface. Hence if $q_1 \cdot x > \beta_1$, x is said to be in front of the plane and if $q_1 \cdot x < \beta_1$, x is said to be in back of the plane. The plane is given a finite size by accepting points which satisfy:

$$0 \leq q_2 \cdot x - \beta_2 \leq |q_2 \cdot (p_2-p_1)|; \quad 0 \leq q_3 \cdot x - \beta_3 \leq |q_3 \cdot (p_3-p_1)|$$

as points which are in the boundaries of the finite plane.

15

Acceptable points are illustrated as the shaded area in the following figure.
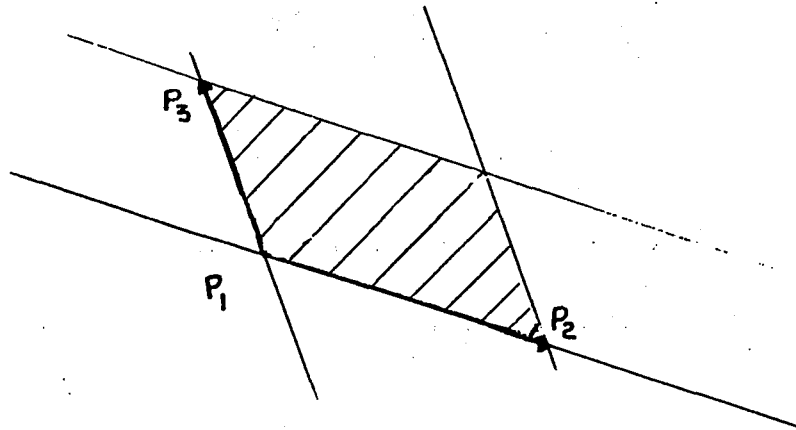
The recommended procedure for defining a planar surface is to use points such that $P_2 - P_1$ is perpendicular to $P_3 - P_1$ as in the following figure.
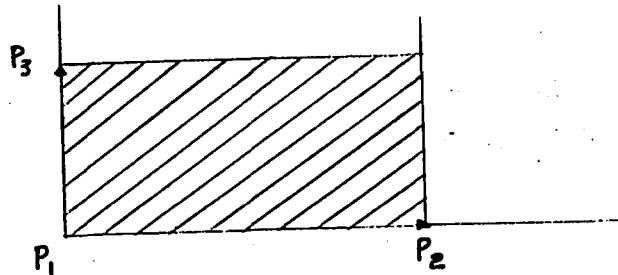
The acceptable region is then a rectangle with P_1, P_2, P_3 on the corners.

Note that in the above figure the front side would be the side seen by the reader. If P_2 and P_3 were interchanged, the reader would be viewing the back side.

16

ELLIPSOIDS. Ellipsoids are used throughout the program for modeling the contact surfaces of the body and other curved surfaces such as the air bags or interior surfaces of the vehicle.
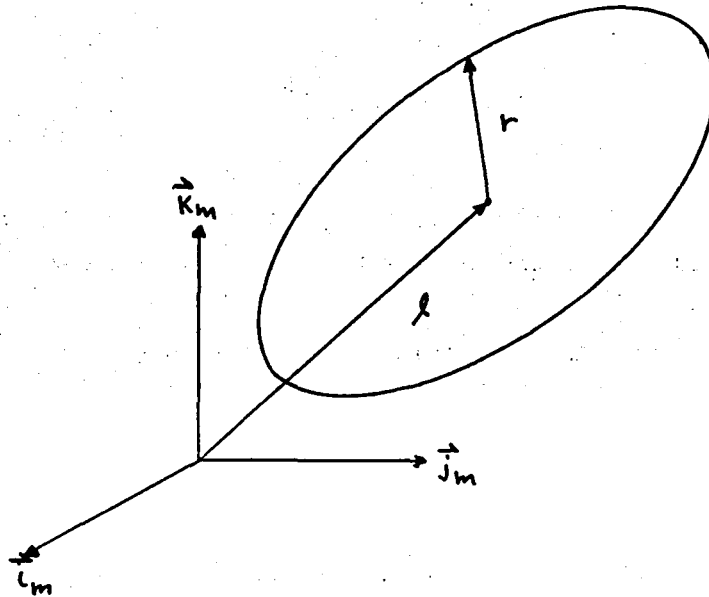
Figure 2.5   ELLIPSOID GEOMETRY

Consider an ellipsoid whose principal axes are aligned with the reference system. Points r and the ellipsoid centered at ℓ satisfy the relation

$$\left(\frac{r_1 - \ell_1}{a_1} \right)^2 + \left(\frac{r_2 - \ell_2}{a_2} \right)^2 + \left(\frac{r_3 - \ell_3}{a_3} \right)^2 = 1 \qquad (2.37)$$

where

$$r = \begin{pmatrix} r_1 \\ r_2 \\ r_3 \end{pmatrix} \quad , \quad \ell = \begin{pmatrix} \ell_1 \\ \ell_2 \\ \ell_3 \end{pmatrix} \qquad \text{and} \quad a_1 , a_2 , a_3 \quad \text{are}$$

the semi axes lengths.

This may be written as

$$(r - \ell) \cdot A \,(r - \ell) = 1$$

<div align="right">(2.38)</div>

where A is the matrix

$$A = \begin{pmatrix} \frac{1}{a_1^2} & 0 & 0 \\ 0 & \frac{1}{a_2^2} & 0 \\ 0 & 0 & \frac{1}{a_3^2} \end{pmatrix}$$

<div align="right">(2.39)</div>

For convenience in the following discussion let the center be at the origin $(\ell = 0)$. This places no restrictions on the development.

The ellipsoid equation is then written

$$r \cdot A\, r = 1$$

<div align="right">(2.40)</div>

If the reference system is rotated by the direction cosine matrix D such that

$$r = DS$$

<div align="right">(2.41)</div>

then

$$r \cdot A\, r = S^T D^T A D S = S \cdot (D^T A D) S = S \cdot B S = 1$$

<div align="right">(2.42)</div>

where $B = D^T A D$, is the matrix describing an ellipsoid whose principal axes are oriented by the rotation specified by the direction cosine matrix D with respect to the reference system of S.

Note that A is a real positive definite matrix and hence B is a real positive definite matrix. (i.e. positive real eigenvalues.) Thus 2.40 may be used to represent a general ellipsoid with the restriction that A be a real positive definite matrix.

Consider a general point X

if	$X \cdot A X > 1$	the point is outside of the ellipsoid
if	$X \cdot A X < 1$	the point is inside the ellipsoid
if	$X \cdot A X = 1$	the point is on the ellipsoid.

$$(2.43)$$

(remember that x is the vector from the center of the ellipsoid to the point X)

Consider a point r on the ellipsoid

Ar is a vector which is perpendicular to the surface at the point r. The outward normal is then

$$t = {}^{A r}\!\!/_{|A r|}$$

$$(2.44)$$

A plane tangent to the surface at the point r would then be defined by the vector t and the distance, β_1 , of plane from the center of the ellipsoid is;

$$\beta_1 = r \cdot t = r \cdot Ar/|Ar| = {}^1\!\!/_{|A r|}$$

$$(2.45)$$

In words, the distance of the tangent plane at the point r on the ellipsoid to the center of the ellipsoid is ${}^1\!\!/_{|Ar|}$.

2.3   ROTATIONS, QUATERNIONS AND DIRECTION COSINE MATRICES

A direction cosine matrix is assigned to each segment to indicate the angular orientation of the segment. The direction cosine matrix is updated during integration by use of a quaternion (Eq. 2.69). The integrator integrates the quaternion equation (Eq. 2.70). Rotation, Quaternions and Direction Cosine Matrices are discussed in this section.

2.3.1   Rotations in 3-D Space

Any rotation in three dimensional space may be considered as rotating a vector $\vec{b}$ about an axis $\vec{\mu}$ through an angle θ in the plane that is perpendicular to $\vec{\mu}$.
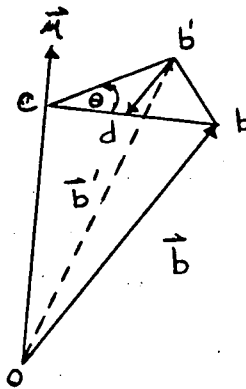
Figure 2.6   ROTATING A VECTOR

Let R be the operator (matrix) which performs the rotation

$$b' = R b$$

(2.46)

R may be expressed as

$$R = \mu^T + \cos\theta\,(I - \mu\mu^T) + \sin\theta\,\mu \otimes$$

(2.47)

where $\mu \cdot \mu = 1$

and I is the identity matrix.

From Figure 2.6 write

$$\vec{b}' = \vec{oc} + \vec{cd} + \vec{db}'$$

(2.48)

where

$$\vec{oc} = \mu\mu^T b = \vec{\mu}\,(\vec{\mu}\cdot\vec{b})$$

$$\vec{cd} = \cos\theta\,(I - \mu\mu^T)b = \cos\theta\,(\vec{b} - \vec{\mu}\,(\vec{\mu}\cdot\vec{b}))$$

$$\vec{db'} = \sin\theta\,\mu\otimes b \qquad = \sin\theta\,\vec{\mu}\otimes\vec{b}$$

Note that

$$(\vec{b} - \vec{\mu}\,(\vec{\mu}\cdot\vec{b}))\cdot(\vec{b} - \vec{\mu}\,(\vec{\mu}\cdot\vec{b})) = (\vec{\mu}\otimes\vec{b})\cdot(\vec{\mu}\otimes\vec{b})$$

$$= \vec{b}\cdot\vec{b} - (\vec{\mu}\cdot\vec{b})^2 \qquad (2.49)$$

The inverse operation (rotation through an angle $-\theta$) is

$$R^{-1} = \mu\mu^T + \cos\theta\,(I - \mu\mu^T) - \sin\theta\,\mu\otimes$$

$$(2.50)$$

In terms of the components μ_1, μ_2, μ_3 of the vector $\vec{\mu}$
R may be expressed as a matrix.

$$R = \begin{pmatrix} \mu_1^2(1-\cos\theta)+\cos\theta & \mu_1\mu_2(1-\cos\theta)-\mu_3\sin\theta & \mu_1\mu_3(1-\cos\theta)+\mu_2\sin\theta \\ \mu_2\mu_1(1-\cos\theta)+\mu_3\sin\theta & \mu_2^2(1-\cos\theta)+\cos\theta & \mu_2\mu_3(1-\cos\theta)-\mu_1\sin\theta \\ \mu_3\mu_1(1-\cos\theta)-\mu_2\sin\theta & \mu_3\mu_2(1-\cos\theta)+\mu_1\sin\theta & \mu_3^2(1-\cos\theta)+\cos\theta \end{pmatrix}$$

$$(2.51)$$

by using the relations

$$\mu\mu^T = \begin{pmatrix} \mu_1 \\ \mu_2 \\ \mu_3 \end{pmatrix}(\mu_1, \mu_2, \mu_3) = \begin{pmatrix} \mu_1^2 & \mu_1\mu_2 & \mu_1\mu_3 \\ \mu_2\mu_1 & \mu_2^2 & \mu_2\mu_3 \\ \mu_3\mu_1 & \mu_3\mu_2 & \mu_3^2 \end{pmatrix}$$

$$(2.52)$$

and

$$\mu\otimes = \begin{pmatrix} 0 & -\mu_3 & \mu_2 \\ \mu_3 & 0 & -\mu_1 \\ -\mu_2 & \mu_1 & 0 \end{pmatrix}$$

Note that
$$R^{-1} = R^T$$

since $(\mu \mu^T)^T = \mu \mu^T$

and $(\mu \otimes)^T = -\mu \otimes$

Additional properties which may prove useful are derived below. The trace and determinant of R are given by

$$tr(R) = 1 + 2 \cos \theta$$

$$|R| = 1$$

and the eigenvalues of R are $1, e^{\hat{i}\theta}$ and $e^{-\hat{i}\theta}$. *

Note that

$$\mu \mu^T = (R + R^T - 2 \cos \theta I)/2(1 - \cos \theta) \qquad (2.53)$$

$$\mu = \frac{1}{2 \sin \theta} \begin{pmatrix} r_{32} - r_{23} \\ r_{13} - r_{31} \\ r_{21} - r_{12} \end{pmatrix} \qquad (2.54)$$

where r_{jk} are elements of the R matrix

$$\mu \otimes = (R - R^T)/2 \sin \theta$$

$$R^2 = R^T + tr(R)(R - I) \qquad (2.55)$$

combining the above, the characteristic equation is given by

$$R^3 - tr(R)R^2 + tr(R)R - I = 0 \qquad (2.56)$$

---

*In this equation, $\hat{i} = \sqrt{-1}$ to distinguish from i used as index below.

The projection operators associated with the eigenvalues are

$$E_1 = \mu \mu^T$$

$$E_2 = E_{e^{i\theta}} = (I - \mu \mu^T - \hat{i} \mu \otimes)/2$$

$$E_3 = E_{e^{-i\theta}} = (I - \mu \mu^T + \hat{i} \mu \otimes)/2$$

(2.57)

Note that

$$E_1 + E_2 + E_3 = I$$

and

$$E_j E_k = \delta_{jk} E_j$$

where δ_{jk} is the Kronecker delta

2.3.2 Quaternions

In the program, quaternions are used to update the direction cosine matrices. A more elaborate development of quaternion theory may be found in Ref. 13 pg.168. The relationship between the rotation operator established in Equation (2.47) and quaternions is presented in this section. A rotation may be expressed in terms of a quaternion

$$\vec{b}' = q \, \vec{b} \, q^*$$

(2.58)

where $\quad q = \cos \theta/2 + \sin \theta/2 \, \vec{\mu}$

and $\quad q^* = \cos \theta/2 - \sin \theta/2 \, \vec{\mu}$

A quaternion may be considered as four component matrix which has a scalar, $\alpha = \cos \theta/2$ as a first term, plus the three vector components, $\vec{u} = \sin \theta/2 \, \vec{\mu}$. This results in the following:

$$\vec{b}' = (\alpha + \vec{u}) \, \vec{b} \, (\alpha - \vec{u})$$

$$\vec{b}' = \alpha \vec{b} \alpha - \alpha \vec{b} \vec{u} + \vec{u} \vec{b} \alpha - \vec{u} \vec{b} \vec{u}$$

(2.59)

Interpreting the results as

$$\alpha b \alpha = \alpha^2 \vec{b} \qquad \text{since } \alpha \text{ is a scalar}$$

$$\alpha \vec{b} \vec{u} = \alpha(-\vec{b} \cdot \vec{u} + \vec{b} \otimes \vec{u})$$

where the product of two vectors has been defined as,

$$\vec{b}\,\vec{u} = -\vec{b} \cdot \vec{u} + \vec{b} \otimes \vec{u}$$

$$\vec{u}\,\vec{b}\,\vec{u} = \vec{u}(\vec{b}\,\vec{u}) = (\vec{u}\,\vec{b})\vec{u}$$

$$= -\vec{b} \cdot \vec{u}\,\vec{u} + \vec{u} \cdot \vec{u}\,\vec{b} - \vec{u} \cdot \vec{b}\,\vec{u}$$

Combining the above relationships yields

$$\vec{b}' = (\alpha^2 - \vec{u} \cdot \vec{u})\vec{b} + 2\,\vec{u} \cdot \vec{b}\,\vec{u} + 2\,\alpha\,\vec{u} \otimes \vec{b} \qquad (2.60)$$

when

$$\alpha = \cos \theta/2$$

$$\vec{u} = \sin \theta/2\ \vec{\mu}$$

then

$$q\,q^* = (\alpha + \vec{u})(\alpha - \vec{u}) = \alpha^2 + \vec{u} \cdot \vec{u} = 1$$

$$(2.61)$$

and

$$\vec{b}' = \cos\theta\,\vec{b} + (1 - \cos\theta)\,\vec{\mu} \cdot \vec{b}\,\vec{u} + \sin\theta\,\vec{\mu} \otimes \vec{b}$$

$$\vec{b}' = R\vec{b} \quad, \text{ or } \quad b' = R\,b \text{ (see equation 2.47)}$$

2.3.3 Relation To Direction Cosine Matrix

If the direction cosine matrix D represents the relation between the vector b' in a reference system and b as measured in a local system, then

$$b = D b'$$
(2.62)

and
$$b' = D^T b$$

Previously we defined a rotation matrix R as an operator which, when applied to a vector measured in a particular coordinate system, would give the components in the same coordinate system of a new vector which was a rotation of the original vector.

The direction cosine matrix represents the relationship of the components of the same vector as expressed in two different coordinate systems, one rotated relative to the other. If the local system is described as have been rotated an angle Θ about an axis μ from the reference, then

$$D^T = R = \mu \mu^T + \cos \theta \, (I - \mu \mu^T) + \sin\Theta \; \mu \otimes$$
(2.63)

2.3.4   Time Derivative Relation Between Quaternions and Direction Cosine Matrix

Relationships are established between the time derivative of the direction cosine matrix and angular velocity which is then related to the time derivative of the quaternion. As previously established, a rotation of a vector b to a vector b' is the following:

$$b' = D^T(t) \, b \qquad \text{at time t.}$$

At a time later $t + \Delta$

$$b'' = D^T(t + \Delta) \, b$$
(2.64)

Then it is possible to write

$$b'' = R(\Delta) \, b' \qquad \text{using the rotation operator.}$$

25

Combining these results in

$$b'' = R(\Delta) D^T(t) b' = D^T(t+\Delta) b'$$ (2.65)

therefore from continuity

$$D^T(t+\Delta) = R(\Delta) D^T(t)$$

or

$$D(t+\Delta) = D(t) R^T(\Delta)$$ (2.66)

Writing the derivative $\dot{D}(t)$ as $\quad \dot{D}(t) = \lim_{\Delta \to 0} \left[\dfrac{D(t+\Delta) - D(t)}{\Delta} \right]$

$$\dot{D}(t) = \lim_{\Delta \to 0} \left[\dfrac{D(t) (R^T(\Delta) - I)}{\Delta} \right]$$

Then

$$\dot{D}(t) = \lim_{\Delta \to 0} \left[\dfrac{D(t)(\mu \mu^T + \cos \theta(\Delta)(I - \mu \mu^T) - \sin \theta(\Delta) \mu \otimes - I)}{\Delta} \right]$$ (2.67)

Using L'Hospitals rule

$$D^{-1}(t) \dot{D}(t) = \frac{-d\theta}{d\Delta} \mu \otimes = -\dot{\theta} \mu \otimes$$ (2.68)

Interpret μ as the instantaneous axis of rotation and θ' as the angular time derivative. Thus the vector $\dot{\theta} \mu$ defined in Equation (2.68) is $D^{-1}\omega$, where ω is the angular velocity in the local reference system associated with D. From the matrix identity

$$(Ab) \otimes (AC) \equiv \det (A) \, (A^T)^{-1} \, b \otimes C$$

we have $\quad (D^{-1}\omega) \otimes (D^{-1}C) = D^{-1} (\omega \otimes C)$ or $(D^{-1}\omega) \otimes D^{-1} \equiv D^{-1} \omega \otimes$

Equation 2.68 may be rewritten as

$$\dot{D} D^{-1} = -D \dot{D}^{-1} = -D \, (D^{-1}\omega) \otimes D^{-1}$$

$$= -D D^{-1} \omega \otimes \quad \text{hence}$$

$$\dot{D}^{-1} = D^{-1} \omega \otimes$$ (2.68a)

In quaternion notation, using q instead of R,

$$D = q^* D_0 q \tag{2.69}$$

where the quaternion is defined to operate on the column vectors of the D matrix, D_0 is the initial value of D,

and
$$q^* q = 1$$
$$q(0) = 1$$

Differentiating equation (2.69) with respect to time, yields

$$\dot{D} = \dot{q}^* D_0 q + q^* D_0 \dot{q}$$
$$= \dot{q}^* q D + D q^* \dot{q}$$
$$= -2 (q^* \dot{q}) \otimes D$$

since $q^* \dot{q}$ and $-q^* \dot{q}$ is a vector. This results the relationship

$$2 q^* \dot{q} = \omega$$

or
$$\dot{q} = q \omega / 2$$

$$\tag{2.70}$$

More explicitly, write $\dot{q}$ as

$$\dot{q} = \frac{1}{2} \begin{pmatrix} 0 & -\omega_1 & -\omega_2 & -\omega_3 \\ \omega_1 & 0 & \omega_3 & -\omega_2 \\ \omega_2 & -\omega_3 & 0 & \omega_1 \\ \omega_3 & \omega_2 & -\omega_1 & 0 \end{pmatrix} \begin{pmatrix} q_0 \\ q_1 \\ q_2 \\ q_3 \end{pmatrix} \equiv T_q \tag{2.71}$$

where $\omega^T \equiv (\omega_1, \omega_2, \omega_3)$

which has the characteristic equation

$$\left(\lambda^2 + \frac{1}{4}\, \omega \cdot \omega \right)^2 = 0$$

(2.72)

and double roots

$$\lambda_1 = \frac{\hat{\imath}}{2}\,|\omega|$$

and

$$\lambda_2 = -\frac{\hat{\imath}}{2}\,|\omega|$$

Note that $T^2 = \lambda^2 I$. The projections are given by

$$E_{\lambda_1} = \frac{1}{2}\left[I - \frac{T}{\lambda_2} \right]$$

and

$$E_{\lambda_2} = I - E_{\lambda_1}$$

If T is a constant, equation (2.71) has a solution

$$q(t) = e^{Tt} q(0)$$

(2.73)

where

$$e^{Tt} = \left(\cos \tfrac{1}{2}\,|\omega|\,t \right) I + \frac{\sin \tfrac{1}{2}\,|\omega|\,t}{\tfrac{1}{2}\,|\omega|}\, T$$

Therefore it is possible to write,

$$q(t) = \left(\cos \tfrac{1}{2}\,|\omega|\,t \right) q(0) + \frac{\sin \tfrac{1}{2}\,|\omega|\,t}{\tfrac{1}{2}\,|\omega|}\, \dot{q}(0)$$

(2.74)

and

$$T\, q(0) = \dot{q}(0)$$

(2.75)

In particular, if

$$q(0) = \begin{pmatrix} 1 \\ 0 \\ 0 \\ 0 \end{pmatrix}.$$

and

$$\dot{q}(o) = T q(o) = \frac{1}{2} \begin{pmatrix} 0 \\ \omega_1 \\ \omega_2 \\ \omega_3 \end{pmatrix}$$

then

$$q(t) = \begin{bmatrix} \cos\left(\frac{1}{2}|\omega|t\right) \\ \sin\left(\frac{1}{2}|\omega|t\right)\frac{\omega_1}{|\omega|} \\ \sin\left(\frac{1}{2}|\omega|t\right)\frac{\omega_2}{|\omega|} \\ \sin\left(\frac{1}{2}|\omega|t\right)\frac{\omega_3}{|\omega|} \end{bmatrix} \qquad (2.76)$$

In quaternion notation, we have

$$q = \cos\left(\frac{1}{2}|\omega|t\right) + \left(\sin\left(\frac{1}{2}|\omega|t\right)\right)\frac{\omega}{|\omega|} \qquad (2.77)$$

which represents a rotation of angle $|\omega|t$ about the axis $\frac{\omega}{|\omega|}$.

2.4   DETERMINATION OF YAW, PITCH AND ROLL ANGLES OR EULER ANGLES FROM DIRECTION COSINE MATRIX

The angular orientation of the segments in the 3-D program are computed and maintained in terms of the direction cosine matrices.

For input and output purposes, it is convenient to express the direction cosine matrices in terms of three rotation angles, either yaw, pitch and roll, or the Euler angles, spin, nutation and precession.

29

2.4.1   Computation of Yaw, Pitch and Roll

A direction cosine matrix can be comput ed as the product of three successive rotations about the coordinate axes (see Figure 2.7). This product can be expressed as $D = T_x(r) \, T_y(p) \, T_z(y)$, or in detail

$$D = \begin{bmatrix} 1 & 0 & 0 \\ 0 & \cos r & \sin r \\ 0 & -\sin r & \cos r \end{bmatrix} \begin{bmatrix} \cos p & 0 & -\sin p \\ 0 & 1 & 0 \\ \sin p & 0 & \cos p \end{bmatrix} \begin{bmatrix} \cos y & \sin y & 0 \\ -\sin y & \cos y & 0 \\ 0 & 0 & 1 \end{bmatrix}$$

$$\qquad\qquad 3 \qquad\qquad\qquad\qquad 2 \qquad\qquad\qquad\qquad 1$$

where in the above matrix product

1 – represents a yaw around the z axis, $T_z(y)$

2 – represents a pitch about the resultant y axis, $T_y(p)$

3 – represents a roll about the resultant x axis, $T_x(r)$.

The complete matrix is given below:

$$D = \begin{bmatrix} \cos p \cos y & \cos p \sin y & -\sin p \\ \begin{pmatrix} -\sin y \cos r \\ +\sin r \sin p \cos y \end{pmatrix} & \begin{pmatrix} \cos y \cos r \\ +\sin r \sin p \sin y \end{pmatrix} & \cos p \sin r \\ \begin{pmatrix} +\sin y \sin r \\ +\cos r \sin p \cos y \end{pmatrix} & \begin{pmatrix} -\sin r \cos y \\ +\cos r \sin p \sin y \end{pmatrix} & \cos p \cos r \end{bmatrix}$$

We have $\operatorname{tr}(D) = 1 + 2 \cos \theta$, (Section 2.31).

$$(\cos y/2 \, \cos p/2 \, \cos r/2 + \sin y/2 \, \sin p/2 \, \sin r/2)^2 = \cos^2 \theta/2$$

The direction cosine matrix defining the same orientation is:

$$D = (d_{ij}) \text{ for i and j = 1 to 3}$$

The present routine computes yaw, pitch and roll angles with the relationships

$$y = \tan^{-1}\left(\frac{d_{12}}{d_{11}}\right), \quad p = -\sin^{-1}(d_{13}), \quad r = \tan^{-1}\left(\frac{d_{23}}{d_{33}}\right) \tag{2.78}$$

Application of expressions (2.78) provide excellent results except in regions approaching $p = \pm\frac{\pi}{2}(\cos p \to o)$. Additional relationships have been derived which may alleviate problems in this special region.

$$d_{22} + d_{31} = \cos(y-r)(1 + \sin p)$$
$$-d_{21} + d_{32} = \sin(y-r)(1 + \sin p)$$
$$d_{22} - d_{31} = \cos(y+r)(1 - \sin p)$$
$$d_{21} + d_{32} = -\sin(y+r)(1 - \sin p)$$

hence if $\qquad \sin p = 1$

we have $\qquad y - r = \tan^{-1}\left(\frac{-d_{21} + d_{32}}{d_{22} + d_{31}}\right)$

and if $\qquad \sin p = -1$
$$y + r = \tan^{-1}\left(\frac{-d_{21} - d_{32}}{d_{22} - d_{31}}\right)$$

At these points (when cos p=0, sin p=± 1) it is impossible to distinguish between yaw and roll hence some arbitrary decision must be made unless further information (such as memory of last point) is available.

2.4.2   <u>Euler Angles: Spin, Nutation and Precession</u>

In a manner similar to the above the Euler angles may be obtained from the direction cosine matrix. The conventional notation as used in Reference 11 is

$$D = T_j(\psi) \, T_x(\theta) \, T_j(\phi)$$

31

where ψ , θ and ϕ are termed the spin, nutation and precession angles, respectively. In particular the direction cosine matrix is expanded in the following manner and is illustrated in Figure (2.8.)

$$\begin{bmatrix} \cos\psi & \sin\psi & 0 \\ -\sin\psi & \cos\psi & 0 \\ 0 & 0 & 1 \end{bmatrix} \begin{bmatrix} 1 & 0 & 0 \\ 0 & \cos\theta & \sin\theta \\ 0 & -\sin\theta & \cos\theta \end{bmatrix} \begin{bmatrix} \cos\phi & \sin\phi & 0 \\ -\sin\phi & \cos\phi & 0 \\ 0 & 0 & 1 \end{bmatrix}$$

when multiplied yield.

$$D = \begin{bmatrix} \cos\psi \ \cos\phi & \cos\psi \ \sin\phi & \sin\psi \ \sin\theta \\ -\sin\psi \ \cos\theta \sin\phi & +\sin\psi \ \cos\theta \cos\phi & \\ & & \\ -\sin\psi \ \cos\phi & -\sin\psi \ \sin\phi & \cos\psi \ \sin\theta \\ -\cos\psi \ \cos\theta \sin\phi & +\cos\psi \ \cos\theta \cos\phi & \\ & & \\ \sin\theta \ \sin\phi & -\sin\theta \ \cos\phi & \cos\theta \end{bmatrix}$$

As before the Euler angles may be computed by

$$\theta = \cos^{-1}(d_{33}) \ , \quad \psi = \tan^{-1}\left(d_{13}/d_{23}\right), \quad \phi = \tan^{-1}\left(d_{31}/-d_{32}\right)$$

in almost all cases (i.e., $\theta \neq 0$, or $\theta \neq \pi$).

For the special cases of $\theta = 0$ or π the following relationships may be used.

$\theta = 0$	$\theta = \pi$
$\psi + \phi = \tan^{-1}\left(\dfrac{d_{12} - d_{21}}{d_{11} + d_{22}}\right)$	$\phi - \psi = \tan^{-1}\left(\dfrac{d_{12} + d_{21}}{d_{11} - d_{22}}\right)$

Again, for these special cases it is impossible to distinguish between the spin and precession. An arbitrary decision could be made such as setting $\psi = 0$ and computing ϕ from the above table. An alternate solution is to use additional information such as memory of the last angle values to alleviate the problem.
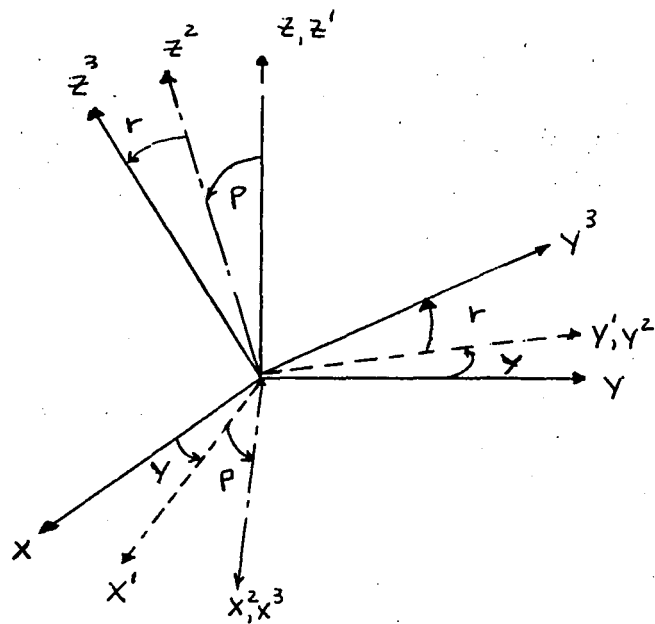
Figure 2.7   YAW, PITCH, ROLL
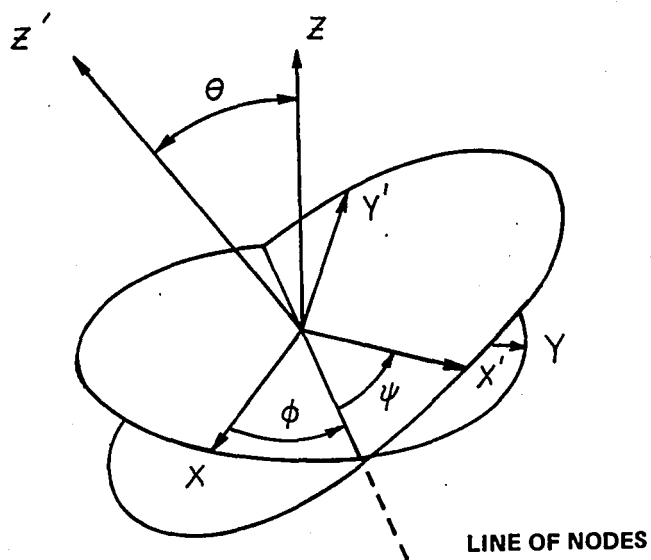
Figure 2.8   EULER ANGLES

34

SECTION 3
VECTOR EXPONENTIAL INTEGRATOR

3.1   INTRODUCTION

In large scale simulations, such as the Calspan Three-Dimensional
Crash Victim Simulation computer program, where the amount of computer time
can become overly excessive to produce integration results to a desired degree
of accuracy, it becomes very desirable to determine those integration techniques
that are capable of producing the best integration accuracy for a minimum
expenditure of computer time. Throughout the development of the CVS, Calspan
has been continually investigating different integration techniques to achieve
these goals.

A new integrator, called the Vector Exponential Integrator, has
been incorporated into CVS-IV that duplicated results obtained with the CVS-III
integrator but required only about 10% of the computer time for a test case
where the CVS-III integration control parameters to achieve comparable results
on IBM and CDC computers were determined by NHTSA personnel. Other studies at
Calspan (Sections 3.4 and 3.5) indicate that, for the same amount of computer
time, the accuracy of integration is significantly improved with the new
integrator.

3.2   MATHEMATICAL FORMULATION OF THE INTEGRATION PROCEDURE

To describe the procedure used by this integrator, consider the first
order differential equation

$$\dot{x} = f(x, t) \qquad\qquad (3.1)$$

The solution of equation 3.1 may be written as

$$x(t) = x(0) + \int_0^t e^{\alpha(t-\tau)} \left[f(x(\tau),\tau) - \alpha(x(\tau)-x(0))\right]d\tau \qquad (3.2)$$

where α is a constant to be determined.

Assume that f may be approximated by

$$\dot{x}(t) = f(x(t),t) \simeq \alpha x(t) + a_0 + a_1 t + a_2 t^2 \qquad (3.3)$$

where α, a_0, a_1 and a_2 are parameters to be determined. We then have

$$x(t) = x(0) + \int_0^t e^{\alpha(t-\tau)} \left[\alpha x(0) + a_0 + a_1\tau + a_2\tau^2\right]d\tau \qquad (3.4)$$

or

$$x(t) = x(0) + (\alpha x(0)+a_0)t\, e_0(t) + a_1 t^2 e_1(t) + a_2 t^3 e_2(t) \qquad (3.5)$$

where

$$e_0(t) = (e^{\alpha t}-1)/(\alpha t) \quad \to 1 \quad \text{as } \alpha t \to 0$$

$$e_1(t) = (e_0^{\alpha t}-1)/(\alpha t) \quad \to 1/2 \text{ as } \alpha t \to 0$$

$$e_2(t) = (2e_1^{\alpha t}-1)/(\alpha t) \to 1/3 \text{ as } \alpha t \to 0$$

(The presence of the exponential function is the reason for the name exponential integrator.)

The behavior of the integrator is determined by the method used for determining the four parameters, α, a_0, a_1 and a_2. In the latest version, the integrator operates in two modes, a reset mode and a memory mode. In both modes the parameters are selected to fit the computed derivatives at $t = 0$,

36

the beginning of an integration interval. Hence we may rewrite equation 3.3 as

$$\dot{x}(t) = \alpha(x(t) - x(0)) + \dot{x}(0) + a_1 t + a_2 t^2 \qquad (3.6)$$

In the memory mode, when a successful integration step has been completed over a time interval h, t + h is substituted for t, so that t = 0 is always the start of a new time interval. This yields

$$\dot{x}(t+h) = \alpha(x(t+h) - x(h)) + (a_1 + 2a_2 h)t + a_2 t^2 \qquad (3.7)$$
$$+ \alpha(x(h) - x(0)) + \dot{x}(0) + a_1 h + a_2 h^2$$

The functions are then redefined so that the form of equation 3.6 is preserved, where

new $a_1 = a_1 + 2a_2 h$

new $a_2 = a_2$

new $\dot{x}(0) = $ old $\dot{x}(h)$ is used in place of $\alpha(x(h)-x(0))+\dot{x}(0)+a_1 h+a_2 h^2$

new $x(t) = $ old $x(t+h)$

These values are used to estimate the value of x(t) at the first half step of the next interval, i.e., when t = h/2. In the reset mode, the parameters α, a_1 and a_2 are set to zero.

3.2.1   Computational Procedure

        The integrator uses a procedure similar to that used by a basic
Runge-Kutta with the steps as follows:

Step 1:   First midpoint calculation at t = h/2.

        a) $x(h/2)$ is evaluated using equation 3.5.

        b) $\dot{x}(h/2)$ is evaluated by calling Subroutine PDAUX.

        c)   The parameter α is unchanged.

        d)   In the memory mode, the parameters a_1 and a_2 are modified so
             that the fit for the derivative is exact at t = 0 and is least
             squares fitted to the values of the derivative at the beginning
             and middle of the previous interval and to the value just
             determined.

        e)   In the reset mode, a_1 is set to give a linear fit to $\dot{x}(0)$ and
             $\dot{x}(h/2)$ with $\alpha = a_2 = 0$.

Step 2:   Second mid-point calculation at t = h/2.

        a) $x(h/2)$ is evaluated using equation 3.5.

        b) $\dot{x}(h/2)$ is evaluated by a call to Subroutine PDAUX.

        c)   The parameter α is updated.

        d)   In the memory mode, parameters a_1 and a_2 are computed to fit
             the values of the derivatives at t = 0, t = previous mid-point
             and the average value of the derivatives obtained in this and
             the previous step.

38

e) In the reset mode, the parameter, a_1, is set to give a linear fit to the value at $t = 0$ and the average value at $t = h/2$.

Step 3: First end point calculation at $t = h$,

a) $x(h)$ is evaluated using equation 3.5.

b) $\dot{x}(h)$ is evaluated by a call to Subroutine PDAUX.

c) The parameter α is unchanged.

d) In both modes, the parameters a_1 and a_2 are computed to fit the value at $t = 0$, the average at $t = h/2$ and the value at $t = h$ just computed.

Step 4: Second end point calculation at $t = h$,

a) $x(h)$ is evaluated using equation 3.5.

b) $\dot{x}(h)$ is evaluated by a call to Subroutine PDAUX.

c) The parameter α is updated.

d) In both modes, the parameters a_1 and a_2 are evaluated as they were in Step 3d.

e) Tests for convergence (to be described later) are performed. If the convergence test passes, the integrator has successfully completed a step and we proceed to the substitution $t \leftarrow t + h$ as explained previously. If the integrator has successfully completed three consecutive steps for the same value of h, the value of h is doubled but is limited to the input parameter h_{max}. Control is then returned to Step 1.

f) If the convergence test has failed and if the specified
    number of iterations of Steps 4 and 5 have not been made
    (as controlled by the input parameter NDINT), control is
    then passed to Step 5.

g) If the convergence test has failed and the specified (NDINT) number
    of iterations have been made, the step size h is halved and the
    process is repeated by returning to Step 1. However, if h is
    already less than the allowed minimum step size (as controlled
    by the input parameter h_{min}), the integration test is considered
    successful and the $t \leftarrow t + h$ substitution is made and control is
    passed to Step 1.

Step 5: Additional calculation at mid-point, $t = h/2$.

a) $x(h/2)$ is evaluated using equation 3.5.

b) $\dot{x}(h/2)$ is evaluated by a call to Subroutine PDAUX.

c) The parameter α is updated.

d) In both modes, the parameters a_1 and a_2 are evaluated to fit
    exactly at $t = 0$, the last value at $t = h$ and the new value
    at $t = h/2$ just computed.

Step 4 is then repeated except that the value just computed at
$t = h/2$ is used for $\dot{x}(h/2)$. Where the standard Runge-Kutta method evaluates
functions only at $t = 0$ (or end of previous step), $t = h/2$, $t = h/2$ and $t = h$,
the new integrator now tests for convergence, and revaluates $t = h/2$ and $t = h$
for NDINT iterations if the convergence test fails. However, the convergence
test may pass at any $t = h$ evaluation. Although it seems that increasing
NDINT may cause extra functional evaluations and hence expend additional
computer time, if the extra functional evaluation can reduce the error and
cause the convergence test to now pass, this may prove to be more efficient

40

than the additional functional evaluations made necessary by halving the step size. The sequence of functional evaluations is summarized in Table 3.1.

The integrator treats each variable separately by the preceeding process. There are two exceptions to this, one is the determination of the value of α and the other is the translation of t in the parameters associated with the quaternions.

3.2.2 Determination of the Value of α

The variables are treated in their three component vector form $\overline{x}$ and $\overline{\overline{x}}$, the same value of α is used for each of the three components of the vector, but a different α is evaluated for each vector. This is the reason for the name Vector Exponential Integrator.

Let

$$\overline{\overline{x}}(t) \simeq \alpha \ (\overline{x}(t) - \overline{x}(0)) + \overline{\overline{x}}(0) + \overline{a}_1 t + \overline{a}_2 t^2 \qquad (3.8)$$

be the vector form of equation 3.5. If two different determinations of $\overline{\overline{x}}(t)$ and $\overline{x}(t)$ are made at the same time point t, we have

$$\overline{\overline{x}}_1(t) \simeq \alpha \ (\overline{x}_1(t) - \overline{x}(0)) + \overline{\overline{x}}(0) + \overline{a}_1 t + \overline{a}_2 t^2$$

$$\overline{\overline{x}}_2(t) \simeq \alpha \ (\overline{x}_2(t) - \overline{x}(0)) + \overline{\overline{x}}(0) + \overline{a}_1 t + \overline{a}_2 t^2$$

Subtraction yields

$$\overline{\overline{x}}_2(t) - \overline{\overline{x}}_1(t) \simeq \alpha \ (\overline{x}_2(t) - \overline{x}_1(t)) \qquad (3.9)$$

41

Table 3.1 SUMMARY OF INTEGRATION STEPS

Step No.	Time Point	Time Point Used to Compute a_1 and a_2	Exponential Factor	Time Point Data Saved
1	$t = h/2$	$t = 0$, least square fit thru $t = -h_s$, $-h_s/2$, $h/2$	same α	middle point, $h/2$
2	$t = h/2$	$t = -h_s/2$, 0, $h/2$	new α	average of middle points
3	$t = h$	$t = 0$, $h/2$, h	same α	end point, h
4	$t = h$	$t = 0$, $h/2$, h	new α	end point, h
5	$t = h/2$	$t = 0$, $h/2$, h	new α	middle point, $h/2$

h = current step size

h_s = previous step size

Sequence of steps: 1, 2, 3, 4(1), 5, 4(2), 5, ----, 4 (NDINT)

If this process is done at several time points, we may make a least square determination of α by

$$\alpha = \frac{\sum_n (\overline{x}_2(t_n) - \overline{x}_1(t_n)) \cdot (\overline{x}_2(t_n) - \overline{x}_1(t_n))}{\sum_n |\overline{x}_2(t_n) - \overline{x}_1(t_n)|^2} = \frac{U}{V} \qquad (3.10)$$

The values of the numerator and denominator are carried separately as U and V so that they may be updated when new data points are obtained. In the memory mode, when t is translated by $t = t + h$, U and V are decreased by a memory factor which depends exponentially on the value of the step size h just completed. In the reset mode, both U and V are initialized to zero.

3.2.3   Integrator Convergence Tests

The Vector Exponential Integrator obtains two sets of derivatives in vector form. One set, considered to be the computed value and denoted by $\overline{x}_c(t)$, is obtained by a call to Subroutine PDAUX. The other, considered to be the estimated value and denoted by $\overline{x}_e(t)$, is evaluated from the functional form of equation 3.8 using the latest values of the parameters (repeated for convenience).

$$\overline{x}_e(t) \simeq \alpha(\overline{x}(t) - \overline{x}(0)) + \overline{x}(0) + \overline{a}_1 t + \overline{a}_2 t^2 \qquad (3.11)$$

If α is large, this estimated value is very sensitive to perturbations of $\overline{x}(t)$. Consider the error measure ε^2 defined by

$$\varepsilon^2 = \frac{|\overline{x}_e(t) + \alpha\overline{\delta} - \overline{x}_c(t)|^2}{|\overline{x}_c(t)|^2} + \lambda \frac{|\overline{\delta}|^2}{|\overline{x}(t)|^2} \qquad (3.12)$$

where

$\bar{\delta}$ = perturbation of $\bar{x}(t)$

λ = arbitrary constant weight (present version assumes $\lambda = 1$)

Equation 3.12 is minimized when

$$\delta = \frac{\alpha \, (\bar{\bar{x}}_c - \bar{\bar{x}}_e)}{\alpha^2 + \lambda \, |\bar{\bar{x}}_c|^2 / |\bar{x}|^2} \qquad (3.13)$$

and has the value

$$\epsilon^2_{min} = \frac{|\bar{\bar{x}}_c - \bar{\bar{x}}_e|^2}{|\bar{\bar{x}}_c|^2 + \alpha^2 |\bar{x}|^2 / \lambda} \qquad (3.14)$$

Note that when $\alpha^2/\lambda = 0$, this reduces to a relative squared error of the derivative as was tested in the previous integrator in CVS-III.

For each vector variable which is integrated, the user supplies three levels of test numbers (T_1, T_2 and T_3) that are used by the Vector Exponential Integrator to test for integrator convergence.

The procedure to test for integrator convergence is as follows:

a. If the magnitude test T_1 is zero, no further testing is performed and the test is considered passed for this vector variable.

b. If $T_1 \neq 0$ and if $|\bar{\bar{x}}_c|^2 \leq T_1^{\,2}$, no further testing is performed and the test is considered passed for this vector variable.

c. If the absolute error test $T_2 \neq 0$ and $|\bar{x}_c - \bar{x}_e|^2 \leq T_2^2$, no further testing is performed for this vector variable and the test is considered to have passed.

d. If $\varepsilon^2_{min} > T_3^2$, the relative error test parameter, the integrator convergence test has failed; otherwise this vector variable has passed and the procedure is then repeated for all vector variables.

It should be noted that for an integration step to be considered as successful, all vector variables must pass the above sequence of tests; whereas any single vector variable failing Step d will cause the integration step to fail.

3.3 ANALYTICAL SOLUTION OF FREE BODY ANGULAR MOTION

The angular momentum vector in inertial reference of a single segment is given by the matrix relation

$$h = D^{-1} \Phi \omega \qquad\qquad (3.15)$$

where

D is the direction cosine matrix

Φ is the inertia matrix (tensor), and

ω is a vector representing the angular velocity about the principal axes in local reference.

45

If the segment has no external torques acting on it, then h is a constant and the equation of motion is obtained by taking the time derivative of equation 3.15.

$$\dot{h} = (D^{-1}\dot{\Phi\omega}) = D^{-1}\dot{\Phi\omega} + D^{-1}\omega \otimes \Phi\omega = 0 \qquad (3.16)$$

Equation 3.16 can be solved for the angular acceleration vector

$$\dot{\omega} = -\Phi^{-1}\omega \otimes \Phi\omega \qquad (3.17)$$

It can be shown that

$$\omega \cdot \dot{\Phi\omega} = 0 \qquad (3.18)$$

hence

$$\omega \cdot \Phi\omega = 2E \qquad (3.19)$$

which is a constant where E is the energy. Also,

$$(\Phi\omega) \cdot (\Phi\omega) = h \cdot h \text{ is constant} \qquad (3.20)$$

If Φ is a diagonal matrix, equation 3.17 may be written as

$$\dot{\omega}_1 = \omega_2 \omega_3 / a_1 \qquad (3.21)$$

$$\dot{\omega}_2 = \omega_3 \omega_1 / a_2$$

$$\dot{\omega}_3 = \omega_1 \omega_2 / a_3$$

where $\qquad a_1 = \Phi_1 / (\Phi_2 - \Phi_3)$

$$a_2 = \Phi_2 / (\Phi_3 - \Phi_1)$$

and $\qquad a_3 = \Phi_3 / (\Phi_1 - \Phi_2)$

The following cases may then be considered:

Case I: The segment has equal principal moments of inertia, i.e.,
$\Phi_1 = \Phi_2 = \Phi_3$.

In this case, equation 3.17 becomes $\dot{\omega} = 0$, hence, ω is a constant.
The instantaneous angular position is described by the quaternion, q, where

$$q = \cos \frac{|\omega|t}{2} + \frac{\omega}{|\omega|} \sin \frac{|\omega|t}{2} \qquad (3.22)$$

and the direction cosine matrix by

$$D = (\cos |\omega|t)\, I + (1 - \cos |\omega|t)\, \frac{\omega\omega^{\cdot}}{\omega\cdot\omega} - (\sin |\omega|t)\, \frac{\omega\otimes}{|\omega|} \qquad (3.23)$$

Case II: The segment has two equal principal moments of inertia, i.e.,
$\Phi_1 = \Phi_2 \neq \Phi_3$.

In this case, since $\dot{\omega}_3 = 0$, $\dot{\omega}_1$ in equation 3.21 may be differentiated
to yield

$$\ddot{\omega}_1 = \dot{\omega}_2 \omega_3/a_1 = \omega_1 \omega_3/a_1 a_2 \qquad (3.24)$$

The solution is

$$\omega_1 = \omega_{1_o} \cos \Omega t + \frac{\omega_{2_o} \omega_{3_o}}{a_1} \frac{\sin \Omega t}{\Omega}$$

$$\omega_2 = \omega_{2_o} \cos \Omega t + \frac{\omega_{3_o} \omega_{1_5}}{a_2} \frac{\sin \Omega t}{\Omega} \qquad (3.25)$$

$$\omega_3 = \omega_{3_o}$$

47

where
$$\Omega = \left(\frac{\omega_{3_o}^2}{-a_1 a_2}\right)^{1/2} = \left|\omega_{3_o}(\Phi_3 - \Phi_1)/\Phi_1\right| \tag{3.26}$$

In terms of the Euler angles[1], ϕ, Θ, ψ (precession, nutation and spin), if we let

$$\Phi_1 \omega_1/|h| = \sin \psi \sin \Theta$$

$$\Phi_2 \omega_2/|h| = \cos \psi \sin \Theta \tag{3.27}$$

and
$$\Phi_3 \omega_3/|h| = \cos \Theta$$

the momentum vector, h, will be aligned with the inertial z axis; the nutation angle, Θ, will be constant; and the spin angle, ψ, may be computed directly as

$$\psi = \tan^{-1} \frac{\omega_1}{\omega_2} \tag{3.28}$$

The precession angle, ϕ, is determined by the relation

$$\dot{\phi} \sin \Theta = \omega_1 \sin \psi + \omega_2 \cos \psi = \frac{|h|}{\Phi_1} \sin \Theta \tag{3.29}$$

Therefore,

$$\dot{\phi} = |h|/\Phi_1 \tag{3.30}$$

is a constant, and

$$\phi = \phi_o + (|h|/\Phi_1)t \tag{3.31}$$

---

[1] See Section 2.4.

48

Case III: The principal moments of inertia are all unequal.

It is no restriction to assume that $\Phi_1 < \Phi_2 < \Phi_3$. Equation 3.21 may then be written as

$$a_1 \dot{\omega}_1 \omega_1 = a_2 \dot{\omega}_2 \omega_2 = a_3 \dot{\omega}_3 \omega_3 = \omega_1 \omega_2 \omega_3 \qquad (3.32)$$

Integrating equation 3.32 yields

$$a_1 (\omega_1^2 - \omega_{1_0}^2) = a_2 (\omega_2^2 - \omega_{2_0}^2) = a_3 (\omega_3^2 - \omega_{3_0}^2) \qquad (3.33)$$

ω_1 and ω_3 may be expressed as functions of ω_2 and substitution then yields

$$a_2 \dot{\omega}_2 = \{ [-a_2 (\omega_2^2 - \omega_{2_0}^2) - a_1 \omega_{1_0}^2][-a_2 (\omega_2^2 - \omega_{2_0}^2) - a_3 \omega_{3_0}^2]/a_1 a_3 \}^{1/2} \qquad (3.34)$$

If we let

$$\text{min} = \text{minimum} (a_2 \omega_{2_0}^2 - a_1 \omega_{1_0}^2, \ a_2 \omega_{2_0}^2 - a_3 \omega_{3_0}^2) \qquad (3.35)$$

$$\text{max} = \text{maximum} (a_2 \omega_{2_0}^2 - a_1 \omega_{1_0}^2, \ a_2 \omega_{2_0}^2 - a_3 \omega_{3_0}^2) \qquad (3.36)$$

$$\omega_2 = y \sqrt{\text{min}/a_2}$$

and $\qquad m = \text{min}/\text{max}$

then equation 3.34 may be written as

$$\dot{y} = \sqrt{\frac{\text{max}}{a_1 a_2 a_3}} \ \sqrt{(1-y^2)(1-my^2)} \qquad (3.37)$$

49

Now by defining

$$u = \int_0^y \frac{dy}{\sqrt{(1-y^2)(1-my^2)}}$$ (3.38)

as an Elliptic Integral of the First Kind, and

$$y = sn(u)$$ (3.39)

as the corresponding Jacobian Elliptic Function[2], one obtains

$$\omega_2 = \sqrt{\frac{min}{a_2}} \; sn \left([t-t_o] \sqrt{\frac{max}{a_1 a_2 a_3}} + sn^{-1} \left[\omega_{2_o} \sqrt{\frac{a_2}{min}} \right] \right)$$ (3.40)

Further, if $min = a_2 \omega_{2_o}^2 - a_1 \omega_{1_o}^2$, then

$$\omega_1^2 = - \left(\frac{min}{a_1} \right) cn^2(u)$$ (3.41)

$$\omega_3^2 = - \left(\frac{max}{a_3} \right) dn^2(u)$$ (3.42)

or, if $min = a_2 \omega_{2_o}^2 - a_3 \omega_{3_o}^2$, then

$$\omega_1^2 = - \left(\frac{max}{a_1} \right) dn^2(u)$$ (3.43)

$$\omega_2^2 = - \left(\frac{min}{a_3} \right) cn^2(u)$$

_____

[2]Reference 10.

50

where u is the argument of the sn function used for ω_2 in equation 3.40. Care must be taken in selecting the signs of the square roots which must be chosen to yield the proper signs for ω and $\dot{\omega}$. Also note that

$$\text{sn}^2(u) + \text{cn}^2(u) \equiv 1 \qquad (3.44)$$

$$\text{dn}^2(u) + m \ \text{sn}^2(u) \equiv 1$$

The angular position may be determined in a manner similar to equation 3.27, namely

$$\Phi_3 \omega_3 / |h| = \cos \Theta \qquad (3.45)$$

$$\frac{\Phi_1 \omega_1}{\Phi_2 \omega_2} = \tan \psi$$

and equation 3.30 becomes

$$\dot{\phi} = |h| \ [\ \frac{\sin^2 \psi}{\Phi_1} + \frac{\cos^2 \psi}{\Phi_2} \ ] \qquad (3.46)$$

$$= |h| \ \frac{\Phi_1 \omega_1^2 + \Phi_2 \omega_2^2}{\Phi_1^2 \omega_1^2 + \Phi_2^2 \omega_2^2}$$

Note that in the general case, Θ and $\dot{\phi}$ are not constant as they were when $\Phi_1 = \Phi_2$.

Further substitution into equation 3.46 yields

$$\dot{\phi} = |h| \ \frac{(\Phi_3 - \Phi_2) + (\Phi_2 - \Phi_1) \ k \ \text{sn}^2(u)}{\Phi_1(\Phi_3 - \Phi_2) + \Phi_3(\Phi_2 - \Phi_1) \ k \ \text{sn}^2(u)}$$

$$= |h| \ [\Phi_3^{-1} + \frac{\Phi_1^{-1} - \Phi_3^{-1}}{1 + nk \ \text{sn}^2(u)} \ ] \qquad (3.47)$$

51

where

$$n = \frac{\Phi_3 \, (\Phi_2 - \Phi_1)}{\Phi_1 \, (\Phi_3 - \Phi_2)}$$

and

$$k = 1 \text{ if min} = a_2 \omega_{2_0}^2 - a_1 \omega_{1_0}^2$$

$$= m \text{ if min} = a_2 \omega_{2_0}^2 - a_3 \omega_{3_0}^2$$

This is now in a form that can be expressed in terms of Elliptic Integrals of the Third Kind which are defined as

$$\pi(n; \, u|m) = \int_0^u [1 - n \, sn^2(\omega)]^{-1} \, d\omega \qquad (3.48)$$

The solution of equation 3.47 may be written as

$$\phi = \phi_0 + |h| \, \frac{t - t_0}{\Phi_3} + C \, [\pi(nk; \, u|m) - \pi(nk; \, u_0|m)] \qquad (3.49)$$

where

$$C = |h| \, (\Phi_1^{-1} - \Phi_3^{-1}) \sqrt{\frac{a_1 a_2 a_3}{max}}$$

$$u = sn^{-1} (\omega_2 \sqrt{a_2/min})$$

$$u_0 = sn^{-1} (\omega_{2_0} \sqrt{a_2/min})$$

52

3.4   SIMULATION OF FREE BODY ANGULAR MOTION

        Users of CVS-III have experienced difficulty in those cases that
involve rapid angular motion of individual body segments. Examples of this
are (1) the basic test case Calspan has supplied on previous program tapes when
the feet make initial contacts with the floorboard and toeboard, and (2) pedestrian
runs by Chrysler Corporation for the RSV program when the hands make initial
contact with the hood. In both cases, these were small body extremities making
hard contacts near the beginning of the simulation. Attempts to control the
resulting rapid angular motion by varying the input of the integrator control
parameters forced the integrator to the specified minimum time step intervals,
resulting in excessive computer CPU time, and produced questionable results.

        It became suspect that the integrating techniques used by CVS-III
were either incorrect or incapable of properly integrating angular motion.
It was decided to run computer simulations of a single rotating segment for
a case where the exact analytical solution is known to study the accuracy of
the integration of angular motion produced by the new integrator. The
analytical solution of free body angular motion is given in Section 3.3.

3.4.1   Computer Simulation Inputs

        The basic inputs for the test case were given by:

        (1)   One segment and zero joints (Card B.1).

        (2)   Principal moments of inertia (Card B.2),
                Φ_x, Φ_y and Φ_z (or Φ_1, Φ_2 and Φ_3) = 1, 2 and 3.

r

53

(3)   The input yaw, pitch and roll (Card G.3),

$$y = \tan^{-1} \frac{2}{-1} = 116.565051 \text{ deg.}$$

$$p = \sin^{-1} \sqrt{5/14} = 36.6992252 \text{ deg.}$$

$$r = 0 \text{ deg.}$$

These were chosen so that the momentum vector would coincide with the Z axis. Note that CVS program normally computes the initial direction cosine matrix by reversing the order of the input rotation angles (yaw, pitch, and roll), i.e.,

$$D = D_y \, D_p \, D_r$$

whereas for output purposes, the rotation angles are defined by

$$D = D_r \, D_p \, D_y.$$

(4)   The initial angular velocities (Card G.3),

$$\omega_x, \, \omega_y \text{ and } \omega_z \text{ (or } \omega_1, \, \omega_2 \text{ and } \omega_3) = 36799.3780 \text{ deg/sec.}$$

These were chosen such that the frequency of the components of angular velocity would be 100 cycles per second, the period of one cycle to be exactly 10 msec. This value is obtained in radians/sec by

$$\omega = 200 \sqrt{3} \; K \, (m)$$

where $K \, (m)$ is the complete elliptic integral of the first kind for $m = 1/2$.

(5)   There are no specified contacts and the segment is falling under the influence of g (Card A.3).

3.4.2 Additional Simulation Outputs

In addition the output routine was modified to give the following outputs for every successful integration step.

(1) The segment angular velocity was changed from rev/sec in vehicle reference to rad/sec in local reference.

(2) The components and magnitude of the momentum vector, h, given by

$$(\Phi\omega)\cdot(\Phi\omega) = h\cdot h$$

This should remain constant, with the x and y components equal to zero.

(3) The constant $\sqrt{2E}$, where E is the energy, given by

$$\omega\cdot(\Phi\omega) = 2E$$

(4) In addition to the angular displacements, y, p and r, computed from

$$D = D_r \, D_p \, D_y$$

the Euler angles, ψ, Θ and ϕ, were printed in degrees from

$$D = T_z(\psi) \, T_x(\Theta) \, T_z(\phi)$$

(5)   The following angles, in degrees, are computed as follows
       and theoretically should equal the indicated rotation
       angles.

$$p^* = \sin^{-1} \frac{-\Phi_1 \omega_1}{|h|} \simeq p$$

$$r^* = \tan^{-1} \frac{\Phi_2 \omega_2}{\Phi_3 \omega_3} \simeq r$$

$$\Theta^* = \cos^{-1} \frac{\Phi_3 \omega_3}{|h|} \simeq \Theta$$

$$\phi^* = \tan^{-1} \frac{\Phi_1 \omega_1}{\Phi_2 \omega_2} \simeq \phi$$

In addition, the other two rotation angles, y and ψ, can be compared
to Jacobian elliptic functions, sn(u), cn(u) and dn(u), but these comparisons
were not made.

3.4.3   Comparison Measures

The resulting time history outputs presented many items whose
accuracy could be determined to study the accuracy of the integrating techniques
used.   They include:

(1)   The x, y and z components of linear acceleration of the
       segment c.g. should be in the ratio of 1:2:3 at the half-
       period (every 5 msec) time points.   The resultant should
       remain at a constant 1 g for all points.

(2)   The z component of linear acceleration at the points (1, 2, 3)
       and (0, 0, 1) appeared to remain constant with small
       fluctuations.   Also, the resultant linear velocity of the
       point (0, 0, 1) appeared to remain constant with small

56

fluctuations. These results were unexpected and have not been studied.

(3)   The components of segment angular acceleration (rev/sec^2) in local reference should follow known elliptic functions with a fixed half-period (5 msec). Their magnitudes are quite large, $\approx 10^6$, and the deviation from the known values at the half-period time points was one of the measures used to study the accuracy of the various simulations that were run.

(4)   The magnitude of the x and y components of the momentum vector h should be zero, and the deviation from zero is a meaningful comparison measure.

(5)   The values of $|h|$ and E should remain constant and their deviation from the known constant value can be used as comparison measures.

(6)   The deviations of the computed values of p^*, r^*, Θ^*, and ϕ^* from the printed values of p, r, Θ and ϕ at the same time points are also useful comparison measures. It was difficult to determine, however, if deviations were caused by inaccuracies in the direction cosine matrix or in the angular velocities.

3.4.4   Simulation Input Parameters

        Several simulations were run for 25 msec, 2 1/2 full cycles,
varying the following parameters.

        (1)   Integrating procedure used.

               a.   New Vector Exponential Integrator.

               b.   Previous integrator of CVS-III.

               c.   Standard Runge-Kutta integrator.

        (2)   Value of the maximum step size, h_{max}.

        (3)   Value of the initial step size, h_o.

        (4)   Value of the relative error test for angular acceleration.

        A summary of the various simulations is presented in Table 3.2.

3.5   RESULTS AND CONCLUSIONS

        A study of Table 3.2 and the finer detail given by the simulation
outputs show the following results and conclusions.

        (1)   The new Vector Exponential Integrator produces very accurate
               results of free body angular motion. The resulting accuracy
               is 50-1000 times better than that produced by the previous
               integrator of CVS-III, using the same integrator control
               parameters and approximately the same amount of computer
               CPU time (as measured by the number of calls to DAUX). In
               order to produce the same degree of accuracy with the CVS-III
               integrator, it would be necessary to tighten the relative error
               controls which would increase the amount of computer CPU time.

Table 3.2

SUMMARY OF COMPUTER SIMULATIONS OF FREE BODY ANGULAR MOTION

Run Number	Integrator	No. Steps	DT (Msec)	h_{max} (Msec)	h_o (Msec)	Relative Error Test For Angular Accel.	No. Integration Steps	No. Calls to DAUX	Max. Error (%) Angular Acceleration At Half-Period Points	Max. Magnitude of X, Y Components of Momentum Vector, h	Max. Deviation (%) of |h| From Constant Value	Max. Deviation (%) of E from Constant Value
8045	CVS-III	25	1	1/2	1/8	10^{-3}	56	317	11.6300	43.29	2.3570	2.9810
6688	R-K	50	1/2	1/2	1/2	--	51	204	0.2138	--	0.0286	0.0224
4393	Vec. Exp.	25	1	1/4	1/16	10^{-3}	105	417	0.0323	0.96	0.0021	0.0025
1176	Vec. Exp.	25	1	1/4	1/8	10^{-3}	103	411	0.0416	0.99	0.0046	0.0051
5816	Vec. Exp.	5	5	1/2	1/16	10^{-3}	58	259	0.0159	10.89	0.0079	0.0108
4376	Vec. Exp.	25	1	1/2	1/16	10^{-3}	58	259	0.0248	10.99	0.0092	0.0108
6793	Vec. Exp.	25	1	1/2	1/8	10^{-3}	56	251	0.0259	10.95	0.0099	0.0114
3717	Vec. Exp.	25	1	1/2	1/4	10^{-3}	53	239	0.0979	9.78	0.0137	0.0146
6190	Vec. Exp.	5	5	1/2	1/2	10^{-3}	51	235	0.0414	8.04	0.0129	0.0178
6502	Vec. Exp.	5	5	1/2	1/2	10^{-4}	51	363	0.0078	0.79	0.0008	0.0006

(2)   The variation of the input parameters, h_{max} and h_o, had
       small but inconclusive effects on the resulting accuracy with
       the new integrator. In some cases a maximum step size of
       1/2 msec produced better results than those of 1/4 msec.

(3)   The most significant increase in simulation accuracy was
       achieved by decreasing the relative error test for angular
       acceleration from 10^{-3} and 10^{-4}. The resulting accuracy
       increased by factors of 6-30, using the largest values of h_{max}
       and h_o tested, but required a 54% increase in computer CPU
       time. It is believed that a further tightening of this input
       parameter would improve the accuracy even further, as long
       as the relative error can decrease rapidly to this test
       parameter for the NDINT (input number of maximum internal
       steps for each integration step) iterations. This appears to
       be true in our one segment simulation, but is not always true
       in a full scale simulation. If the relative error test is not
       satisfied after NDINT internal steps, the integrator fails
       for that time step, and the current integration time step is
       halved to try again. There were no such integrator failures
       in all of these simulations for the one segment model.

(4)   A more detailed study of the individual simulations indicated
       that there are two sources of error in the integration results.
       They are:

       (a) A transient error seems to exist at the very first
            integration step. The new Vector Exponential Integrator
            has a built-in memory to integrate to the mid-point of
            the next step, but this is zero at the start. This
            transient error may also be influenced by the accuracy
            of the input numbers, the inputs to the one segment model
            were supplied with nine significant figures. The error
            should be minimized by starting out with a small h_o.

60

(b) A cumulative error buildup dependent on the number of
     integration steps. The individual errors are controlled
     by the relative error test. If a particular variable
     remains fairly constant, the cumulative error is limited
     by the number of integration steps times the relative
     error test times the magnitude of the variable.

     In the individual simulations, some of the actual errors
     followed a definite quadratic function behavior after
     5 msec, but not between 0 and 5 msec. It is believed that
     this was due to extra integration steps that are performed
     when $h_o < h_{max}$, which in some cases more than offsets
     the improvement in the transient error that exists at the
     beginning by taking a small h_o.

(5) Differences between simulation results obtained previously with
     the CVS-III and the new Vector Exponential Integrator are
     probably due to loose tests on the relative error for angular
     acceleration and the new Vector Exponential Integrator probably
     yields much more accurate results.

(6) It must be realized that the angular velocities for the
     simulations listed in Table 3.2 are much larger than those one
     would normally expect in a full scale simulation. Also, the
     2 1/2 complete revolutions of a single segment, achieved here
     in 25 msec, is much larger than the rotations usually occurring
     in full scale simulations. We therefore do not think that a
     relative error test of 10^{-4} is necessary under normal conditions.
     The following integrator control parameters are recommended as
     a result of these and other studies.

NDINT: 6

NSTEPS: · As necessary to control length of simulation.

DT: An integral multiple of h_{max}.

h_o: 1/8 or 1/16 msec.

h_{max}:   1/2 or 1 msec but a power of 2 multiple of h_o.

h_{min}:   Equal to h_o.

Relative
Error
Test: 10^{-2} for angular acceleration (all segments),

           10^{-3} for linear accelerations (reference segments

           only).

SECTION 4

EQUATIONS OF MOTION OF A SET OF CONNECTED RIGID BODIES

4.1   SEGMENT MOTION EQUATIONS

This section presents the equations of motion of a set of rigid bodies
using matrix notation which has a direct relation to the actual program code.

In this analysis each of the segments is assumed to be a rigid body
connected to another segment by means of a joint. As indicated in Figure 4.1
only one joint is assumed present between any two segments. It is possible now
to disconnect these segments into free bodies by supplying (for each segment
in the appropriate direction) the forces and torques that exist at the joint.
A diagram of this step is presented in Figure 4.2. In this form the equations
of motion may be written separately and simply for each rigid body with a cor-
responding set of constraint equations which allow the computation of the forces
and torques of constraint. By this method extension of the equations to any
number of segments linked in this way is a simple matter.

Define the location of the center of gravity (c.g.) of the nth segment
in an inertial reference system by x_n denoting.

$$X_h = \begin{pmatrix} X_o \\ Y_o \\ Z_o \end{pmatrix}_n$$

where X_o, Y_o, Z_o are orthogonal

coordinates in the inertial reference system.

Define a principal axis system fixed in the segment by $\begin{pmatrix} i \\ j \\ k \end{pmatrix}_n$

Then denote D_n as the direction cosine matrix associated with segment n.
Such that if $\begin{pmatrix} a \\ b \\ c \end{pmatrix}$ locates a point in the local system, and $\begin{pmatrix} x \\ y \\ z \end{pmatrix}$ locates the same
point in the inertial system then D_n satisfies the following relationship:

63
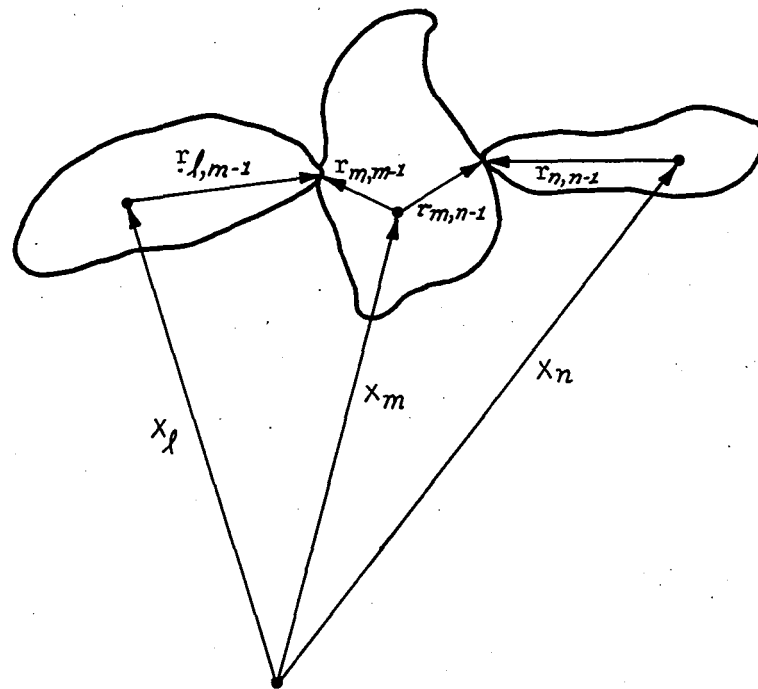
Figure 4.1 SYSTEM OF CONNECTED RIGID BODIES

EXTERNAL FORCE

(SUM OF EXTERNAL TORQUES) $_l$

ρ_{l_1}

$-f_{l,m-1}$

$+f_{l,m-1}$

EXTERNAL FORCE

ρ_{m_1}

$-f_{m,n-1}$

$+f_{m,n-1}$

EXTERNAL FORCE

$\rho_{n,1}$

$\rho_{l,2}$

EXTERNAL FORCE

(SUM OF EXTERNAL TORQUES) $_m$

$\rho_{m,2}$

EXTERNAL FORCE

(SUM OF EXTERNAL TORQUES) $_n$

x_l

x_m

x_n
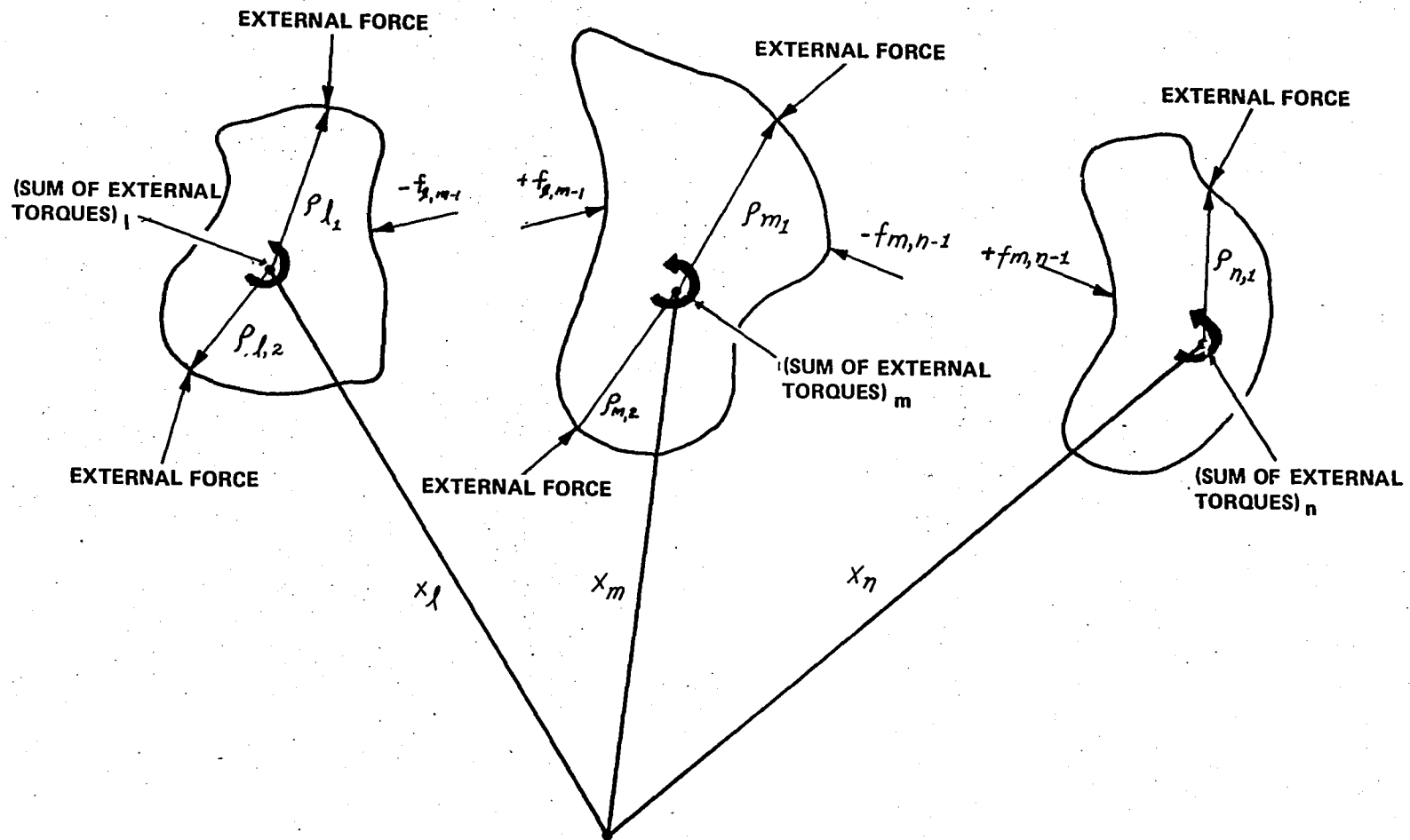
Figure 4.2. FREE BODY CONFIGURATION

$$
\begin{pmatrix} a \\ b \\ c \end{pmatrix} = \mathcal{D}_n \left[\begin{pmatrix} x \\ y \\ z \end{pmatrix} - X_n \right] \tag{4.1}
$$

or equivalently

$$
\begin{pmatrix} a \\ b \\ c \end{pmatrix} = \mathcal{D}_n \begin{bmatrix} (x - x_o) \\ (y - y_o) \\ (z - z_o) \end{bmatrix} \tag{4.2}
$$

Define also the k th external force acting on the nth segment by F_{nk}. The point of application as indicated in Figure 4.2 is P_{n_k} measured in the nth local system.

Let f_{n_j} be the constraint force at joint j acting on segment n. This of course assumes the segment n is connected to another segment by joint j. Due to the nature of the free body configuration assumed, if segment n is connected to segment m by joint j then f_{n_j} acts on segment n and $-f_{n_j} = f_{m_j}$ acts on segment m.

The position of the c.g. of the nth segment is X_n and the velocity of the c.g. is then $\dot{X}_n$. Denote the mass of the nth segment to be M_n then the linear momentum is $M_n \dot{X}_n$. The dynamic equation of motion for the nth segment is then

$$
\frac{d}{dt} \left(M_n \dot{X}_n \right) = \sum_k F_{n_k} + \sum_j f_{n_j} \tag{4.3}
$$

where $k = 1, 2 \ldots$, total number of external forces acting on segment n and $j = 1, 2$; the joints connected to segment n.

Since the mass of each segment is constant with respect to time, this equation may be rewritten as

$$
M_n \ddot{X}_n = \sum F_{n_k} + \sum f_{n_j}
$$

This is the linear (translational) dynamic equation. $\tag{4.4}$

For development of the angular equation denote ω_n as the angular velocity vector of segment n and ϕ_n as the inertia matrix about the c.g. of segment n. The angular momentum of segment n about the c.g. is written as $\phi_n \omega_n$. Note that $\phi_n \omega_n$ is in local reference so care must be used when taking the derivative. With this in mind, the angular dynamic equation in inertial system components is:

$$\frac{d}{dt}\left(D_n^{-1}\phi_n\,\omega_n\right) = D_n^{-1}\sum \text{Torques} \qquad (4.5)$$

Now taking the derivative yields

$$\dot{D}_n^{-1}\phi_n\,\omega_n + D_n^{-1}\dot{\phi}_n\,\omega_n + D_n^{-1}\phi_n\,\dot{\omega}_n = D_n^{-1}\sum \text{Torques}.$$

Note that ϕ_n is a constant property of the segment therefore $\dot{\phi}_n = 0$. Also note that $\dot{D}_n^{-1} = -D_n^{-1}\dot{D}_n\,D_n^{-1}$ and $\dot{D}_n\,D_n^{-1} = -\omega_n \otimes$, which is a matrix defined by equation (2.68.) The angular dynamic equation may be written as

$$D_n^{-1}\left(\omega_n\otimes\right)\phi_n\,\omega_n + D_n^{-1}\phi_n\,\dot{\omega}_n = D_n^{-1}\sum \text{Torques} \qquad (4.6)$$

Now the torques may be catalogued as follows:

$$D^{-1}\sum \text{Torques} = \sum\left(D_n^{-1}\rho_{n_k}\right)\otimes F_{n_k} \qquad \text{due to external forces}$$

$$+\sum\left(D_n^{-1}r_{n_j}\right)\otimes f_{n_j} \qquad \begin{array}{l}\text{due to forces of constraint}\\ \text{at joint}\end{array}$$

$$+\sum \tau_{cons.} \qquad \text{due to constraint torques}$$

$$+\sum \tau_{ex} \qquad \text{due to external torques}$$

Rewriting equation (4.6) yields

$$\phi_n\,\dot{\omega}_n = -\left(\omega_n\otimes\right)\phi_n\,\omega_n + D_n\left[\sum\left(D_n^{-1}\rho_{n_k}\right)\otimes F_{n_k} + \sum\left(D_n^{-1}r_{n_j}\right)\otimes f_{n_j}\right.$$
$$\left.+\sum \tau_{cons} + \sum \tau_{ex}\right]$$

$$(4.7)$$

4.2 CONNECTIVITY

The connectivity of the model is described by a joint vector (array) JNT(j) which is interpreted as joint j connects segment JNT(j) to segment j+1. The use of this joint array limits the model to a "tree structure", Figure 4.3. That is, no closed paths can be found which leave a segment via a joint and return to the same segment through another joint. This also requires that a numbering system be used in which joint j is associated with segment j+1. This imposes no constraint on the tree structure.

The program is so written that JNT(j) may be zero, defining a null joint. This results in the capability of defining sets of disjoint segments. Segment 1 is always taken as a reference segment. For each joint j where JNT(j)=0 segment j+1 is the reference segment. For each such set of segments the identifying numbers must be sequential. The lowest numbered segment in each set is used as the reference. An example of this is the following:

(1,2,3) (4) (5,6,7,8,9,10,11,12,13)

where JNT(3) and JNT(4) are zero. Thus segments 1,2,3 would be treated as one set of connected rigid bodies with segment 1 as a reference. Segment 4 would be an isolated segment with 4 as a reference. Segments 5 through 13 would be treated as a connected set with segment 5 as a reference.

The integrator integrates for the linear motion of the reference segments only. The linear position and velocities of the other segments are determined by use of a chain algorithm (subroutine CHAIN.)
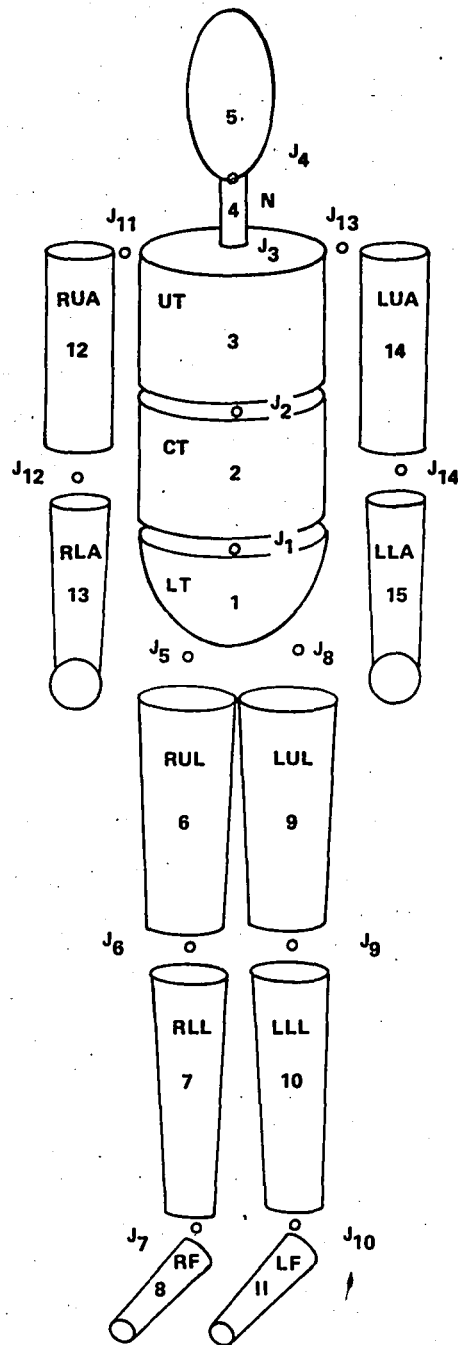
JOINT J CONNECTS SEGMENT JNT(J) WITH SEGMENT J+1

JNT(i) = 1 2 3 4 1 6 7 1 9 10 3 12 3 14
    i   = 1 2 3 4 5 6 7 8 9 10 11 12 13 14

Figure 4.3 EXAMPLE TREE STRUCTURE FOR FIFTEEN SEGMENT MAN

4.3   <u>CONSTRAINT EQUATIONS</u>

Derivation of the additional equations required for solution of the system equations is presented in this section. The first two are constraints at the joints and arise from model considerations. For instance, at a joint the segments must have a point in common (linear position constraint) also the type of joints specified such as free, pinned, or locked require constraint equations (joint angular position constraint). The third equation pertains to other more general types of constraints such as a fixed distance between points on segments, or sliding or rolling motion of one segment over another segment or over a vehicle surface.

The general procedure for applying a constraint between segments m and n is to introduce a constraint force q into the system of equations as:

$$M_m \ddot{X}_m - \sum_j f_{m_j} + Pq = u_{1_m}$$

$$M_n \ddot{X}_n - \sum_k f_{n_k} - Pq = u_{1_n}$$

$$\phi_m \dot{\omega}_m - \sum_j \left(D_m^{-1} r_{m_j} \right) \otimes f_{m_j} + \left(\ell_m + r_m \right) \otimes D_m \, Pq = u_{2m}$$

$$\phi_n \dot{\omega}_n - \sum_k \left(D_n^{-1} r_{n_k} \right) \otimes f_{n_k} - \left(\ell_n + r_n \right) \otimes D_n \, Pq = u_{2n} \tag{4.8}$$

where the matrix*P depends on the type of constraint and q is determined by adding a constraint equation to the system of equations. The constraint equations are derived in following sections.

*Note: In all cases P may be taken as the identity matrix or it may be chosen to impose symmetry of the equations where this is possible. These equations, along with the constraint equations, are referred to as the system equations.

4.3.1   Linear Position Constraint

Consider the joint j connecting segment n=JNT(j) to segment
m=j+1. Because it is assumed that the joint does not separate, the following
expression

$$X_n + D_n^{-1} r_{nj} = X_m + D_m^{-1} r_{mj} \qquad (4.9)$$

holds for each joint. These equations can be used to calculate X_n the
position of segment n, if D_n, D_m and X_m are known. Differentiating equa-
tion (4.9) results in

$$\dot{X}_n + D_n^{-1}\left(\omega_n \otimes r_{nj}\right) = \dot{X}_m + D_m^{-1}\left(\omega \otimes r_{mj}\right) \qquad (4.10)$$

noting that r_{nj} and r_{mj} are constant in their local reference system. Differ-
entiating equation (4.10) results in

$$\ddot{X}_n + D_n^{-1}\left[\dot{\omega}_n \otimes r_{nj} + \omega_n \otimes (\omega_n \otimes r_{nj})\right] = \ddot{X}_m + D_m^{-1}\left[\dot{\omega}_m \otimes r_{mj} + \omega_m \otimes (\omega_m \otimes r_{mj})\right] \qquad (4.11)$$

which relates the accelerations. Rearranging yields.

$$\ddot{X}_n - \ddot{X}_m - D_n^{-1}\left(r_{nj} \otimes \dot{\omega}_n\right) + D_m^{-1}\left(r_{mj} \otimes \dot{\omega}_m\right) = D_m^{-1}\left[\omega_m \otimes \left(\omega_m \otimes r_{mj}\right)\right] - D_n^{-1}\left[\omega_n \otimes (\omega_n \otimes r_{nj})\right] \qquad (4.12)$$

Equation (4.12) is the linear joint position constraint
equation

4.3.2   Angular Joint Constraint

Again consider joint j connecting segments n=JNT(j) and
m=j+1. The free body method of describing the motion of connected rigid
bodies require specification of the constraint torque at the joint. The
particular equation defining this torque depends on the type of joint con-
sidered.

Consider the following two cases:

CASE 1 Locked Joint

The relative angular position remains constant thus the direction cosine matrices satisfy the equation

$$C = D_m D_n^{-1}$$

(4.13)

where C is a constant matrix.

Rearranging $D_m^{-1} C = D_n^{-1}$

Differentiating; $D_m^{-1} \left(\omega_n \otimes \right) C = D_n^{-1} \left(\omega_n \otimes \right)$

eliminating C yields $D_m^{-1} \left(\omega_m \otimes \right) D_m = D_n^{-1} \left(\omega_n \otimes \right) D_n$

which implies

$D_m^{-1} \omega_m = D_n^{-1} \omega_n$ as the velocity constraint.

Differentiating and rearranging yields the acceleration constraint as:

$$D_n^{-1} \dot{\omega}_n - D^{-1} \dot{\omega}_m = 0$$

(4.14)

CASE 2 Pinned Joint

The segments are constrained to rotate about some pin axis which is fixed relative to each segment. Let h_m, h_n be unit vectors defining the pin axis in their respective coordinate systems. Then the position constraint is

$$D_m^{-1} h_m = D_n^{-1} h_n = h$$

(4.15)

72

where h_m and h_n are constant and h is the pin axis in inertial reference.

Differentiating yields the velocity constraint

$$D_n^{-1}(\omega_n \otimes)h_n = D_m^{-1}(\omega_m \otimes)h_m$$

or

$$D_n^{-1}(\omega_n \otimes h_n) = D_m^{-1}(\omega_m \otimes h_m)$$

(Note: when the matrix $\omega \otimes$ operates on a vector, it is equivalent to the vector cross product $i.e.\ (\omega \otimes)h = \omega \otimes h$.) This velocity constraint may be interpreted as specifying that the components of angular velocity perpendicular to the pin must be equal. That is

or

$$D_n^{-1}(\omega_n - h_n(h_n \cdot \omega_n)) = D_m^{-1}(\omega_m - h_m(h_m \cdot \omega_m))$$

$$(I - hh\cdot)\ D_n^{-1}\omega_n = (I - hh\cdot)D_m^{-1}\omega_m$$

(Note: h is a column vector, h· is h transpose [a row vector], hh· is a square matrix.)

Differentiating again yields the acceleration constraint

$$D_n^{-1}\dot{\omega}_n \otimes h_n + D_n^{-1}\omega_n \otimes (\omega_n \otimes h_n) = D_m^{-1}\dot{\omega}_m \otimes h_m + D_m^{-1}\omega_m \otimes (\omega_m \otimes h_m)$$

which may be written as

$$h \otimes \left[D_n^{-1}\dot{\omega}_n - D_m^{-1}\dot{\omega}_m\right] = D_n^{-1}\omega_n \otimes (\omega_n \otimes h_n) - D_m^{-1}\omega_m \otimes (\omega_m \otimes h_m)$$

Taking the dot product with h yields

$$0 = h \cdot \left[D_n^{-1}\omega_n \otimes (\omega_n \otimes h_n) - D_m^{-1}(\omega_m \otimes \omega_m \otimes h_m m)\right]$$

$$= (\omega_n \cdot h_n)^2 - \omega_n \cdot \omega_n - (\omega_m \cdot h_m)^2 + \omega_m \cdot \omega_m$$

which may be written as

$$\omega_n \cdot \omega_n - (\omega_n \cdot h_n)^2 = \omega_m \cdot \omega_m - (\omega_m \cdot h_m)^2$$

This is satisfied if the velocity constraint is satisfied.

Taking the cross product with h yields

$$-h \otimes \left[h \otimes (D_n^{-1}\dot{\omega}_n - D_m^{-1}\dot{\omega}_m)\right] = \omega_n \cdot h_n\ D_n^{-1}\omega_n \otimes h_n - \omega_m \cdot h_m\ D_m^{-1}\omega_m \otimes h_m$$

which may be written as

$$(I - hh\cdot)(D_n^{-1}\dot{\omega}_n - D_m^{-1}\dot{\omega}_m) = \omega_n \cdot h_n\ D_n^{-1}\omega_n \otimes h_n - \omega_m \cdot h_m\ D_m^{-1}\omega_m \otimes h_m$$

(Note: that we have used the matrix identity $I - \tilde{h}\tilde{h}\cdot = -h_\otimes\, h_\otimes$ which is valid when h is a unit vector.) In addition, we must impose the condition that the constraining torque have no component on the pin axis, that is

$$h \cdot t = 0$$

This may be put in matrix form as $\tilde{h}\tilde{h}\cdot t = 0$ and added to the above constraint on accelerations to produce a single constraint equation for a pinned joint as

$$\left(I - \tilde{h}\tilde{h}\cdot \right)\left(D_n^{-1}\dot{\omega}_n - D_m^{-1}\dot{\omega}_m \right) + \lambda\, \tilde{h}\tilde{h}\cdot t = \left(\omega_n \cdot h_n^- \omega_{n}^{\doteq} h_m \right) D_n^{-1}\omega_n \otimes h_n$$

$$(4.16)$$

where λ is an arbitrary scalar $(\lambda \neq 0)$

We note that since $\left(I - \tilde{h}\tilde{h}\cdot \right) t = t$ the original system equations may be written as

$$\phi_n\, \dot{\omega}_n + D_n\!\left(I - \tilde{h}\tilde{h}\cdot \right) t = u_{2_n}$$

$$\phi_m\, \dot{\omega}_m - D_m\!\left(I - \tilde{h}\tilde{h}\cdot \right) t = u_{2_m}$$

$$(4.17)$$

This form has the advantage of making the system matrix symmetrical.

4.3.4   <u>Additional Constraint Relationships</u>

In addition to the joint constraints developed in Section 4.3.3, other relationships are derived in this section for two types of distance constraints, a rolling constraint and a sliding constraint.

TYPE 1

The zero distance constraint requires a point on a segment be the same as a point on another segment, as indicated in Figure (4.4). In general, consider two segments m and n such that r_m locates a point in segment m relative to its own c.g. and r_n locates a point in segment n relative to its own c.g. The zero distance constraint equation then is written as:

$$X_m + D_m^{-1} r_m = X_n + D_n^{-1} r_n \qquad (4.18)$$

X_m, X_n locates the c.g of segments m and n w.r.t an inertial reference system.

Twice differentiating this equation yields the constraint equation

$$\ddot{X}_m - \ddot{X}_n - D_m^{-1} r_m \otimes \dot{w}_m + D_n^{-1} r_n \otimes \dot{w}_n = V_{3_n} \qquad (4.19)$$

where

$$V_{3_n} = D_n^{-1} \left[\omega_n \otimes \left(\omega_n \otimes r_n \right) \right] - D_m^{-1} \left[w_m \otimes \left(\omega_m \otimes r_m \right) \right]$$

TYPE II   Fixed Distance Constraint

The fixed distance constraint allows a specified point on one segment to be a fixed (constant) distance from a specified point on another segment, as illustrated in Figure (4.5).   Consider   two segments m and n such that r_m locates a point in segment m and r_n locates a point in segment n . Also define ρ to be a fixed distance vector between these two points. The constraint equation is written simply as

$$\rho \cdot \rho = d^2 = |\rho|^2 \qquad (4.20)$$

where

$$\rho = X_m + D_m^{-1} r_m - X_n - D_n^{-1} r_n \qquad (4.21)$$

Twice differentiating eqn (4.20) yields

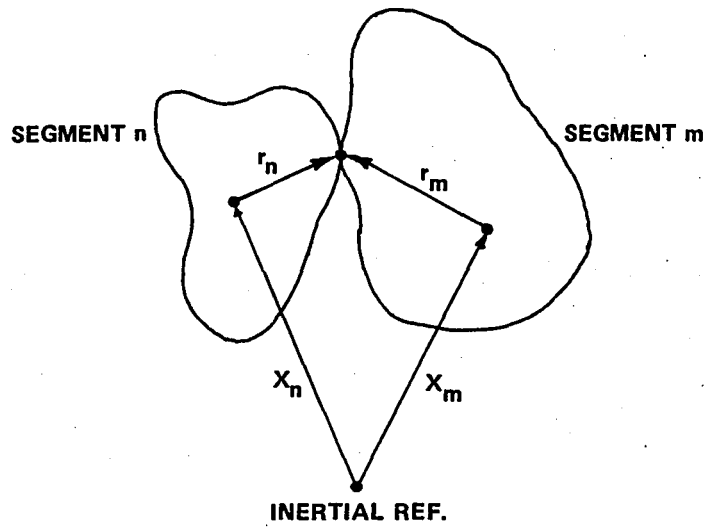$$\ddot{\rho} \cdot \rho + |\dot{\rho}|^2 = 0$$
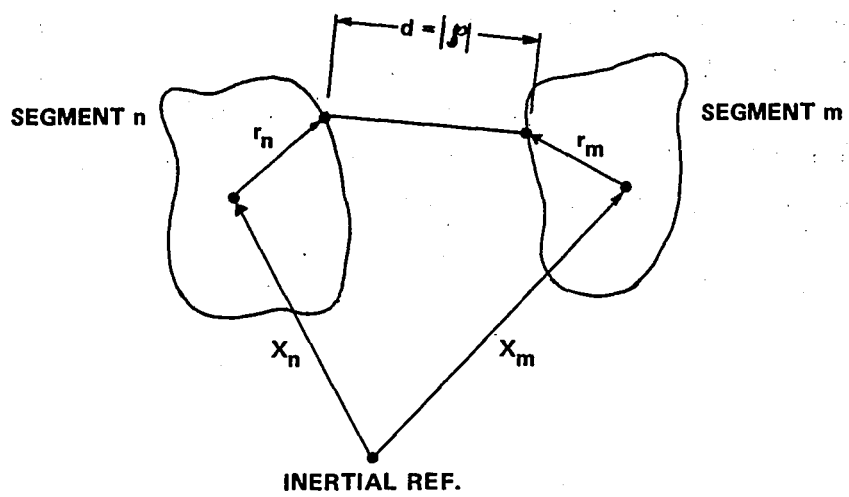
where

75

Figure 4.4   ZERO DISTANCE CONSTRAINT

Figure 4.5   FIXED DISTANCE CONSTRAINT

76

$$\ddot{\rho} = \ddot{X}_m + D_m^{-1}\left[\dot{\omega}_m \otimes r_m + \omega_m \otimes \left(\omega_m \otimes r_m\right)\right]$$
$$-\ddot{X}_n - D_n^{-1}\left[\dot{\omega}_n \otimes r_n + \omega_n \otimes \left(\omega_n \otimes r_n\right)\right]$$

$$(4.22)$$

rearranging $\quad \ddot{X}_m - \ddot{X}_n + D_m^{-1}\left[\dot{\omega}_m \otimes r_m\right] - D_n^{-1}\left[\dot{\omega}_n \otimes r_n\right]$

$$= \ddot{\rho} + D_n^{-1}\left[\omega_n \otimes \left(\omega_n \otimes r_n\right)\right] - D_m^{-1}\left[\omega_m \otimes \left(\omega_m \otimes r_m\right)\right] \quad (4.23)$$

For the distance constraint the constraint force q must be directed along ρ . Define then a unit vector h in the direction of ρ .

$$h = \frac{\rho}{|\rho|} = \frac{X_m + D_m^{-1} r_m - X_n - D_n^{-1} r_n}{\left|X_m + D_m^{-1} r_m - X_n - D_n^{-1} r_n\right|}$$

$$(4.24)$$

Although only the magnitude of the constraint force q need be computed, for purposes of symmetry and computation logic the vector nature of the constraint equation is maintained.

For this reason the constraint force is defined along h by $h \cdot q$, then maintained as a vector by $h(h \cdot q)$. The same procedure is performed on the constraint relation yielding the following:

$$h\left\{h \cdot \left[\ddot{X}_m - \ddot{X}_n + D_m^{-1}\left[\dot{\omega}_m \otimes r_m\right] - D_n^{-1}\left[\dot{\omega}_n \otimes r_n\right]\right]\right.$$

$$+ \lambda(I - h h \cdot) q = h\left\{h \cdot \left[D_n^{-1}\omega_n \otimes \left(\omega_n \otimes r_n\right) - D_m^{-1}\omega_m \otimes \left(\omega_m \otimes r_m\right)\right] - \frac{|\dot{\rho}|^2}{d}\right\} (4.25)$$

λ is an arbitrary scalar $\neq 0$.

TYPE III & IV   Rolling and Sliding Constraints

These constraints provide the capability of modeling the motion of surfaces which are rolling or sliding over each other. A diagram of the geometrical configuration and appropriate variable definition is presented in Figure 4.6. The relationship at the point of contact is

$$X_m + D_m^{-1}(l_m + r_m) = X_n + D_n^{-1}(l_n + r_n) \tag{4.26}$$

The time derivative of this expression is

$$\dot{X}_m + D_m^{-1}\omega_m \otimes (l_m + r_m) + D_m^{-1}r_m' = \dot{X}_n + D_n^{-1}\omega_n \otimes (l_n + r_n) + D_n^{-1}r_n' \qquad *$$

$$\tag{4.27}$$

The relative velocity of the surfaces at the point of contact is

$$V_{REL} = \dot{X}_m + D_m^{-1}\omega_m \otimes (l_m + r_m) - \dot{X}_n - D_n^{-1}\omega_n \otimes (l_n + r_n) \tag{4.28}$$

The rolling constraint requires that the relative velocity be zero and the
sliding constraint requires that the normal component of the relative
velocity be zero. Thus

$$V_{REL} = 0 \quad \text{for roll}$$
$$t \cdot V_{REL} = 0 \quad \text{for slide} \tag{4.29}$$

We have from (4.27) and (4.28)

$$V_{REL} + D_m^{-1}r_m' = D_n^{-1}r_n' \tag{4.30}$$

Note that for the rolling constraint, Equation (4.30) requires that $D_m^{-1}r_m' = D_n^{-1}r_n'$

---

* Note: The prime on r_m and r_n, indicates the time derivative of the respective
variables in its local reference system.

SEGMENT m

SEGMENT n

c.g.

ℓ_m

r_m

t

q

r_n

X_m

c.g.

ℓ_n

X_n
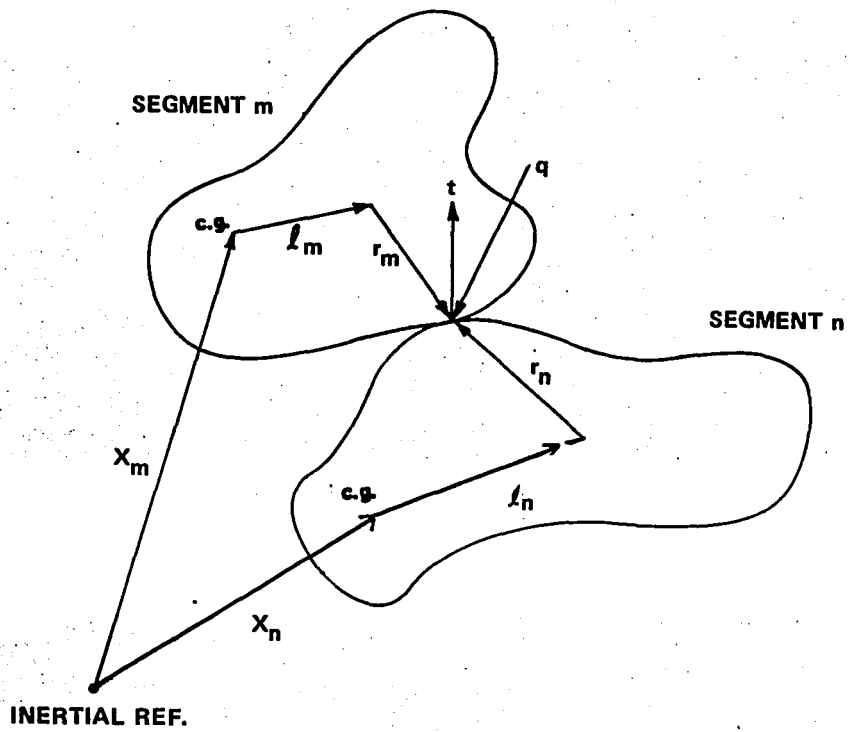
INERTIAL REF.

X_m, X_n INERTIAL REF. POSITION OF c.g. FOR SEGMENTS m AND n.

ℓ_m, ℓ_n OFFSET OF SURFACE m AND n FROM c.g.

r_m, r_n VECTOR TO POINT OF CONTACT EACH IN ITS OWN LOCAL REFERENCE FRAME.

t NORMAL TO SURFACE AT POINT OF CONTACT.

q CONSTRAINT FORCE

Figure 4.6   GEOMETRY FOR GENERAL ROLLING CONSTRAINT

79

The distinction between rolling and sliding is made by computing the force required to impose a rolling constraint. The magnitude of the tangential component of this force is compared to the magnitude of the normal component times a specified friction coefficient.

Thus, $|\mathcal{G}_t|$ (tangential force) is compared to $\beta_s|\mathcal{G}_n|$ where β_s is the static friction coefficient and $|\mathcal{G}_n|$ is the normal component of the constraint force.

If $|\mathcal{G}_t| \leq \beta_s|\mathcal{G}_n|$ then the surface characteristics will sustain a roll. If $|\mathcal{G}_t| > \beta_s|\mathcal{G}_n|$ sliding will occur.

When sliding occurs the direction of the constraint force is along the vector h where

$$ h = \left(t - \rho \frac{V}{|V|} \right) / \sqrt{1 + \rho^2} $$

(4.31)

where t is the normal vector, ρ is the coefficient of sliding friction and V is the tangential component of the relative velocity which will be equal to V_{REL} for a true slide (since $t \cdot V_{REL} = 0$.)

The constraint equation in acceleration form are found by differentiating equation (4.29). They are:
for rolling;

$$ \ddot{X}_m - D_m^{-1}(\ell_m + r_m) \otimes \dot{\omega}_m - \ddot{X}_n + D_n^{-1}(\ell_n + r_n) \otimes \dot{\omega}_n = D_n^{-1}(\omega_n \otimes (\omega_n \otimes (\ell_n + r_n))) - D_m^{-1}\omega_m \otimes (\omega_m \otimes (\ell_m + r_m)) + D_n^{-1}\omega_n \otimes r_n' - D_m^{-1}\omega_m \otimes r_m' $$

and for sliding;

(4.32)

$$ t \cdot \left[\ddot{X}_m - D_m^{-1}(\ell_m + r_m) \otimes \dot{\omega}_m - \ddot{X}_n + D_n^{-1}((\ell_n + r_n) \otimes \dot{\omega}_n) \right] = t \cdot \left[D_n^{-1}(\omega_n \otimes (\omega_n \otimes (\ell_n + r_n))) \right. $$

$$ \left. - D_m^{-1}\omega_m \otimes (\omega_m \otimes (\ell_m + r_m)) + D_n^{-1}\omega_n \otimes r_n' - D_m^{-1}\omega_m \otimes r_m' \right] - t \cdot \left(D_n^{-1}r_n' - D_m^{-1}r_m' \right) $$

(4.33)

30

and $(I - hh \cdot) \dot{q} = 0$, where $\dot{t}$ is the time derivative of t

The two equations for the sliding constraint may be combined into one matrix equation as

$$h t \cdot \left[\ddot{X}_m - D_m^{-1} (\ell_m + r_m) \otimes \dot{\omega}_m - \ddot{X}_n + D_n^{-1} (\ell_n + r_n) \otimes \dot{\omega}_n \right] + \lambda \, (I - hh) \dot{q}$$

$$= h t \cdot \left[D_n^{-1} \omega_n \otimes \left(\omega_n \otimes (\ell_n + r_n) \right) - D_m^{-1} \left(\omega_m \otimes \left(\omega_m \otimes (\ell_m + r_m) \right) \right) \right.$$

$$\left. + D_n^{-1} \omega_n \otimes r_n' - D_m^{-1} \omega_m \otimes r_m' \right] - h \dot{t} \cdot \left(D_n^{-1} r_n' - D_m^{-1} r_m' \right) \qquad (4.34)$$

The right hand side of these constraint equations contains the unknowns $\dot{t}$, r_n' and r_m' which depend on the kinematics and the geometric properties of the surfaces.

The contact routines normally will compute the point of contact which yields r_m, r_n and the vectors t and h.

In the program when a roll-slide constraint is specified, no force deflection characteristic is specified but the impulse option should be used to insure that the normal component of relative velocity is reduced to zero. That is one should specify the impulse option with a coefficient of restitution equal to zero. This will insure that $t \cdot V_{REL} = 0$ at the instant of first contact.

Calculation of r'_m, r'_n, $\dot{t}$ in the Program

The current version of the program considers ellipsoid-plane (Subroutine PLELP) and ellipsoid-ellipsoid (Subroutine SEGSEG) contacts. Since the calculations of $\dot{t}, r'_m$ and r'_n are similar the equations will be derived together.

The equation of the ellipsoids are

$$r_m \cdot A_m \, r_m = 1$$
$$r_n \cdot A_n \, r_n = 1$$

and the equation of the plane is

$$r_n \cdot t_n = \gamma$$

where A_m, A_n are the ellipsoid matrices, constant in the local coordinate systems and t_n is the normal to the plane, a constant in the local coordinate system.

For the ellipsoid plane contact we have (Figure 4.7)

$$D_m^{-1} \frac{A_m \, r_m}{|A_m \, r_m|} = -t = -D_n^{-1} t_n \qquad (4.35)$$

For the exterior ellipsoid-ellipsoid contact we have (Figure 4.8)

$$D_m^{-1} \frac{A_m \, r_m}{|A_m \, r_m|} = -t = -D_n^{-1} \frac{A_n \, r_n}{|A_n \, r_n|}$$

For the interior ellipsoid-ellipsoid contact (the exterior of ellipsoid A_m contacts the interior of ellipsoid A_n)we have (not illustrated)

$$D_m^{-1} \frac{A_m \, r_m}{|A_m \, r_m|} = -t = D_n^{-1} \frac{A_n \, r_n}{|A_n \, r_n|}$$

For convenience we define (for ellipsoids)

$$t_m = -\frac{A_m \, r_m}{|A_m \, r_m|} \quad , \quad t_n = \pm \frac{A_n \, r_n}{|A_n \, r_n|}$$

Note $\quad t = D_m^{-1} t_m = D_n^{-1} t_n$
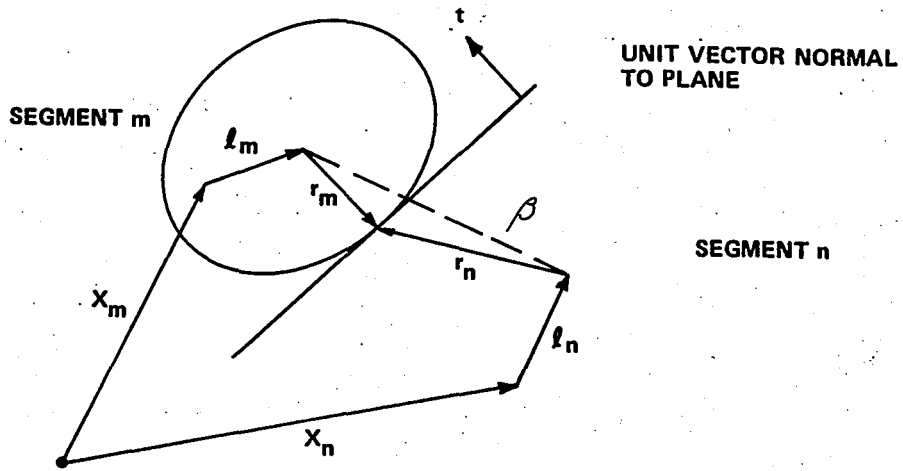
82

Figure 4.7   ELLIPSOID ROLLING (OR SLIDING) OVER A PLANE
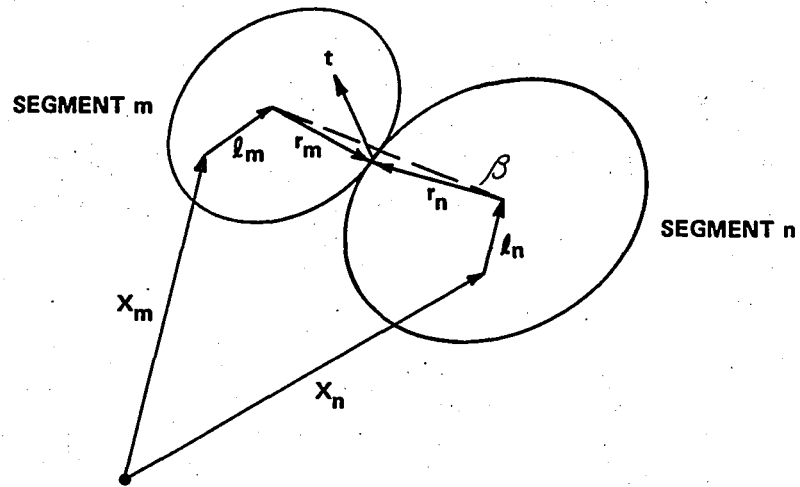
Figure 4.8   ELLIPSOID ROLLING (OR SLIDING) OVER AN ELLIPSOID

Differentiating the equations of the ellipsoids and planes yields

$$r_m' \cdot t_m = 0 \quad,$$

$$r_n' \cdot t_n = 0 \qquad also \quad t \cdot \dot{t} = 0 \quad.$$

Differentiating the ellipsoid plane normal equation

$$D_m^{-1}\, \omega_m \otimes \frac{A_m\, r_m}{|A_m\, r_m|} + D_m^{-1} \left[\frac{A_m\, r_m'}{|A_m\, r_m|} - A_m\, r_m\, \frac{A_m\, r_m \cdot A_m\, r_m'}{|A_m\, r_m|^3} \right] = -\dot{t} = -D_n^{-1}\, \omega_n \otimes t_n$$

which may be written as

$$-D_m^{-1}\, \omega_m \otimes t_m + D_m^{-1} \left[I - t_m\, t_m \cdot \right] \frac{A_m\, r_m'}{|A_m\, r_m|} = -\dot{t} = -D_n\, \omega_n \otimes t_n$$

Differentiating the exterior ellipsoid-ellipsoid equation

$$-D_m^{-1}\, \omega_m \otimes t_m + D_m^{-1} \left[I - t_m t_m \right] \frac{A_m\, r_m'}{|A_m\, r_m|} = -\dot{t} = -D_n^{-1}\, \omega_n \otimes t_n - D_n^{-1} \left(I - t_n t_n \cdot \right) \frac{A_n\, r_n}{|A_n\, r_n|}$$

Differentiating the interior ellipsoid-ellipsoid equations yields

$$-D_m^{-1}\, \omega_m \otimes t_m + D_m^{-1} \left[I - t_m\, t_m \right] \frac{A_m\, r_m'}{|A_m\, r_m|} = -\dot{t} = -D_n^{-1}\, \omega_n \otimes t_n + D_n^{-1} \left(I - t_n\, t_n \cdot \right) \frac{A_n\, r_n'}{|A_n\, r_n|}$$

If we add the relation

$$V_{REL} + D_m^{-1}\, r_m' = D_n^{-1}\, r_n'$$

to the above equation we have a sufficient number of equations to solve for $\dot{t}, r_m', r_n'$. These may be summarized as follows:

$$\begin{bmatrix} E & 0 & D_m \\ 0 & F & -D_n \\ D_m^{-1} & -D_n^{-1} & 0 \end{bmatrix} \begin{bmatrix} r_m' \\ r_n' \\ \dot{t} \end{bmatrix} \begin{bmatrix} \omega_m \otimes t_m \\ -\omega_n \otimes t_n \\ -V_{REL} \end{bmatrix} \tag{4.36}$$

84

where $E = \left[I - t_m\, t_m \cdot \right] \dfrac{A_m}{|A_m\, r_m|} + \lambda\ t_m t_m \cdot$

and

$$F = 0 \qquad \text{for plane}$$

$$F = \pm\ (I - t_n\, t_n \cdot) \dfrac{A_n}{|A_n\, r_n|} \qquad \text{for ellipsoid } n,\ +\ \text{ external contact}$$

$$\text{— internal contact}$$

λ is an arbitrary constant chosen such that the matrix is nonsingular (in practice $\lambda \sim \dfrac{1}{|r_m|}$).

The solution may be written in the form

$$D_n^{-1}\, r_n' = C^{-1} W - C^{-1} t\ \frac{t \cdot C^{-1} W}{t \cdot C^{-1} t}$$

$$D_m^{-1}\, r_m' = D_n^{-1}\, r_n' - V_{REL}$$

$$\dot{t} = D_n^{-1} \left[\omega_n \otimes t_n + F\, r_n' \right] \tag{4.37}$$

where

$$W = D_m^{-1}\, \omega_m \otimes t_m - D_n^{-1}\, \omega_n \otimes t_n + D_m^{-1}\, A_m\, D_m\, V_{REL} \Big/ (|\, A_m\, r_m|)$$

for the ellipsoid-ellipsoid contact

$$C = D_m^{-1}\, A_m\, D_m \Big/ |\, A_m\, r_m| + D_n^{-1}\, A_n\, D_n \Big/ (\pm|\, A_n\, r_n|) \tag{4.38}$$

and for the ellipsoid — plane contact

$$C = D_m^{-1}\, A_m\, D_m \Big/ |\, A_m\, r_m| \tag{4.39}$$

4.4   TENSION ELEMENT

4.4.1   Specifications

The primary purpose of the tension element (TE) is the simulation of the longitudinal muscles of the human body. It behaves statically in a manner simular to a linear spring in that when it is subjected to a tension force $\overline{F}$, it increases in length by an amount proportional to $\overline{F}$. However, in contrast to a spring, the TE displays no stiffness when subjected to a compression force. In this respect it is similar to a longitudinal body muscle.

The TE has been designed so that, under the action of rapidly varying tension forces, the distribution of strains within the element is uniquely defined by the strains at the two ends of the element. As a consequence, the equations of motion of the element are simplified: they depend only on the positions, velocities, and accelerations of the two ends of the element.

The computer program inputs required for complete specification of the TE are denoted by L_o, M_A, M_B, M_{AB}, k, d . These quantities are defined in the following discussion.

Figure 4.9 depicts the geometry of the TE when subjected to a static tension $\vec{F}$
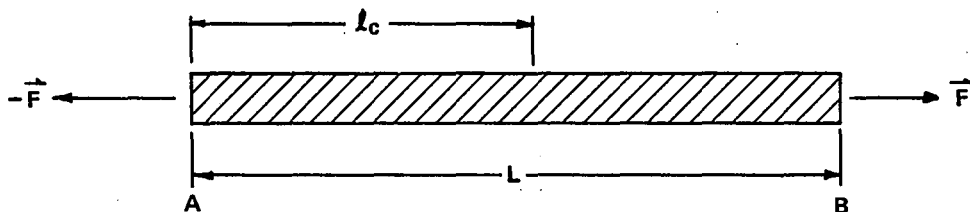
Figure 4.9   TENSION ELEMENT GEOMETRY

The two ends of the element are denoted by A and B. In connection with Figure 4.9 quantities are defined as follows:

L = length of TE when subjected to a tension force

ℓ_c = distance from the end A to the center of mass of the TE

L_o = length of TE when the tension force $\vec{F}$ is infinitesimal.

ℓ = the value of ℓ_c when the tension force $\vec{F}$ is infinitesimal.

The cross section of the TE is treated as negligible. Thus, the moment of inertia about its long axis is negligible. The inertial properties of the element are completely determined by the quantities L and ℓ defined above, and the quantities M_T and ϕ_A defined as follows:

M_T = total mass of TE

ϕ_A, ϕ_B = moment of inertia of TE about the point A,B and about an axis perpendicular to the long axis of the element when the tension force $\vec{F}$ is negligible.

In terms of the quantities L, L_o, M_T and ϕ_A, the quantities M_A and M_B and M_{AB} are given by

$$M_B = \phi_A / L_o^2 \qquad (4.40)$$

$$M_A = \phi_B / L_o^2 \qquad (4.41)$$

$$M_{AB} = \frac{1}{2} \left(M_T - M_A - M_B \right) \qquad (4.42)$$

The computer program input, k, is a force constant given by

$$k = \frac{|\vec{F}|}{(L - L_o)} \qquad (4.43)$$

Where F denotes the magnitude of the static tension force $\vec{F}$. The quantities $\vec{F}$, L and L_o are defined above.

To define the program input, d, it is noted that when the TE is <u>not</u> in static equilibrium, the tension force, $\vec{F}$, can be expressed as the sum of the force of inertia, the force of stiffness, and the force of viscosity (or dissipation.) The parameter d is a constant of dissipation defined by the relation

$$\vec{F}_{dissipation} = d\dot{L}$$

Where $\vec{F}_{dissipation}$ denotes the force of dissipation and $\dot{L}$ denotes the time rate of change of the length, L, of the TE.

4.4.2   <u>Derivation</u>

Represent the TE by the discrete system depicted in Figure 4.10
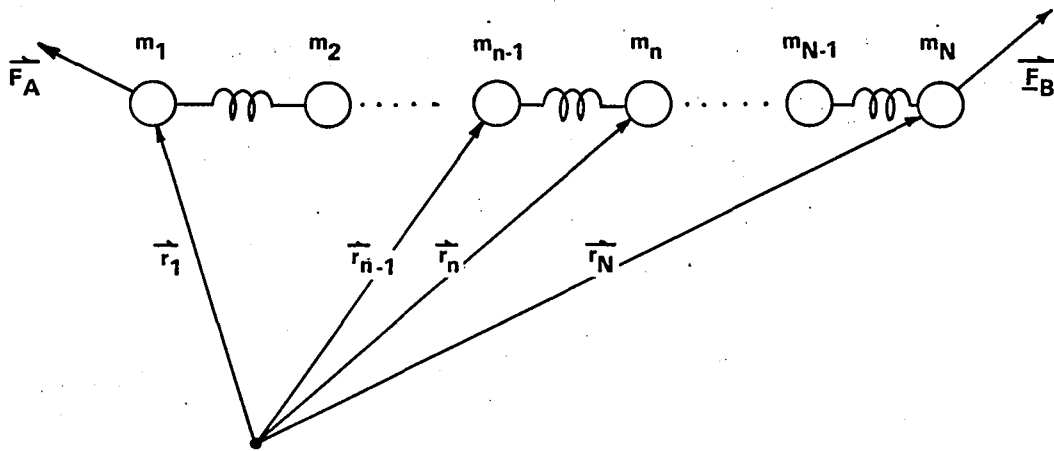
Figure 4.10   TENSION ELEMENT MODEL

88

As shown, the discrete system is composed of N particles connected by N-1 springs. The mass of the Nth particle is denoted by m_n. The position vector of the Nth particle relative to the inertial coordinate system is denoted by $\vec{r}_n$, $\vec{F}_A$ and $\vec{F}_B$ denote external forces applied to the first and Nth particles respectively. Since the element cannot support externally applied torques, it must be coupled to other elements in such a way that it will not be subjected to external torques (or force couples.)

The springs can exert forces of tension when stretched but they cannot exert forces of compression. Each spring has viscous damping.

The TE is subject to constraints (not shown in Figure 4.10) which insures that all of the particles lie on a straight line (regardless of the directions of the applied forces $\vec{F}_A$ and $\vec{F}_B$) and that the strains and relative motions within the element are uniquely determined by the positions and motions of the two ends of the element. The constraint relations are:

$$\left(\vec{r}_n - \vec{r}_1 \right) = \xi_n \left(\vec{r}_N - \vec{r}_1 \right) \tag{4.44}$$

Where the ξ_n are constants which satisfy

$$0 = \xi_1 < \xi_n < \xi_{n+1} \leq \xi_N = 1 \tag{4.45}$$
$$n = 2, N-1$$

Putting
$$\vec{r}_1 = \vec{r}_A$$
$$\vec{r}_N = \vec{r}_B$$

Equation 4.44 may be re-expressed

$$\vec{r}_n = \left(1 - \xi_n \right) \vec{r}_A + \xi_n \vec{r}_B \tag{4.46}$$

The equation of motion of the TE will be obtained by the D'Alembert method. That is, the equations will be expressed first for motion in the absence of the constraints, then the modified equations, which take account of the constraints, can be inferred.

The equations of motion in the absence of the constraints in (4.46) are

$$\frac{d}{dt}\left(\frac{\partial T}{\partial \dot{\vec{r}}_n}\right) - \frac{\partial T}{\partial \vec{r}_n} + \frac{\partial V}{\partial \vec{r}_n} + \frac{\partial D}{\partial \dot{\vec{r}}_n} = \vec{F}_A \, \delta_{n_I} + \vec{F}_B \, \delta_{n_N}.$$

$$(4.47)$$

*

Where T, V, D denote, respectively, the total kinetic energy, total potential energy, and Rayleigh Dissipation Function for the system depicted in Figure 4.16. T, V, and D are expressed as functions of the coordinates $\vec{r}_n$ and velocities $\dot{\vec{r}}_n$ of the particles. In (4.47) $\partial/\partial \vec{r}_n$ denotes the gradient with respect to the components of $\vec{r}_n$.

To obtain the equations of motion which include the constraints, T, V, and D are re-expressed as functions of $\vec{r}_A, \dot{\vec{r}}_A, \vec{r}_B \, \dot{\vec{r}}_B$ by direct substitution, employing the constraint relations in (4.46). The equations of motion can then be expressing

$$\frac{d}{dt}\left(\frac{\partial T}{\partial \dot{\vec{r}}_A}\right) - \frac{\partial T}{\partial \vec{r}_A} + \frac{\partial V}{\partial \vec{r}_A} + \frac{\partial D}{\partial \dot{\vec{r}}_A} = \vec{\tau}_A$$

$$\frac{d}{dt}\left(\frac{\partial T}{\partial \dot{\vec{r}}_B}\right) - \frac{\partial T}{\partial \vec{r}_B} + \frac{\partial V}{\partial \vec{r}_B} + \frac{\partial D}{\partial \dot{\vec{r}}_B} = \vec{\tau}_B \qquad (4.48)$$

where

$$\vec{\tau}_A = \sum_{n=1}^{d} \frac{\partial \vec{r}_n}{\partial \vec{r}_A} \cdot \left(\vec{F}_A \, \delta_{n_I} + \vec{F}_B \, \delta_{n_N}\right)$$

---

*Since we are working in 3 space it seems simpler to write equations (4.47), (4.48) and (4.49) in a vector form where each equation represents 3 equations in the more conventional notation where $\vec{r}_n$ would have 3 generalized coordinates $q_{n_1}, q_{n_2}, q_{n_3}$ and $\dot{\vec{r}}_n$ the coordinates $\dot{q}_{n_1}, \dot{q}_{n_2}, \dot{q}_{n_3}$. In this scheme (4.47) would be written as

$$\frac{d}{dt}\left(\frac{\partial T}{\partial \dot{q}_{n_i}}\right) - \frac{\partial T}{\partial q_{n_i}} + \frac{\partial V}{\partial q_{n_i}} + \frac{\partial D}{\partial \dot{q}_{n_i}} = F_{A_i} + F_{B_i} \qquad i = 1,3$$

90

$$\vec{\tau}_B = \sum_{n=1}^{N} \frac{\partial \vec{r}_n}{\partial \vec{r}_B} \cdot \left(\vec{F}_A \, \delta_{n1} + \vec{F}_B \, \delta_{n_N} \right) \qquad (4.49)$$

From Figure 4.10 the total kinetic energy of the system is given by

$$T = \frac{1}{2} \sum_{n=1}^{N} m_n \, |\dot{\vec{r}}_n|^2$$

Substituting from (4.46) and rearranging leads to

$$T = \frac{1}{2} M_A \, |\dot{\vec{r}}_A|^2 + \frac{1}{2} M_B \, |\dot{\vec{r}}_B|^2 + M_{AB} \left(\dot{\vec{r}}_A \cdot \dot{\vec{r}}_B \right)$$

$$(4.50)$$

where

$$M_A = \sum_{n=1}^{N} m_n \left(1 - \xi_n \right)^2$$

$$M_B = \sum_{n=1}^{N} m_n \, \xi_n^2$$

$$M_{AB} = \sum_{n=1}^{N} m_n \, \xi_n \left(1 - \xi_n \right)$$

$$(4.51)$$

The potential energy, V, contributed by the stiffness of the springs may be expressed

$$V = \frac{1}{2} \sum K_n \left(\Delta \ell_n \right)^2 \qquad \Delta \ell_n > 0$$
$$= 0 \qquad\qquad\qquad \Delta \ell_n < 0$$

$$(4.52)$$

Where $\Delta \ell_n$ denotes the relative elongation of the spring connecting the nth and (n+1)th particles, and K_n denotes the corresponding force constant. The second of the relations (4.52) expresses the condition that the springs exert no forces of compression. Evidently,

$$\Delta \ell_n = |\vec{r}_{n+1} - \vec{r}_n| - |\vec{r}_{n+1} - \vec{r}_n|_o \qquad (4.53)$$

Where $|\vec{r}_{n+1} - \vec{r}_n|_o$ denotes the length of the spring connecting the particles n and n+1 when this spring is subjected only to a negligible tension. From

(4.46)

$$\left(\vec{r}_{n+1} - \vec{r}_n\right) = \left(\xi_{n+1} - \xi_n\right)\left(\vec{r}_B - \vec{r}_A\right)$$

(4.54)

and so

$$\Delta \ell_n = \left(\xi_{n+1} - \xi_n\right)\left[\left|\vec{r}_B - \vec{r}_A\right| - L_o\right]$$

(4.55)

Where L_o denotes the overall length of the TE when it is subjected to a negligible static tension.

Substitution of (4.55) into (4.52) leads to

$$V = \tfrac{1}{2} K \left[\left|\vec{r}_B - \vec{r}_A\right| - L_o\right]^2 \qquad \text{if } \left|r_B - r_A\right| > L_o$$

$$V = 0 \qquad\qquad \text{otherwise}$$

(4.56)

Where

$$K = \sum_{n=1}^{N-1} k_n \left(\xi_{n+1} - \xi_n\right)^2$$

(4.57)

The Rayleigh Dissipation Function, D, is equal to half the rate of dissipation of energy resulting from the viscous forces. It is assumed that a dissipation element is connected between each pair of particles.

Thus,

$$D = \tfrac{1}{2} \sum_{n=1}^{N-1} d_n \left(\Delta \dot{\ell}_n\right)^2$$

(4.58)

Where d_n denotes the dissipation coefficient for the dissipative element between the nth and (n+1) the particles and $\Delta \ell_n$ is defined in (4.55). Substituting (4.55) into (4.58), one obtains

$$D = \tfrac{d}{2} \left|\dot{\vec{r}}_B - \dot{\vec{r}}_A\right|^2$$

(4.59)

92

where

$$d = \sum_{n=1}^{N-1} d_n \left(\dot{\xi}_{n+1} - \dot{\xi}_n \right)^2 \tag{4.60}$$

Substitution of the relations (4.50), (4.52), (4.59) and (4.46) into (4.48) and (4.49) yields the equations of motion for the TE:

$$M_A \ddot{\vec{r}}_A + M_{AB} \ddot{\vec{r}}_B - d \left(\dot{\vec{r}}_B - \dot{\vec{r}}_A \right) - \vec{F}_s = \vec{F}_A$$

$$M_B \ddot{\vec{r}}_B + M_{AB} \ddot{\vec{r}}_A + d \left(\dot{\vec{r}}_B - \dot{\vec{r}}_A \right) + \vec{F}_s = \vec{F}_B \tag{4.61}$$

where

$$\vec{F}_s = K \left(\vec{r}_B - \vec{r}_A \right) \left[1 - L_0 / | \vec{r}_B - \vec{r}_A | \right] \qquad \text{if } | r_B - r_A | > L_0$$

$$\vec{F}_s = 0 \qquad\qquad\qquad\qquad \text{otherwise} \tag{4.62}$$

The definitions of the parameters M_A, M_B, M_{AB}, K, d given in the first subsection follows from the equations of motion in (4.61) and the relations in (4.51) and (4.46).

For purposes of implementing the tension element in the framework of the program, let the point r_A be fixed in one rigid segment and let the point r_B be fixed in another rigid segment. Then the following relationships may be written.

$$r_A = X_m + D_m^{-1} r_m$$
$$r_B = X_n + D_n^{-1} r_n$$

where X_m, X_n - location of the c. g. of segments m and n respectively in inertial reference.

r_m - location of point r_A with respect to the c. g. of segment m this is a constant in m's local reference.

93

r_n location of point r_B with respect to the c.g. of segment this is a constant in n's local reference

D_m, D_n are the direction cosine matrices of segment m and segment n

The inputs required for each tension element are

r_m, m, r_n, n and the values of the scalars M_A, M_B, M_{AB}, K, d and L_o

With each tension element are associated the two constraint forces F_A and F_B. Equations 4.61 are the constraint equations. The force $(-F_A)$ and the torque $(-r_m \otimes D_m F_m)$ are applied to segment m and the force (F_B) and the torque $(r_n \otimes D_n F_B)$ are applied to segment n (This is done by use of the system matrices A_{13} and A_{23}). The expressions for $\vec{r}_A, \vec{r}_B, \ddot{\vec{r}}_A, \ddot{\vec{r}}_B$ are given:

$$r_A = X_m + D_m^{-1} r_m$$
$$\dot{r}_A = \dot{X}_m + D_m^{-1} \omega_m \otimes r_m$$
$$\ddot{r}_A = \ddot{X}_m + D_m^{-1} \dot{\omega}_m \otimes r_m + D_m^{-1} \omega_m \otimes (\omega_m \otimes r_m)$$
$$r_B = X_n + D_n^{-1} r_n$$
$$\dot{r}_B = \dot{X}_n + D_n^{-1} \omega_n \otimes r_n$$
$$\ddot{r}_B = \ddot{X}_n + D_n^{-1} \dot{\omega}_n \otimes r_n + D_n^{-1} \omega_n \otimes (\omega_n \otimes r_n)$$

where ω_m and ω_n are the angular velocities of the respective segments. Substitution of these terms into the constraint equation 4.61 results in the form needed by the program. The simularity of this constraint to the other types of constraints (fixed point, etc.) should be noted. The tension element is another example of a case where the system equations are non-symmetrical as was true for the sliding constraint.

94

4.5   FLEXIBLE ELEMENT PARAMETERS

The flexible element is intended for representations of complex, flexible portions of the human body, including, in particular, the neck, torso, and trunk. It is composed of a chain of N joined rigid segments. Each joint has three degrees of freedom with three corresponding stiffness constants. In addition, each of the N-2 interior segments of the flexible element is constrained so that its orientation is uniquely determined by the orientations of the end (or outer) segments of the element. These constraints have been introduced to approximate the effects of body muscles which are so connected that, rather than acting on individual joints, they determine the overall flexural characteristics of the represented body member. Fidelity of representation can be insured by determination of flexible element parameters from measurements.

Table 4.1 is a summary list of proposed computer program inputs for the flexible elements. The last column of the table indicates where the definition of each input is given.

The orientation of segment n relative to segment 1 is designated by the three angles θ_{1n}, θ_{2n}, θ_{3n} (see the discussion in the context of Figure 4.12). In order to avoid singularities in certain transform matrices employed in the calculations (see equation (4.10)), it is necessary to restrict θ_n to the domain

$$-\pi/2 < \theta_{2n} < \pi/2$$

Since there are no restrictions on the ranges of variations of θ_{1n} and θ_{3n}, θ_{1n} should be chosen for the angle of bend maximum range of variation. For example, in the representation of the human torso, forward bending should correspond to the angles θ_{1n} and not to θ_{2n}. θ_{2n} would correspond to sidewise bending of the torso. It should then be possible to satisfy the above bounds on θ_{2n} since few people (if any) can bend their torsos sidewise through 90°.

Table 4.1

COMPUTER PROGRAM INPUTS

FOR FLEXIBLE ELEMENT

SYMBOL		BRIEF DESCRIPTION	WHERE DEFINED
θ_{in}^{b}	$i = 1,3$ $n = 1, N-1$	set of bias angles	Equation (4.64)
N		number of segments in element	First paragraph
$f_{ij}(n)$	$i,j = 1,3$ $n = 1,N$	first-order taper function in constraint relation	Equation (4.64)
$g_{ij}(n)$	$i,j = 1,3$ $n = 1,N$	second-order, interaction taper function in constraint relation	Equation (4.64)
$h_{ij}(n)$	$i,j = 1,3$ $n = 1,N$	second-order, quadratic-form taper function in constraint relation	Equation (4.64)
ϕ_i^n	$i = 1,3$ $n = 1,N$	moments of inertia elements of nth segment	Context of Equation (4.69)
M_n	$n = 1,N$	mass of nth segment	Context of Equation (4.69)
$\theta_{1n}, \theta_{2n}, \theta_{3n}$	$n = 1,N$	yaw, pitch and roll angles	Context of Equation (4.63)
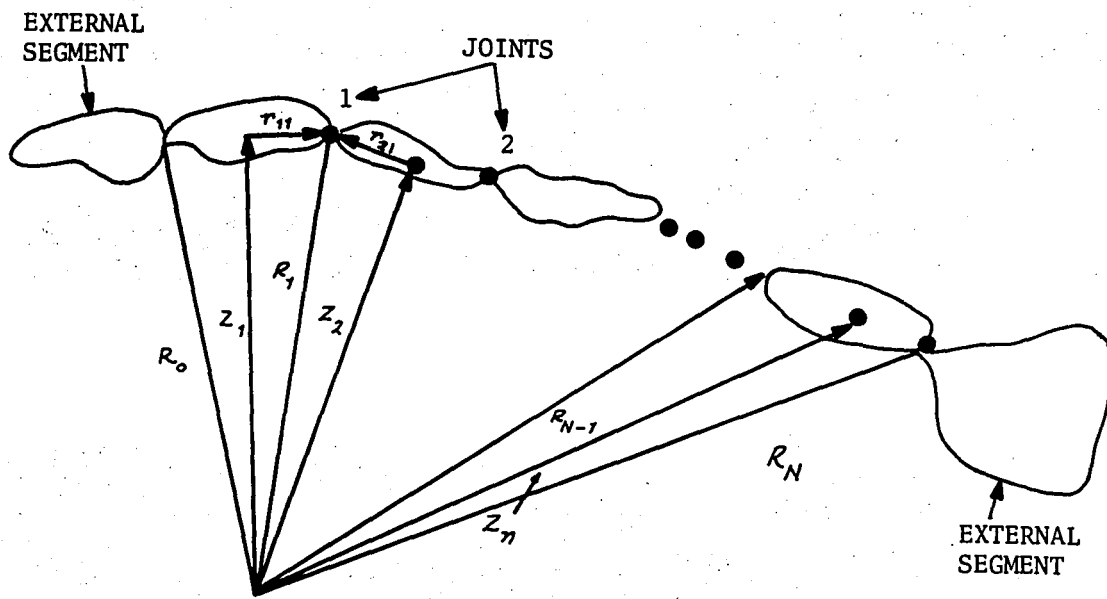
FIGURE 4.11 MODEL OF FLEXIBLE SEGMENT

In the rest of this subsection, all of the basic geometry of the flexible element, except details on the joints, is presented. The latter are discussed in the third subsection. Development of the equations of motion is undertaken in the second subsection.

As noted above, the flexible element is composed of N joined segments which are labelled 1 to N. In each segment there is a rigid local coordinate system with orthogonal unit vectors $\hat{e}_1^n$, $\hat{e}_2^n$, $\hat{e}_3^n$. As depicted in Figure 4.12, the unit vectors $\hat{e}_i^n$ are aligned with the principal inertia axes. Z_n is the position vector of the c.g. of segment n.

The orientation of the $\hat{e}_j^n$ vector of the nth segment relative to segment 1 is shown in Figure 4.12 and are in agreement with yaw, pitch and roll angles described in Figure 2.7.

Figure 4.12 COORDINATES FOR FLEXIBLE SEGMENT

The first rotation is through an angle θ_{1_n} about $\hat{e}_3^1$, the second rotation is through an angle $+\theta_{2_n}$ about the new $\hat{e}_2^1$; the final rotation is through an angle θ_{3_n} about $\hat{e}_1^n$ (which is the new $\hat{e}_1^1$.) The relation between $\hat{e}_1^n, \hat{e}_2^n, \hat{e}_3^n$ and $\hat{e}_1^1, \hat{e}_2^1, \hat{e}_3^1$ is

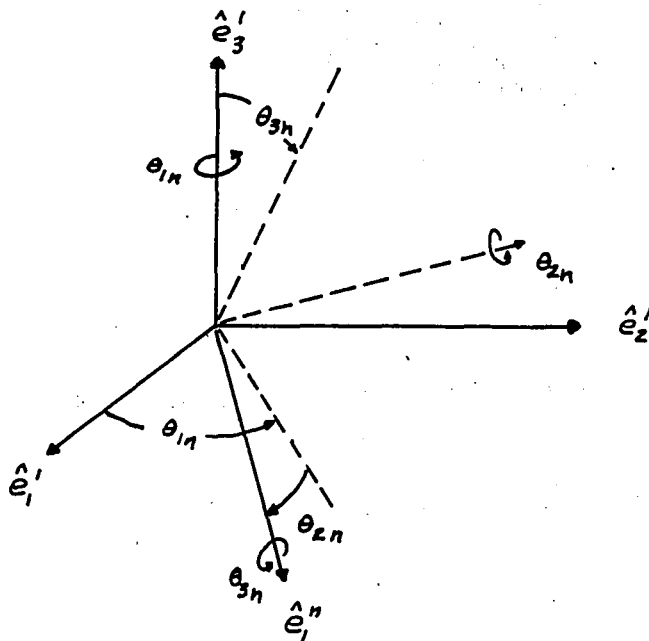$$\begin{pmatrix} \hat{e}_1^n \\ \hat{e}_2^n \\ \hat{e}_3^n \end{pmatrix} = \begin{pmatrix} 1 & 0 & 0 \\ 0 & \cos\theta_{3_n} & \sin\theta_{3_n} \\ 0 & -\sin\theta_{3_n} & \cos\theta_{3_n} \end{pmatrix} \begin{pmatrix} \cos\theta_{2_n} & 0 & -\sin\theta_{2_n} \\ 0 & 1 & 0 \\ +\sin\theta_{2_n} & 0 & \cos\theta_{2_n} \end{pmatrix} \begin{pmatrix} \cos\theta_{1_n} & \sin\theta_{1_n} & 0 \\ -\sin\theta_{1_n} & \cos\theta_{1_n} & 0 \\ 0 & 0 & 1 \end{pmatrix} \begin{pmatrix} \hat{e}_1^1 \\ \hat{e}_2^1 \\ \hat{e}_3^1 \end{pmatrix}$$

$$\text{(4.63)}$$

In accord with a suggestion of Dr. Ovenshire, $\theta_{1_n}, \theta_{2_n}, \theta_{3_n}$ will be represented by the second degree polynomials in the relations

$$\theta_{i_n} = \theta_{i_n}^t + f_{i1}(n)\,\theta_{1N} + f_{i2}(n)\,\theta_{2N} + f_{i3}(n)\,\theta_{3N}$$

$$+ g_{i1}(n)\,\theta_{2N}\theta_{3N} + g_{i2}(n)\,\theta_{3N}\theta_{1N} + g_{i3}(n)\,\theta_{1N}\theta_{2N}$$

$$+ h_{i1}(n)\,\theta_{1N}^2 + h_{i2}(n)\,\theta_{2N}^2 + h_{i3}(n)\,\theta_{3N}^2$$

$$\begin{array}{c} n = 2, N \\ i = 1, 3 \end{array} \qquad \text{(4.64)}$$

where

$$\theta_{i_n}^t = \text{a bias function with} \qquad \theta_{i_n}^t = 0 \qquad \text{for} \quad n = N$$

$$f_{ij}(N) = \delta_{ij} \quad , \quad g_{ij}(N) = 0 \; , \quad h_{ij}(N) = 0 \qquad \text{(4.65)}$$

The bias functions $\theta_{i_n}^t$ and the taper functions $f_{ij}(n), g_{ij}(n), h_{ij}(n)$ are all program inputs.

The joints are located in the standard manner:

$$\vec{R}_n = \vec{Z}_n + \vec{r}_{nn} \qquad\qquad (4.66)$$

where $\vec{R}_n$ is the location of the nth joint, also

$$\vec{R}_n = \vec{Z}_{n+1} + \vec{r}_{n+1,n} \qquad n = 1, N-1 \qquad (4.67)$$

where $\vec{r}_{ij}$ are defined in Figure 4.11.

The connection constraints (that is, the condition that the joints connecting segments do not pull apart) are contained in the relations (4.66) and (4.67). ·

The introduction of the bias functions, θ_{in}^b also allows the latitude of choosing the principal axes for the nth segment to coincide with the unit vectors $\hat{e}_i^n$. Thus, the Moment of Inertia Tensor for the nth segment is given by

$$\phi_n = \sum_{i=1}^{3} \phi_i^n \, \hat{e}_i^n \, \hat{e}_i^n$$

$$(4.68)$$

The inertia elements ϕ_i^n are program inputs, as are the masses M_n of the segments.

The Equations of Motion

The translation equation of motion of the nth segment of the flexible element may be expressed

$$M_n \, \ddot{\vec{r}}_n = \vec{F}_1 \, \delta_{n1} + \vec{F}_n^c + \vec{F}_n \, \delta_n + \vec{f}_n^c .$$

$$(4.69)$$

where M_η, and $\vec{r}_\eta$ are as previously defined, and

$\vec{F}_1$ =   an external applied force at the point with position vector $\overline{R}_o$ (see Figure 4.11)

$\vec{F}_N$ =   an external applied force at the point with position vector (R_N)

$\vec{F}_\eta^{\,c}$ =   an external force applied to a point of the contact surface which is rigidly connected to the segment n

$\vec{f}_\eta^{\,c}$ =   the summation of all constraint forces acting on segment n as a result of the configuration constraints on the flexible element

The rotational equation of motion of the nth segment may be expressed

$$\frac{d}{dt}\left[\phi_\eta \cdot \vec{\omega}_\eta\right] = \vec{N}_1\,\delta_{\eta 1} + \vec{N}_N\,\delta_{\eta N} + \vec{r}_c^{\,\eta} \otimes \vec{F}_\eta^{\,c} + N_\eta^{-joints} + \vec{n}_\eta^{\,c}$$

$$(4.70)$$

where ϕ_η and $\vec{F}_\eta^{\,c}$ are as previously defined and

$\vec{\omega}_n$ =   total angular velocity of nth segment

$\vec{N}_1$ =   an external torque (that is, force moment and/or force couple) applied to segment 1 through application at the point with position vector $\vec{R}_1$.

$\vec{N}_N$ =   same as N_1 except applied to segment N through application at the point with position vector $(R_N + \rho_\eta\,\hat{e}_1^{\,N})$.

$\vec{r}_c^{\,\eta}$ =   position vector of point of application of the force $\vec{F}_\eta^{\,c}$ relative to the c.m. of segment n. This vector depends on many things including the dimensions of the contact surface.

$\vec{N}_n^{JOINTS}$ = net torque applied to segment n as a result of stiffness of the joints which connect this segment to the adjacent segments n-1 and n+1.

$\vec{h}_n^{\,c}$ = the summation of all constraint torques acting on segment n as a result of the configuration constraints on the flexible element.

In the successive sections, the necessary expressions for forces, torques and constraint relations are derived.

Expressions For Torques Due To Stiffness Of Joints

Let $\vec{N}_{n,\,n+1}$ denote the torque exerted on segment n due to the stiffness of the joint between segment n and segment n+1. The definitions of $\vec{N}_{n,\,n+1}$ and $\vec{N}_n^{JOINTS}$ result in the following equations:

$$\vec{N}_n^{JOINTS} = \vec{N}_{n,n+1} - \vec{N}_{n-1,n} \qquad n=1,N \qquad (4.71)$$

where

$$\vec{N}_{N,N+1} = \vec{N}_{0,1} = 0 \qquad (4.72)$$

The $\vec{N}_{n,n+1}$ are computed using the same coordinate designation as described in Section 6.0 and indicated in Figure 4.13.
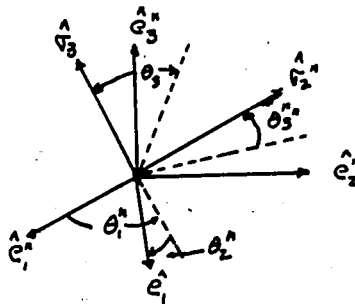
Figure 4.13 JOINT COORDINATE SYSTEM

where

$(\hat{e}_1^n, \hat{e}_2^n, \hat{e}_3^n)$ = orthonormal coordinates defining the segment axes for the nth segment

$$(4.73)$$

$(\hat{\sigma}_1^n, \hat{\sigma}_2^n, \hat{\sigma}_3^n)$ = orthonormal coordinates defining the joint axes for the nth segment   (4.74)

The program provides several methods of determining the torques between the segments defining the flexible element as indicated below.

$\vec{N}_{n,n+1}$ torque equations developed in Section 6.1 (4.75)

$\vec{N}_{n,n+1}$ torque equations developed in Section 6.1
using globolgraphic representation of joint
stops (Section 6.2)   (4.76)

$\vec{N}_{n,n+1}$ torque equations developed in Section 6.3
(Euler Joint)   (4.77)

$\vec{N}_{n,n+1}$ torque equations developed in Section 6.3
using the Globalgrpahic representation of the
joint stop torque .   (4.78)

.103

The Force-Type Constraint Relations

From Figure 4.17 and the discussion in the context of (4.66) and (4.67) the connection constraint for the joint between segment n and segment n+1 is

$$\vec{Z}_n + \vec{r}_{n,n} = \vec{Z}_{n+1} + \vec{r}_{n,n+1}$$

(4.79)

These relations do not include the connection constraints between the Flexible Element and other segments it is connected to. Differentiating (4.79) twice yields

$$\ddot{\vec{Z}}_n + \dot{\vec{\omega}}_n \otimes \vec{r}_{n,n} - \ddot{\vec{Z}}_{n+1} - \dot{\vec{\omega}}_{n+1} \otimes \vec{r}_{n,n+1} = -\vec{\omega}_n \otimes (\vec{\omega}_n \otimes \vec{r}_{n,n}) + \vec{\omega}_{n+1} \otimes (\vec{\omega}_{n+1} \otimes \vec{r}_{n,n+1})$$

(4.80)

Let

$$\vec{f}_n = \text{constraint force exerted on segment n due to connection constraint between segment n and segment n+1.}$$

Then

$$\vec{f}_n^{\,c} = \vec{f}_n - \vec{f}_{n-1} \qquad n = 1, N$$

(4.81)

$$\vec{n}_n^{\,c} = \vec{r}_{n,n} \otimes \vec{f}_n - \vec{r}_{n-1,n} \otimes \vec{f}_{n-1} + \vec{n}_n^{\,torque}$$

(4.82)

where $\vec{f}_n^{\,c}$ and $\vec{n}_n^{\,c}$ are the total constraint forces and torques on segment n (previously defined) and

$$\vec{f}_o = \vec{f}_N = 0$$

(4.83)

104

Forces and torques resulting from connecting the Flexible Element to external segments are represented separately by $\vec{F}_1$, $\vec{F}_N$, $\vec{N}_1$ and N_N. $\vec{n}_n^{torque}$ denotes the net constraint torque acting on segment n as the result of torque-type constraints.

The Torque-Type Constraint Relations

This subsection covers the formulation of the torque-type constraint relations. The corresponding compatibility relations are considered in the next subsection.

The relations in (4.64) can be expressed more generally

$$\theta_{in} = G_{in}\left[\theta_{1n}, \theta_{2n}, \theta_{3n}\right] \qquad \begin{array}{l} i = 1,3 \\ n = 2,N \end{array}$$

$$(4.84)$$

The functions G_{in} can be evaluated in a separate subroutine. This procedure will allow more latitude for generalizations in the functional form.

From (4.84)

$$\dot{\theta}_{in} = \sum_{j=1}^{3} G_{nij}\left[\theta_{1n}, \theta_{2n}, \theta_{3n}\right] \dot{\theta}_{jN}$$

$$(4.85)$$

where

$$G_{nij} = \frac{\partial G_{in}}{\partial \theta_{jN}} \qquad n = 2,N$$

$$(4.86)$$

Now, the $\dot{\theta}_{in}$ are nonorthogonal components of the relative angular velocity $\vec{\omega}_n - \vec{\omega}_1$. From (4.65) and Figure 4.12

$$\omega_n - \omega_1 = \dot{\theta}_{1n}\,\hat{e}_3^1 + \dot{\theta}_{3n}\,\hat{e}_1^n + \dot{\theta}_{2n}\left[-\hat{e}_1^1 \sin\theta_{1n} + \hat{e}_2^1 \cos\theta_{1n}\right]$$

$$(4.87)$$

Put

$$\vec{a}_1^{\,n} = \hat{e}_3^{\,1}$$

$$\vec{a}_2^{\,n} = -\hat{e}_1^{\,1} \sin\theta_{1n} + \hat{e}_2^{\,1} \cos\theta_{1n}$$

$$\vec{a}_3^{\,n} = \vec{e}_1^{\,n}$$

$$(4.88)$$

Then, (4.87) may be reexpressed

$$\vec{\omega}_n - \vec{\omega}_1 = \sum_{i=1}^{3} \dot{\theta}_{in} \, \vec{a}_i^{\,n}$$

$$(4.89)$$

Introduce reciprocal unitary vectors $\vec{t}_i^{\,n}$ such that

$$\vec{t}_i^{\,n} \cdot \vec{a}_j^{\,n} = \delta_{ij}$$

$$(4.90)$$

From (4.85), (4.89) and (4.90)

$$\sum_{i=1}^{3} \dot{\theta}_{in} \, \vec{a}_i^{\,n} = \sum_{i=1}^{3} \sum_{j=1}^{3} a_i^{\,n} \, G_{nij} \, \dot{\theta}_{jN}$$

$$= \left\{ \sum_{i=1}^{3} \sum_{j=1}^{3} \vec{a}_i^{\,n} \, G_{nij} \, \vec{t}_j^{\,N} \right\} \cdot \left\{ \sum_{K=1}^{3} \vec{a}_K^{\,N} \, \dot{\theta}_{KN} \right\}$$

or, employing (4.89)

$$\vec{\omega}_n - \vec{\omega}_1 = G_n^+ \cdot \left[\vec{\omega}_N - \vec{\omega}_1 \right]$$

$$(4.91)$$

where G_n^+ denotes the tensor

$$G_n^+ = \sum_{i=1}^{3} \sum_{j=1}^{3} \vec{a}_i^{\,n} \, G_{nij} \, \vec{t}_j^{\,N}$$

$$(4.92)$$

Rearranging (4.91), one obtains*

$$\vec{\omega}_n + \left(G_n^+ - I \right) \cdot \vec{\omega}_1 - G_n^+ \cdot \vec{\omega}_N = 0$$

$$n = 2, N-1$$

$$(4.93)$$

_____

*Note that $G_N^+ = I$ (where I denotes the identity tensor.) So (4.93) vanishes identically when n = N.

106

Differentiating (4.93):

$$\dot{\vec{\omega}}_n + \left[G_n^+ - I \right] \cdot \dot{\vec{\omega}}_1 - G_n^+ \cdot \dot{\vec{\omega}}_N$$

$$= - \dot{G}_n^+ \cdot \vec{\omega}_1 + \dot{G}_N^+ \cdot \vec{\omega}_N$$

(4.94)

In employing (4.94), it is to be observed that

$$\dot{\vec{\omega}}_n = \sum_{i=1}^{3} \dot{\omega}_n^i \, \hat{e}_i^n \qquad n = 1, N$$

(4.95)

A logical base system in which to express the elements of the tensor G_N^+ is the $\hat{e}_i^1$ system. In this system

$$G_n^+ = \sum_{i=1}^{3} \sum_{j=1}^{3} G_{ij}^{1n} \, \hat{e}_i^1 \, \hat{e}_j^1$$

(4.96)

To evaluate G_{ij}^{1n}, $\vec{a}_i^n$ and $\vec{t}_j^N$ can be expressed in terms of the unit vectors $\hat{e}_i^1$.

From Figure 4.12

$$\hat{e}_1^n = \hat{e}_1^1 \cos\theta_{2n} \cos\theta_{1n} + \hat{e}_2^1 \cos\theta_{2n} \sin\theta_{1n} - \hat{e}_3^1 \sin\theta_{2n}$$

(4.97)

Substituting (4.97) into (4.88) yields

$$\vec{a}_i^n = \sum_{j=1}^{3} c_{ij}^n \, \hat{e}_j^1$$

(4.98)

107

where

$$(c_{ij}^n) = \begin{pmatrix} 0 & 0 & 1 \\ -\sin\theta_{1n} & +\cos\theta_{1n} & 0 \\ \cos\theta_{2n}\cos\theta_{1n} & \cos\theta_{2n}\sin\theta_{1n} & -\sin\theta_{2n} \end{pmatrix} \qquad (4.99)$$

$$\vec{t}_i^{\,n} = \sum_{j=1}^{3} \widetilde{(c^n)}_{ij}^{-1} \, \hat{e}_j^{\,1} \qquad (4.100)$$

where $\widetilde{(c^n)}^{-1}$ denotes the transpose inverse of c^n, given by

$$(c^n)^{-1} = \begin{pmatrix} \dfrac{-\cos\theta_{1n}\sin\theta_{2n}}{\cos\theta_{2n}} & -\sin\theta_{1n} & \dfrac{\cos\theta_{1n}}{\cos\theta_{2n}} \\[4mm] -\dfrac{\sin\theta_{1n}\sin\theta_{2n}}{\cos\theta_{2n}} +\cos\theta_{1n} & & \dfrac{\sin\theta_{1n}}{\cos\theta_{2n}} \\[4mm] 1 & 0 & 0 \end{pmatrix}$$

$$(4.101)$$

The singular points of the matrix in (4.101) can be avoided by limiting the range of variation of θ, as discussed in the first subsection.

Substitution of (4.98) and (4.100) into (4.92) leads to

$$G_n^+ = \sum_{i=1}^{3}\sum_{j=1}^{3} \hat{e}_i^{\,1} \left\{ \sum_{K=1}^{3}\sum_{\ell=1}^{3} \widetilde{c}_{iK}^{\,n} \, G_{nK\ell} \, \widetilde{(c^N)}_{\ell j}^{-1} \right\} \hat{e}_j^{\,1}$$

Comparing this relation with (4.96), it is concluded that

$$G_{ij}^{\prime n} = \sum_{K=1}^{3}\sum_{\ell=1}^{3} \widetilde{c}_{iK}^{\,n} \, G_{nK\ell} \, \widetilde{(c^n)}_{\ell j}^{-1} \qquad (4.101)$$

The next step is to differentiate G_n^+ .

From (4.96)

$$\dot{G}_n^+ = \vec{\omega}_1 \otimes G_n^+ - G_n^+ \otimes \vec{\omega}_1 + \sum_{i=1}^{3}\sum_{j=1}^{3} \dot{G}_{ij}^{\prime n} \, \hat{e}_i^{\,1} \hat{e}_j^{\,1}$$

$$n = 2, N-1 \qquad (4.103)$$

108

From (4.102)

$$\dot{G}^{'n}_{ij} = \sum_{K=1}^{3} \sum_{\ell=1}^{3} \dot{\widetilde{c}^n_{iK}} \; G_{nK\ell} \; \widetilde{(c^N)}^{-1}_{\ell j}$$

$$+ \sum_{K=1}^{3} \sum_{\ell=1}^{3} \widetilde{c}^n_{iK} \; G_{nK\ell} \; \dot{\widetilde{(c^N)}^{-1}_{\ell j}}$$

$$+ \sum_{K=1}^{3} \sum_{\ell=1}^{3} \widetilde{c}^n_{iK} \; \dot{G}_{nK\ell} \; \widetilde{(c^N)}^{-1}_{\ell j}$$

(4.104)

Now

$$\dot{\widetilde{c}^n_{iK}} = \frac{\partial \widetilde{c}^n_{iK}}{\partial \theta_{1n}} \dot{\theta}_{1n} + \frac{\partial \widetilde{c}^n_{iK}}{\partial \theta_{2n}} \dot{\theta}_{2n}$$

or

$$\dot{\widetilde{c}^n_{iK}} = \widetilde{D^n_{1iK}} \; \dot{\theta}_{1n} + \widetilde{D^n_{2iK}} \; \dot{\theta}_{2n}$$

(4.105)

where

$$D^n_{\ell iK} = \frac{\partial c^n_{iK}}{\partial \theta_{\ell n}}$$

(4.106)

Also

$$\dot{\widetilde{(c^N)}^{-1}_{\ell j}} = \widetilde{E^N_{\ell j 1}} \; \dot{\theta}_{1n} + \widetilde{E^N_{\ell j 2}} \; \dot{\theta}_{2n}$$

(4.107)

where

$$E^n_{\ell j m} = \frac{\partial (c^n)^{-1}_{\ell j}}{\partial \theta_{mn}} \quad ; \; m = 1, 2$$

(4.108)

Further,

$$\dot{G}_{nK\ell} = \sum_{m=1}^{3} \frac{\partial G_{nK\ell}}{\partial \theta_{mn}} \; \dot{\theta}_{mn}$$

or

$$\dot{G}_{nK\ell} = \sum_{m=1}^{3} G_{nK\ell m} \; \dot{\theta}_{mn}$$

(4.109)

where

$$G_{nK\ell m} = \frac{\partial G_{nK\ell}}{\partial \theta_{mn}}$$

(4.110)

$G_{nK\ell m}$ can be evaluated in the subroutine which evaluates $G_{nK\ell}$ and G_{in}.

109

In summary, $\dot{G}_{ij}^{m}$ can be evaluated piecewise. First, the quantities $\dot{\vec{\omega}}_{N}$ and $\dot{\vec{\omega}}_{1}$ are integrated to obtain $\vec{\omega}_{N}$ and $\vec{\omega}_{1}$. Then $\dot{\theta}_{1n}$ can be determined from the inverse of (4.89):

$$\dot{\theta}_{1n} = \vec{t}_{c}^{n} \cdot \left(\vec{\omega}_{N} - \vec{\omega}_{1} \right)$$

(4.111)

The quantities θ_{iN}, $i=1,\ldots,3$ can be evaluated either by integrating $\dot{\theta}_{iN}$ or by employing the direction cosines of segments 1 and N, which are obtained by integration. The quantities θ_{in} and $\dot{\theta}_{in}$ ($i=1,3$; $n=2,N-1$) can then be obtained from the relations (4.84) and (4.85). This procedure insures the satisfaction of the configuration constraints. $G_{nK\ell m}$ and $\dot{G}_{nK\ell}$ can be evaluated from (4.109) and (4.110) nd $\widetilde{D}_{\ell jm}^{n}$ can be evaluated from (4.107) and (4.108). Then $\widetilde{C}_{ik}^{n}$, $\widetilde{C}_{ik}^{n}$, $(\widetilde{C}_{\ell j}^{N})^{-1}$ and $(\widetilde{C}^{N})_{\ell j}^{-1}$ can be evaluated from (4.99), (4.105), (4.101) and (4.107). Finally, $\dot{G}_{ij}^{1n}$ can be computed from (4.105).

The discussion of the quantities which appear in the torque-type constraint relations is complete. In the last subsection, the representation of the constraint torques is considered.

The Constraint Torques

From (4.70) and (4.82), the rotational equations of motion may be expressed

$$\dot{\vec{H}}_{n} - \vec{n}_{n}^{force} - n_{n}^{torque} = \vec{N}_{n} \; applied$$

$$n = 1, N \qquad (4.112)$$

where

$$\dot{\vec{H}}_{n} = \frac{d}{dt} \left[\phi_{n} \cdot \vec{\omega}_{n} \right]$$

(4.113)

$$\vec{N}_{n} \; applied = \vec{N}_{1} \, \delta_{n1} + \vec{N}_{N} \, \delta_{nN} + \vec{r}_{c}^{n} \otimes F_{n}^{c} + \vec{N}_{n}^{joints}$$

(4.114)

$$\vec{n}_n^{\,force} = \overline{r_{n,n}} \otimes \vec{f}_n - \overline{r_{n-1,n}} \otimes \overline{f_{n-1}} \qquad (4.115)$$

and $\vec{n}_n^{\,torque}$ denotes the constraint torques resulting from the constraint relations .

$$\vec{\omega}_n + \left[G_n^+ - I \right] \cdot \vec{\omega}_1 - G_n^+ \cdot \vec{\omega}_N = 0$$
$$n = 2, N-1 \qquad (4.116)$$

The easiest way to infer the compatibility relations among the constraint torques is by the Lagrange-multiplier method. If the constraint relations in (4.116) are represented in the form

$$\sum_{n=1}^{N} A_n^m \cdot \vec{\omega}_n = 0 \qquad m = 2, N-1 \qquad (4.117)$$

$$\vec{n}_n^{\,torque} = \sum_{m=2}^{N-1} \vec{\lambda}_m \cdot A_n^m \qquad (4.118)$$

where the $\vec{\lambda}_m$ are vector Lagrange multipliers.

Comparing (4.117) with (4.116) it is readily concluded that

$$\vec{n}_n^{\,torque} = \vec{\lambda}_n \qquad n = 2, N-1 \qquad (4.119)$$

$$\vec{n}_1^{\,torque} = \sum_{m=2}^{N-1} \vec{\lambda}_m \cdot \left[G_m^+ - I \right] \qquad (4.120)$$

$$\vec{n}_N^{\,torque} = -\sum_{m=2}^{N-1} \vec{\lambda}_m \cdot G_m^{'+} \qquad (4.121)$$

Elimination of $\vec{\lambda}_m$ from the relations (4.119)-(4.121) is immediate, and leads to the compatibility relations among the torques.

It is apparent that the equations of motion in (4.112) in conjunction with the constraint relations in (4.116) can be solved uniquely for the $\vec{\omega}_n$ and the $\vec{\lambda}_m$.

4.6 SINGULAR SEGMENTS (MASSLESS ELEMENTS)

In some simulations, it may be desirable to ignore the mass and/or particular components of the inertia tensor. This is feasible if sufficient constraints exist to define the motion (i.e. the system matrix is non-singular.) Because of the generality of the program, it is difficult to establish a necessary or sufficient condition for the assurance of a non-singular system matrix. But, for example, a segment connected between two other segments in a chain with at least one pinned joint may be assigned a singular mass or inertia matrix.

The program will accept these singular segments without special input. If the mass or any principal component of the inertia tensor is zero, the program will treat that segment as singular. It is assumed that the user will supply sufficient constraints to avoid a singular system matrix.

The effect of this singular feature is unknown, but it is conjectured that if a mass or inertia component of a particular segment is very small, the use of a zero value may eliminate undesirable modes of oscillation in the system. As a matter of interest, the program will accept negative values of mass and/or principal components of inertia*.

---

*In the spring of 1973 Dr. Ovenshire asked Calspan to make a series of runs using modified masses and inertia tensors. Dr. Kane at Stanford University had shown that in a connected set of rigid bodies that the definitions of mass and inertia were not unique. Calspan does not know what Dr. Kane's method is for determining equivalent systems but the following theorem was proved by Dr. Fleck at Calspan and used to compute accurate equivalent sets. Dr. Fleck assumes that this must be Kane's result.

113

Theorem on Equivalent Systems.

The following is a proof for equivalent systems applied to a system
of n rigid bodies connected by joints. Consider n rigid segments linked
together in a tree structure. That is there is only one path through the
structure which leads from any segment to any other segment.

Define: $\vec{X}_k$ be the location of the center of mass of the kth
segment

m_k be the mass of the kth segment

φ_k be the inertia matrix of the kth segment

$\vec{\omega}_k$ be angular velocity of the kth segment

$\vec{r}_{kj}$ be the location of joint j relative to the center
of mass of k th segment. This is defined only for
joints linking segment k to adjoining segments.

$\vec{f}_{kj}$ be the constraint force acting on segment k at joint j
which prevents the joint from separating

$\vec{F}_{k\ell}$ be the lth external force acting on segment k

$\vec{\rho}_{k\ell}$ location relative to c. m. of point of application
of the lth force on kth segment

$\vec{T}_k$ be external torques (couples) acting on segment k.

The equations of motion of this system are:

$$m_k \, \ddot{\vec{X}}_k + \sum_j \vec{f}_{kj} = \sum_\ell \vec{F}_{k\ell} \qquad \kappa = 1, N \qquad \text{(linear)}$$

(4.122)

$$\frac{d}{dt}\left(\varphi_k \, \vec{\omega}_k \right) + \sum_j \vec{r}_{kj} \otimes \vec{f}_{kj} = \sum_\ell \vec{\rho}_{k\ell} \otimes \vec{F}_{k\ell} + \vec{T}_k \qquad \kappa = 1, N \qquad \text{(angular)}$$

(4.123)

114

Subject to the constraints

$$\vec{x}_k + \vec{r}_{kj} = \vec{x}_\ell + \vec{r}_{\ell j} \qquad\qquad j = 1, M_{joint} \qquad (4.124)$$

Note that the sum over j in the linear and angular equations is taken over only those joints which are directly connected to segment k.

Consider the transformation of variable:

$$m_k^* = m_k + \delta_k \qquad\qquad \sum_{k=1}^{N} \delta_k = 0$$

$$\varphi_k^* = \varphi_k + \sum_j \delta_{kj} \; \vec{r}_{kj}^* \otimes \left(\vec{r}_{kj}^* \otimes \right.$$

$$\vec{r}_{kj}^* = \vec{r}_{kj} + \vec{c}_k \qquad\qquad\qquad\qquad (4.125)$$

$$\vec{\rho}_{kj}^* = \vec{\rho}_{kj} + \vec{c}_k$$

$$\vec{x}_k^* = \vec{x}_k - \vec{c}_k$$

$$\vec{f}_{kj}^* = \vec{f}_{kj} + \delta_{kj} \frac{d^2}{dt^2}\left(\vec{x}_k + \vec{r}_{kj} \right)$$

where δ_{kj} is the sum of the δ_ℓ of the segments which may be reached through joint j from segment k. The C_k are determined by the relation

$$m_k^* \; \vec{c}_k = \sum_j \delta_{kj} \cdot \vec{r}_{kj}$$

___Theorem:___ This transformation leaves the equations invariant; that is the new equations of motion can be written as:

$$m_k^* \ddot{\vec{x}}_k^* + \sum_j \vec{f}_{jk}^* = \sum_\ell \vec{F}_{k\ell}$$

$$\frac{d}{dt}\left(\varphi_k^* \vec{\omega}_k \right) + \sum_j \vec{r}_{kj}^* \otimes \vec{f}_{kj}^* = \sum_\ell \vec{\rho}_{kj}^* \otimes \vec{F}_{k\ell} + \vec{T}_k \qquad (4.126)$$

Subject to the constraint

$$\vec{x}_k^* + \vec{r}_{kj}^* = \vec{x}_\ell^* + \vec{r}_{\ell j}^* \qquad\qquad (4.127)$$

The proof is straightforward by substitution:

$$m_k^* \, \ddot{\vec{x}}_k^* + \sum_j \vec{f}_{k_j}^{\,*} = (m_k + \delta_k)(\ddot{\vec{x}}_k - \ddot{\vec{c}}_k) + \sum_j (\vec{F}_{k_j} + \delta_{k_j}(\ddot{\vec{x}}_k + \ddot{\vec{r}}_{k_j}))$$

$$= m_k \ddot{\vec{x}}_k + \sum_j \vec{F}_{k_j} - m_k \ddot{\vec{c}}_k + \sum_j \delta_{k_j} \ddot{\vec{r}}_{k_j} + (\delta_k + \sum_j \delta_{k_j}) \ddot{\vec{x}}_k^*$$

Then

$$m_k^* \, \ddot{\vec{x}}_k^* + \sum_j \vec{f}_{k_j}^{\,*} = m_k \ddot{\vec{x}}_k + \sum_j \vec{F}_{k_j}$$

because

$$m_k \vec{c}_k = \sum_j \delta_{k_j} \vec{r}_{k_j}^{\,*}$$

$$\vec{x}_k + \vec{r}_{k_j} = \vec{x}_k^* + \vec{r}_{k_j}^{\,*}$$

and

$$\delta_k + \sum_j \delta_{k_j} = 0$$

For the angular equation, consider the following substitution:

$$\sum_j \vec{r}_{k_j}^{\,*} \otimes \vec{f}_{k_j}^{\,*} - \sum_\ell \vec{p}_{k\ell}^{\,*} \otimes \vec{F}_{k\ell} = \sum_j \vec{r}_{k_j} \otimes \vec{f}_{k_j} - \sum_\ell \vec{p}_{k\ell} \otimes \vec{F}_{k\ell}$$

$$+ \vec{c}_k \otimes \sum_j \vec{f}_{k_j}^{\,*} - \vec{c}_k \otimes (m_k^* \ddot{\vec{x}}_k^* + \sum_j \vec{f}_{k_j}^{\,*}) + \sum_j \delta_{k_j} \vec{r}_{k_j} \otimes (\ddot{\vec{x}}_k^* + \ddot{\vec{r}}_{k_j}^{\,*})$$

rearranging

$$\sum_j \vec{r}_{k_j}^{\,*} \otimes \vec{f}_{k_j}^{\,*} - \sum_\ell \vec{p}_{k\ell}^{\,*} \otimes \vec{F}_{k\ell} = \sum_j \vec{r}_{k_j} \otimes \vec{f}_{k_j} - \sum_\ell \vec{p}_{k\ell} \otimes \vec{F}_{k\ell} + (\sum_j \delta_{k_j} \vec{r}_{k_j}$$

$$- m_k^* \vec{c}_k) \otimes \ddot{\vec{x}}_k + \sum_j \delta_{k_j} \vec{r}_{k_j} \otimes \ddot{\vec{r}}_{k_j}^{\,*}$$

but

$$\sum_j \delta_{k_j} \vec{r}_{k_j} \otimes (\ddot{\vec{r}}_{k_j}^{\,*}) = - \sum_j \delta_{k_j} \vec{r}_{k_j} \otimes \frac{d}{dt}\left[\vec{r}_{k_j}^{\,*} \otimes \vec{\omega}_k \right]$$

$$= - \frac{d}{dt}\left[\sum_j \delta_{k_j} \vec{r}_{k_j}^{\,*} \otimes (\vec{r}_{k_j} \otimes \vec{\omega}_k) \right]$$

which results in

$$\sum_j \vec{r}_{k_j}^{\,*} \otimes \vec{f}_{k_j}^{\,*} - \sum_\ell \vec{p}_{k\ell}^{\,*} \otimes \vec{F}_{k\ell} = \sum_j \vec{r}_{k_j} \otimes \vec{f}_{k_j} - \sum_\ell \vec{p}_{k\ell} \otimes \vec{F}_{k\ell} - \frac{d}{dt} \sum_j \delta_{k_j} \vec{r}_{k_j}^{\,*} \otimes (\vec{r}_{k_j} \otimes \vec{\omega}_k)$$

$$+ (\sum_j \delta_{k_j} \vec{r}_{k_j} - m_k^* \vec{c}_k) \otimes \ddot{\vec{x}}_k^*$$

116

and noting that

$$\left(\sum_j \delta_{k_j} \bar{F}_{k_j} - m_k \vec{c}_k^{\,*} \right) = 0$$

yields

$$\sum_j \vec{r}_{k_j}^{\,*} \otimes \vec{f}_{k_j}^{\,*} - \sum_\ell \vec{\rho}_{k_\ell}^{\,*} \otimes \bar{F}_{k_\ell} = \sum_j \bar{r}_{k_j} \otimes \vec{f}_{k_j} - \sum_\ell \vec{f}_{k_\ell} \otimes \bar{F}_{k_\ell} - \frac{d}{dt} \sum_j \delta_{k_j} \vec{r}_{k_j}^{\,*} \otimes \left(\bar{r}_{k_j} \otimes \vec{\omega}_k \right)$$

which completes the proof.

DESCRIPTION OF THE MATRICES IN THE SYSTEM EQUATIONS

Now that the constraint relationships have been derived, it is appropriate to discuss the overall set of system equations indicated below in matrix form.

$$M\ddot{X} + A_{11}f + A_{13}\,q = u_1$$ linear acceleration   (4.128)
(inertial ref.)

$$\phi\,\dot{\omega} + A_{21}f + A_{22}t + A_{23}\,q + A_{24}\tau = u_2$$ angular acceleration   (4.129)
(local ref.)

with constraint equations of the form:

$$B_{11}\ddot{X} + B_{12}\,\dot{\omega} + B_{13}f = V_1$$ joint linear position   (4.130)
constraint

$$B_{22}\,\dot{\omega} + B_{24}t = V_2$$ joint angular position   (4.131)
constraint

$$B_{31}\ddot{X} + B_{32}\,\dot{\omega} + B_{35}\,q = V_3$$ other constraints*   (4.132)

$$B_{42}\,\dot{\omega} = V_4$$ flexible element constraints
(4.133)

When discussing the matrices of vectors of the model, it is convenient to talk in terms of the 3 x 3 submatrices, or 3 x 1 vectors that are involved. For example, the inertia matrix ϕ for a model with N segments may be described as consisting of N, 3 x 3 submatrices ϕ_i . The matrix ϕ_i is a diagonal matrix (since we are using principal axes as a coordinate system) with the

---

* Note, for the sliding constraint, or when tension elements are used, B_{31} and B_{32} are not the transposes of A_{13} and A_{23}. Thus when a sliding constraint or tension element is active the system equations are not symmetrical.

diagonal elements equal to the components of inertia about the x, y, and z
local axes of segment i. The matrix ϕ is the diagonal matrix which is the
collection of the n matrices ϕ_i. Similarly the mass matrix M is diagonal
and is the collection of the submatrices m_i ; which is a diagonal 3 x 3
matrix with the mass of segment i on the diagonal. Thus, unless it is speci-
fically stated to the contrary, when we refer to the element in the ith row
and j^{th} column of a system matrix we are referring to the ij^{th} submatrix. A
diagram of the M and ϕ matrices illustrating the above convention is pre-
sented in Figure 4.14.

Linear Joint Constraint

Consider the linear joint constraint equation derived in the previous
section and repeated below for comparison.

$$\ddot{X}_n - \ddot{X}_m - D_n^{-1}\left(r_{n_j} \otimes \dot{\omega}_n\right) + D_m^{-1}\left(r_{m_j} \otimes \dot{\omega}_m\right) = D_m^{-1}\left[\omega_m \otimes \left(\omega_m \otimes r_{m_j}\right)\right] - D_n^{-1}\left[\omega_n \otimes \left(\omega_n \times r_{n_j}\right)\right]$$

Compared with the system equation

$$B_{11}\ddot{X} + B_{12}\dot{\omega} + B_{13}f = V_1$$

There will be an equation for each joint j for j = $1, J$. The
matrix B_{11} will then be an NXJ group of 3x3 matrices. For joint j there will
be the identity matrix in row j column m and -I in row j column n of B_{11}. A
schematic diagram of B_{11} is presented in Figure 4.15. Matrix B_{12} is also
J x N with the entry for joint j indicated in Figure 4.1 . V_1 then is the
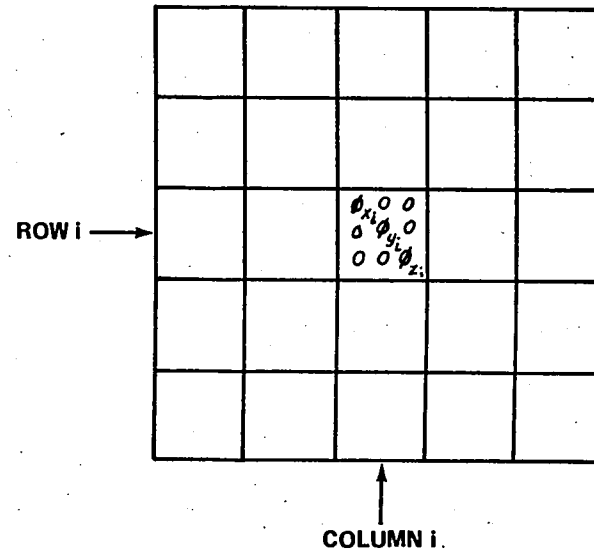right hand side of the equation and also appears in Figure 4.16.

119
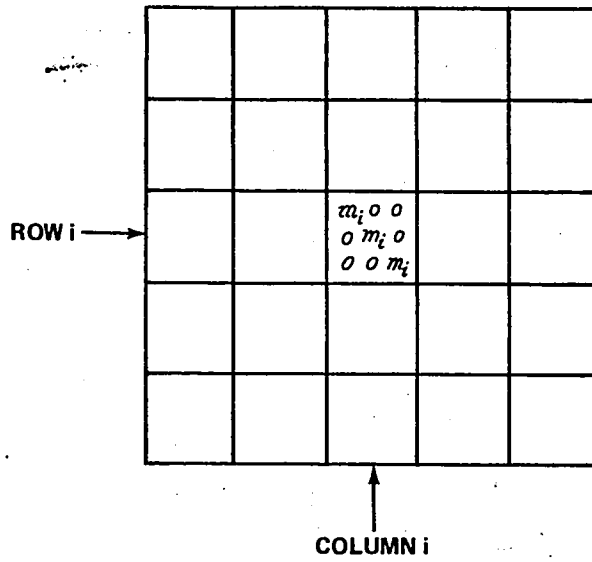
Figure 4.14. THE ith ENTRY IN THE MASS AND INERTIA MATRICES

Figure 4.15. B_{11} MATRIX ENTRY FOR JOINT j

121

B$_{12}$

V$_1$

ROW j →

α_m α_n

ROW j → γ

COL.   COL.
JNT(j)   j+1

$\alpha_m = -D_m^{-1} (r_{mj} \otimes)$

$\alpha_n = D_n^{-1} (r_{nj} \otimes)$

$\gamma = D_m^{-1} [\omega_m \otimes (\omega_m \otimes r_{mj})]$

$- D_n^{-1} [\omega_n \otimes (\omega_n \otimes r_{nj})]$

$m = JNT(j)$
$n = j+1$

Figure 4.16. B$_{12}$ MATRIX ENTRY AND V$_1$ VECTOR ENTRY FOR JOINT j

122

Angular Joint Constraint

The angular joint constraint equations have three different forms depending on the type of joint specified. These equations are the following:
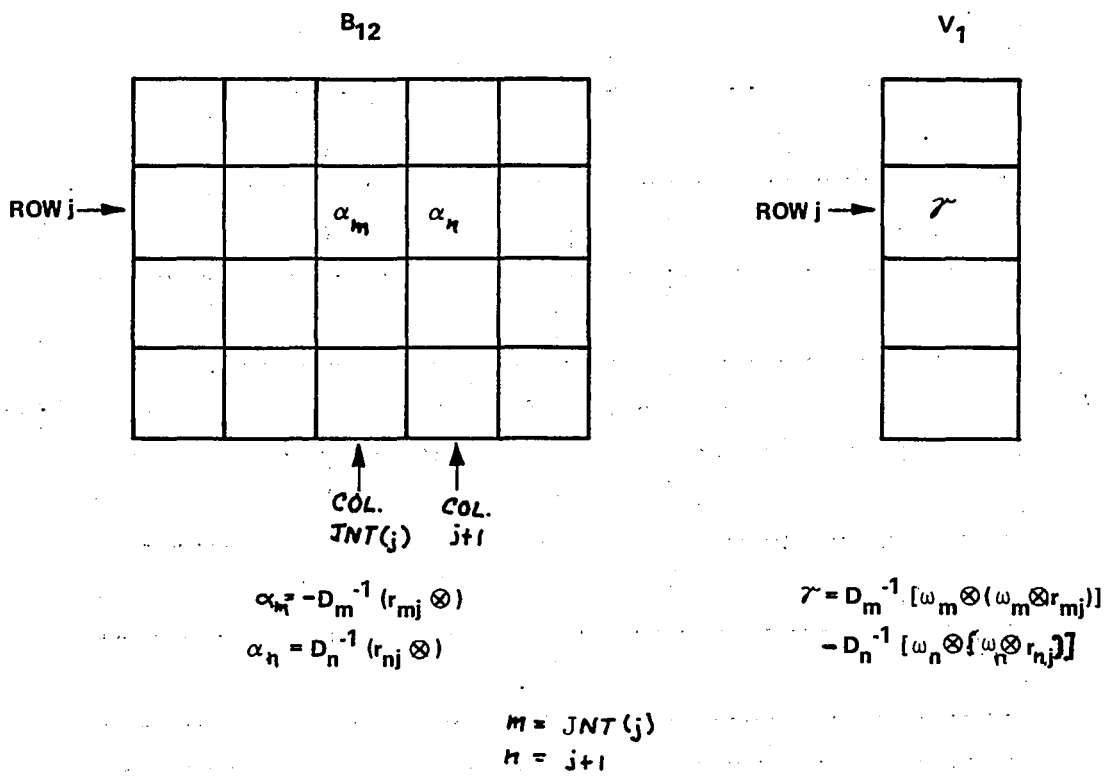
$$t = 0 \quad \text{free (ball \& socket) joint}$$

$$D_n^{-1} \dot{\omega}_n - D_m^{-1} \dot{\omega}_m = 0 \quad \text{locked joint}$$

and

$$(I - hh \cdot)(D_n^{-1} \dot{\omega}_n - D_m^{-1} \dot{\omega}_m) + \lambda hh \cdot t$$
$$= \left[(\omega_n \cdot h_n) - (\omega_m \cdot h_m) \right] D_n^{-1} \omega_n \otimes h_n \quad \text{pinned joint}$$

The matrix equation for the above equations is

$$B_{22} \dot{\omega} + B_{24} t = V_2$$

Again for N segments and J joints B_{22} will be $J \times N$ collection of 3x3 sub-matrices. The particular entries depend on the type of joint specified. A typical entry for joint j is given for B_{22}, B_{24} and V_2 in Figure (4.17).

Other Constraint Equations

The distance, rolling and sliding constraints derived in the previous section are summarized below. The fixed distance constraint is:

$$h \left\{ h \cdot \left[\ddot{x}_m - \ddot{x}_n \, D_m^{-1} r_m \otimes \dot{\omega}_m + D_n^{-1} r_n \otimes \dot{\omega}_n \right] \right\} + \lambda (I - hh \cdot) q = V_3$$
$$V_3 = h \left\{ h \cdot \left[D_n^{-1} (\omega_n \otimes (\omega_n \otimes r_n)) - D_m^{-1} (\omega_m \otimes \omega_m \otimes r_m) \right] - \left| \frac{\dot{\rho}}{d} \right|^2 \right\}$$

The rolling constraint equation is:

$$\ddot{x}_m - \ddot{x}_n - D_m^{-1} (l_m + r_m) \otimes \dot{\omega}_m + D_n^{-1} \left[l_n + r_n \right] \otimes \dot{\omega}_n = V_3$$

$$V_3 = D_n^{-1} \left[\omega_n \otimes (\omega_n \otimes (l_n + r_n)) \right] + D_n^{-1} \omega_n \otimes r_n' - D_m^{-1} \left[\omega_m \otimes (\omega_m \otimes (l_m + r_m)) \right] - D_m^{-1} \omega_m \otimes r_m'$$
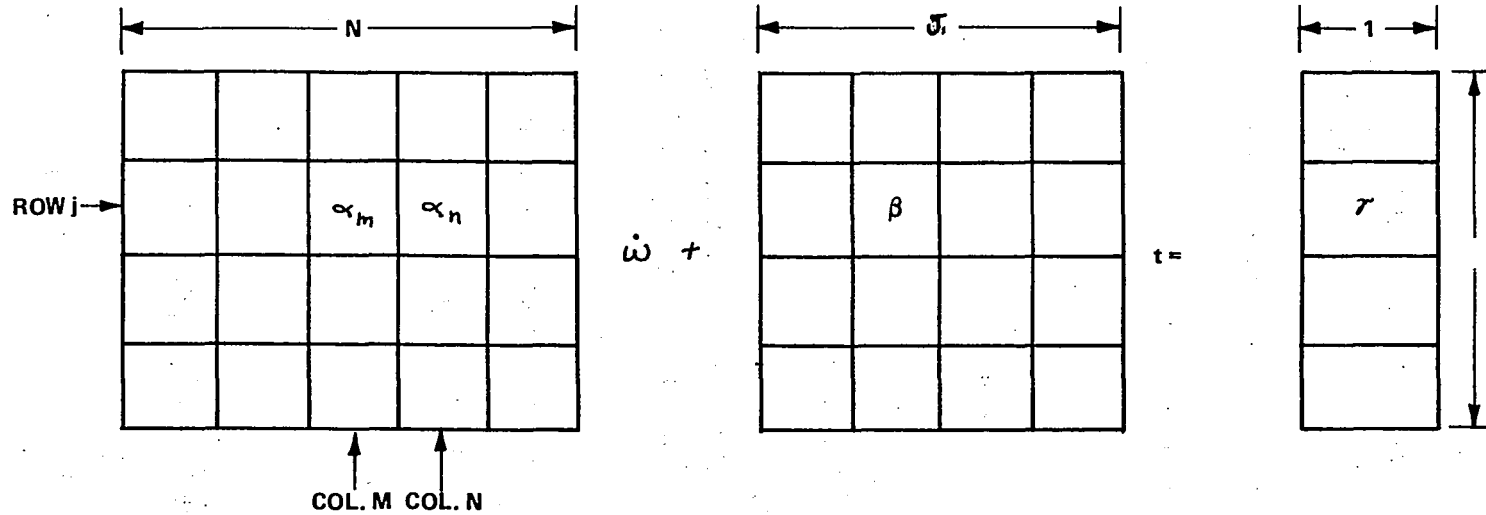
The sliding constraint equation is

$$h t \cdot \left[\ddot{x}_m - \ddot{x}_n - D_m^{-1} (l_m + r_m) \otimes \dot{\omega}_m + D_n^{-1} (l_n + V_n) \otimes \dot{\omega}_n \right] + \lambda (I - hh \cdot) q = V_3$$
$$V_3 = h (t \cdot V_{3_{roll}} - t \cdot V_{REL})$$

$$\dot{\omega} \ + \ \mathsf{t} =$$

		β		

	FREE	$\alpha_m = \alpha_n = 0$	$\beta = I$	$\gamma = 0$
	LOCKED	$\alpha_m = D_m^{-1}$ $\alpha_n = D_n^{-1}$	$\beta = 0$	$\gamma = 0$
				See Eq. 4.16
	PINNED	$\alpha_m = (I\text{-}hh)D_m^{-1}$ $\alpha_n = (I\text{-}hh) D_n^{-1}$	$\beta = (\lambda hh \cdot)$	$\gamma = \left(\omega_n \cdot h_n - \omega_m \cdot h_m\right)D_n^{-1} \ \omega_n \otimes h_n$

Figure 4.17. B_{22}, B_{24} AND V_2 MATRIX ENTRIES FOR JOINT j

$\dot{t}$ is the derivative of the normal vector at the point of contact and $V_{3\,roll}$ is the expression for V_3 used in the rolling constraint. V_{REL} is the relative velocity at the point of contact,

$$V_{REL} = \dot{X}_m - \dot{X}_n + D_m^{-1}\,\omega_m \otimes (\ell_m + r_m) - D_n^{-1}\omega_n \otimes (\ell_n + r_n)$$

The matrix equation for the above constraints

$$B_{31}\ddot{X} + B_{32}\,\dot{\omega} + B_{35}\,\dot{q} = V_3$$

Define L to be the number of these constraints. The matrices B_{31} and B_{32} then will be L x N and B_{35} will be L x L. (See Figure 4.18.)

It should be noted that for the sliding constraint the entries in and B_{32} are not the transposes of the entries in A_{13} and A_{23}. For example, B_{31} has an entry $h\dot{t}$. but A_{13} must have the entry hh. or the entry I (unit matrix)

Flexible Element Constraint

The constraint equation for the flexible element is equation (4.94). The matrix form of this equation is written as
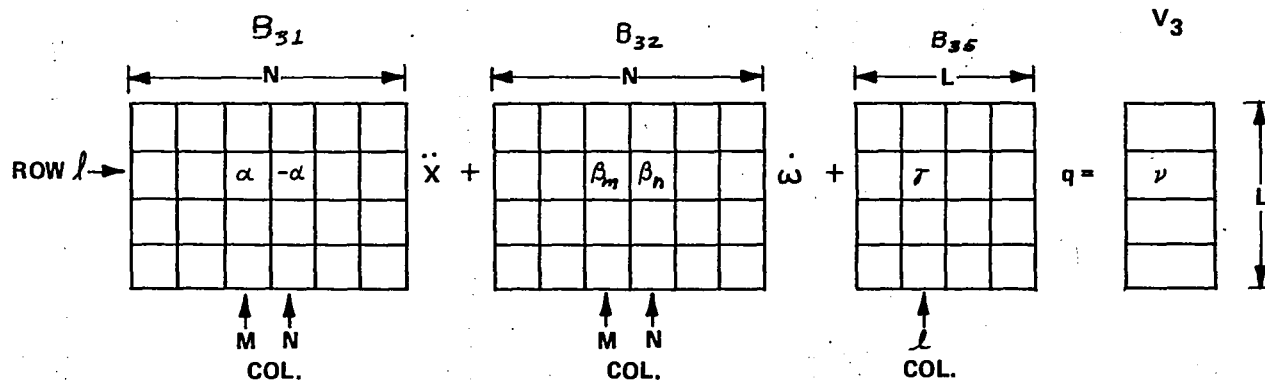
$$B_{42}\,\dot{\omega} = V_4$$

Definition of the System Matrix

The system equations, (4.128 - 4.133) can be written in general matrix form as:

$$S\ddot{X} = u \qquad\qquad (4.134)$$

where S is defined as the system matrix and the components of equation (4.134)

125

ZERO DIST. $\alpha = I$ $\beta_m = -D_m^{-1}(r_m \otimes$
$\beta_n = D_n^{-1}(r_n \otimes$

$\tau = 0$

$\nu = D_n^{-1}[\omega_n \otimes (\omega_n \otimes r_n)]$
$\quad - D_m^{-1}[\omega_m \otimes (\omega_m \otimes r_m)]$

FIXED DIST. $\alpha = h(h \cdot)$ $\beta_m = -h \; h \cdot D_m^{-1}(r_m \otimes$
$\beta_n = h \; h \cdot D_n^{-1}(r_n \otimes$

$\tau = (I - hh \cdot)$

$\nu = h\{h \cdot D_n^{-1}\omega_n \otimes (\omega_n \otimes r_n) -$
$\quad D_m^{-1}(\omega_n \otimes (\omega_m \otimes r_m)]\} - |\dot{\rho}|^2/\alpha\}$

ROLLING $\alpha = I$ $\beta_m = -D_m^{-1}((\ell_m + r_m) \otimes$
$\beta_n = D_n^{-1}((\ell_n + r_n) \otimes$

$\tau = 0$

$\nu_{ROLL} = D_n^{-1}[\omega_n \otimes (\omega_n \otimes (\ell_n + r_n))] + D_n^{-1}\omega_n \otimes r_n$
$\quad - D_m [\omega_m \otimes (\omega_m \otimes (\ell_m + r_m))] - D_m^{-1}\omega_n \otimes r_m$

SLIDING $\alpha = h(t \cdot)$ $\beta_m = -h \; t \cdot D_m^{-1}((\ell_m + r_m) \otimes$
$\beta_n = h \; t \cdot D_n^{-1}((\ell_n + r_n) \otimes$

$\tau = I - hh \cdot$

$\nu = h[t \cdot \nu_{roll} - \dot{t} \cdot V_{REL}]$

WHERE V$_{REL}$ IS THE RELATIVE VELOCITY AT THE POINT OF CONTACT

Figure 4.18. B_{31}, B_{32}, B_{35} and V_3 MATRIX ENTRIES FOR ADDITIONAL CONSTRAINTS

are defined below.

$$
\begin{bmatrix}
M & 0 & A_{11} & 0 & A_{13} & 0 \\
0 & \phi & A_{21} & A_{22} & A_{23} & A_{24} \\
B_{11} & B_{12} & B_{13} & 0 & 0 & 0 \\
0 & B_{22} & 0 & B_{24} & 0 & 0 \\
B_{31} & B_{32} & 0 & 0 & B_{35} & 0 \\
0 & B_{42} & 0 & 0 & 0 & 0
\end{bmatrix}
\begin{bmatrix}
\ddot{x} \\
\dot{\omega} \\
f \\
t \\
g \\
\tau
\end{bmatrix}
=
\begin{bmatrix}
u_1 \\
u_2 \\
v_1 \\
v_2 \\
v_3 \\
v_4
\end{bmatrix}
$$

(4.135)

127

SECTION 5

SOLUTION OF THE SYSTEM EQUATIONS

The system contains 6N+6M+3L equations. The current version is dimensioned to handle 30 segments plus the vehicle and ground with 21 joints and 20 other types of constraints yielding 420 equations.

Due to the large system size, sparse matrix techniques are employed. In addition, since M and $\mathcal{D}$ are diagonal, special subroutines (DAUX$_{ij}$) were written to produce the reduced set of equations involving only the constraints by block reduction of the system equation (4.135)

$$C_{11} f + C_{12} t + C_{13} q + C_{14} \tau = V_1^*$$
$$C_{12} f + C_{22} t + C_{23} q + C_{24} \tau = V_2^*$$
$$C_{13} f + C_{23} t + C_{33} q + C_{34} \tau = V_3^*$$
$$C_{14} f + C_{24} t + C_{34} q + C_{44} \tau = V_4^*$$

The above equations are solved by subroutine FSMSOL which is a routine using a Gauss elimination process specifically designed for sparse matrices of the type encountered in the model. The current version of FSMSOL takes advantage of the symmetry when symmetry exists. Although the equations are written in a symmetrical form, the addition of the sliding constraint and the tension elements destroy symmetry.

After FSMSOL has computed f, t, q, and τ subroutine DAUX computes the linear and angular accelerations from equations (4.54) and (4.55)

5.1   SYMMETRY OPTION

If either of the symmetry modes is exercised modifications are made in DAUX after the contact routines are executed and before the solving

of the system equations for f, t, q and τ. The following tables indicate the specific symmetrical configurations available by specifying elements of the NSYM array and the corresponding modifications in the DAUX routine.

NSYM(J) = o   Normal three dimensional motion for body segment J. Therefore a complete blank card will enable the program to operate in a normal manner.

NSYM(J) = J   The motion of body segment J will be restricted to the x-z plane with no lateral motion. Hence it will be two dimensional.

NSYM(J) = K   Body segments J and K are to remain symmetrical with no lateral motion. The motion of each will be replaced with their average and restricted to the x-z plane. NSYM(K) must be equal to J.

NSYM(J) = -K   Body segments J and K are to remain mirror symmetrical with respect to the x-z plane. Equal but opposite lateral motion is permitted. NSYM(K) must be equal to -J.

NSYM(J)	$f = U1_y, U2_x$ and $U2_z$	$f = U1_x, U1_z$ and $U2_y$
= 0	no change	no change
= J	$f_J = o$	no change
= K(K>J)	$f_J = o$	$f_J = 1/2(f_J + f_K)$
= K(K<J)	$f_J = o$	$f_J = f_K$
= -K(K>J)	$f_J = (f_J - f_K)/2$	$f_J = (f_J + f_K)/2$
= -K(K<J)	$f_J = -f_K$	$f_J = f_K$

* Reference to the x-z plane are to a plane parallel to the x-z inertial plane.

SECTION 6

COMPUTATION OF JOINT TORQUES

For purposes of computing torques at the joint a separate coordinate system is defined for the joint. The joint coordinate system is related to the principal axes of the segment by the standard yaw, pitch and roll angles as displayed in Figure 6.0. Note that the joint coordinates are defined for both segments that are attached at the joint and joint torques are then computed using the relative angular orientation and velocity of these two coordinate systems. These two coordinate systems are fixed in each segment and do not move relative to the segment.

As an example consider the two coordinate systems presented in Figure 6.1. The h_A and h_B displayed there would correspond to the $\hat{\sigma}_3$ and $\hat{\sigma}_2$ axes respectively. The h_A' and h_B' axes would correspond to the $\hat{\sigma}_3'$, $\hat{\sigma}_2'$ axes defined for the adjoining segment.

Joint torques in the program are computed by a choice of three routines. Subroutine VISPR is described in Section 6.1. It is used to compute torques in the standard ball and pin joint. A special model of a mechanical joint termed an Euler joint is described in Section 6.3, Subroutine EJOINT. This is based on the standard Euler angles as displayed in Figure 2.8 using three axes of rotation. Either VISPR or EJOINT may be used with or without the global graphic joint stop representation described in Section 6.2.

The ball or pinned joint may lock. The Euler joint may lock on any combination of its prinicpal axes. If a joint goes from a free to a locked state or if the Euler Joint changes its state (free or locked axes) a special impulse subroutine (IMPLS2) is called to correct the angular velocities of the segments so that the required components of relative angular velocity of the adjoining segments (those connected by the joint) are set to zero.

The ball joint is either free or completely locked. The pinned joint, of course, can lock on only one axis, in which case it is completely locked. The Euler Joint has seven different locked states and one completely free state.

130

The decision to unlock a locked joint is made by comparing the locking torque to an input torque that is prescribed by the user. If the locking torque exceeds the prescribed level, the joint is unlocked. In an Euler Joint, the user may specify a breaking torque on each of the three axes.

The user specifies a minimum torque and a minimum relative angular velocity at which the joint may remain unlocked. If the locking torque or the velocity fall below these specified levels, the joint will relock and the velocities corrected by use of the impulse routine.

The spring functions used to define the restoring torque on the ball pinned, or Euler Joint are defined in Section 6.1. In this definition, a linear torque vs. angle is prescribed until a specified joint stop angle is reached. For angles greater than the joint stop, a quadratic and cubic restoring torque is added. This effectively defines the joint stop as a 'soft' stop instead of a 'hard' stop. That is, the angular motion of the joint may actually exceed the specified stop but a progressively increasing restoring torque will be applied. When the Globalgraphic option is used, the restoring torque can be defined using the general function definitions as described in Section 7.5.

The user has the option of specifying that an impulsive torque be applied when a joint first enters or reenters a stop. In a ball joint, this will be applied on either the flexure or twist axis. For an Euler Joint, this torque will be applied on the particular axis involved. If the Globalgraphic option is used, an impulse may also be specified on the axis determining the Global-graphic equation

$\left(\hat{e}_{1},\hat{e}_{2},\hat{e}_{3}\right) \doteq$ principal axes of the segment

$\left(\hat{\sigma}_{1},\hat{\sigma}_{2},\hat{\sigma}_{3}\right) \triangleq$ joint coordinate system

$\theta_{1} \doteq$ YAW

$\theta_{2} \doteq$ PITCH

$\theta_{3} \doteq$ ROLL
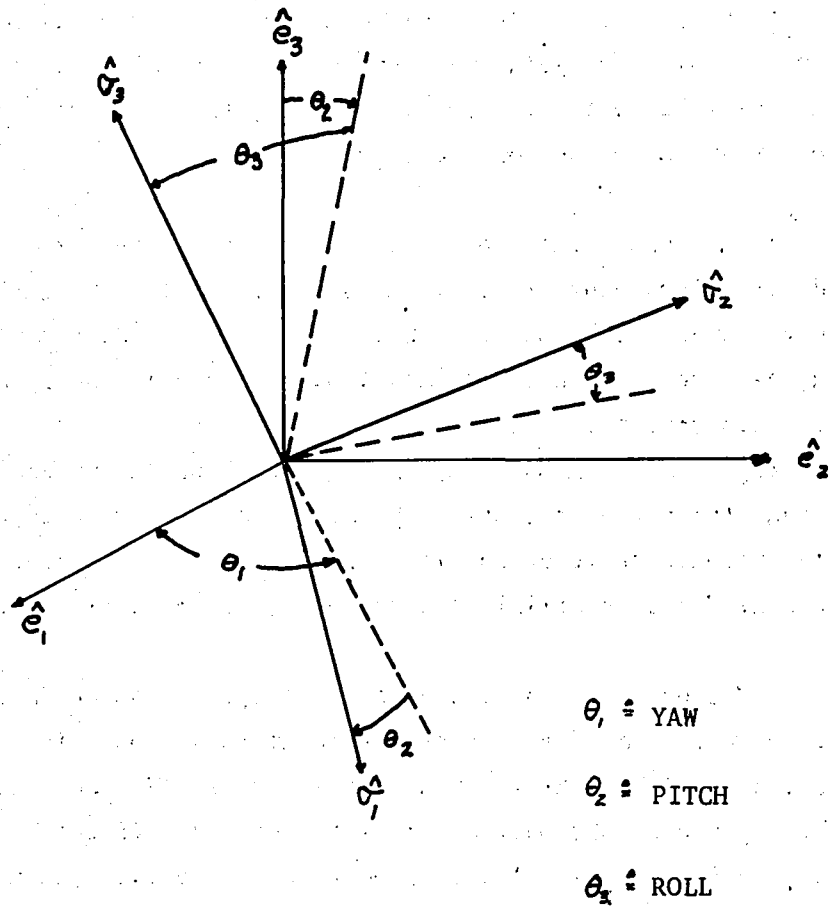
Figure 6.0   DEFINITION OF THE JOINT COORDINATE SYSTEM

132

6.1 SPRING AND VISCOUS TORQUES

Subroutine VISPR computes the torques at the joints as functions of the relative angular orientation and velocity of the adjoining segments. The spring and viscous coefficients specified on the input cards are used for the functional evaluation. The coordinates used for the joint torque computation are illustrated below.
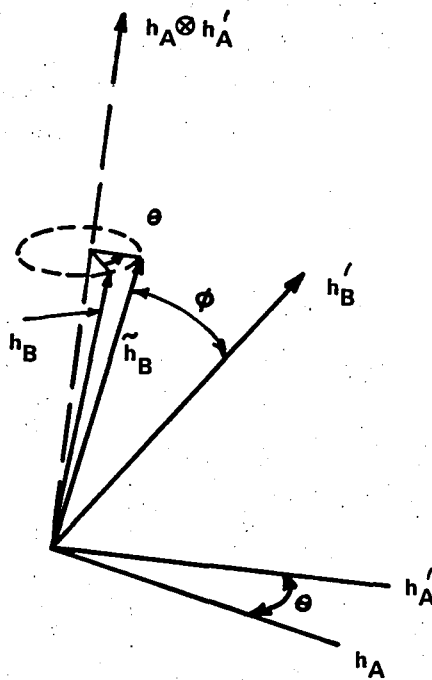

Figure 6.1 JOINT FLEXURE AND TORSION (TWIST)

Two orthogonal unit vectors are associated with each segment at each joint. Let h_A and h_B be the vectors for segment k(k=jnt(j)) and h'_A and h'_B be the vectors for segment j+1. In the rest position (no torques) h_A is aligned with h'_A and h_B is aligned with h'_B. The present input routines allow the user to specify the orientation of these unit vectors with respect to principal co-ordinate system of the segment. Thus, for each joint the user specifies the yaw-pitch and roll angles of the axes of the joint as they are located relative to the prinicpal system of segment k and as they are located relative to the principal system of segment j+1. If all zero angles are specified for any of these segments, the h_A vector will be parallel to the z axis of the segment and the h_B vector will be parallel to the y axis.

The flexure angle (θ) at the joint is computed from the relation:

$$\theta = \cos^{-1}\left(h_A \cdot h'_A\right) \tag{6.1}$$

The magnitude of the flexure torque is computed using the flexure spring co-efficients. The torque vector is parallel to the vector $h_A \otimes h'_A$.

The twist angle (ϕ) may be computed from the relation:

$$\phi = \cos^{-1}\left(\tilde{h}_B \cdot h'_B\right) \tag{6.2}$$

where $\tilde{h}_B$ is the unit vector obtained by rotating h_B through the angle θ about the $h_A \otimes h'_A$ axis. In relation to Euler angles θ is nutation and ϕ is precession plus spin.

The rotation operation is

$$\tilde{h}_B = \left(\mu\mu \cdot h_B + (h_B - \mu\mu \cdot h_B)\right)\cos\theta + \sin\theta\ \mu \otimes h_B$$

where μ is a unit vector in the $h_A \otimes h'_A$ direction.

The magnitude of the twist torque is computed using the torsional spring characteristics. The torque vector is taken along the h'_A axis.

134

For a pinned joint, only the flexure torque is computed.

The present routine computes a viscous torque from the magnitude of the relative angular velocity vector using the flexural viscous characteristics. The torsional viscous characteristics are not used by the present routine. The viscous torque opposes the angular relative velocity.

The spring (and stop) torques are computed by subroutine EFUNCT which uses the following algorithm to compute the torque T from the parameters s_1, s_2, s_3, s_4, and s_5, as illustrated in Figure 6.2.

If $|\theta| \le s_5$

$$T = s_1|\theta|$$

If $|\theta| > s_5$, an additional torque T_s is computed as

$$T_s = s_2(|\theta|-s_5)^2 + s_3(|\theta|-s_5)^3$$

If $\dot{\theta} < 0$ (unloading) T_s is modified by

$$T_s = s_4 T_s$$

For small values of $|\dot{\theta}|$ the routine interpolates between the loading and unloading characteristics.

The total torque $T+T_s$ is returned as the function value.

The coulomb and viscous torque, as illustrated in Figure 6.3, is computed in subroutine VISCOS from the parameters V_1, V_2, V_3 in array VISC. The algorithm uses the following expressions:

$$\text{if } |\dot{\theta}| < V_3, \; Z = V_3/(2-|\dot{\theta}|/V_3); \; \text{if } |\dot{\theta}| > V_3, \; Z = |\dot{\theta}| \qquad (6.3)$$

$$= V_1 + V_2/Z$$

135

where $|\omega|$ is the magnitude of the angular velocity. Thus V_1 is the linear viscous coefficient and V_2 is the constant coulomb torque which is reduced to zero quadratically as $\omega \to 0$. This is done for the purpose of avoiding numerical instability in the integration. These effects need further study.

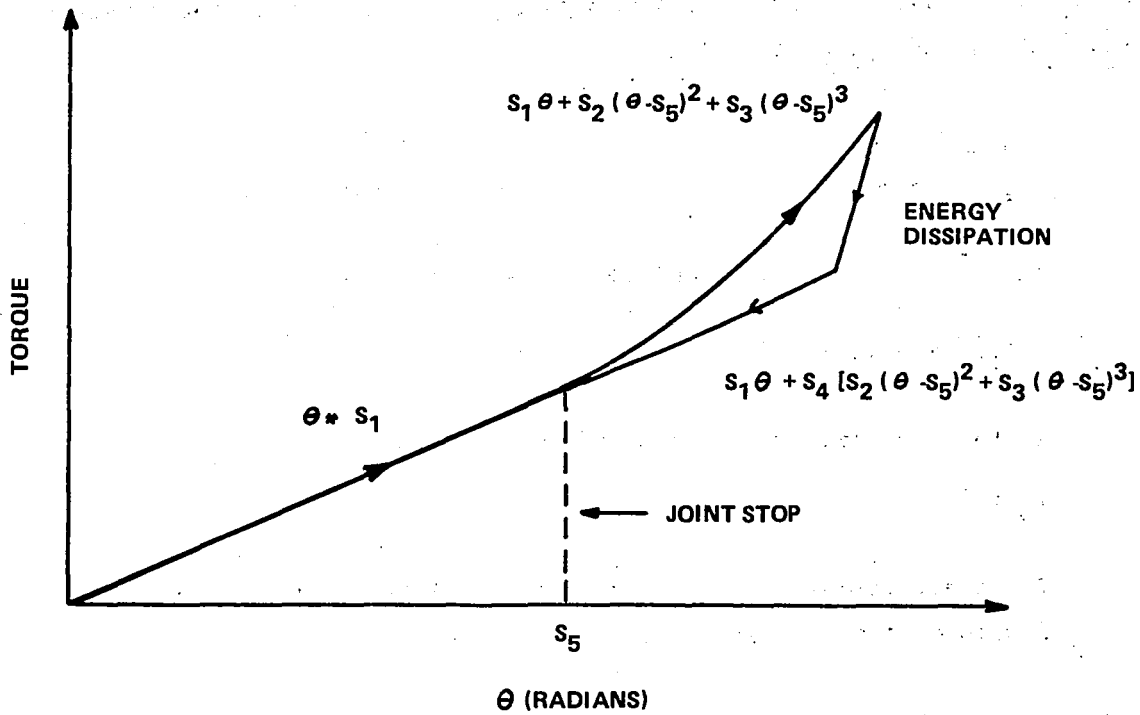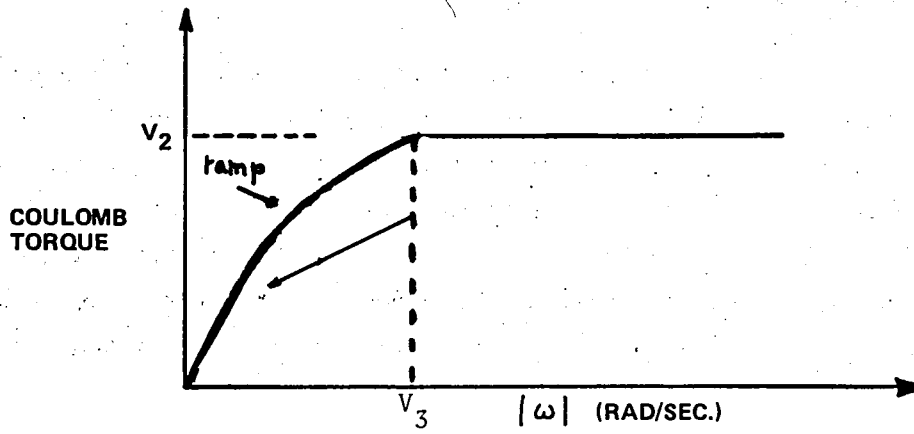Figure 6.2 JOINT SPRING TORQUE

JOINT TORQUE DUE TO RELATIVE ANGULAR VELOCITY AT THE JOINT

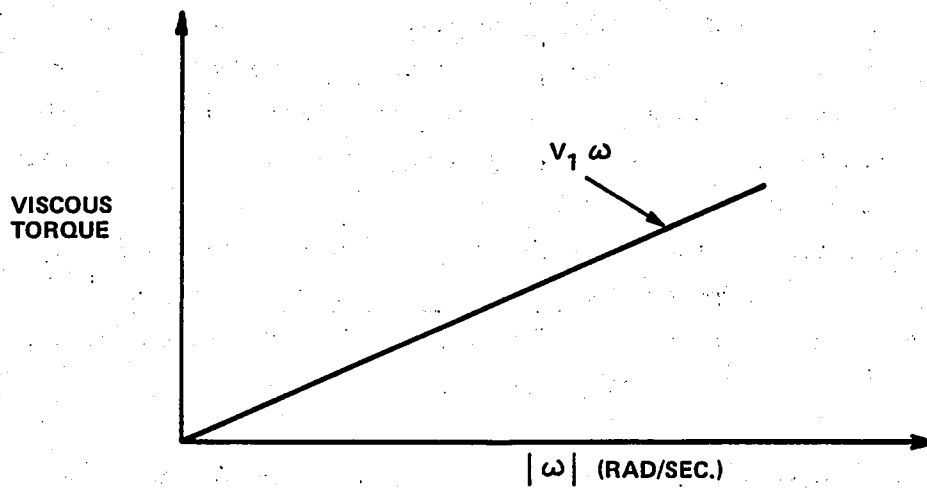ω IS THE RELATIVE ANGULAR VELOCITY

Figure 6.3   JOINT TORQUE DUE TO RELATIVE ANGULAR VELOCITY AT THE JOINT

6.2   JOINT STOP MODEL

6.2.1   General Features

Joints always have definite restrictions on orientation which are
imposed by the internal or external geometry of the joint proper. Two types
of restrictions are recognized. The first type, which limits the number of
degrees of freedom in the joint, can be treated by holonomic constraint rela-
tions, which are discussed elsewhere in this report. This section is concer-
ned with the second type of restriction, which does not limit the number of
degrees of freedom, but which bounds the range(s) of variation of the angle(s)
which express the orientation of the joint. These bounds are usually termed
joint stops (or, on occasion, joint-stop contours when the joint has two or
more degrees of freedom). Since the treatment of such bounds in the case of
hinge joints is covered elsewhere in this report, this section is devoted to
the discussion of such bounds in the case of joints with two or three degrees
of freedom.

It is clear that in the most general case, the bounds on the variation
of a given orientation angle are functions of both of the remaining orienta-
tion angles. For reasons brought out in the next subsection, 6.2.2, the model pre-
sented here is limited to joints for which the bounds on a given orientation
angle depend on only one of the remaining orientation angles. As will be
shown, this restriction of the model leads to a particularly simple descrip-
tion of joint stops in terms of the global-graphic representation. The gen-
eralization of the model for more general types of joint stops awaits future
development.

The next subsection also provides the groundwork for the model
formalism which is developed in the third and fourth subsections. In the
fifth subsection of this section the stop-torque formalism is applied to the
spherical-coordinate representation of the joint-stop contour.

6.2.2   The Global-Graphic Representation

A joint connects two members which are here designated Segment 1 and Segment 2. The orientation of the joint is completely prescribed by the specification of this orientation of Segment 2 relative to Segment 1. Figure 6.4 depicts three orthogonal unit vectors, $\hat{\sigma}_1$, $\hat{\sigma}_2$, $\hat{\sigma}_3$ which are fixed rigidly in Segment 1, and a unit vector, $\vec{r}$, which is fixed rigidly in Segment 2.
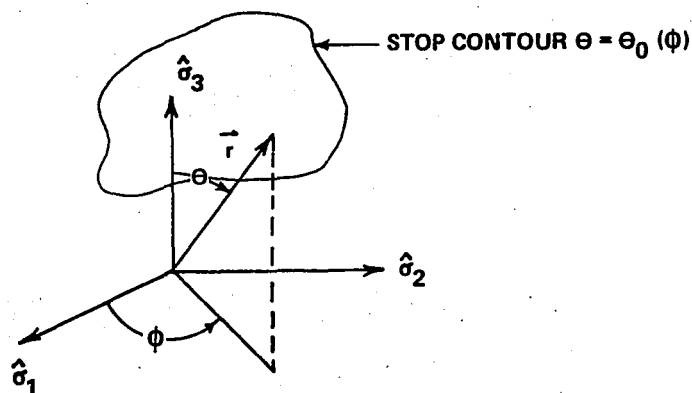
Figure 6.4 JOINT STOP COORDINATES

The orientation of $\vec{r}$ relative to 1 is completely determined by the spherical-coordinate angles θ and ϕ. More generally, the orientation of $\vec{r}$ can be specified by two independent coordinates, u_1, u_2 which are functions of θ and ϕ.

If the joint has two degrees of freedom its orientation is completely determined by the orientation of $\vec{r}$; further, any bounds on the orientation of $\vec{r}$ are functions only of u_1 and u_2. In this case, the bounds on the orientation of $\vec{r}$ can be represented by a single closed contour on the surface of a unit sphere which is centered at the joint. This representation of the joint stops is termed the global-graphic representation.

139

If the joint has three degrees of freedom, its orientation is not solely determined by the orientation of $\overline{r}$, but requires additionally the specification of the relative orientation of a second unit vector, $\overline{s}$, which is fixed rigidly in body 2 and which is noncolinear with $\overline{r}$. Further, the complete specification of the relative orientations of $\overline{r}$ and $\overline{s}$, depends upon three coordinates u_1, u_2, u_3. As before, the orientation of $\overline{r}$ is still a function only of u_1 and u_2. However, (depending on the joint geometry), bounds or stops on the orientation of $\overline{r}$ can be functions of <u>all three coordinates</u> u_1, u_2, u_3. In this case the global graphic representation of the stops on $\overline{r}$ would consist of a family of closed contours on the unit sphere, with u_3 as the parameter of the family. A similar representation could be introduced for stops on the orientation of $\overline{s}$.

As indicated in the first subsection, the joint stop model considered here is limited to joints for which the bounds on the orientation of $\overline{r}$ are functions only of u_1 and u_2. Also the model does not contain provisions for including those bounds on the orientation of $\overline{s}$ which are distinct from bounds on the orientation of $\overline{r}$.

In applying the model, it is important that the coordinate system $\hat{\sigma}_1$ $\hat{\sigma}_2$ $\hat{\sigma}_3$ and the unit vector $\overline{r}$ are chosen so that the reference orientation (see Figure 6.4) is within the joint-stop contour. Also, it is necessary that when contour is expressed in the form

$$\theta = \theta_o \left(\phi \right) \qquad\qquad 6.1$$

$\theta_o(\phi)$ is a single-valued function of ϕ. Fortunately this condition is satisfied by the joints of interest. The version of the model which is presently programmed (and which is discussed in the subsection 6.2.5) employs the representation in (6.1) for the joint-stop contour. However, the more general model developed in the fourth subsection is not limited to the representation in (6.1). It is based on the employment of any coordinates u_1, u_2 which are adequate for the specification of the orientation of $\overline{r}$. For example, if the

140

stop contour bounded θ in the range $0 \le \theta \le \frac{\pi}{2}$, one could employ

$$u_1 = \vec{r} \cdot \hat{e}_1$$
$$u_2 = \vec{r} \cdot \hat{e}_2$$

Or, more generally, u_1 could be equated to $\vec{r} \cdot \hat{e}_3$, and u_2 would be identified with $\vec{r}, \hat{e}_2$ for some ranges of orientation of $\vec{r}$, and with $\vec{r}, \hat{e}_1$ for other ranges of orientation of $\vec{r}$. This particular choice of coordinates would lead to a more complicated representation of joint-stop contour than the employment of the coordinates θ and ϕ. However, the evaluation of arctangents would be avoided, and so computer running time might be reduced.

Throughout the development, the equation

$$f(u_1, u_2) = 0$$

(6.2)

is employed for the joint-stop contour. This contour represents a hard stop. As in the case of the hinge joint, the hard stop is replaced by a soft stop. That is, no stop torque is applied to the joint when the terminal point of $\vec{r}$ is contained within the joint-stop contour in (6.2). But when the terminal point of $\vec{r}$ is outside the joint-stop contour in (6.2) a stop torque is applied to the joint. This torque acts in such a direction to tend to restore the terminal point of $\vec{r}$ to the region inside the joint-stop contour; and the magnitude of the torque increases with the extent of penetration of the terminal point of $\vec{r}$ into the region <u>outside</u> the joint-stop contour. The general approach which is taken to obtain a stop torque with the desired characteristics is brought out in the remainder of this subsection. The detailed development is given in the following subsections.

The stop torque, $\vec{M}$, can be expressed as the sum of stop torques in the direction of and perpendicular to the unit vector $\vec{r}$. It is clear that a stop torque in the direction $\vec{r}$ tends only to produce rotations of about the $\vec{r}$ axis. Such rotations could not restore the terminal point of $\vec{r}$ to the region inside the joint-stop contour hence is not applied. It is clear, therefore, that M should be perpendicular to $\vec{r}$. This perpendicularity is assumed by the relation:

$$\vec{M} = \vec{r} \otimes \vec{F} \qquad\qquad (6.3)$$

It is convenient to visualize $\vec{F}$ as a force applied at the terminal point of $\vec{r}$. In actuality, of course, the desired restoring action is obtained by applying the torque $\vec{M}$ to Segment 2 and a torque $-\vec{M}$ to Segment 1.

The force $\vec{F}$ which is required to obtain restoring action is not unique. First, it is apparent from (3) that components of $\vec{F}$ which are parallel to $\vec{r}$ do not contribute to $\vec{M}$. Therefore, $\vec{F}$ will be chosen perpendicular to $\vec{r}$. In the case of a hard stop, $\vec{F}$ could (conceptually, at least) have components parallel to the joint-stop contour. On the basis of symmetry arguments, such components would not in general serve a useful function. Therefore, $\vec{F}$ would be chosen in a direction perpendicular to the joint-stop contour. In the generalization to a soft stop, it is logical to choose $\vec{F}$ in a direction which is close to perpendicular to that portion of the joint-stop contour which is nearest to the terminal point of $\vec{r}$. In accord with the desired characteristics of the torque, $\vec{M}$, the magnitude of the force, $\vec{F}$, should increase with the extent of penetration of the terminal point of $\vec{r}$ into the region outside of the joint-stop contour. The joint-stop model has been designed so that the force $\vec{F}$, displays the characteristics just discussed. The model is described in the following:

The function $f(u_1, u_2)$ is defined so that

(i) $f(u_1, u_2) = 0$ on the joint-stop contour

(ii) The contour $f(u_1, u_2) = c$ encloses or is enclosed by the contour $f(u_1, u_2) = 0$. (That is, these contours do not intersect)

(iii) On the contour $f(u_1, u_2) = \theta$ is a single valued function of ϕ.

(iv) The surface gradient of $f(u_1, u_2)$ is in the direction of the external normal to the contour.

142

Figure 6.5 depicts the geometry for the determination of the force $\vec{F}$. This figure shows polar ($\theta \, vs \, \phi$) plots of the contours of interest.
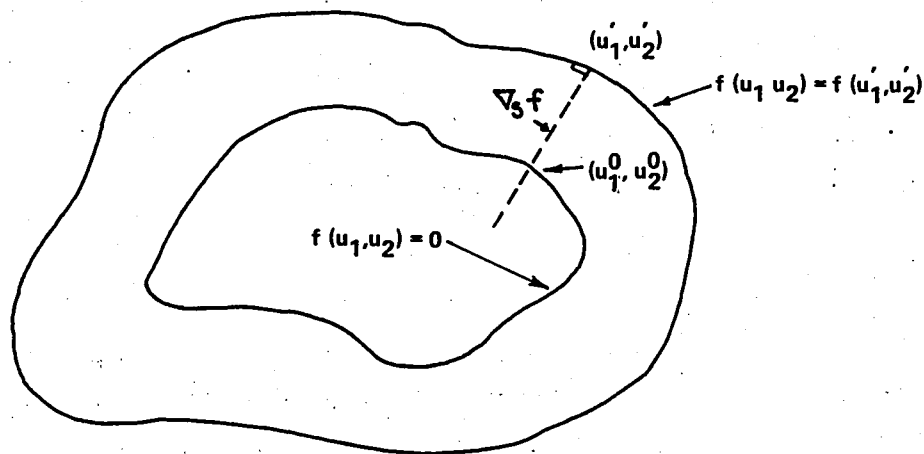
Figure 6.5 JOINT STOP CONTOURS

u_1', u_2' denote the coordinates of $\vec{r}$. The force $\vec{F}$ is obtained from a differential approximation to the construction described in the next paragraph.

Through the point (u_1', u_2') the contour

$$f(u_1, u_2) = f(u_1', u_2')$$

(6.4)

can be constructed. Then a geodesic of the sphere (depicted by a broken line in the figure) can be constructed to pass through the point (u_1', u_2') and to be perpendicular to the contour in (6.4) at the point. The geodesic will intersect the joint-stop contour ($f(u_1, u_2) = 0$) at some point (u_1^o, u_2^o). The force $\vec{F}$ is parallel to the geodesic tangent at the point (u_1', u_2')(and in the opposite direction to the external normal to the contour in (6.4) at the point (u_1', u_2')). The magnitude of the force $\vec{F}$ is an increasing function of the magnitude of the vector $\Delta \vec{r}$ given by

$$\Delta \vec{r} = \vec{r}(u_1', u_2') - \vec{r}(u_1^o, u_2^o)$$

(6.5)

143

In the model, the force $\vec{F}$ is obtained exactly as just described with the exception that $(u_1' - u_1^o)$ and $u_2' - u_2^o$ are treated as differentials, and $\Delta \vec{r}$ and $f(u_1', u_2') - f(u_1^o, u_2^o)$) are evaluated in the differential approximation.

As a preliminary to the mathematical development of the model, an expression will be derived for the surface gradient in terms of the general coordinates u_1, u_2.

6.2.3 The Surface Gradient

The surface gradient is just the operator $-\vec{n} \otimes (\vec{n} \otimes \nabla)$ where ∇ denotes the usual three-dimensional gradient operator, and $\vec{n}$ is the normal to the surface of interest. In the current application $\vec{n}$ is equated to $\vec{r}$. It is convenient to employ the <u>modified</u> surface-gradient operator given by

$$\nabla_S = -\vec{r}\,\vec{r} \otimes \left(\vec{r} \otimes \nabla\right)$$

$$(6.6)$$

where $\vec{r}$ denotes the radius of the spherical surface. In the case of the unit sphere , $\vec{r} = 1$. Thus, for simplicity, in the rest of this section $\nabla_S f$ will be termed the surface gradient of f .

The fundamental property of the surface gradient which is utilized in the model is that the vector given by

$$\nabla_S f\left(u_1, u_2\right) \Big|_{u_1 = u_1', \, u_2 = u_2'}$$

is normal to $\vec{r}$ and to the contour

$$f\left(u_1, u_2\right) = f\left(u_1', u_2'\right)$$

$$(6.7)$$

at the point $u_1 = u_1', u_2 = u_2'$. As stated in the previous subsection, $f(u_1 u_2)$ must be chosen so that $\nabla_S f$ evaluated at (u_1' , u_2') is in the direction of the <u>exterior</u> normal to the contour in (6.7).

The surface gradient of any differentiable function V of u_1 and u_2 satisfies

$$dV = d\vec{r} \cdot \nabla_s V \tag{6.8}$$

where dV is the total differential of V and $d\vec{r}$ is the total differential of $\vec{r}$. $d\vec{r}$ is expressible as a function of u_1 and u_2. Its total differential may be expressed

$$d\vec{r} = \vec{a}_1 du_1 + \vec{a}_2 du_2 \tag{6.9}$$

where

$$\vec{a}_i = \frac{\partial \vec{r}}{\partial u_i} \qquad i = 1, 2 \tag{6.10}$$

The unitary vectors, $\vec{a}_i$, are not in general orthogonal. Thus, in accord with the formalism for nonorthogonal curvilinear coordinates, reciprocal unitary vectors $\vec{a}^j (j = 1, 2)$ are introduced. These vectors are coplanar to the vectors $\vec{a}_i (i = 1, 2)$ and they satisfy

$$\vec{a}_i \cdot \vec{a}^j = \delta_{ij} \tag{6.11}$$

where δ_{ij} denotes the Kronecker delta.

From (6.8),(6.9), and (6.11), it is readily concluded that

$$\nabla_s V = \vec{a}^1 \frac{\partial V}{\partial u_1} + \vec{a}^2 \frac{\partial V}{\partial u_2} \tag{6.12}$$

Equation (6.12) is the general expression for the surface gradient of a function V of u_1 and u_2.

145

6.2.4 The Mathematical Formulation

     This subsection is devoted to the mathematical development of the stop-torque model described in the second subsection. As before, $u_1{}', u_2{}'$ denote the coordinates of $\vec{r}$, and u_1^o, u_2^o , denote the coordinates of the intersection of the joint-stop contour with the geodesic depicted in Figure (6.3). From (6.5).

$$\Delta \vec{r} = \vec{r}\left(u_1{}', u_2{}'\right) - \vec{r}\left(u_1^o, u_2^o\right) \tag{6.13}$$

As explained in subsection 6.2.2, $\Delta \vec{r}$ is evaluated in the differential approximation. From (6.9) and (6.13)

$$\Delta \vec{r} = \vec{a}_1 \Delta u_1 + \vec{a}_2 \Delta u_2 \tag{6.14}$$

where

$$\Delta u_i = u_i{}' - u_i^o \tag{6.15}$$

and $\vec{a}_i$ is evaluated at $(u_1{}', u_2{}')$.

     Since (u_1^o, u_2^o) lies on the joint-stop contour,

$$f\left(u_1^o, u_2^o\right) = 0$$

or, employing (6.15)

$$f\left(u_1{}' - \Delta u_1, u_2{}' - \Delta u_2\right) = 0 \tag{6.16}$$

In the differential approximation, (6.16) becomes

$$\frac{\partial f\left(u_1{}', u_2{}'\right)}{\partial u_1{}'} \Delta u_1 + \frac{\partial f\left(u_1{}', u_2{}'\right)}{\partial u_2{}'} \Delta u_2 = f\left(u_1{}', u_2{}'\right) \tag{6.17}$$

     The exterior normal at the point ($u_1{}', u_2$) of the contour

$$f\left(u_1, u_2\right) = f\left(u_1{}', u_2{}'\right)$$

is in the direction of the surface gradient $\nabla_S f(u_1', u_2')$. From (6.12)

$$\nabla_S f(u_1', u_2') = \vec{a}^1 \frac{\partial f}{\partial u_1'} + \vec{a}^2 \frac{\partial f}{\partial u_2'} \qquad (6.18)$$

Where $\vec{a}^j$ is evaluated at (u_1', u_2').

Now, $\Delta \vec{r}$ is the chord of the geodesic depicted in Figure 6.5. Therefore, in the differential approximation, $\Delta \vec{r}$ is directed parallel to the surface gradient in (6.18). This condition and (6.17) uniquely determines Δu_1 and Δu_2. To evaluate Δu_1 and Δu_2, (6.11) is employed to reexpress (6.14) in this form (dot $\bar{a}_1$ and $\bar{a}_2$ with 6.14 to get coefficients of $\vec{a}^1$ and $\vec{a}^2$)

$$\Delta \vec{r} = \left[\vec{a}_1 \cdot \vec{a}_1 \Delta u_1 + \vec{a}_2 \cdot \vec{a}_1 \Delta u_2 \right] \vec{a}^1$$
$$+ \left[a_1 \cdot \vec{a}_2 \Delta u_1 + \vec{a}_2 \cdot \vec{a}_2 \Delta u_2 \right] \vec{a}^2 \qquad (6.19)$$

In the expressions for the final solution, the superscript 1 on u_1^1, u_2^1 is dropped so that u_1, u_2 are the coordinates of $\vec{r}$. The stop torque, $\vec{M}$, defined in the second subsection, is given by

$$\vec{M} = 0 \quad \text{if } (u_1, u_2) \text{ is within the joint-stop contour} \qquad (6.20)$$

$$\vec{M} = -A\left(/\Delta \vec{r}/\right) \frac{\vec{r} \otimes \Delta \vec{r}}{/\Delta \vec{r}/} \quad \text{otherwise}$$

$A\left(/\Delta \vec{r}/\right)$ denotes a suitably chosen non-negative, increasing function of the magnitude $/\Delta \vec{r}/$ of $\Delta \vec{r}$, which is given by

$$\Delta \vec{r} = \vec{a}_1 \Delta u_1 + \vec{a}_2 \Delta u_2 \qquad (6.21)$$

The unitary vectors $\vec{a}_i$ are defined in the previous subsection, and

$$\Delta u_1 = \frac{\left[a_{22} f_1 - a_{12} f_2 \right] f}{\left[a_{22} f_1^2 - 2 a_{12} f_1 f_2 + a_{11} f_2^2 \right]} \qquad \Delta u_2 = \frac{\left[a_{11} f_2 - a_{12} f_1 \right] f}{\left[a_{22} f_1^2 - 2 a_{12} f_1 f_2 + a_{11} f_2^2 \right]} \qquad (6.22)$$

147

$$f = f(u_1, u_2)$$

$$f_i = \partial f / \partial u_i \qquad i = 1,2$$

$$a_{ij} = \vec{a}_i \cdot \vec{a}_j \qquad i,j = 1,2$$

The conditions on the function $f(u_1, u_2)$ are given in the second subsection of this development.

In the next subsection, $\vec{M}$ is evaluated for the coordinates θ and ϕ.

6.2.5 Application to Spherical Coordinates

In the computer program, the spherical coordinate representation
$$\theta = \theta_o(\phi)$$
is employed for the joint-stop contour. To evaluate the stop torque, $\vec{M}$, in the coordinates θ, ϕ the formalism of the above subsection is applied with

$$u_1 = \theta \,, \quad u_2 = \phi$$

$$\vec{a}_1 = \hat{\theta} \,, \quad \vec{a}_2 = \hat{\phi} \sin\theta$$

$$f(u_1, u_2) = \theta - \theta_o(\phi)$$

Here $\hat{\theta}$ denotes a unit vector in the direction of increasing θ and $\hat{\phi}$ denotes a unit vector in the direction of increasing ϕ .

The evaluation of $\vec{M}$ is straightforward. The final expression is:

for $\quad 0 \leq \theta_o(\phi)$, $\qquad \vec{M} = -\dfrac{A(|\Delta\vec{r}|)(\hat{\phi}\sin\theta + \hat{\theta}\,\theta_o')}{\sqrt{\sin^2\theta + (\theta_o')^2}}$

and for $\quad 0 > \theta_o(\phi)$, $\vec{M} = 0$

where $\qquad \theta_o' = \dfrac{\partial \theta_o(\phi)}{\partial \phi}$

$$|\Delta\vec{r}| = \left[\theta - \theta_o(\phi)\right]\sin\theta \Big/ \sqrt{\sin^2\theta + (\theta_o')^2}$$

The non-negative function $A(|\Delta\vec{r}|)$ is computed by employing the force versus deflection subroutine in the computer program. As noted above, the torque $\vec{M}$ is applied to body 2 and a torque $-\vec{M}$ is applied to body 1.

6.2.6 Stop Contour

The representation of the stop contour is taken from the work of Dr. R.E. Herron where he uses a trigonometric polynomial of the form.[*]

$$\theta_0 (\phi) = \sum_{n=1}^{N} \cos^{n-1} \phi \left(C_{2n-1} + C_{2n} \sin \phi \right)$$

The degree of θ depends on the particular joint. Stop contours and the corresponding numerical values for the coefficients as supplied by the Biostereometrics Laboratory of the Texas Institute for Rehabilitation and Research are presented in Figures 6-6 thru 6-14.

---

[*] See equation 11 pg 40 of Reference 14.

Polynomial
Coefficients
Of Envelope

1	0.1178192746D 01
2	0.5256826831D - 01
3	0.2205680734D- 01
4	-0.6080622115D - 01
5	-0.7495043784D 00
6	-0.3721774873D 00
7	-0.7770362813D - 01
8	0.5596024691D - 01
9	0.2758183454D 00
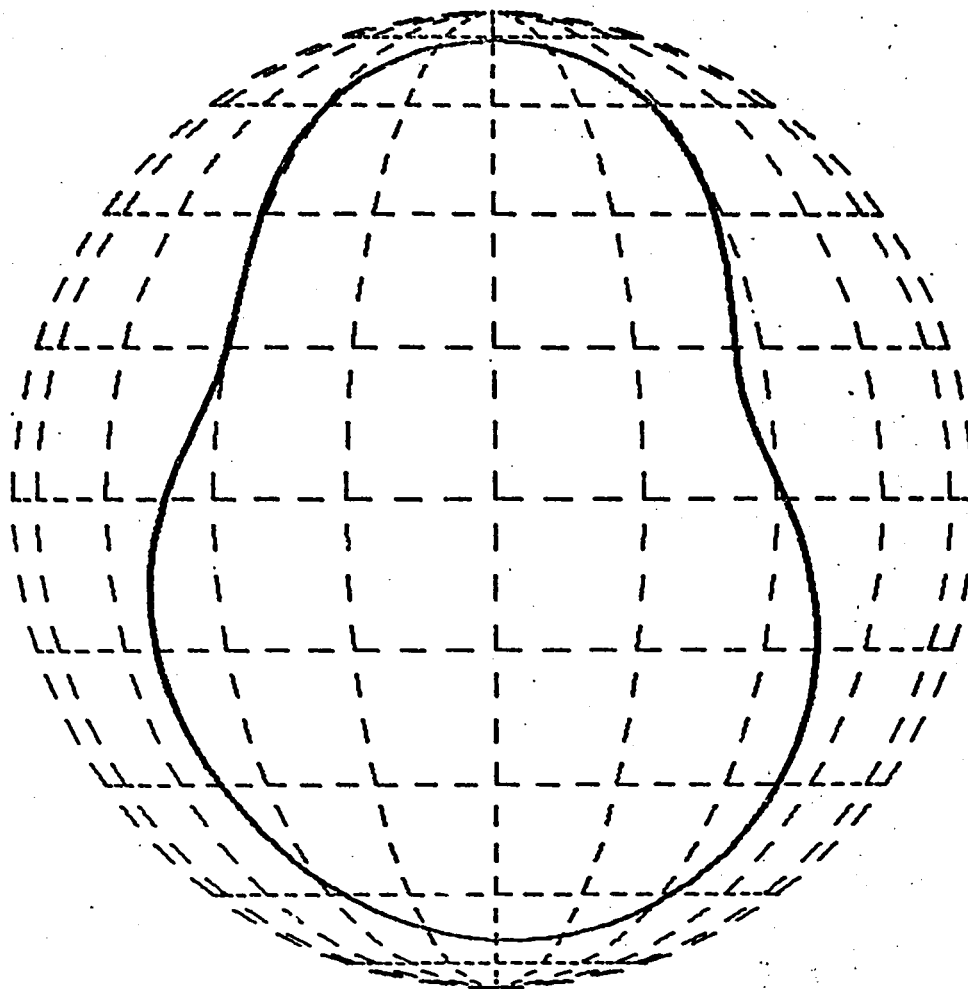
GLOBOGRAPHIC DESCRIPTION OF JOINT SINUS SHOULDER

FIGURE 6.6

Polynomial
Coefficients
Of Envelope

1   0.9133825523D 00
2   0.7077697944D-01
3 -0.6927252967D-02
4 -0.1802609949D-01
5 -0.3069872675D 00
6 -0.2363953324D 00
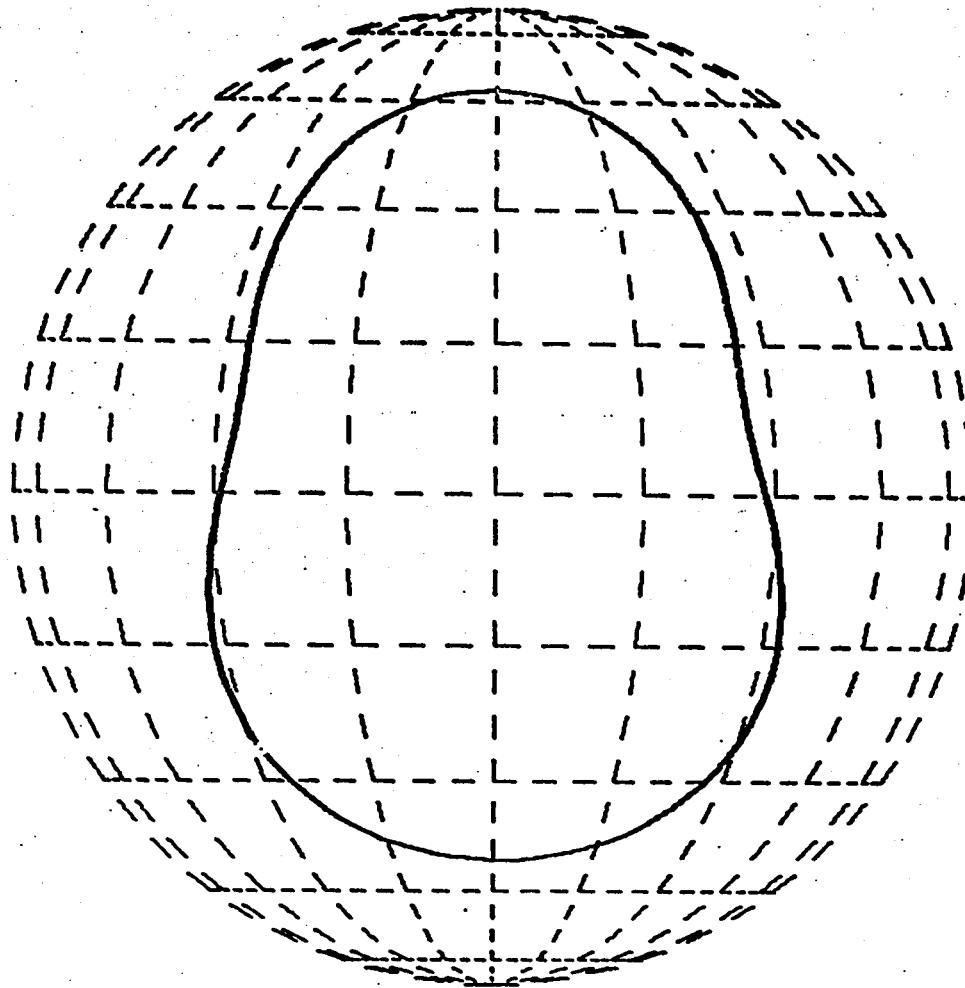
GLOBOGRAPHIC DESCRIPTION OF JOINT SINUS WRIST

FIGURE   6.7

Polynomial
Coefficient
Of Envelope

1   0.1014025777D 01
2   0.7702397177D-02
3   0.7838368820D-01
4 -0.3089546611D -01
5 -0.2201073048D 00
6 -0.4947257259D-02
7 -0.1662438636D 00
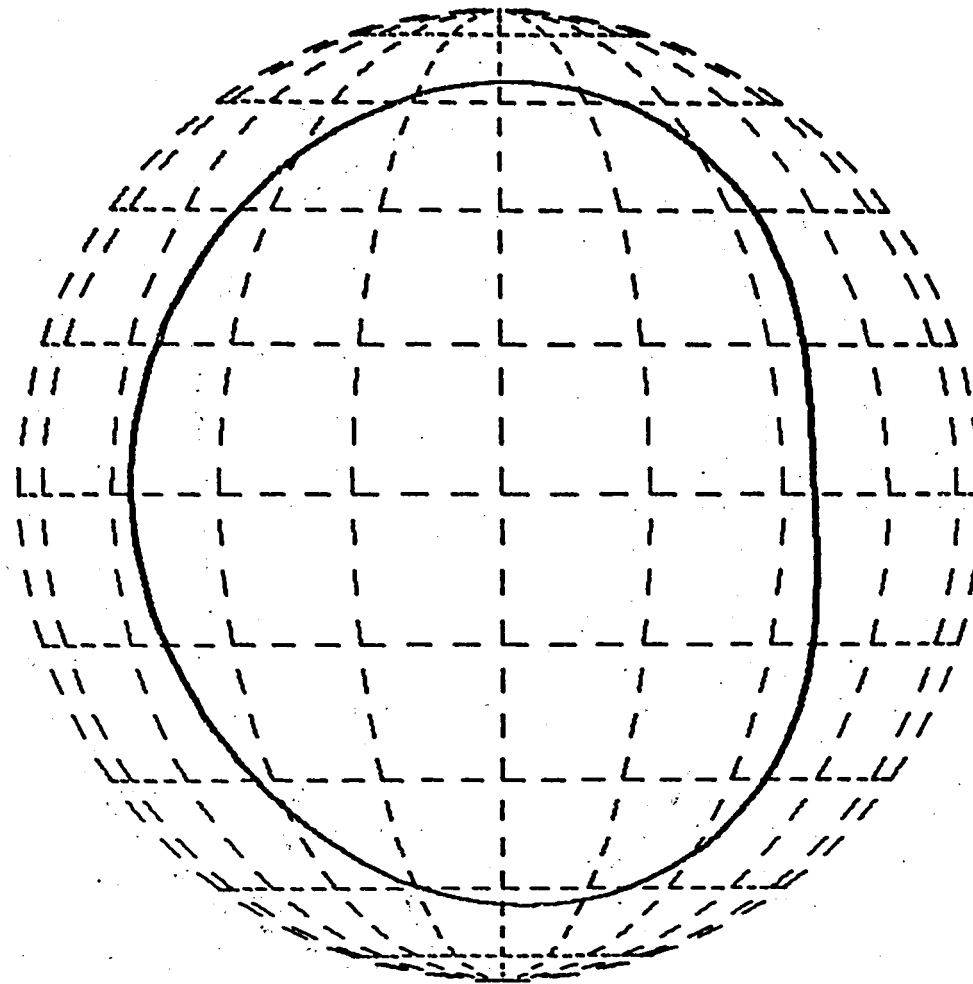
GLOBOGRAPHIC DESCRIPTION OF JOINT SINUS ELBOW

FIGURE   6.8

Polynomial
Coefficient
Of Envelope

1   0.7507378074D   00
2   0.2541109524D - 01
3 -0.1462134894D   00
4   0.1483473597D   00
5 -0.1229647095D   00
6 -0.3318729303D - 01
7   0.2079118345D   00
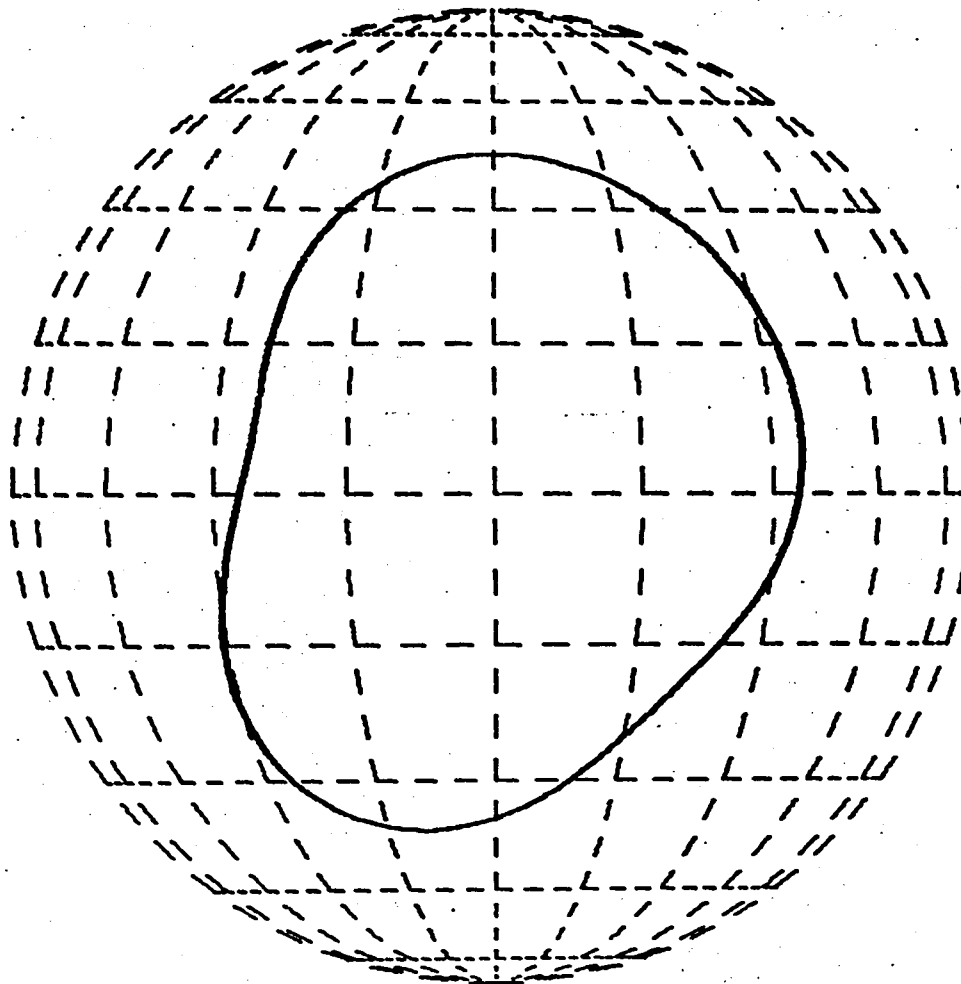
GLOBOGRAPHIC DESCRIPTION OF JOINT SINUS ANKLE

FIGURE 6.9

Polynomial
Coefficient
Of Envelope

1	0.5236919132D 00
2	0.9627570647D-01
3	0.3538946830D 00
4	-0.1790400355D-01
5	0.1411701119D 00
6	0.2673494846D 00
7	-0.4270560352D 00
8	-0.8629601954D-01
9	0.3372349196D 00
10	-0.5424383277D 00
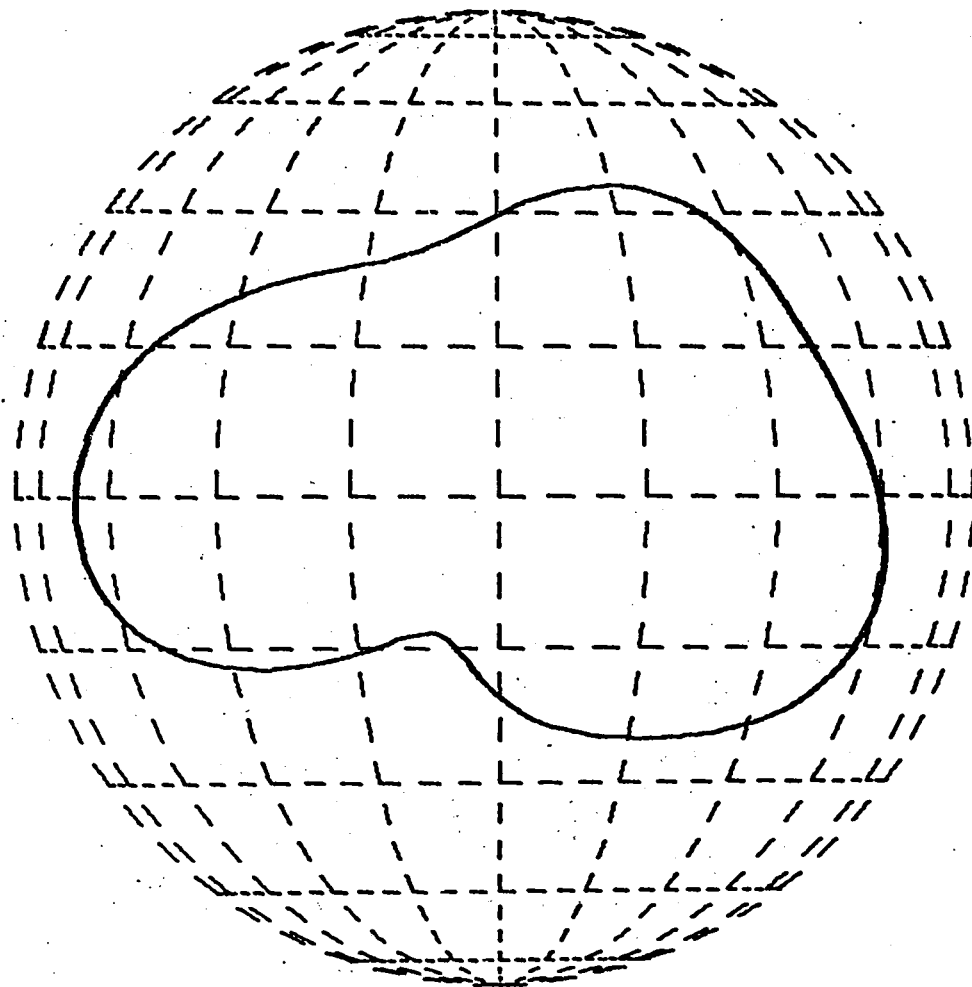
GLOBOGRAPHIC DESCRIPTION OF JOINT SINUS KNEE

FIGURE 6.10

Polynomial
Coefficient
Of Envelope

1	0.4180794933D 00
2	0.3019400526D-02
3	-0.4991239637D-01
4	-0.9908697133D-01
5	0.3609323951D-00
6	-0.5650999723D-01
7	0.6113666808D-01
8	-0.7913587292D-01
9	-0.2706717721D 00
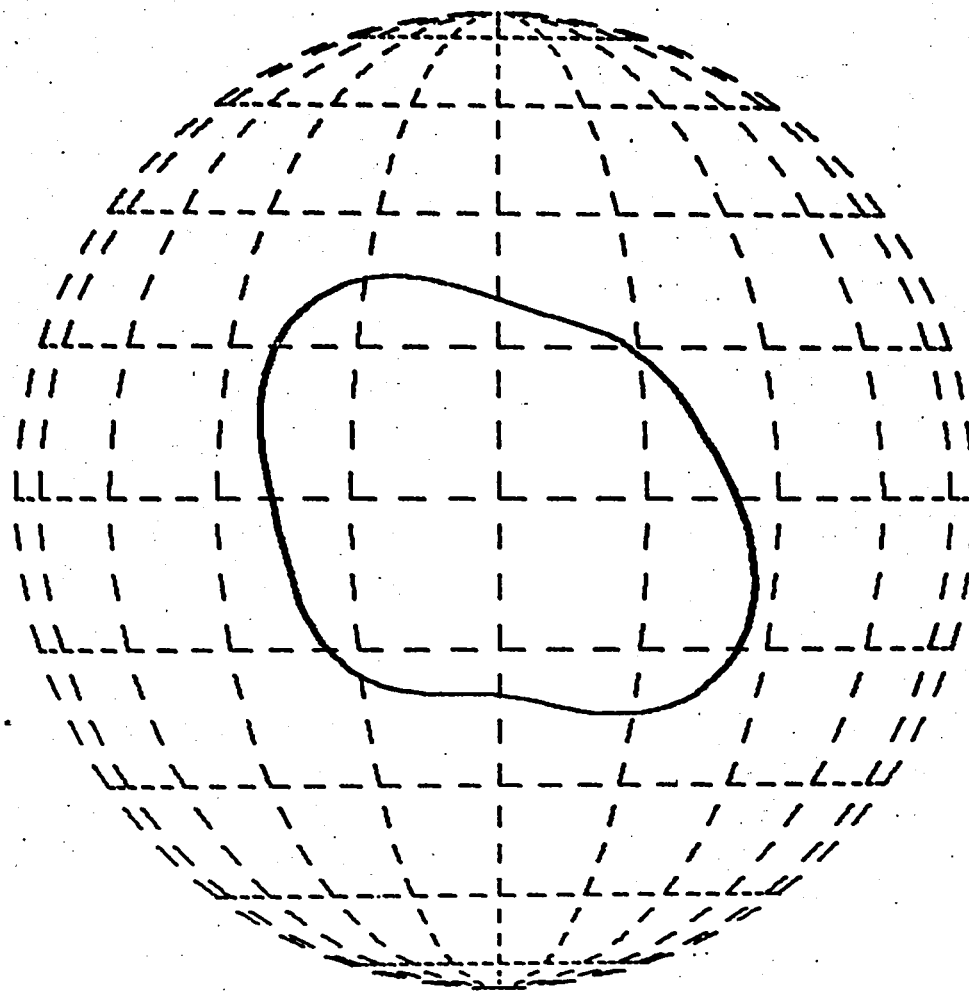
GLOBOGRAPHIC DESCRIPTION OF JOINT SINUS HIP

FIGURE 6.11

GLOBOGRAPHIC DESCRIPTION OF JOINT SINUS LUMBAR PIVOT

FIGURE 6.12

Polynomial
Coefficient
Of Envelope

1   0.4706707921D 00
2   -0.7015183779D -02
3   -0.1127470633D -01
4   0.1717095553D 00
5   0.2567280845D 00

156

Polynomial
Coefficient
Of Envelope

1	0.1090517284D	01
2	0.1502519396D	-01
3	-0.7417370842D	-01
4	0.1947527865D	00
5	0.4326310319D	00
6	-0.2240639189D	00
7	0.1825421568D	00
8	-0.2655333031D	00
9	-0.3454897556D	00
10	0.3462342717D	00
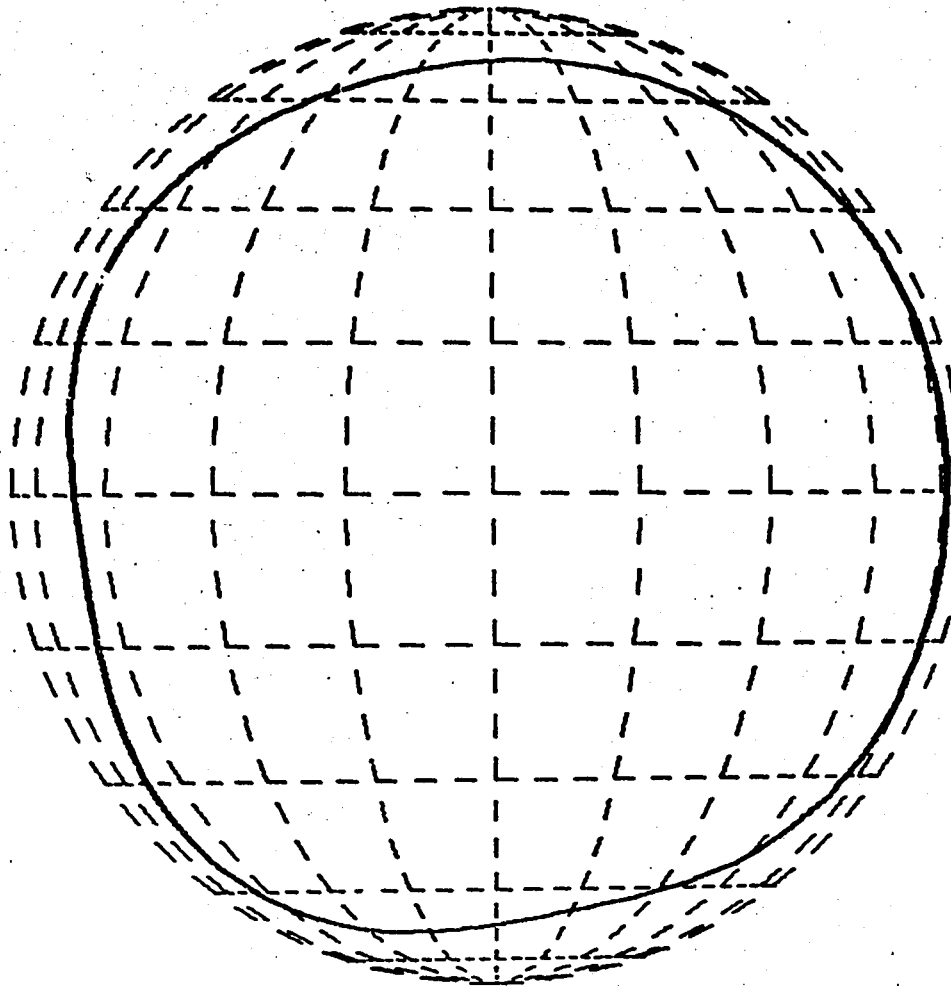
GLOBOGRAPHIC DESCRIPTION OF JOINT SINUS COLLAR BONE

FIGURE 6.13

Polynomial
Coefficient
Of Envelope

1   0.6990754441D 00
2   0.2907723195D -01
3   0.4716935001D -03
4   0.2755491672D -02
5   0.1740819131D 00
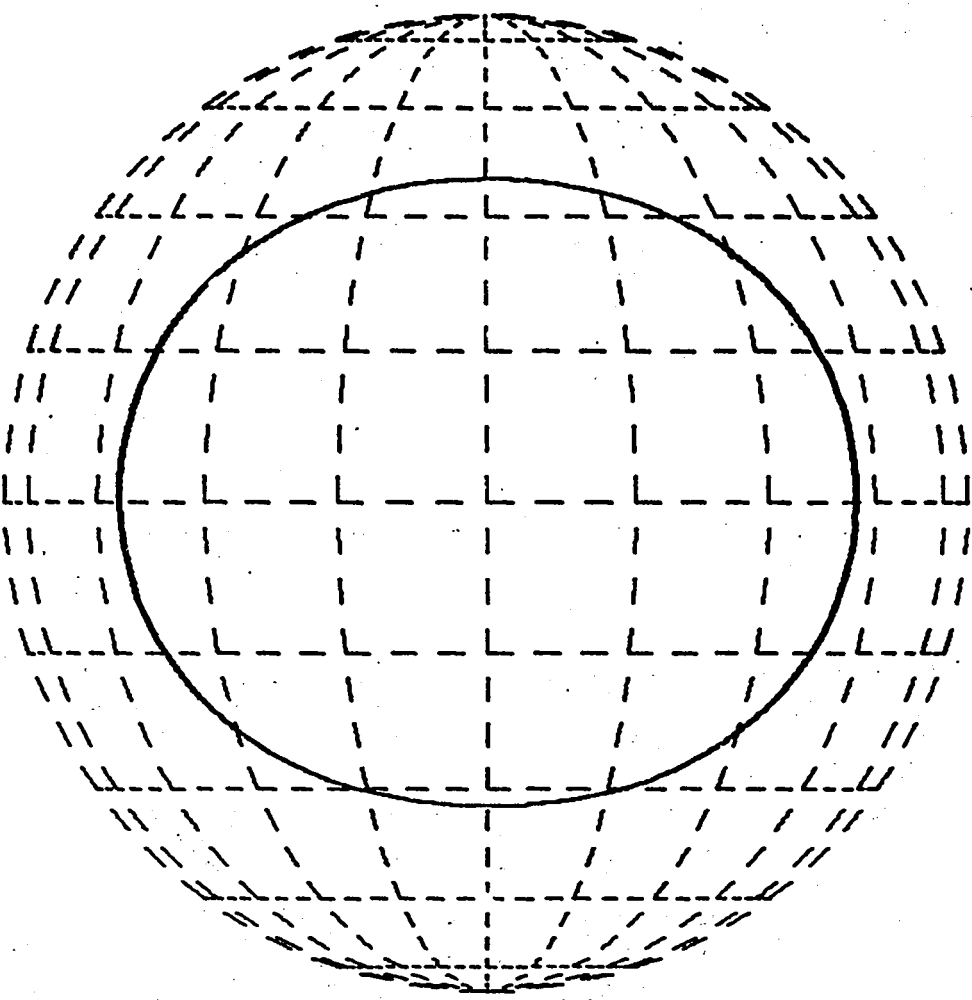
GLOBOGRAPHIC DESCRIPTION OF JOINT SINUS NECK

FIGURE   6.14

6.3   EULER JOINT MODEL

As a means of more accurately modeling mechanical joints used in dummies, a joint termed an Euler joint illustrated in Figure 6.15 has been defined. For purposes of discussion consider a composite joint attaching segments 1 and 4.
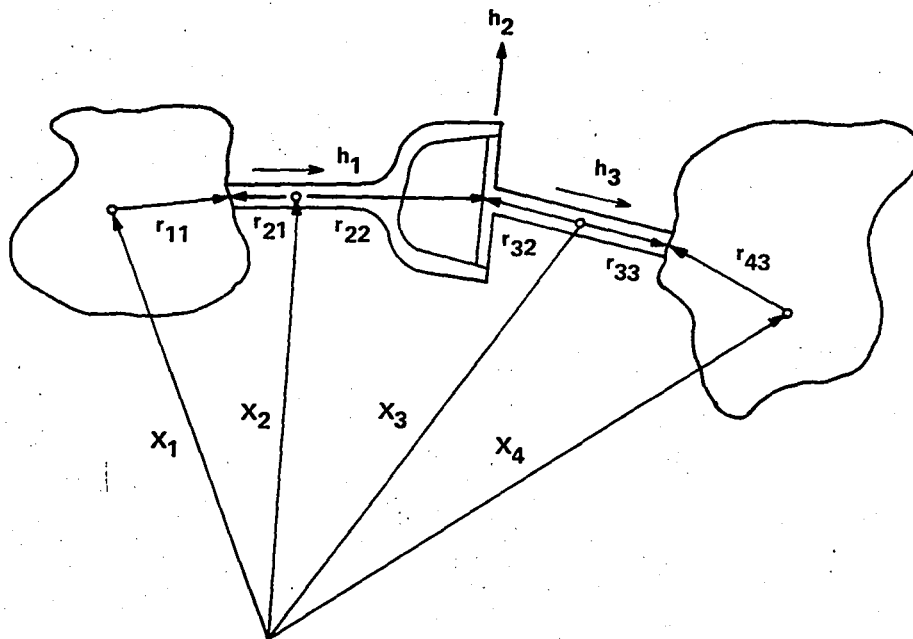
Figure 6.15 EULER JOINT

The composite joint itself is comprised of two segments; segments 2 and 3, and 3 pin joints.

Joint 1 connects 1 to 2, rotation about h_1

Joint 2 connects 2 to 3, rotation about h_2

Joint 3 connects 3 to 4, rotation about h_3

The equations of motion are:

$$m_1 \ddot{x}_1 + f_1 = u_{11}$$

$$m_2 \ddot{x}_2 - f_1 + f_2 = u_{12}$$

$$m_3 \ddot{x}_3 - f_2 + f_3 = u_{13}$$

$$m_4 \ddot{x} - f_3 = u_{14}$$

$$\frac{d}{dt}\left(\phi_1 w_1\right) + r_{11} \otimes D_1 f_1 + D_1 t_1 = u_{21} + D_1 \tau_1$$

$$\frac{d}{dt}\left(\phi_2 w_2\right) - r_{21} \otimes D_2 f_1 + r_{22} \otimes D_2 f_2 - D_2 t_1 + D_2 t_2 = u_{22} - D_2 \tau_1 + D_2 \tau_2$$

$$\frac{d}{dt}\left(\phi_3 w_3\right) - r_{32} \otimes D_3 f_2 + r_{33} \otimes D_3 f_3 - D_3 t_2 + D_3 t_3 = u_{23} - D_3 \tau_2 + D_3 \tau_3$$

$$\frac{d}{dt}\left(\phi_4 w_4\right) - r_{43} \otimes D_4 f_3 - D_4 t_3 = u_{33} - D_4 \tau_3$$

with the constraint equations:

$$X_1 + D_1^{-1} r_{11} = X_2 + D_2^{-1} r_{21}$$

$$X_2 + D_2^{-1} r_{22} = X_3 + D_3^{-1} r_{32}$$

$$X_3 + D_3^{-1} r_{33} = X_4 + D_4^{-1} r_{43}$$

and angular constraints:

$$D_1^{-1} h_{11} = D_2^{-1} h_{21} = h_1$$

$$D_2^{-1} h_{22} = D_3^{-1} h_{32} = h_2$$

$$D_3^{-1} h_{33} = D_4^{-1} h_{43} = h_3$$

Where h_1, h_2, h_3 are pin vectors parallel to permitted axis of rotation. The f_1, f_2, f_3 are constraint forces, and t_1, t_2 and t_3 are constraint torques at the joints. Also τ_1, τ_2 and τ_3 are additional torques generated at the joints (h_{nj} is pin vector h_j as measured in system n.)

Define an axis system in segment 1 where the z axis is aligned with the pin vector h . Let H_1 be the relative direction cosine matrix associated with this system such that a vector γ in the reference system will be transformed into the local system by $\gamma_{local} = H_1 D_1 \gamma_{ref}$. Define a reference system in segment 2 whose z axis is aligned with the pin vector h_1 and whose x axis is aligned with pin vector h_2 . Also define a system in segment 3 whose z axis is aligned with the pin vector h_2 and whose x axis is aligned with pin vector h_3. (Note that $h_1 \cdot h_3 = \cos\theta$, $h_1 \cdot h_2 = 0$ and $h_2 \cdot h_3 = 0$) Define an axis system in segment 4 whose z axis is aligned with the pin h_3 . Let H_4 be the relative direction cosine matrix in a manner similar to that used for segment 1. Let ϕ be the rotation of segment 2 relative to segment 1 about the h_1 axis. Let θ be the rotation of segment 3 relative to segment 2 about the h_2 axis. Let ψ be the rotation of segment 4 relative to segment 3 about the h_3 axis. Then

$$D_2 = T_z(\phi) H_1 D_1$$
$$D_3 = T_x(\theta) D_2$$
$$D_4 = H_4^T T_z(\psi) D_3 = H_4^T T_z(\psi) T_x(\theta) T_z(\phi) H_1 D_1$$
$$T_z(\psi) T_x(\theta) T_z(\phi) = H_4 D_4 D_1^{-1} H^{-1}$$

here $T_x(\theta)$ indicates a rotation through an angle θ about the local x axis and $T_z(\phi)$ indicates a rotation through an angle ϕ about the local z axis. Also note that $T_z(\psi) T_x(\theta) T_z(\phi)$ is the standard Euler transformation relating segment 4 to segment 1. Where ϕ is precession θ is nutation and ψ is spin.

Make the following simplifications:

      (1) The masses and inertias of segments 2 and 3 are negligible
$$m_2 = m_3 = \emptyset_2 = \emptyset_3 = 0$$

      (2) The dimensions of the joints are negligible
$$r_{21} = r_{22} = r_{32} = r_{33} = 0$$

(3) No forces or torques act on segments 2 and 3 other than those produced by constraint forces and torques, or torques generated by the relative Euler angles at the joints themselves.

$$\begin{pmatrix} u_{22} = u_{23} = 0 \\ u_{12} = u_{13} = 0 \end{pmatrix}$$

These assumptions reduce the model to two effective segments (1 and 4) connected by a massless joint.

The reduced set of equations are:

$$m_1 \ddot{X}_1 + f_1 = u_{11}$$

$$-f_1 + f_2 = 0$$

$$-f_2 + f_3 = 0$$

$$m_4 \ddot{X}_4 - f_3 = u_{14}$$

$$\frac{d}{dt}\left(\phi_1 w_1'\right) + r_{11} \otimes D_1 f_1 + D_1 t_1 = u_{21} + D_1 \tau_1$$

$$-D_2 t_1 + D_2 t_2 = -D_2 \tau_1 + D_2 \tau_2$$

$$-D_3 t_2 + D_3 t_3 = -D_3 \tau_2 + D_3 \tau_3$$

$$\frac{d}{dt}\left(\phi_4 w_4'\right) - r_{43} \otimes D_4 f_3 - D_4 t_3 = u_{24} - D_4 \tau_3$$

Since

$$f_1 = f_2 = f_3$$

and

$$t_2 = t_1 - \tau_2 + \tau_2$$

$$t_3 = t_2 - \tau_2 + \tau_3$$

If we let $t = t_1 - \tau_1$

We may write the equations as

$$m_1 \ddot{X}_1 + f_1 = u_{11}$$

$$m_4 \ddot{X}_4 - f_1 = u_{14}$$

$$\left(\phi_1 w_1'\right) + r_{11} \otimes D_1 f_1 + D_1 t = u_{21}$$

$$\left(\phi_4 w_4'\right) - r_{43} \otimes D_4 f_1 - D_4 t = u_{24}$$

$$X_1 + D_1^{-1} r_{11} = X_4 + D_4^{-1} r_{43}$$

For the axes of rotation we have:

for precession ϕ , $h_1 = D_1^{-1} h_{11} = D_2^{-1} h_{21}$,

nutation θ , $h_2 = D_2^{-1} h_{22} = D_3^{-1} h_{32}$,

spin ψ , $h_3 = D_3^{-1} h_{33} = D_4^{-1} h_{43}$

162

For the direction cosines,

$$D_2 = T_{\not z}(\phi) H_1 D_1$$
$$D_3 = T_x(\theta) D_2$$
$$H_4 D_4 = T_{\not z}(\psi) D_3$$

Where H_1 and H_4 are defined such that when $\phi = \theta = \psi = 0$, the local x, y, z axis of each system are aligned.

Thus

$$h_{11}^* = \begin{pmatrix} 0 \\ 0 \\ 1 \end{pmatrix} = h_{11} = h_{33} = h_{43}^*$$

$$h_{22} = \begin{pmatrix} 1 \\ 0 \\ 0 \end{pmatrix} = h_{32}$$

Explicitly for the h_i in the inertial reference system we have

$$h_1 = D_1^{-1} H_1^{-1} \begin{pmatrix} 0 \\ 0 \\ 1 \end{pmatrix}$$

or equivalently

$$h_2 = D_1^{-1} H_1^{-1} T_{\not z}^{-1}(\phi) \begin{pmatrix} 1 \\ 0 \\ 0 \end{pmatrix} = D_1^{-1} H_1^{-1} \begin{pmatrix} \cos \phi \\ \sin \phi \\ 0 \end{pmatrix}$$

$$h_2 = D_4^{-1} H_4^{-1} T_{\not z}(\psi) \begin{pmatrix} 1 \\ 0 \\ 0 \end{pmatrix} = D_4^{-1} H_4^{-1} \begin{pmatrix} \cos \psi \\ -\sin \psi \\ 0 \end{pmatrix}$$

$$h_3 = D_4^{-1} H_4^{-1} \begin{pmatrix} 0 \\ 0 \\ 1 \end{pmatrix}$$

The relative angular velocity is

Thus we have

$$\Delta w = D_4^{-1} w_4 - D_1^{-1} w_1$$
$$\dot{\phi} + \cos \theta \, \dot{\psi} = h_1 \cdot \Delta w$$
$$\dot{\theta} = h_2 \cdot \Delta w$$
$$\cos \theta \, \dot{\phi} + \dot{\psi} = h_3 \cdot \Delta w$$

It should be noted that a singular case arises when $\cos \theta = \pm 1$. For these cases it is impossible to distinguish between ϕ and ψ from the rotation matrix ($T_{\not z}(\psi) T_x(\theta) T_{\not z}(\phi)$) alone, some auxiliary information must be used.

Consider the case where all axes are free –
then

$$t = \alpha h_1 + \beta h_2 + \gamma h_3$$

163

where

$$\alpha = -f(\phi, \dot{\phi})$$
$$\beta = -g(\theta, \dot{\theta})$$
$$\gamma = -h(\psi, \dot{\psi})$$

Where f, g, h are the torques generated on the free axes.

Note that

$$h_i \cdot h_i = 1 \qquad \text{for } i\ 1,2,3$$
$$h_1 \cdot h_2 = h_2 \cdot h_3 = 0$$
$$h_1 \cdot h_3 = \cos\theta$$

It should also be noted that when $\sin\theta = 0$ the components of angular velocity of segments 1 and 4 projected on the $h_1 \otimes h_2$ axis must be equal. This is a constraint in the system.

Consider the case where the precession axis is locked. The constraint torque t_c must lie on an axis which is perpendicular to h_2 and h_3. This axis is

$h_1{}^* = h_2 \times h_3$, $h_1{}^*$ will be a unit vector since $h_2 \cdot h_3 = 0$.

where
$$t = -t_c + \beta h_2 + \gamma h_3 = -t_c - g h_2 - h h_3$$
$$t_c = \alpha h_1{}^* = h_1{}^* \cdot t_c h_1{}^*$$

The constraint equation is a statement of the fact that the components of angular velocity on the h_1 axis of the adjoining segments must be equal.

That is,

$$h_1{}^* \cdot \left[D_1^{-1} w_1 - D_4^{-1} w_4 \right] = 0 .$$

When the system is constrained we will write the equations of motion as

$$\frac{d}{dt}\left(\phi_1 w_1 \right) + r_{11} \otimes D_1 f_1 + D_1 {}^{Pt}{}_c = u_{21} + D_1 \left(t \cdot + t_c \right)$$

$$\frac{dt}{dt}\left(\phi_4 w_4 \right) - r_{43} \otimes D_4 f_1 - D_4 {}^{Pt}{}_c = u_{24} - D_4 \left(t + t_c \right)$$

with the constraint $(I - h_1{}^* h_1{}^* \cdot) t_c = (I-P) t_c = 0.$

164

Where P is a projection operator with the property $P t_c = t_c$

The constraint equation in acceleration form may be expressed as

$$P\left[D_1^{-1}\dot{w}_1 - D_4^{-1}\dot{w}_4\right] + \lambda\left[I-P\right]t_c = -\dot{h}_1^*\left[D_1^{-1}w_1 - D_4^{-1}w_4\right] h_1^*$$

Where

$$P = h_1^* h_1^{*T} = h_1^* h_1^*.$$

h_2 has the angular velocity of segment 1 and h_3 has the angular velocity of segment 4.

Similarly if the spin axis is locked we have

$$t = -t_c - fh_1 - gh_2$$

where

$$t_c = \alpha h_3^* \quad and \quad P = h_3^* h_3^{*T}$$

and $h_3^* = h_1 \times h_2$

The rest of the development is the same. (h_1 has angular velocity of segment 1 and h_2 has the angular velocity of segment 4.)

If the nutation axis is locked, then we find that

$$t = -t_c - fh_1 - hh_3$$

where

$$t_c = \alpha h_2 \quad and \quad P = h_2^* h_2^{*T}$$
$$h_2^* = h_2$$

When any two of the axes are locked the unlocked axes is treated in a manner identical to that of a pin or hinge joint. The constraint torque must be perpendicular to the axes

$$h_j \cdot t_c = 0$$

and the constraint equation is derived from

In this case $\quad h_j \otimes \left(D_1^{-1}w_1 - D_4^{-1}w_4\right) = 0$

$$P = I - h_j h_j^T = -h_j \otimes (h_j \otimes$$

165

locked pair	pin axis	projection P
ϕ, θ	h_3	$I - h_3 h_3{}^T$
ϕ, ψ	h_2	$I - h_2 h_2{}^T$
θ, ψ	h_1	$I - h_1 h_1{}^T$

When all axes are locked the constraint equation is

$$D_1^{-1} w_1 - D_4^{-1} w_4 = 0$$

and P = I, the identity matrix.

Table 6.1

SUMMARY OF EULER JOINT RELATIONSHIPS

IND	LOCK	P	TORQUE	CONSTRAINT EQ $P(D_1^{-1}\dot{w}_1 - D_2^{-1}\dot{w}_2) =$
1	ϕ	$h_1 h_1^T$	$t_c - g h_2 - h h_3$	$\overset{*}{h}_1 \cdot \overset{*}{h}_1 \cdot \Delta w$
2	θ	$h_2 h_2^T$	$t_c - f h_1 - h h_3$	$h_2 \overset{*}{h}_2 \cdot \Delta w$
3	ψ	$h_3 h_3^T$	$t_c - f h_1 - g h_2$	$h_3 \overset{*}{h}_3 \cdot \Delta w$
4	$\theta \psi$	$I - h_1 h_1^T$	$t_c - f h_1$	$-\dot{h}_1 \; h_1 \cdot \Delta w$
5	$\phi \psi$	$I - h_2 h_2^T$	$t_c - g h_2$	$-\dot{h}_2 \; h_2 \cdot \Delta w$
6	$\phi \theta$	$I - h_3 h_3^T$	$t_c - h h_3$	$-h_3 h_3 \cdot \Delta w$
7	$\phi \theta \psi$	I	t_c	0
8	none	none	$-f h_1 - g h_2 - h h_3$	none

$$\Delta w = D_2^{-1} w_2 - D_1^{-1} w_1$$

$$f = f(\phi, \dot{\phi}) \quad h_1 = D_1^{-1} H_1^{-1} \begin{pmatrix} 0 \\ 0 \\ 1 \end{pmatrix}, \quad h_2 = D_1^{-1} H_1^{-1} T_z(\phi) \begin{pmatrix} 1 \\ 0 \\ 0 \end{pmatrix}, \quad h_3 = D_4^{-1} H_4^{-1} \begin{pmatrix} 0 \\ 0 \\ 1 \end{pmatrix}$$

$$g = g(\theta, \dot{\theta})$$

$$h = h(\psi, \dot{\psi}) \quad \dot{h}_1 = (D_1^{-1} w_1) \otimes h_1, \quad \dot{h}_2 = (D_1^{-1} w_1) \otimes h_2 + \dot{\phi} \, h_1^*, \quad \dot{h}_3 = (D_4^{-1} w_4) \otimes h_3$$

$$h_1^* = h_2 \times h_3, \quad h_2^* = h_2, \quad h_3^* = h_1 \times h_2$$

$$T_z(\psi) \, T_x(\theta) \, T_z(\phi) = H_4 D_4 D_1^{-1} H_1^{-1}$$

$$\dot{\phi} + \dot{\psi} \cos\theta = h_1 \cdot (\Delta w), \qquad -\dot{\phi} \sin\theta = h_1^* \cdot \Delta w$$
$$\dot{\theta} = h_2 \cdot (\Delta w)$$
$$\dot{\phi} \cos\theta + \dot{\psi} = h_3 \cdot (\Delta w), \qquad -\dot{\psi} \sin\theta = h_3^* \cdot \Delta w$$

Each of the functions f, g, h is defined as the sum of a spring torque, a viscous and a coulomb torque as defined in Section 6.1 and illustrated in Figures 6.2 and 6.3.

SECTION 7

FORCES PRODUCED BY CONTACT

The present version of the program has four basic contact routines:

(1) ellipsoid with plane

(2) ellipsoid with ellipsoid

(3) ellipsoid with restraint belt

(4) ellipsoid with air bag

Each segment has an ellipsoidal contact surface defined for it.
Additional ellipsoidal and/or planar surfaces (finite rectangles) may be
associated with each segment. The vehicle may have planar or ellipsoidal
surfaces. Any combination may be used with contact routines 1 and 2. The
restraint belt may be attached to any segment (usually the vehicle) at two
anchor points (these must be separate) and is assumed to pass around the
principal ellipsoid through a specified point associated with the segment.
Belts may be associated with any segment, but it is assumed that the belts lie
in a plane determined by the anchor points and the specified point in the
ellipsoid. The number of belts (8 maximum) is limited only by storage.

In each of the first three types of contact, the force is determined
by a force deflection routine which allows for energy losses (hysteresis),
permanent offset, and impulsive forces. The force deflection is associated with
each paired contact, hence it is important to specify a mutual force deflection
characteristic which allows for the specific paired contacts being considered.
For example a head ellipsoid contacting a planar dashboard should be assigned
a different force defelction response than the upper torso (ellipsoid) contacting
the same planar dashboard. Proper definition of the mutual force deflection
allows the user to partially account for the deformation of the contacting
segments.

It should be noted that the contact routines which are inputted
force-deflection characteristics compute the force as a function of only one
parameter (related to the penetration distance) and apply the force at a single

point. However, the modular structure of the program permits easy insertion of more sophisticated routines in which, for example, the force might also be made a function of penetration rate and/or the contact area.

The air bag routine is special in that the air bag is assumed to be ellipsoidal and contacted only by surfaces (occupant segments or vehicle reaction panels) that also are ellipsoids. No contact forces are computed until the air bag is fully inflated and the motion of the bag is then dynamically integrated. Although several segments may contact the air bag, no provision is made for the interaction of simultaneous contacts, i.e., the volume and the effective area associated with a segment (or reaction panel) contact with the bag are computed separately for each contact.* The bag pressure is determined from the total change of bag volume, which is the sum of the volumes computed for the separate contacts, and the forces on the bag and the contacting elements are computed using the pressure and the effective contact areas. The computer program currently provides storage for a maximum of five air bags.

A separate subroutine is used to compute the force resulting from a specific type of contact. The general pattern for defining the forces and torques produced by contact is the following:

1. Detect contact.
2. Determine the parameter (penetration) for use in the force deflection routine.
3. Compute a normal force and friction force.
4. Apply the total force and torque on one segment.
5. Apply the corresponding reaction force and torque to the other segment.

The following sections develop the method used in each of the four types of contact.

---

*It should be noted that simultaneous bag contacts, if too closely spaced, can result in errors due to overlapping of volumes and areas which is not accounted for in the computations.

7.1   PLANE - ELLIPSOID CONTACT (SUBROUTINE PLELP)

The geometrical configuration of the plane ellipsoid contact along with the appropriate variable definitions is presented in Figure (7.1). The following equations refer to an ellipsoid A_m attached to segment m contacting a plane P_n attached to segment n.

At the point of maximum penetration

$$\mu\, A_m\, r_m = D_m\, D_n^{-1}\, t_1 = -t \qquad (7.1)$$

μ - is a scalar quantity

t - is the outward normal to the plane in m's reference system.

t_1 is the outward normal to the plane in n's reference system.

     The ellipsoid equation is written in the form

therefore
$$r_m^T\, A_m\, r_m = 1$$

or
$$\mu^2 = t^T A_m^{-1} t$$
$$\mu = \sqrt{t^T A_m^{-1} t}$$

This results in

$$r_m = -A_m^{-1}\, t \Big/ \sqrt{t^T A_m^{-1} t}$$

The penetration distance p is given by the following equation

$$p = t^T [\ell_m + r_m] - t_1^T [D_n(-x_n + x_m] + \beta \qquad (7.2)$$

where β is the distance of the plane from x_n (see Figure 7.1)

For $p < 0$ no penetration has occurred, and if $p > 2\mu$, the ellipsoid has fully penetrated. In both of these cases no contact is assumed and therefore no forces are generated. The assumption of no contact for full penetration is a crude method of preventing an erroneous contact when an object comes behind a plane from the side.

170

The point of force application can be specified as occurring at any point between the point of maximum penetration to the point of intersection of the vector r_m with the plane. This point is the center of the ellipse formed by the plane-ellipsoid intersection.*

Then

$$y_m = (1-\rho)r_m + \rho\left(\frac{\mu-\rho}{\mu}\right)r_m + \lambda_m \qquad (7.3)$$

defines the point of application of the force as measured from the c.g. of the segment m. Then

$$y_n = D_n D_m^{-1} y_m + D_n(x_m - x_n) \qquad (7.4)$$

is the same point as measured from the c.g of segment n.

If the plane P_n is bounded (i.e a finite rectangle) the projection of y_n on the plane is checked to see if it lies on the rectangle by comparing

and

$$0 \le t_2^T y_n - \alpha_2 \le \beta_2$$
$$0 \le t_3^T y_n - \alpha_3 \le \beta_3 \qquad (7.5)$$

t_1, t_2, t_3 are vectors defining the plane, t_1 is the outward normal to the plane. The scalar quantities $\beta_1, \beta_2, \beta_3, \alpha_2, \alpha_3$ define the location and size of the plane.

If β_2 or β_3 is zero or negative this check will not be made.

The magnitude of the normal force is computed by the force deflection routine using the penetration distance and the specific material properties. The normal force is then used to generate a friction force existing between the two contacting surfaces. Information concerning the relative velocity is important here, therefore the following equations are needed. The relative velocity between the surfaces at the point of contact is

* If the plane is soft and the ellipsoid is hard, a value of $\rho = 0$ seems appropriate. If the plane is hard and the ellipsoid is soft, a value of $\rho = 1$ seems appropriate.

171
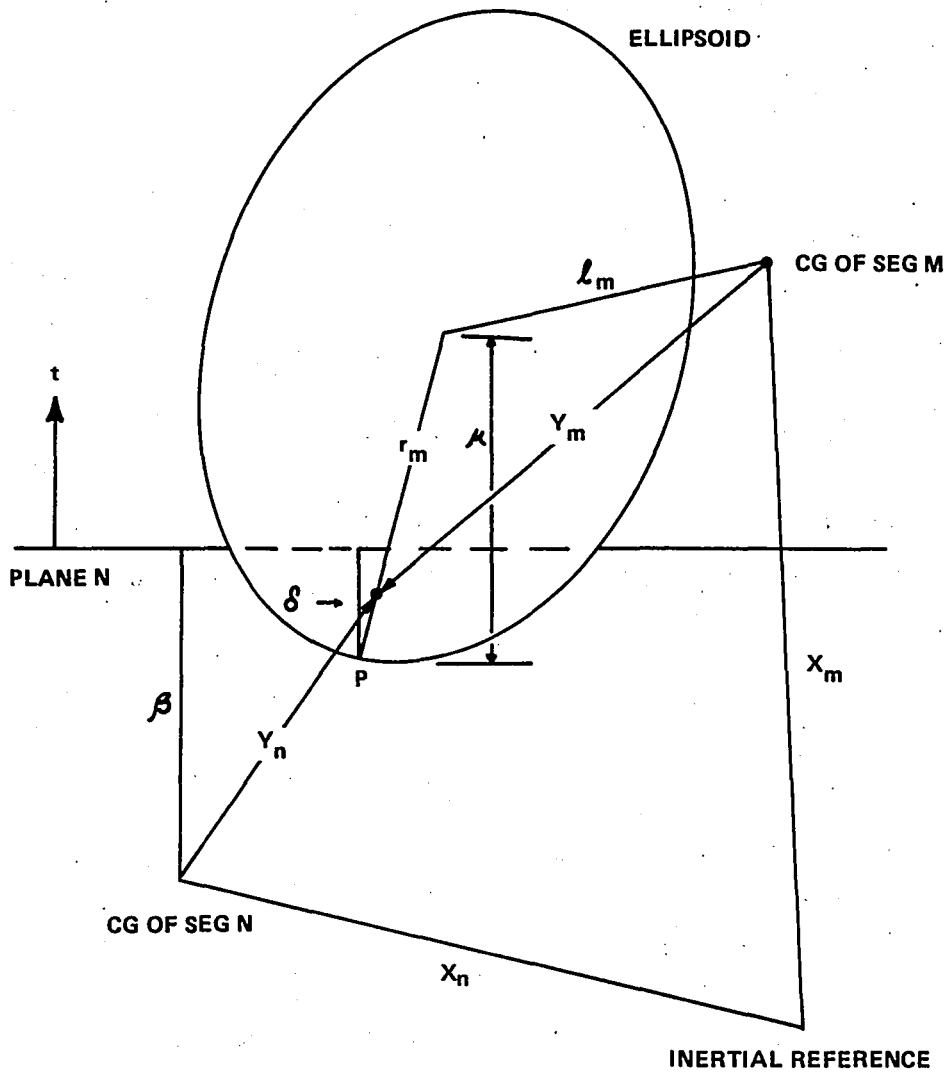
Figure 7.1 PLANE-ELLIPSOID CONTACT

computed in m's reference as

$$V_r = D_m \left(\dot{X}_m - \dot{X}_n \right) + \omega_m \otimes \mathcal{Y}_m - D_m D_n^{-1} \left(\omega_n \otimes \mathcal{Y}_n \right) \qquad (7.6)$$

The magnitude of the normal component is given by $t^T V_r$.
The tangential component then is

$$V_{r_t} = V_r - \left(t^T V_r \right) t \qquad (7.7)$$

The friction force is computed as C_f (coefficient of friction) times the normal force. If the magnitude of the tangential velocity is less than one unit a ramp function is applied which allows the friction force to decrease to zero as the tangential velocity decreases to zero.

The total force is then computed as

$$f = \left| f_{nor} \right| t - C_f \left| f_{nor} \right| V_{rt} / \left| v_{rt} \right| \qquad (7.8)$$

The force $-f$ is applied to segment n and f is applied to segment m. The torque $- \mathcal{Y}_n \otimes f$ is applied to segment n and $\mathcal{Y}_m \otimes f$ to segment m.

7.2   INTERSECTION OF ELLIPSOIDS (SUBROUTINE INTERS)

In the program it is necessary to recognize the intersection of two ellipsoids A and B. For the ellipsoid-ellipsoid contact routine (Subroutine SEGSEG) both the exterior and interior contact (ellipsoid A is interior to ellipsoid B) are considered as indicated in Figure 7.2. For the airbag routine only the exterior contact is considered. The technique used is based on the following algorithm.

173

EXTERIOR CONTACT
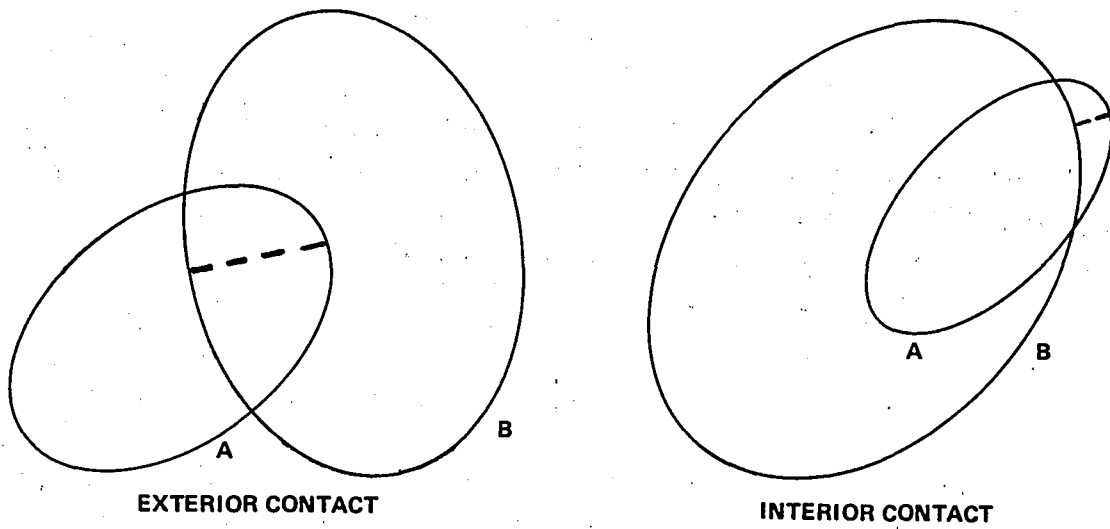
INTERIOR CONTACT

Figure 7.2 ELLIPSOID-ELLIPSOID CONTACT

174

7.2.1   Ellipsoid-Ellipsoid Algorithm

If an exterior contact is specified the ellipsoids A and B are expanded or contracted about their centers until a single point of contact is achieved. If contraction was necessary to establish this single point of contact the ellipsoids are said to intersect, otherwise no intersection is assumed.

If an internal contact is specified, ellipsoid A is contracted and ellipsoid B is expanded or vice versa until a single point of contact is achieved. If a contraction of ellipsoid A (expansion of B) was necessary to achieve this single point of contact an intersection is assumed, otherwise no intersection is assumed.

This algorithm is executed by subroutine INTERS. The equations are described below. In the current version of the program a memory knowledge is used, hence the algorithm may fail for large penetrations. This is provided which uses the last solution as the starting point for a new solution. Use of this prior knowledge should reduce the number of iterations which are done to obtain a solution.

Consider the case illustrated in Figure 7.3 of two ellipsoids A and B which just touch at a single point.
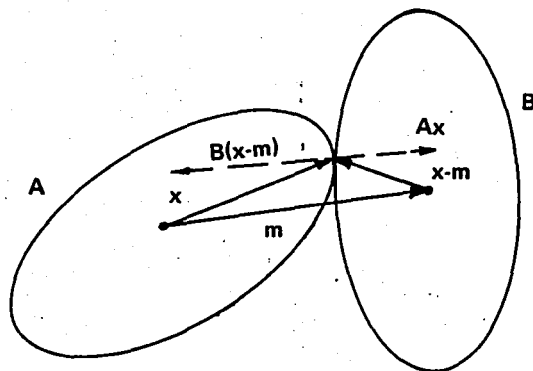
Figure 7.3   ELLIPSOID-ELLIPSOID CONTACT GEOMETRY

175

The basic geometrical relationships are then

$$\nu \mu A x = -n$$
$$\mu B (x - m) = n$$

where n is the normal directed outward from ellipsoid B and ν, μ are scalars.

For an exterior contact ν, μ are both positive and for an interior contact (A is interior to B) ν, μ are both negative. Hence in either case

which yields

$$\nu A x = -B (x - m)$$
$$(\nu A + B) x = B m$$
$$(x - m) = -\nu (\nu A + B)^{-1} A m$$

Thus the value of the single point of contact X is determined by the parameter ν .

The basic equations of the ellipsoids are

Let

$$X \cdot A x = 1$$
$$(x - m) \cdot B (x - m) = 1$$
$$f_A (\nu) = X \cdot A x$$

and

$$f_B (\nu) = (x - m) \cdot B (x - m)$$

For a particular X

if $f_A (\nu) > 1$ ellipsoid A has been expanded, i.e x lies outside of the ellipsoid

if $f_A (\nu) < 1$ ellipsoid A has been contracted, i.e x is inside the ellipsoid

Now define the function g(ν) such that

$$g(\nu) = f_A(\nu) - f_B(\nu) \quad \text{for exterior contact}$$

and/or

$$g(\nu) = \frac{1}{f_A(\nu)} - f_B(\nu) \quad \text{for interior contact}$$

The single point of contact is then determined as the value of where g(ν) = 0.

Investigation of the equations shows that solving for the ν where g(ν) = 0 is equivalent to solving a sixth degree polynomial in ν . Rather than solve the polynomial a Newton-Raphson procedure is used where g(ν) is expanded in a Tayler series.

$$g(\nu + \delta\nu) = g(\nu) + \delta\nu \left.\frac{dg}{d\nu}\right|_\nu$$

Since it is desired that $g(\nu + \delta\nu) = 0$ then

$$\delta\nu = \frac{-g(\nu)}{\left(\frac{dg}{d\nu}\right)_\nu}$$

This procedure is iterated until a specific degree of convergence is achieved ($\left|\frac{\delta\nu}{\nu}\right| < \xi$) or until a specified number of steps have been executed and convergence has failed in which case an error message is printed.

The initial value of ν is estimated as

$$\nu = \left(m \cdot Bm \middle/ m \cdot Am\right)^{1/2}$$

for the exterior contact and the negative of this for interior contact. This produces a ν of about the right order of magnitude.

Using the expressions for f_A and f_B, the following equations result

$$\frac{df_A}{d\nu} = 2 \; \frac{dx}{d\nu} \cdot Ax,$$

$$\frac{df_B}{d\nu} = -\nu \; \frac{df_A}{d\nu},$$

$$\frac{dx}{d\nu} = -[\nu A + B]^{-1} Ax,$$

for exterior contact, $\dfrac{dg}{d\nu} = \dfrac{df_A}{d\nu} - \dfrac{df_B}{d\nu} = (1+\nu) \; \dfrac{df_A}{d\nu}$

and for interior contact, $\dfrac{dg}{d\nu} = -\dfrac{1}{f_A^2} \; \dfrac{df_A}{d\nu} - \dfrac{df_B}{d\nu} = \left(\nu - \dfrac{1}{f_A^2}\right)\dfrac{df_A}{d\nu}$

The functions f_A, f_B and $\dfrac{1}{f_A}$ are illustrated below as functions of ν.
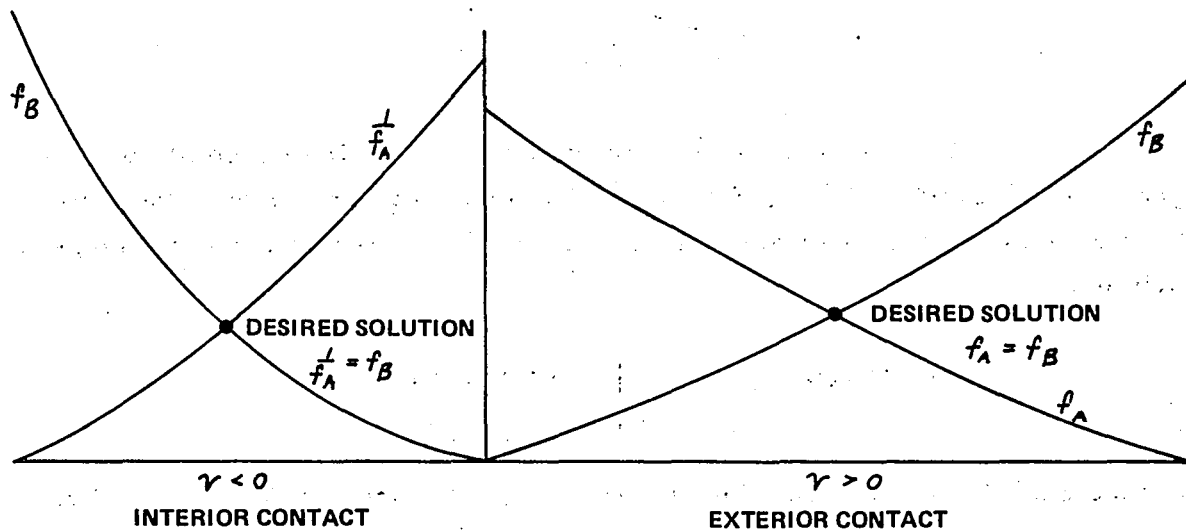
Figure 7.4   ELLIPSOID FUNCTIONS FOR INTERIOR AND EXTERIOR CONTACTS

178

When the solution is obtained, the expansion factor is

$$\epsilon_f = \sqrt{f_A}$$

If no solution is obtained after 50 iterations, the statement "INTERS ITERATION DID NOT CONVERGE" is printed and the program continues.

7.2.2   Depth of Penetration for Ellipsoid-Ellipsoid Contacts

The depth of penetration for the ellipsoid-ellipsoid contact is computed by subroutine SEGSEG by the following algorithm, using the results of subroutine INTERS.

1.   For an exterior contact where the ellipsoids have been contracted by an amount ϵ_f as determined by subroutine INTERS they have a single point of contact at the point x when contracted. The location of the same point on A when not contracted is

$$X_A = X/\epsilon_f$$

and on B is

$$X_B = (X - m)/\epsilon_f + m$$

The vector between these points is then

$$X_A - X_B = \left(\frac{1}{\epsilon_f} - 1\right)m$$

The depth of penetration, p, is taken as the magnitude of this vector i.e.

$$p = \left(\frac{1}{\epsilon_f} - 1\right)|m|$$

179

2.   For an internal contact, A has been contracted and B expanded. Hence,

$$X_A = X/\epsilon_f$$

$$X_B = \epsilon_f (X-m) + m$$

Then

$$X_A - X_B = X/\epsilon_f - \epsilon_f (X-m) - m = \left(\frac{1}{\epsilon_f} - \epsilon_f\right)X - (1-\epsilon_f)m$$

The depth of penetration is then taken as

$$P = |X_A - X_B| = \left|\left(\frac{1}{\epsilon_f} - 1\right)X + \epsilon_f (x-m)\right|$$

7.3   RESTRAINT BELT CONTACT

The CVS IV program provides two options for modeling of belt restraint systems: (1) the original method, which is described in detail below and (2) a new approach developed for the Air Force Aerospace Medical Research Laboratory at Wright-Patterson Air Force Base which allows modeling of interactive belts that can slip over multiple deformable segments (References 5 and 6).

In the simpler treatment, each restraint belt is assumed to lie in a plane defined by two anchor points attached to a segment (usually the vehicle) and by a fixed point on a contact ellipsoid rigidly attached to some other segment (see Figure 7.5). The calculation of the belt length from the fixed point to the two anchor points is done separately. The friction of the contact between the belt and the segment ellipsoid may be assumed to be either zero or infinite. In the zero friction option the total belt length is used to compute the strain and a single force-strain history is used to determine the force which is applied equally at each of the tangent points. In the infinite friction option each of the partial belt lengths (one from the fixed point to anchor point A and the other from the fixed point to anchor point B) are treated
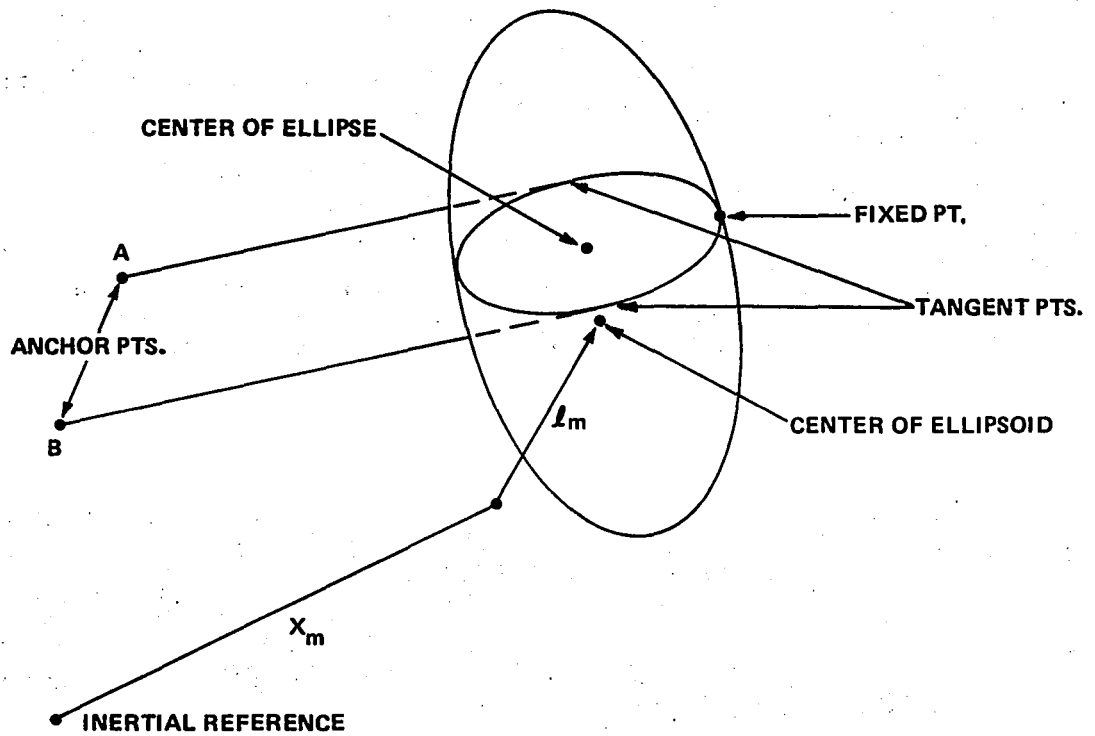
Figure 7.5   RESTRAINT BELT GEOMETRY

independently. Separate force-straint histories are carried for each part resulting in different forces. It is assumed that the force-strain functions are defined in such a manner as to account for deformation of the contact ellipsoid (i.e., they are mutual force-strain functions).

The center of the ellipsoid is used as a reference for the calculation of the tangent points and the belt length.

The following vectors are defined:

$\mathcal{P}_A, \mathcal{P}_B$ - location of anchor points w. r. t. the ellipsoid

T_A, T_B - vectors from the anchor points to fixed point

T_C - vector defining the belt plane

All quantities such as these are matrices in the reference system of the segment associated with the contact ellipsoid.

$$T_C = \frac{T_B \otimes T_A}{|T_B \otimes T_A|} \tag{7.9}$$

The distance, $\tilde{\beta}$, of the center of the ellipsoid to the belt plane is computed by

$$\tilde{\beta} = T_C \cdot \mathcal{P}_C = T_C \cdot \mathcal{P}_A = T_C \cdot \mathcal{P}_B \tag{7.10}$$

An ellipse is formed by the intersection of the belt plane with the ellipsoid. The center of the ellipse is given by:

$$X_E = \frac{E^{-1} T_C}{T_C \cdot E^{-1} T_C} \tilde{\beta} \tag{7.11}$$

E is the ellipsoid matrix.

182

7.3.1 Calculation of the Tangent Points

The belt plane is illustrated in Figure 7.6.

Let $$p = \alpha x + \beta z + \tau t \otimes Ez$$

Since x, z, and p terminate in the belt plane, the following relationships hold, $t \cdot p = t \cdot x = t \cdot z$

Then

$$t \cdot p = \alpha t \cdot x + \beta t \cdot z$$
$$\alpha + \beta = 1$$

yields

$$(7.12)$$

p may now be written;

$$p = x + \beta(z - x) + \tau t \otimes Ez \qquad (7.13)$$

Since z-p is tangent to the ellipsoid it must be perpendicular to the normal at p. Applying this yields.

$$(z - p) \cdot Ep = 0$$

and since p lies in the ellipsoid the ellipsoid equation states that $p \cdot Ep = 1$. Therefore

yielding

$$z \cdot Ep = 1$$
$$1 = \alpha z \cdot Ex + \beta z \cdot Ez$$

$$(7.14)$$

Equations (7.12) and (7.14) may be used to define α and β. To determine τ use; $1 = p \cdot Ep$

$$1 = \alpha^2 x \cdot Ex + 2\alpha\beta x \cdot Ez + 2\alpha\tau x \cdot E(t \otimes Ez)$$
$$+ \beta^2 z \cdot Ez + 2\beta\tau z \cdot E(t \otimes Ez) + \tau^2(t \otimes Ez) \cdot (t \otimes Ez)$$

$$(7.15)$$

But $x \cdot E(t \otimes Ez) = Ex \cdot t \otimes Ez = 0 = Ez \cdot (t \otimes Ez) = z \cdot E(t \otimes Ez)$

$$\tau^2 = \frac{\alpha[1 - x \cdot Ex]}{(t \otimes Ez) \cdot E(t \otimes Ez)}$$
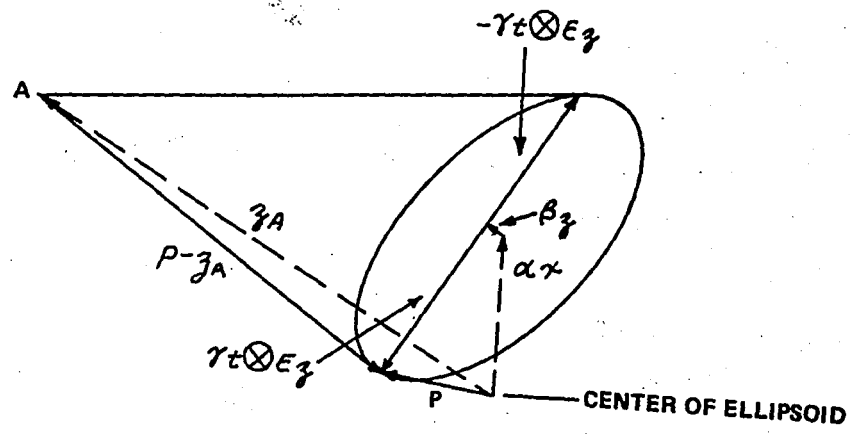
Figure 7.6   ELLIPSE IN BELT PLANE

184

The choice of the sign of τ distinguishes between the possible tangent vectors from the anchor points to the ellipse. The possible belt plane configurations are illustrated in Figure 7.7. Note that if the fixed point does not lie on the arc of contact the belts are assumed to be attached directly to the fixed point as in (d) of Figure 7.7.

Determination of the arc length begins with the definition of a right handed coordinate system uc, up, Tc as; uc is the unit vector in the direction of the fixed point c from the center of the ellipse, Tc is the vector defining the belt plane and $up = Tc \otimes uc$.

Let $p = x(uc) + y(up) + X_E$, be a vector from the center of the ellipsoid to a point on the ellipse. Applying the equation of an ellipsoid yields:

$$p \cdot E p = x^2 uc \cdot E(uc) + 2xy \, uc \cdot E(up) + y^2 up \cdot E up$$
$$+ X_E \cdot E X_E = 1 \tag{7.16}$$

then writing

where
$$a x^2 + 2 b x y + c y^2 = 1$$

$$a = \frac{uc \cdot E uc}{1 - X_E \cdot E X_E} \qquad b = \frac{uc \cdot E(up)}{1 - X_E \cdot E X_E}$$

$$c = \frac{up \cdot E(up)}{1 - X_E \cdot E X_E}$$

$$\tag{7.17}$$

The values of x and y are computed for the two tangent points. Denote them as X_A, Y_A then X_B, Y_B and

$$\theta_A = \tan^{-1}(Y_A / X_A) \quad , \quad \theta_B = \tan^{-1}(Y_B / X_B)$$

$$\tag{7.18}$$

185

FIXED POINT
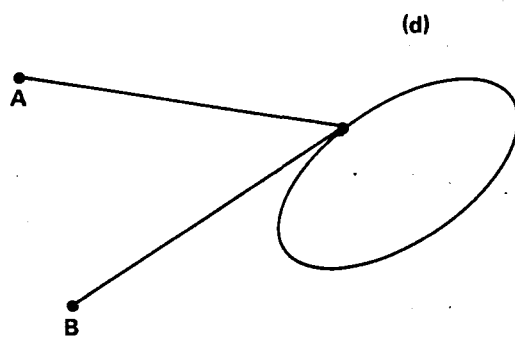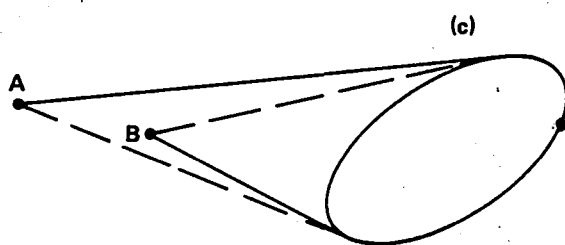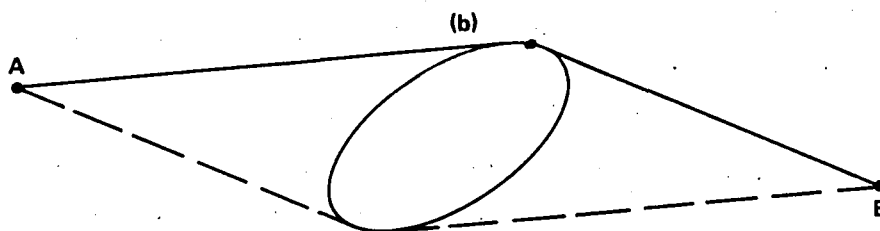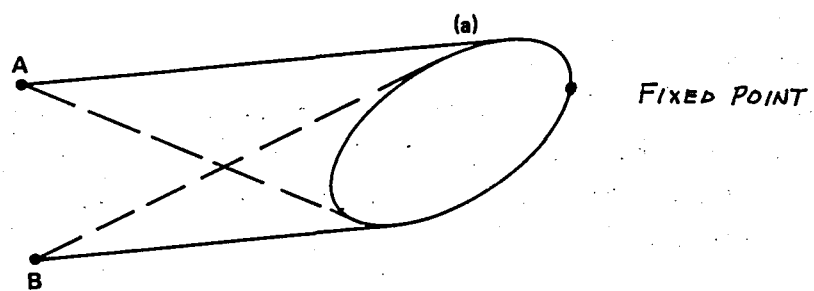
Solid Lines Indicate
Accepted Solutions

Figure 7.7   BELT CONFIGURATIONS

186

The arc length is then computed by Simpson's Rule integration using (a, b, c, step size and θ ,) as input. The Function Routine Elong performs this operation. The form of the integration is found by considering the following equations:

Write the equation of an ellipse:

$$a x^2 + 2 b x y + c y^2 = 1 \tag{7.19}$$

Let
$$x = r \cos \theta, \quad y = r \sin \theta$$

Then
$$r = 1 \Big/ \sqrt{a \cos^2 \theta + 2 b \sin \theta \cos \theta + c \sin^2 \theta} \tag{7.20}$$

The arc length ds is;

$$ds = \sqrt{dr^2 + (r \, d\theta)^2} = d\theta \sqrt{r^2 + \left(\frac{dr}{d\theta}\right)^2} \tag{7.21}$$

Substituting for r yields

$$\sqrt{r^2 + \left(\frac{dr}{d\theta}\right)^2} = r^2 \sqrt{a + c + r^2 (b^2 - ac)}$$

The equation for the arc length L is then given by:

$$L = \int_0^{\theta_1} d\theta \sqrt{r^2 + \left(\frac{dr}{d\theta}\right)^2} \tag{7.22}$$

The sign of L will be defined to agree with the sign of θ_1 .

The following assumptions and/or restrictions apply to the derivation and use of the belt routine:

(1)   Anchor points A and B are distinct, therefore A, B and the fixed point on the ellipsoid are sufficient to define a plane.

(2)   The fixed point lies on the arc of contact from tangent point A to tangent point B. If the fixed point does not lie on the

187

on the contact arc, the belts are run to the fixed point and the
arc lengths are set to zero.

7.4   AIR BAG CONTACT

        The airbag model is based on the assumption of a stretchless
bag of ellipsoidal shape which interacts with contact ellipsoids attached to
selected segments of the crash victim or the vehicle*. Each interaction of
a contact ellipsoid and the bag is treated separately by the geometry routine
which computes the decrease in volume of the bag, the effective area of the
contact and the force and torque per unit pressure. After all the contacts
have been considered the total decrease in volume is used to compute the
pressure of the gas in the bag and then the forces and torques are applied to
the various segments.

        In using the airbag at least one contact ellipsoid must be attached
to the vehicle. This is called the primary reactional panel. A point is speci-
fied on this panel as the deployment point. At the beginning of the program
(time = 0) the bag is assumed to have zero volume (zero size) and is located
at the deployment point of the primary reaction panel, after a specified time
delay the bag is inflated by using the gas dynamic relations for the choked
flow of gas through a nozzle. The gas source is a high pressure tank of con-
stant volume, that the total gas which has come through the nozzle, would
occupy at atmospheric pressure. Until this computed volume plus the volume
of the intersections from the contacts reaches the geometric volume of the bag

---

* The contact ellipsoids attached to the vehicle which are used by the airbag
  routines are distinct from the other contact ellipsoids in the program and
  are referred to as reaction panels in the program comments. The loca-
  tion and orientation of these panels is arbitrary.

(when fully inflated) the bag is assumed to be at atmospheric pressure and hence no forces are produced. When this volume reaches the geometric volume, the bag is said to be fully inflated and the addition of more gas from the cylinder or an increase in the volume of intersection will cause the pressure in the bag to increase and thus produce contact forces on any segment intersecting the bag.

During inflation the size of the bag is determined by scaling the semi-axes of the ellipsoid by the cube root of the volume. The center of the bag lies on a vector which has one end at the deployment point and is parallel to the X axis of the primary reaction panel but in the minus X-direction, and the distance is equal to the semi major X axis of the sealed bag from the deployment point.

When the bag is fully inflated it is moved dynamically. A mass and inertia matrix is assigned to the bag. Until fully inflated the orientation of the bag with respect to the vehicle is held constant and equal to its initial orientation. The dynamic motion of the bag is updated by the program integrator. An artificial spring force is applied at the end of the positive X axis of the bag and is exterior to the primary reaction panel. This was done to hold the bag to the panel.

7.4.1   Geometry of the Airbag During Inflation

The airbag geometry during the inflation process is illustrated in Figure 7.8.

AIRBAG

PRIMARY REACTION PANEL

DEPLOYMENT POINT

U_x **AXIS OF PANEL**

$\mathcal{J}_d$

$\mathcal{J}_b$

$\mathcal{J}$

VEHICLE REFERENCE POINT
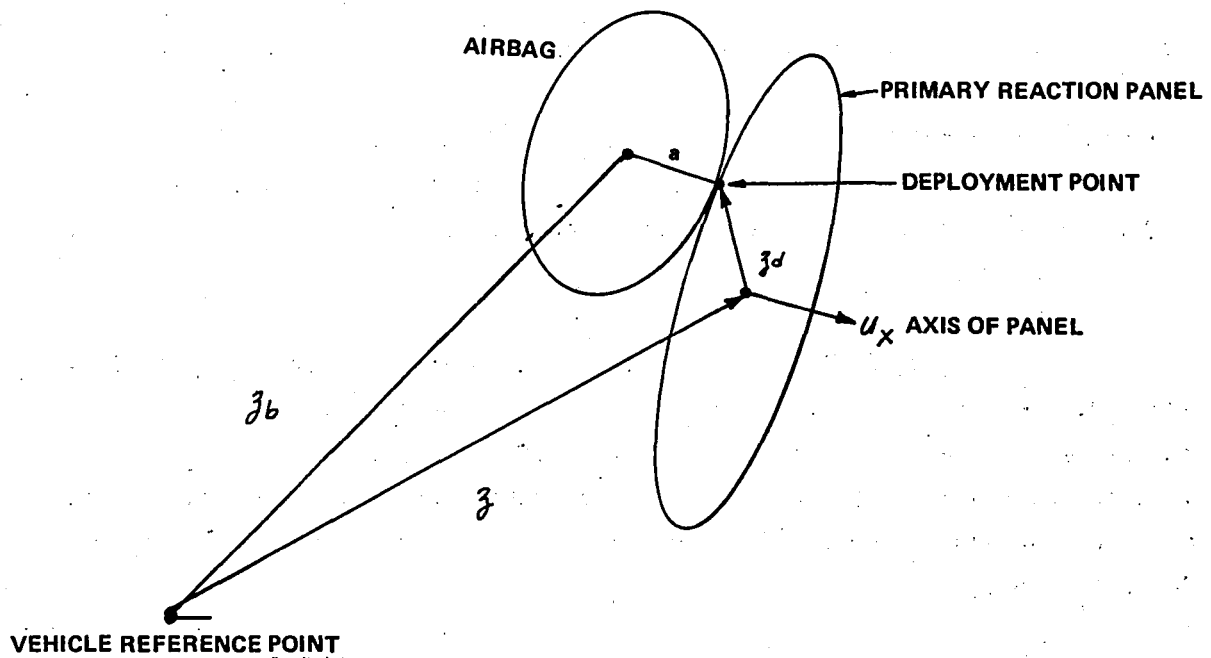
Figure 7.8   AIRBAG GEOMETRY DURING INFLATION

During inflation the following algorithm is used to compute the center of the airbag.

Let $\mathcal{J}$ location of the center of the primary reaction panel with respect to the vehicle reference

$\mathcal{J}_d$ be the location of the deployment point with respect to the center of the panel

u_x be a unit vector in the positive X direction of the panel

a be the scaled semi-axis (X axis of the airbag)

$\mathcal{J}_b$ be the location of the center of the airbag with respect to the vehicle origin.

190

Then $\mathcal{J}_b = \mathcal{J} + \mathcal{J}_d - a \mathcal{U}_x$

The velocity of the c.g. of the bag is computed as the time derivation of this expression plus the velocity of the vehicle.

It should be noted that in the present coding of the program it is tacitly assumed that the X axis of the bag is parallel to the X axis of the primary reaction panel because the above algorithm does not consider the orientation of the bag. This assumption affects only the computation of the artificial spring force which is used to hold the bag to the panel. The spring forces applied only if the end of the X axis of the bag is exterior to the panel and is proportional to the distance of this point from the deployment point. Hence, if the bag X axis is not parallel to the X axis of the primary panel the only error would be in the computation of a possible spring force when the bag is moved dynamically.

The scaled semi axes of the bag are computed by the following algorithm. Let a_1, b_1, c_1 be the semi axes of the fully inflated bag as specified by input.

Then the geometric volume of the bag is

$$V_g = (4/3) \pi a_1 b_1 c_1$$

Let V_b be the instantaneous volume of the bag computed from the gas dynamic relations.

Then

$$a = a_1 \left(\frac{V_b}{V_g} \right)^{1/3}$$

$$b = b_1 \left(\frac{V_b}{V_g} \right)^{1/3}$$

$$c = c_1 \left(\frac{V_b}{V_g} \right)^{1/3}$$

are the semi axes during inflation.

The components of inertia of the bag per unit mass are computed from the relations

$$\phi_{xx} = (b_1{}^2 + c_1{}^2) / 5$$

$$\phi_{yy} = (a_1{}^2 + c_1{}^2) / 5$$

$$\phi_{zz} = (a_1{}^2 + b_1{}^2) / 5$$

which are the principle components of inertia for a thin ellipsoid (ellipsoidal shell).

7.4.2   Dynamic Motion of the Air Bag

When the bag is fully inflated the sum of the forces and torques acting on the bag are used to determine the airbag position, orientation and velocities by integration of the equations of motion. The bag position and velocity is updated only at the completion of a successful main program integration step and is held constant during the integration step.

7.4.3   Air Bag Contact Geometry
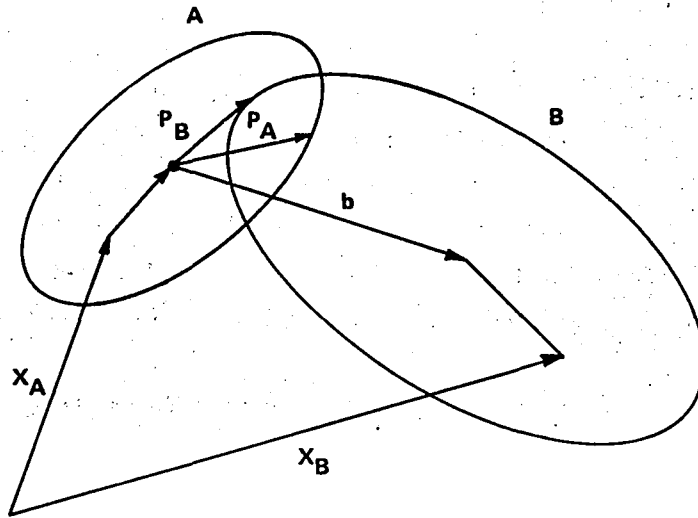
Figure 7.9 AIR BAG GEOMETRY

Subroutine EDEPTH computes the points of maximum penetration$\left(\text{i. e. } |P_A - P_B| \right.$
is maximized$\left. \right)$

$$P = |P_A - P_B|^2 \qquad\qquad (7.23)$$

If P is less than 10^{-6} no further computations are done, zero penetration is
assumed.

If P is greater than or equal to 10^{-6}, two orthogonal planes are defined con-
taining the line from P_B to P_A, using subroutine ORTHO.

In each plane the ellipsoids are replaced by circles with the same radii of curvature as the ellipsoids.

Two cases are considered:

Case I: The radius of curvature of the airbag r_A is greater than the radius of curvature of the contacting ellipsoid r_B . Two circles are constructed with a radius $r = (r_A - r_B)/2$ and center located a distance $r_c = \frac{r_A + r_B}{2}$ from the centers of the circles A and B. These circles are located such that they are tangent to the circles r_A and r_B as shown in Figure 7.10.

The airbag is deformed to the shape described by the arc 1-2-3-4-5-6-7. This arc is the same length as the arc along the circle A from 1-PA-7. This may be established by considering the angle ϕ in the figure. We have

$$\text{Arc } P_A\text{-}7 = r_A \phi = (r_A - r_B)\, 2\phi + r_B \phi \over 2 \tag{7.24}$$

The line from 2 to 6 is tangent to the circles. Points 2 and 6 are the same distance from the center line as are the centers of the tangent circles.

This distance α is

$$\alpha^2 = r_c^2 - (r_c - \tfrac{p}{2})^2 \tag{7.25}$$

The volume of revolution of a sector of a circle as shown in the figure below is

$$V_s = \pi r^3 \left[2/3 - \cos \phi \left(1 - \cos^2 \phi/3 \right) \right] \tag{7.26}$$

194
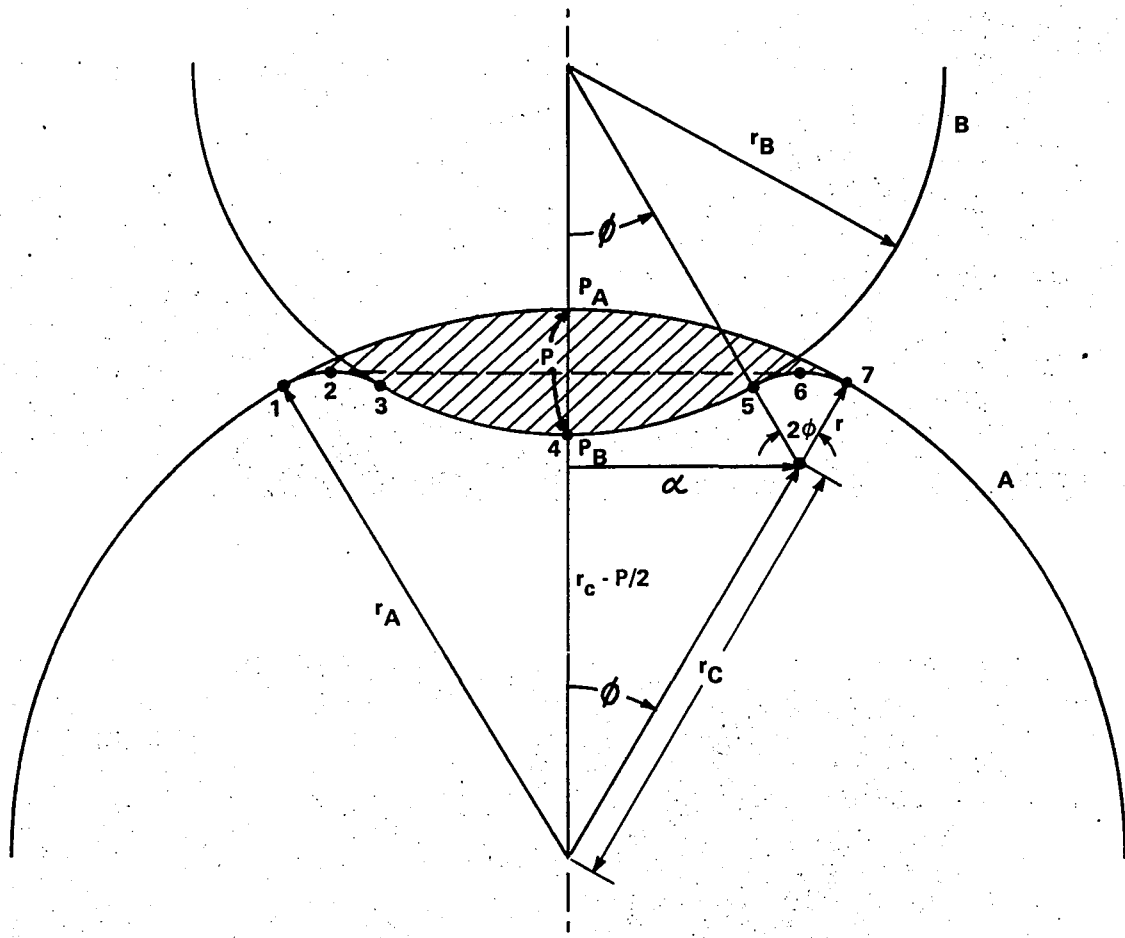
Figure 7.10 CASE I AIR BAG CONTACT GEOMETRY
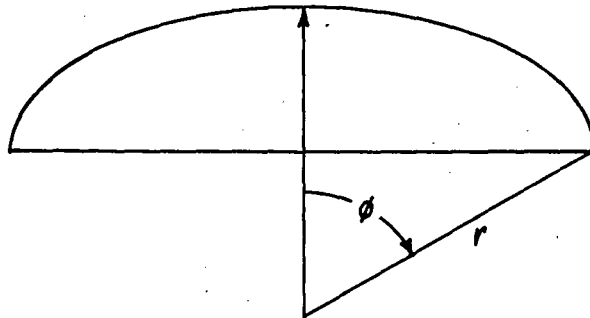
And the volume of a ring as below is
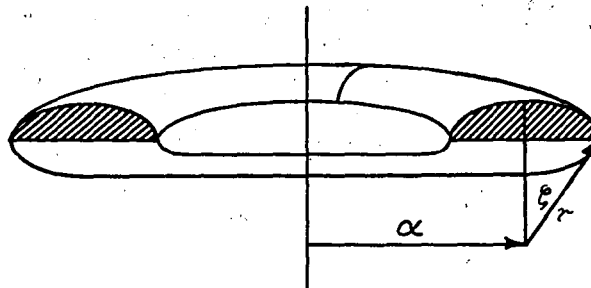
$$V_R = 2 \pi \alpha \, r^2 \left[\phi - \sin \phi \, \cos \phi \right]$$

(7.27)

Hence the volume of the shaded area in the figure above is

$$V = \pi \, r_A^3 \left[2/3 - \cos \phi \left(1 - \cos^2 \phi / 3 \right) \right]$$

$$+ \pi \, r_B^3 \left[2/3 - \cos \phi \left(1 - \cos^2 \phi / 3 \right) \right]$$

$$- 2 \pi \, r_C \, r^2 \sin \phi \left[\phi - \sin \phi \, \cos \phi \right]$$

(7.28)

where
$$\cos \phi = 1 - P / (r_A + r_B)$$
$$\alpha = r_C \sin \phi$$

$$V = \pi \left\{ \left(r_A^3 + r_B^3 \right) \left(\frac{P}{r_A + r_B} \right)^2 \left(1 - 1/3 \, \frac{P}{r_A + r_B} \right) \right.$$

$$\left. - \alpha \, r^2 \left[\pi - 2 \sin^{-1} \left(1 - \frac{P}{r_A + r_B} \right) - 2 \frac{\alpha}{r_C} \left(1 - P / r_A + r_B \right) \right] \right\}$$

(7.29)

196

Case II: The radius of curvature r_A is smaller than r_B
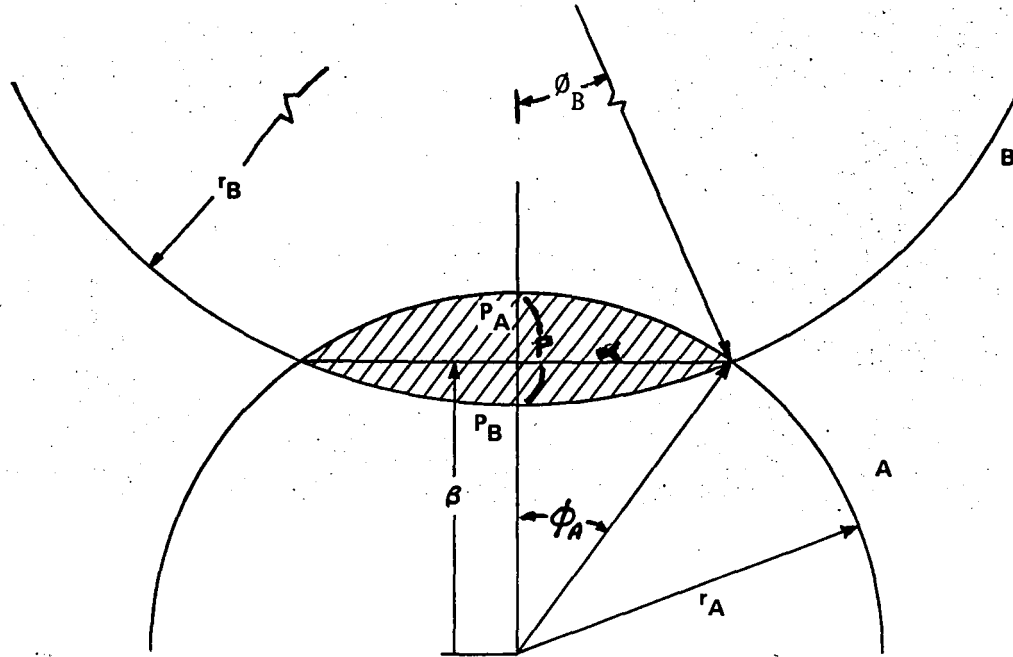
Figure 7.11   CASE II AIR BAG CONTACT GEOMETRY

In this case no tangent circle is constructed since the arc
length along the bag is greater than the arc of the contacting
surface.

Alpha, α is computed as the distance to the point of intersec-
tion as follows:

$$\beta = \left(r_A^2 - r_B^2 + \left(r_A + r_B - \rho \right)^2 \right) / 2 \left(r_A + r_B - \rho \right)$$
$$\alpha^2 = r_A^2 - \beta^2$$

(7.30)

The volume is

$$V = \pi r_A^3 \left[2/3 - \cos \phi_A \left(1 - \cos^2 \phi_A / 3 \right) \right]$$

$$+ \pi r_B^3 \left[2/3 - \cos \phi_B \left(1 - \cos^2 \phi_B / 3 \right) \right] \qquad (7.31)$$

Since

$$\cos \phi_A = \beta / r_A \qquad\qquad (7.32)$$

and $\cos \phi_B = 1 - (P + \beta - r_A) / r_B$

It is now possible to write

$$V = \pi r_A^3 \left(1 - \beta / r_A \right)^2 \left(1 - \left(1 - \beta / r_A \right) / 3 \right)$$

$$+ \pi r_B^3 \left(1 - \left(P + \beta - r_A \right) / r_B \right)^2 \left(1 - \left(1 - \left(P + \beta - r_A / r_B \right) / 3 \right) \right) \quad (7.33)$$

After the above computations are made in each plane the volume of intersection is computed as the average of the volumes of revolution obtained in each plane and the area is estimated as π times the product of the α_S' (the area of our ellipse).

(Note: If the penetration is greater than the radius of curvature of the air-bag in any plane the computations are done by replacing the radius of curvature r_A with the penetration P_B . This serves to limit the volume in cases of extreme penetration where the algorithm is probably no longer valid).

The forces on the bag and on the contacting surface are assumed to be applied at the point P_B . A friction force is computed which apposes the tangential relative velocity of the two surfaces at this point using a friction coefficient supplied by the user. A ramp function is used to limit the frictional force for small relative velocities.

198

7.4.4   <u>Depth of Penetration for Air Bag Routines</u>
         <u>(Subroutine EDEPTH)</u>

         The airbag routines which consider the intersection of ellip-
soid contact surfaces with an ellipsoidal airbag require the points of maxi-
mum penetration. Intersection is determined by subroutine INTERS as de-
sired in Section 7.2.2. If an intersection is detected then subroutine EDEPTH
is used to compute the points of maximum penetration. The geometry of the
ellipsoid-airbag contact is illustrated in Figure 7.12.
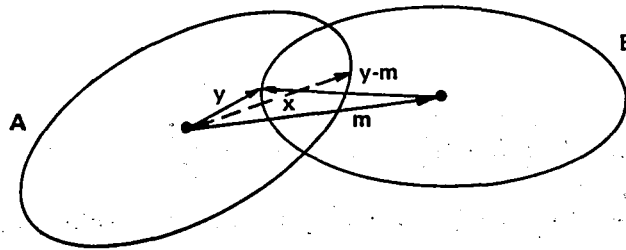
Figure 7.12   ELLIPSOID-ELLIPSOID PENETRATION

         Consider ellipsoids A and B whose centers are separated by
the vector m. It is desired to find the point X on A and y on B such that
the distance $|y-x|$ is a maximum and represents the maximum penetra-
tion in the region of intersection of the ellipsoids.

At the point of maximum penetration, the vector $y-x$ will be aligned with the normals at the ellipsoids. That is

$$\lambda A x = y - x = -\nu B(y-m) \tag{7.34}$$

where $x \cdot A x = 1, (y-m) \cdot B(y-m) = 1$ and ν and λ are negative scalars. Eliminating x we get

$$(\lambda \nu A B + \lambda A + \nu B)(y-m) = -\lambda A m \tag{7.35}$$

Thus

$$y - m = -(\lambda \nu A B + \lambda A + \nu B)^{-1} \lambda A m \tag{7.36}$$

If $y - m$ is known x is given by

$$x = y + \nu B(y-m) \tag{7.37}$$

The scalars λ and ν must be chosen such that

$$x \cdot A x = 1 = (y-m) \cdot B(y-m) \tag{7.38}$$

The procedure used is an iterative Newton Raphson scheme. Starting values of λ and ν are estimated. From these $y - m$ and x may be evaluated. The ellipsoid equations are considered as functions of λ and ν. That is

$$f(\lambda, \nu) = x \cdot A x - 1 \tag{7.39}$$

and

$$g(\lambda, \nu) = (y-m) \cdot B(y-m) - 1$$

Determining λ, ν such that $f(\lambda, \nu) = g(\lambda, \nu) = 0$

Using a Taylor series expansion yields

200

$$f(\lambda + \delta\lambda, \nu + \delta\nu) = f(\lambda, \nu) + \frac{\partial f}{\partial \lambda}\delta\lambda + \frac{\partial f}{\partial \nu}\delta\nu$$

$$g(\lambda + \delta\lambda, \nu + \delta\nu) = g(\lambda, \nu) + \frac{\partial g}{\partial \lambda}\delta\lambda + \frac{\partial g}{\partial \nu}\delta\nu$$

(7.40)

Thus $\delta\lambda$ and $\delta\nu$ may be estimated from the equations

$$\frac{\partial f}{\partial \lambda}\delta\lambda + \frac{\partial f}{\partial \nu}\delta\nu = -f(\lambda, \nu)$$

$$\frac{\partial g}{\partial \nu}\delta\lambda + \frac{\partial g}{\partial \nu}\delta\nu = -g(\lambda, \nu)$$

(7.41)

Replace λ by $\lambda + \delta\lambda$ and ν by $\nu + \delta\nu$ and repeat the procedure until $\left|\frac{\delta\lambda}{\lambda}\right|$, $\left|\frac{\delta\nu}{\nu}\right|$ are less than some test.

To evaluate the partials it is necessary to have

$$\frac{\partial x}{\partial \lambda}, \frac{\partial x}{\partial \nu}, \frac{\partial y}{\partial \lambda}, \frac{\partial y}{\partial \nu}$$

Differentiating with respect to λ, ν yields:

$$\frac{\partial y}{\partial \lambda} = -(\nu\lambda AB + \lambda A + \nu B)^{-1}Ax$$

$$\frac{\partial x}{\partial \lambda} = \frac{\partial y}{\partial \lambda} + \nu B \frac{\partial y}{\partial \lambda}$$

$$\frac{\partial x}{\partial \nu} = -(\nu\lambda \text{ BA} + \lambda A + \nu B)^{-1}B(y-m)$$

$$\frac{\partial y}{\partial \nu} = \frac{\partial x}{\partial \nu} + \lambda A \frac{\partial x}{\partial \nu}$$

(7.42)

and for f and g,

$$\frac{\partial f}{\partial \lambda} = 2x \cdot A \frac{\partial x}{\partial \lambda}$$

$$\frac{\partial f}{\partial \nu} = 2x \cdot A \frac{\partial x}{\partial \nu}$$

$$\frac{\partial g}{\partial \lambda} = 2(y-m) \cdot B \frac{\partial y}{\partial \lambda}$$

$$\frac{\partial g}{\partial \nu} = 2(y-m) \cdot B \frac{\partial y}{\partial \nu}$$

(7.43)

This completes the evaluation of the necessary derivatives.

7.4.5   Gas Dynamics of the Inflatable Restraint System   (Air bag)

The gas dynamics model for the airbag is considered in separate parts. One part consists of the gas supply model and the other part consists of the gas dynamics of the inflating or deflating bag.

Gas Supply Model

The basic assumptions are:

(1)   Perfect gas

(2)   One-dimensional, quasi-steady, isentropic flow

(3)   The flow through the nozzle is choked for the time duration of interest

(4)   The mean velocity of the gas in the supply is small

The mass flow per unit area in a choked nozzle is given by*

$$\omega = \left[\gamma \, g \, P \, \rho \left(\frac{2}{\gamma + 1} \right)^{\frac{\gamma + 1}{\gamma - 1}} \right]^{1/2} \tag{7.44}$$

where ω is the flow in (lbs/sec in^2)

g is the acceleration of gravity (in/sec^2)

p is the pressure (lb/in^2)

ρ is the density (lb/in^3)

γ is the ratio of specific heats ($\sim$1.4)

The change in density of the constant volume supply cylinder is

$$\frac{d\rho}{dt} = - \frac{\omega \, c_D \, A}{V_o} \tag{7.45}$$

where

V_o is the volume of the supply (in^3)

A   is the area of the throat (in^2)

C_D is the discharge coefficient of the nozzle (throat)

For adiabatic flow the following relation is valid

$$P = P_o \left(\rho / \rho_o \right)^{\gamma}$$

(7.46)

where P_o and ρ_o are a reference pressure and density.

The ideal gas law is

$$P = \rho RT = m RT / V_o$$

(7.47)

where   T .   is the temperature ($^\circ$Rankine)

.R   is the gas constant   (in per $^\circ$Rankine)

M   is the mass   (lb)

Combining equations (7.44) thru (7.47) and integrating yields,

$$\rho = \rho_o \big/ Q^{2/\gamma-1}$$

(7.48)

where

ρ_0 = is the initial density

Q = 1 + c (t-t$_o$)

$$c = \frac{C_D A}{V_o} \left(\frac{\gamma-1}{2} \right) \sqrt{\gamma g \, \frac{P_o}{\rho_o} \left(\frac{2}{\gamma+1} \right)^{\frac{\gamma+1}{\gamma-1}}}$$

(7.49)

t = is the time (sec)

(7.50)

and where the subscript o refers to the initial values of the respective variables.

We also have

p = p$_o$ / Q$^{2\gamma/\gamma-1}$

T = T$_o$ / Q^2

(7.51)

Initially, the mass of air in the cylinder (m_0) is

$$M_0 = V_0 \rho_0$$

hence the mass of air discharged into the bag M_m is given by

$$M_m = M_0 - V_0 \rho$$

$$= V_0 \rho_0 \left(1 - \rho/\rho_0\right) \qquad (7.52)$$

Gas Dynamics of the Airbag

During inflation, the volume of the bag, V_b, is estimated by

$$V_b = V_{max} \left(1 - P/P_0\right) \qquad (7.53)$$

where

$$V_{max} = \frac{V_0 P_0}{\gamma P_a} \qquad (7.54)$$
$$P_a = \text{atmospheric pressure}$$

When the calculated value of V_b is equal to the geometric volume of the fully inflated bag the gauge pressure in the bag, P_b, is computed by

$$P_b = P_a \left(\rho_b/\rho_a\right)^\gamma - P_a \qquad (7.55)$$

where ρ_a is the density of the gas in the bag when it was first fully inflated (i. e. when its calculated volume equalled the geometric volume at atmospheric pressure)

$$\rho_b = M_b/V_b$$
$$m_b = \text{mass of air in bag}$$
$$V_b = \text{volume of bag}$$

The volume V_b of the bag is the geometric volume minus the decrease in volume due to the contacting surfaces. The mass of gas in the

205

bag is the mass of the gas discharged into the bag less the mass of gas exhausted through the bag exhaust orifices

$$M_t = M_{in} - M_{out}$$

where M_{in} is given by equation (7.52) and M_{out} is the mass of gas exhausted.

The quantity of gas exhausted is estimated from the relation

$$\frac{d M_{out}}{dt} = 0 \qquad \text{if } p_b \text{ is less than a specified vent pressure}$$

$$\frac{d M_{out}}{dt} = \left(C_D A g \sqrt{2 P_a \, \partial P_t} \middle/ v_s \right) \qquad \text{if } p_b \text{ exceeds vent pressure}$$

206

7.5   FORCE DEFLECTION MODEL

In this model surface contact forces are replaced by a single force which is applied at a specific point and in a specific direction as determined by the various contact routines. The magnitude of the normal force is computed as a function of a single parameter which for the ellipsoid-plane and ellipsoid-ellipsoid contact routines is a measure of the maximum penetration. In addition a friction force is computed which is proportioned to the normal force and is in such a direction as to oppose the tangential velocity. The model does not allow for the addition of viscous or inertial forces except as provided by the "inertial" spike described in the following or the impulse described in section 7.7.

In the force deflection calculation, hysteresis effects are approximated by specification of an energy absorption factor R which may be a function of the force deflection parameter δ . Permanent offset may be specified as a deflection factor G which may be a function of the parameter δ . A unique force deflection characteristic is assigned to each contract hence one should specify the force deflection characteristic as representative of the mutual properties of the contact involved. In specifying a mutual force deflection it is important to remember that the parameter δ as computed in the program is a geometric property of the contact surfaces which is computed as if the surfaces were not deformed during the impact.

Five functions are associated with each contact. These are:

1.   Base Force Deflection
2.   Inertial spike
3.   Energy Absorption factor (R)
4.   Deflection factor (G)
5.   Friction Coefficient

In the current model these functions are assumed to be functions of the penetration factor (force deflection parameter.) No provision is made for variation with velocity.

Each of these functions may be subdivided, if desired, into two separate parts $f_1(\delta)$ and $f_2(\delta)$ where,

$\qquad f_1(\delta)$ is defined for $\quad 0 \leq \delta_o \leq \delta \leq \delta_1$

and

$\qquad f_2(\delta)$ is defined for $\quad \delta_1 \leq \delta \leq \delta_2$

If δ is greater than the last defined value the function is assumed to be a constant equal to the last defined value. Each of these functions may be any of three functional forms; a constant, tabular data, or a fifth degree polynomial in δ .

The force deflection is constructed in the following manner using the first four functions
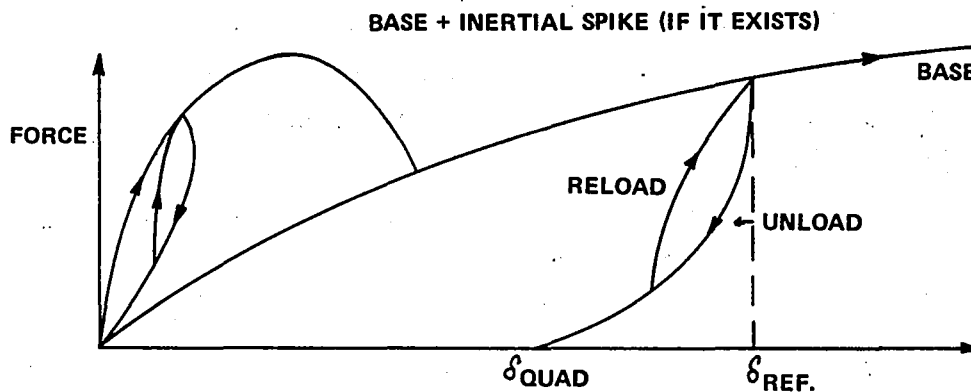
Figure 7.13 FORCE DEFLECTION CURVE

208

Initial loading occurs along the base curve plus the inertial spike(need not be used.) As long as continuous loading occurs the characteristic obtained will be the base plus the inertial spike. Unloading will proceed down an unloading curve. If unloading occurs after a specified deflection is achieved, the inertial spike is deleted from further calculations of the force.

Since the program uses a variable step integrator which may reject a particular step and repeat the calculations for a smaller step size it is not possible to detect whether loading or unloading is occuring by comparing the present δ with the previous δ. To circumvent this problem, a complete force deflection characteristic is defined at the beginning of each new integrating step and is retained until a successful integration step has been achieved.

The subroutine then redefines a new force-deflection function depending on current value of δ as follows:

1. $\delta \leq 0$, or if $\delta = \delta_{last}$, return to calling program.

2. If $\delta < \delta_{CUBIC}$, unloading is occurring, define reloading cubic:

    (a)   If inertial spike exists and if $\delta_{REF} > \mathcal{D}_{IMAX}$, remove inertial spike from further consideration

    (b)   Set

$$\delta_{CUBIC} = max \left(\delta, \delta_{QUAD} \right)$$
$$\delta_{C_0} = \delta_{CUBIC}$$
$$\Delta = \delta_{REF} - \delta_{CUBIC}$$

(7.56)

    (c)   Define new cubic $F_c(\delta) = C_0 + C_1 \left(\delta - \delta_{CUBIC} \right) + C_2 \left(\delta - \delta_{CUBIC} \right)^2 + C_3 \left(\delta - \delta_{CUBIC} \right)^3$
    for $\delta_{CUBIC} \leq \delta \leq \delta_{REF}$ that satisfies the following conditions:

$$F_c \left(\delta_{REF} \right) = F_{BASE} \left(\delta_{REF} \right) \qquad F_c \left(\delta_{CUBIC} \right) = F_Q \left(\delta_{CUBIC} \right)$$
$$F_c' \left(\delta_{REF} \right) = F_{BASE}' \left(\delta_{REF} \right) \qquad F_c' \left(\delta_{CUBIC} \right) = F_Q' \left(\delta_{CUBIC} \right)$$

(7.57)

209

by

$$C_o = F_Q\,(\delta_{CUBIC})$$
$$C_1 = F_Q'\,(\delta_{CUBIC})$$

and C_2 and C_3 by solving simultaneously

$$C_2\,\Delta^2 + C_3\,\Delta^3 = F_{BASE}\,(\delta_{REF}) - C_o - C_1\,\Delta$$
$$2\,C_2\,\Delta + 3\,C_3\,\Delta^2 = F_{BASE}'\,(\delta_{REF}) - C_1$$

(7.58)

(d)   If local minimum of new cubic definition lies between δ_{CUBIC} and δ_{REF} and is negative, then replace cubic definition a straight line between the points [δ_{CUBIC} , $F_Q\,(\delta_{CUBIC})$] and [δ_{REF} , $F_{BASE}\,(\delta_{REF})$] by

$$C_o = F_Q\,(\delta_{CUBIC})$$
$$C_1 = \frac{1}{\Delta}\left[F_{BASE}\,(\delta_{REF}) - F_Q\,(\delta_{CUBIC})\right]$$
$$C_2 = C_3 = 0$$

(7.59)

and return to calling program.

3.   If $\delta_{CUBIC} \leq \delta \leq \delta_{REF}$, reloading is occurring; define new quadratic unloading curve from cubic curve

let $$y_2 = F_C\,(\delta_{C_o})$$

and $$A_{REA} = \int_{\delta_{QUAD}}^{\delta_{CUBIC}} F_Q\,(\delta)\,d\delta + \int_{\delta_{C_o}}^{\delta} F_C\,(\delta)\,d\delta - \int_{\delta_{C_o}}^{\delta_{CUBIC}} F_C\,(\delta)\,d\delta$$

(7.60)

and go to step number 5.

(Note: δ_{C_o} was the value of δ_{CUBIC} when $F_C\,(\delta)$ was defined.)

210

4. Otherwise, $\delta_{REF} < \delta$; define new quadratic unloading curve from base curve.

    (a)   If $\delta \geq \delta_{INER}$, remove inertial spike from further consideration.

    (b)   Determine R factor and place into R_{LAST} .
          If $R = 1$, use base curve for unloading by setting

$$\delta_{QUAD} = \delta_{CUBIC} = \delta_{REF} = q_0 = q_1 = q_2 = 0$$

          and return to calling program.

    (c)   Determine G factor and place into G_{LAST} .
          Fetch D_0 from input data for base function and compute

$$\delta_{QUAD} = D_0 + G_{LAST}(\delta - D_0)$$
$$y_2 = F_{BASE}(\delta)$$
$$y_2 = y_2 + F_{inertial}(\delta) \tag{7.61}$$

    if the inertial spike exists.

$$AREA = \int_0^{\delta} F_{BASE}(\delta)\,d\delta \tag{7.62}$$

5. Using values of y_2 and AREA defined in either step 3 or 4 determine new quadratic unloading function

$$F_Q(\delta) = q_0 + q_1(\delta - \delta_{QUAD}) + q_2(\delta - \delta_{QUAD})^2 \tag{7.63}$$

for $\delta_{QUAD} \leq \delta \leq \delta_{CUBIC}$ that satisfies the following conditions where

$$\delta_{CUBIC} = \delta$$
$$F_Q(\delta_{QUAD}) = 0$$
$$F_Q(\delta_{CUBIC}) = y_2 \tag{7.64}$$

and
$$\int_{\delta_{QUAD}}^{\delta_{CUBIC}} F_q(\delta)\,d\delta = R_{LAST} * AREA$$

by setting

$$q_0 = 0$$

$$q_1 = \frac{2}{\delta_{CUBIC} - \delta_{QUAD}} \left[\frac{3 R_{LAST} * AREA}{\delta_{CUBIC} - \delta_{QUAD}} - y_2 \right]$$

(7.65)

If $q_1 < 0$, q_1 is set to 0 to guarantee non-negative derivative at $\delta = \delta_{QUAD}$

and

$$q_2 = \frac{1}{\delta_{CUBIC} - \delta_{QUAD}} \left[\frac{y_2}{\delta_{CUBIC} - \delta_{QUAD}} - q_1 \right]$$

(7.66)

If $q_2 < 0$ $q_2 = \dfrac{y_2}{\delta_{CUBIC} - \delta_{QUAD}}$ to guarantee non-negative derivative at $\delta = \delta_{CUBIC}$

7.6   <u>IMPULSE FORCES</u>

For the first contact it is necessary to account for the sudden momentum change caused by impulsive type forces. For perfectly elastic impact an energy approach would be sufficient. For impacts which are not perfectly elastic a coefficient of restitution is generally used to define the force magnitude. In the literature most of the cases for which a coefficient of restitution is defined are for simple one or two dimensional problems. A more general treatment is given in Reference 16, but general three dimensional results are sparse for the type of materials of interest in the occupant crash environment. For this reason, the impulse capability has been incorporated in the program in the following manner.

The program has the capability of making a step change in the linear velocity, $\dot{x}$, and the angular velocity, ω, as a result of an impulsive force.

212

The model computes accelerations from forces, and from a computational point of view must distinguish between two types of impulses. The first type is one in which the direction of the impulsive force is specified and its magnitude is unknown, such as the force at the first instant of contact of a body segment with a vehicle surface or with another body segment.

The second type is one in which neither the direction nor the magnitude of the force is known, but a desired change in velocity is specified, such as the case where a joint is changed from an unlocked to a locked state. At the instant of locking, an impulsive torque must be applied which is sufficient to reduce the relative angular velocity of the segments adjoining the joint to zero.

For purposes of this discussion, the system equations may be represented in the form

$$\ddot{X} = \vec{S}' u$$

(7.67)

where u is the generalized applied forces and torques

S is the system matrix

$\ddot{X}$ is the resultant acceleration (linear and angular.)

Integrating from time t to $t + \xi$ yields

$$\dot{X}(t+\xi) - \dot{X}(t) = \int_{t}^{t+\xi} \vec{S}' u \, du$$

(7.68)

Taking the limit as ϵ goes to zero yields

$$\Delta \dot{X} = \vec{S}' \delta u$$

(7.69)

Where $\Delta \dot{X}$ is the impulsive change in velocity and

δu is the impulse (impulsive force.)

In the program the matrix S is not explicitly evaluated. It is implicit since the program computes forces and then solves a set of simultaneous equations using a sequence of matrix block type operation to obtain the acceleration.

Impulses will only be applied at the completion of a successful integration step before proceeding to the next step. Also, the integrator is reset and the step size is reduced to its starting value.

Consider the two types:

TYPE I

The direction of the impulse is known, its magnitude is not known. If more than one impulse occurs simultaneously it will be assumed that they are decoupled so that they can be handled sequentially by the technique developed for one. In this case the program steps are as follows:

1. Detect and identify the impulse to be considered.

2. Call the appropriate contact routine to apply an impulsive force of the proper direction as under a normal call. This is the only force applied (all other forces and gravity are set to zero.)

3. Solve the system equations.

4. Interpreting the computed acceleration as step changes in velocity per unit of force, determine the magnitude of the force using the coefficient of restitution. The normal component of relative velocity after the impulse at the point of contact will be the negative of the coefficient of restitution times the normal component of the relative velocity before the impulse.

5. Scale the $\Delta\dot{X}$ to the value determined in step 4 and add them to the $\dot{X}$ in the program.

6. Repeat steps 2-5 for all impulses to be considered at this time.

7. Make normal call to DAUX and reset integrator.

8. Proceed with normal program.

It should be noted that the impulsive force is applied in a direction that has a component normal to the surface and a component tangent to the surface. The tangential component is determined from the prescribed coefficient of friction and is opposed to the direction of the relative tangential velocity. Application of this type of impulse may or may not cause the direction of the tangential velocity to reverse. The exact treatment of an impulsive contact in three dimensions considering both linear and angular momentum is quite complex and has not been solved (Reference 16.) It should be noted that a reversal of relative tangential velocity is not unusual as the tennis or billiard player is well aware.

The coefficient of restitution, as interpreted by the program is the ratio of the negative of the resultant normal relative velocity after the impulse to the normal relative velocity before the impulse. Thus a coefficient of restitution of one (1) will reverse the normal component of the relative velocity while a value of zero (0) will result in a zero relative velocity after impact, and a coefficient of restitution equal minus one (-1) will produce no change in the relative velocity. No restriction is placed on the value of the coefficient of restitution by the program (i.e. a value of +2 or -8 will be accepted.) In normal usage, it is assumed that the value will be between ± 1.

TYPE II

   A resultant velocity change is specified, the impulse is unknown. For example, consider the case where an unlocked joint is locked, say the joint connecting segments i and j. Determine the impulse torque vector, t, applied at the joint which will determine $\Delta \omega_j$ and $\Delta \omega_i$ such that the resulting velocities are equal i.e.,

$$w_i + \Delta w_i = w_j + \Delta w_j \tag{7.70}$$

The system equation is

$$\Delta \dot{X} = S^{-1} t = S^{-1} \delta u \tag{7.71}$$

where

$$t = \begin{pmatrix} t_x \\ t_y \\ t_z \end{pmatrix} \tag{7.72}$$

and S is a 6*(number of segments) by 3 matrix then

$$\Delta w_i = S_i^{-1} \delta u$$
$$\Delta w_j = S_j^{-1} \delta u$$

Where S_i^{-1} are the three rows of S^{-1} that correspond to the $\Delta \dot{X}$ representing Δw_i and S_j^{-1} are the three rows of S^{-1} that correspond to the $\Delta \dot{X}$ representing $\Delta \omega_j$;

$$\delta u = t \tag{7.73}$$

Thus

$$\dot{w}_i + S_i^{-1} \delta u = w_j + S_j^{-1} \delta u \tag{7.74}$$

Solving for δu,

$$\delta u = (S_i^{-1} - S_j^{-1})^{-1} (w_j - w_i) \tag{7.75}$$

216

It is assumed that $S_i^{-1} - S_j^{-1}$ has an inverse. If it is singular, the problem cannot be solved.

The remaining $\Delta \dot{X}$ may now be evaluated from equation (7.71). The matrix S may be determined by repeated calls to the routine which solves the system equations, each call produces a solution vector which is a column of S^{-1}. In the first call, put a unit x component of torque on segment i and a negative unit x component of torque on segment j. The second call uses a y component and the third a z component.

In general, in order to consider the simultaneous application of impulses to one or more joints, $\mathcal{J}\mu$ is a vector of length 3*k, where k is the number of joints to be considered as impulsive. S has dimension 6* NSEG by 3*k and must be determined. There are k sets of equation (7.74). Equation (7.75) represents the solution of a 3*k by 3*k system of equations.

This development may be modified for the case where its joint is not completely locked in this case equation (7.70) is replaced with the equation

$$ p \, (\omega_i + \Delta \omega_i) \; = \; p \, (\omega_j + \Delta \omega_j) $$

where p is the appropriate projection operator;

if the joint is fully locked   p = I, the identity

if the joint is locked on axis h   p = hh·

if the joint is free on axis h   p = I-hh·

Equations (7.71) through (7.75) are modified accordingly.

SECTION 8

REFERENCES

1. Bartz, John A., "A Three-Dimensional Computer Simulation of a Motor Vehicle Crash Victim, Phase 1 - Development of the Computer Program," Calspan Report No. VJ-2978-V-1, July, 1971.

2. Bartz, John A. and Butler, Frank E., "A Three-Dimensional Computer Simulation of a Motor Vehicle Crash Victim, Phase 2 - Validation Study of the Model," Calspan Report No. VJ-2978-V-2, December, 1972.

3. Bartz, John A., Butler, Frank E. and Ryan, Charles T., "A Three-Dimensional Computer Simulation of a Motor Vehicle Crash Victim, Further Development - Mutual Force-Deflection Characteristics and Comprehensive 'Debug' Facility," Calspan Report No. ZQ-5326-V-2, September, 1974.

4. Fleck, J. T., Butler, F. E., and Vogel, S. L., "An Improved Three-Dimensional Computer Simulation of Motor Vehicle Crash Victims," Volumes I-IV, Report Nos., DOT-HS-801507, -508, -509, -510, July, 1974.

5. Fleck, J. T. and Butler, F. E., "Development of an Improved Computer Model of the Human Body and Extremity Dynamics," Report No. AMRL-TR-75-14, July, 1975 (AD A-014816).

6. Butler F. E. and Fleck, J. T., "Advanced Restraint System Modeling," Report No. AFAMRL-TR-80-14, May, 1980.

7. Federal Motor Vehicle Safety Standard 208, Part 572, "Anthropomorphic Test Dummy."

8. "Development of Approximating Solutions for CVS Program and of Dummy Design Information," Contract No. DOT-HS-6-01418 (in progress).

9. DeLeys, Norman J., "Data For Validation of Crash Victim Simulator," Calspan Report No. 6197-V-1, August, 1981.

10. Abramowitz, M. and Stegun, I. A., Handbook of Mathematical Functions, National Bureau of Standards, Chapters 16 and 17.

11. Goldstein, H., Classical Mechanics, Addison-Wesley Publishing Co., Inc. Reading, Mass., 1950, Seventh Edition, 1965.

12. Uspensky, J. V., Theory of Functions, McGraw Hill Book Co., 1948.

13. Corben, H. C. and Stehle, P., Classical Mechanics, John Wiley & Sons, Inc., New York, 1950.

14.   Herron, R. E., "Experimental Determination of Mechanical Features of
       Children and Adults." Biostereometrics Laboratory, Texas Institute for
       Rehabilitation and Research, Houston, Texas, Report No. DOT-HS-231-2-
       397, February, 1974.

15.   Cheers, F. Elements of Compressible Flow, John Wiley & Sons, Inc.,
       New York, 1963.

16.   Goldsmith, W., Impact, Edward Arnold Publications, London, 1960.

APPENDIX A

THE RIGID-BODY EQUATIONS OF MOTION

A-1   Basic Equations of General Rigid Body Motions

The dynamics of a system of rigid bodies depends upon the forces of interaction of the bodies and upon the single-body equations of motion. These basic rigid-body equations are summarized and derived in this section.

From Chasles' theorem (Reference 11, page 124), the general motion of a rigid body can be expressed as a translation plus a rotation. It follows that the complete differential equations of motion of the body are composed of a translational equation and a rotational equation. The most general forms of these equations are obtained when the rotational equations are expressed in terms of the rigid-body rotational inertia tensor about an arbitrary point of the body space. These most general forms are not necessary since the tensor of rotational inertia about an arbitrary point is simply related to the tensor of rotational inertia about the center of mass (c. m.) of the body. Accordingly, this discussion is limited to the simplest forms of the equations of motion. These equations are

$$m\, \ddot{\vec{X}} \;=\; \vec{F} \tag{A.1}$$

$$\dot{\vec{H}} \;=\; \vec{N} \tag{A.2}$$

where

$\vec{X}$ =   the center of mass (c. m.) of the body

m =   the total mass of the body

$\vec{H}$ =   the angular momentum (moment of linear momentum) of the body about its c. m.

$\vec{F}$ =   the sum of all external forces applied to the body

$\vec{N}$ =   the sum of the moments about the body c. m. of all forces applied to the body plus the sum of all force couples (torques) applied to the body.

The angular momentum about the c.m. is given by

$$\vec{H} = \phi \cdot \vec{\omega} \qquad\qquad\qquad (A.3)$$

where

ϕ = the tensor of rotational inertia of the body about its c.m.

$\vec{\omega}$ = the angular velocity of the body about its c.m.

Since the tensor of inertia is symmetric, it is diagonal when expressed in a special coordinate system, the principal-axis system of the body. In this system, the diagonal element ϕ_{ii} of ϕ is equal to the moment of inertia of the body about its ith principal axis. Thus, the component, H_i, of $\vec{H}$ in the direction of the ith principal axis is given by

$$H_i = \phi_i \omega_i$$

where

$$\phi_i = \phi_{ii}$$

and ω_i denotes the component of $\vec{\omega}$ in the direction of the ith principal axis. The component, $(\vec{H})_1$, of $\vec{H}$ in the direction of principal axis 1 of the body is given by

$$(\dot{\vec{H}})_1 = I_1 \dot{\omega}_1 - \omega_2 \omega_3 (I_2 - I_3) \qquad\qquad (A.4)$$

$(\dot{\vec{H}})_2$ and $(\dot{\vec{H}})_3$ can be obtained by cyclic permutations $1 \to 2$, $2 \to 3$, $3 \to 1$ of the subscripts in (A4)

The equations of motion in (A.1) and (A.2) are derived in the next subsection.

A-2

Derivation
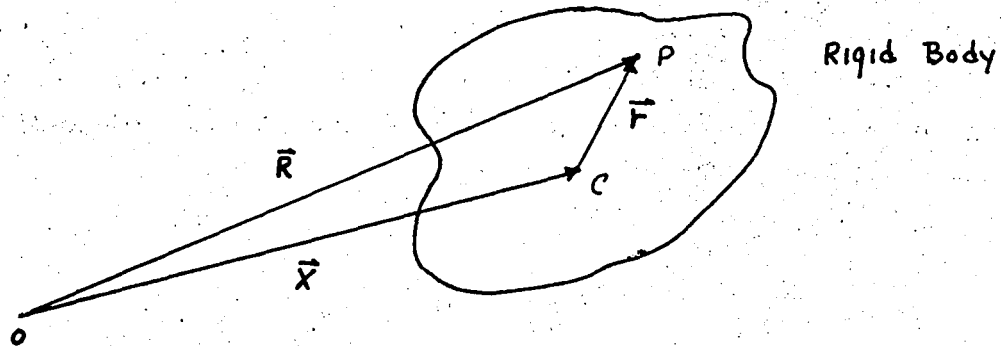
Figure A.1   VECTORS DEFINING A POINT IN A RIGID BODY

Figure A-1 depicts the geometry of the position vectors employed in the developments.   The point O is the origin of the space-fixed (inertial) reference frame.   Point C is a fixed point in the body which, for the present, is arbitrary but which is later identified with the body c.m..   Point p is any other fixed points in the body.   The position vector $\vec{r}$, which is directed from the point C to the point p, is rigidly fixed in the body.

From Newton's second law of motion, the equation of motion for the point p may be expressed

$$\rho(\vec{r})\ddot{\vec{R}} \;=\; \int \vec{f}(\vec{r}, \vec{r}^{1}) dv^{1} \;+\; \vec{F}(\vec{r}) \tag{A.5}$$

In (A.5), $\vec{R}$ denotes the position vector of the point p relative to the origin of the space-fixed coordinate system and $\vec{r}$ is as defined above.   Since $\vec{r}$ uniquely

A-3

defines the point p (when the point C has been defined), functions which depend on the position of p may be expressed as functions of $\vec{r}$.*

The function $\vec{F}(\vec{r})$ is the volume density at the point p of <u>external forces</u> applied to the body. $F(\vec{r})$ may include discrete forces by the employment of the formalism of Dirac delta functions. The function $\vec{f}(\vec{r}, \vec{r}^1)dV^1$ denotes the volume density of the force exerted at the point p due to the <u>direct action</u> of particles in a differential volume element dV^1 about a point p^1 with position vector $\vec{r}^1$ relative to the point C. In contrast to $\vec{F}(\vec{r})$, $\vec{f}(\vec{r}, \vec{r}^1)$ represents the effects of <u>internal forces</u> in the body. From Newton's third law of motion

$$\vec{f}(\vec{r}, \vec{r}^1) = -\vec{f}(\vec{r}^1, \vec{r}) \tag{A.6}$$

The integral in (A.5) is taken over the entire body, and dV^1 is to be expressed in terms of the components of $\vec{r}^1$ in a body-fixed reference frame.

From Figure A.1

$$\vec{R} = \vec{X} + \vec{r} \tag{A.7}$$

The time derivative of (A.7) relative to the <u>space-fixed</u> reference frame is

$$\dot{\vec{R}} = \dot{\vec{X}} + \dot{\vec{r}} \tag{A.8}$$

It will be shown that

$$\dot{\vec{r}} = \vec{\omega} \otimes \vec{r} \tag{A.9}$$

where $\vec{\omega}$ denotes the angular velocity of the body.

---

* In the present context, a function of $\vec{r}$, such as $p(\vec{r})$ is actually a function only of the components of $\vec{r}$ in a <u>body-fixed</u> coordinate system. $\vec{f}(\vec{r}, \vec{r}')$ and and $F(\vec{r})$ and (D) are also functions of time.

Let $\hat{e}_i$, ($i = 1, 2, 3$) denote orthogonal unit vectors rigidly fixed in the body and $\hat{e}_i^*$, ($i = 1, 2, 3$) denote orthogonal unit vectors in the space-fixed reference frame. Then

$$\hat{e}_i = \sum_{j=1}^{3} D_{ij} \hat{e}^j \qquad \text{(A.10)}$$

where

$$D_{ij} = \hat{e}_i \cdot \hat{e}^j$$

Since the matrix D with elements D_{ij} is orthogonal

$$D^T D = I \qquad \text{(A.11)}$$

where D^T denotes the transpose of D and I denotes the identity matrix. From (A.11) the inverse of (A.10) is

$$\hat{e}^j = \sum_{i=1}^{3} D_{ji}^T \hat{e}_i \qquad \text{(A.12)}$$

and so

$$r^j = \sum_{i=1}^{3} D_{ji}^T r_i$$

where r^j and r_i denote components of $\vec{r}$ in the space-fixed and body-fixed systems, respectively.

Equation (A.12) may be reexpressed

$$r^o = D^T r^b \qquad \text{(A.13)}$$

where r^o and r^b denote column vectors with components r_j and r_i respectively.

Since $\vec{r}$ is rigidly fixed in the body the column vector r^b is time independent. Thus, the time derivative of (A.13) is

A-5

$$\dot{r}^{\circ} = \dot{D}^{T} r^{b}.$$

or employing the inverse of (B.13)

$$\dot{r}^{\circ} = \dot{D}^{T} D r^{\circ}$$

(A.14)

Differentiating (B.11), one obtains

$$\dot{D}^{T} D + D^{T} \dot{D} = O$$

or

$$\dot{D}^{T} D + (\dot{D}^{T} D)^{T} = O$$

So $\dot{D}^{T} D$ is a skew symmetrix matrix. Accordingly, there exists a psuedo vector $\vec{\omega}$ such that *

$$\dot{D}^{T} D = (\omega \otimes I)$$

(A.15)

where $\tilde{I}$ denotes the identity tensor (or tensor idemfactor) and $(\omega \otimes I)$ denotes the matrix of the tensor $\vec{\omega} \otimes \tilde{I}$. Substituting (A.15) into (A.16) leads to

$$\dot{r}^{\circ} = (\omega \otimes I)r^{\circ}$$

(A.16)

Since the time derivative of $\dot{\hat{e}_{i}}$ is zero, the vector equivalent of (A.16) is

$$\dot{\vec{r}} = (\vec{\omega} \otimes \tilde{I})\vec{r}$$

(A.17)

or

$$\dot{\vec{r}} = \vec{\omega} \otimes \vec{r}$$

which agrees with A.9

---

* It is clear from (A.14) that in (A.16) and (A.15) the elements of $(\omega \otimes I)$ must be expressed in the space-fixed coordinate system. By contrast, in the relation $D \dot{D} = (\omega \otimes I)$ the elements of $(\omega \otimes I)$ must be expressed in the body-fixed coordinate system. In the vector relations (A.9) and (A.17), $\vec{\omega}$, $\tilde{I}$, and $\vec{r_0}$ may be expressed in any coordinate system.

A-6

The translational equation of motion is obtained by integrating $(A.5)$ with respect to $\vec{r}$ over the entire body:

$$\int p(\vec{r})\ddot{\vec{R}}\, dV = \int\int \vec{f}(\vec{r}, \vec{r}^1)\, dV^1\, dV + \vec{F}$$

(A.18)

where

$$\vec{F} = \int F(\vec{r})\, dV$$

(A.19)

evidently, $\vec{F}$ is equal to the net external force applied to the body. In $(A.18)$, dV is a volume element about the terminal point of $\vec{r}$. It is to be expressed in terms of the components of $\vec{r}$ in the body-fixed coordinate system. From $(A.6)$, it is concluded that

$$\int\int \vec{f}(\vec{r}, \vec{r}^1)\, dV\, dV^1 = 0$$

(A.20)

Since $p(\vec{r})$ is a function only of the components of $\vec{r}$ in the body-fixed reference frame, it is to be treated as time independent in the integrand in the left member of $(A.18)$. It follows that

$$\int p(\vec{r})\ddot{\vec{R}}\, dV = \frac{d^2}{dt^2} \int p(\vec{r})\vec{R}\, dV$$

(A.21)

It is convenient to identify the point C with the c.m. of the body. Then (see Figure $A.1$)

$$\vec{X} = \frac{1}{m} \int p(\vec{r})\vec{R}\, dV$$

(A.22)

where m is the total mass, given by

$$m = \int p(\vec{r})\, dV$$

(A.23)

A-7.

Employing (A.19 - A.22), (A.18) reduces to

$$m \ddot{\vec{X}} = \vec{F}$$

which agrees with (A.1).

The rotational equation is obtained from the volume integral of the first moment of (A.5) about the point C (that is, about the c.m.):

$$\int \rho(\vec{r}) \vec{r} \otimes \ddot{\vec{R}} \, dV = \int\int \vec{r} \otimes \vec{f}(\vec{r}, \vec{r}^1) \, dV^1 dV + \vec{N}$$

(A.24)

where

$$\vec{N} = \int \vec{r} \otimes \vec{F}(\vec{r}) \, dV$$

Interchanging the dummy variables $\vec{r}$ and $\vec{r}^1$ in the double integral in (A.24) it is concluded that

$$\int\int \vec{r} \otimes \vec{f}(\vec{r}, \vec{r}^1) \, dV dV^1 = \int\int \vec{r}^1 \otimes f(\vec{r}^1, \vec{r}) \, dV dV^1$$

It follows from this relation and (A.6) that

$$\int\int \vec{r} \otimes \vec{f}(\vec{r}, \vec{r}^1) \, dV dV^1 = \frac{1}{2} \int\int [\vec{r} \otimes f(\vec{r}, \vec{r}^1) + \vec{r}^1 \otimes f(\vec{r}^1, \vec{r})] \, dV dV^1$$

$$= \frac{1}{2} \int\int [\vec{r} - \vec{r}^1) \otimes \vec{f}(\vec{r}, \vec{r}^1) \, dV dV^1$$

Now, it is assumed that the internal forces in the body are central forces. Therefore $\vec{f}(\vec{r}, \vec{r}^1)$ is parallel to a vector directed from the point p^1 to the point p, that is, parallel to $(\vec{r} - \vec{r}^1)$. From the foregoing relation

$$\int\int \vec{r} \otimes \vec{f}(\vec{r}, \vec{r}^1) \, dV dV^1 = O$$

(A.25)

Since the vector $\vec{r}$ is directed from the body c.m. to the point p, the total angular momentum (moment of linear momentum), $\vec{H}$, about the c.m. is given by

$$\vec{H} = \int \rho(\vec{r})\, \vec{r} \otimes \dot{\vec{R}}\, dV$$

(A.26)

Equation (A.26) may be reexpressed

$$\vec{H} = \iiint \rho(r_1, r_2, r_3)\, [r_1\hat{e}_1 + r_2\hat{e}_2 + r_3\hat{e}_3] \otimes \dot{\vec{R}}\, dr_1 dr_2 dr_3$$

(A.27)

where r_i and $\hat{e}_i$ are as defined above. Since (A.9) is valid for arbitrary body-fixed vectors it follows that

$$\dot{\hat{e}}_i = \vec{\omega} \otimes \hat{e}_i$$

Employing this relation, one obtains for the time derivative of (A.27)

$$\dot{\vec{H}} = \int \rho(\vec{r})\, (\vec{\omega} \otimes \vec{r}) \otimes \dot{\vec{R}}\, dV \ + \int \rho(\vec{r})\, r \otimes \ddot{\vec{R}}\, dV$$

(A.28)

From (A.8) and (A.9)

$$\int \rho(\vec{r})\, (\vec{\omega} \otimes \vec{r}) \otimes \dot{\vec{R}}\, dV = \int \rho(\vec{r})\, (\vec{\omega} \otimes \vec{r}) \otimes \left(\vec{\omega} \otimes \vec{r} \ \times\ \dot{\vec{X}} \right) dV$$

$$= [\vec{\omega} \otimes \int \rho(\vec{r})\vec{r}\, dV] \otimes \dot{\vec{X}} = 0$$

The vanishing of this term is a consequence of the relations

$$\int \rho(\vec{r})\vec{r}\, dV = 0$$

(A.29)

which follows from (A.22), (A.23) and (A.7). Employing (A.25), (A.27) and (A.24), (A.28) reduces to

$$\dot{\vec{H}} = \vec{N}$$

A-9

which agrees with (A.2).

Substituting (A.8) into (A.26) and employing (A.9) results in

$$\vec{H} = \int \rho(\vec{r}) \, \vec{r} \otimes \dot{\vec{X}} \, dV + \int \rho(\vec{r}) \, \vec{r} \otimes (\vec{\omega} \times \vec{r}) \, dV$$

which reduces, by virtue of (A.29) and the triple cross product expansion, to

$$\vec{H} = \phi \cdot \vec{\omega}$$

where

(A.30)

$$\phi = \int \rho(\vec{r}) \, [\vec{r} \cdot \vec{r} \, \tilde{I} - \vec{r} \, \vec{r}] \, dV$$

(A.31)

Equation (A.31) is the fundamental defining relation for the tensor of rotational inertia about the c.m. It is apparent that ϕ is symmetric.

A.2   COMPARISON OF LAGRANGIAN AND NEWTONIAN TECHNIQUES FOR DERIVING
         EQUATIONS OF MOTION

         This section is included for completeness so that one skilled in the
classical treatment of rigid body dynamics may fully understand the techniques
used in the Calspan model and realize that the resultant equations of motion
are equivalent. Understanding of this section is not essential for use of the
program.*

A.2.1   Methods

         The classical treatments of holonomic constraints in rigid-body dy-
namics include the Newtonian method, the Lagrange method, and what may be termed
the independent-coordinate method. The treatment employed in the Calspan 3D
Crash-Simulation Model differs from each of the classical methods. It is similar
to the Newtonian method in that constraint forces are explicitly contained in the
equations of motion without the employment of Lagrange multipliers. However, in
contrast to the classical Newtonian method (in which explicit expressions invol-
ving the constraint forces are obtained by force-diagram analysis), the Calspan
Model employs constraint relations of the type employed in the Lagrange method.
In lieu of the employment of Lagrange multipliers, these constraint relations
are supplemented by additional relations, called compatibility relations, which
are inforced from Newton's third law and/or analysis of constraint-force geometry.

         Since the method employed in the Calspan Model does not appear to be
documented in the published literature, the objective of this section is to show
that this method is equivalent to the Lagrange method. The first step toward
this objective is the proof, in the next subsection, that Lagrange-type constraint

---

* The classical methods do not apply to the sliding constraint as indicated in
   Reference 11, page 15.

terms can be included in the Euler equations of motion. This proof is desirable since the equations of motion employed in the Calspan Model are of the Euler type.

In the subsection titled <u>Equivalence Relations</u>, the equivalence of the Calspan method to the Lagrange method is formally demonstrated, and it is shown that the compatibility relations which are employed in the Calspan formalism can be inferred from the relations connecting the Lagrange multipliers and the constraint forces and torques. Finally, in the subsection titled <u>Examples</u>, the equivalence of the Calspan method to the Lagrange method is demonstrated for a few simple joints.

A.2.2   Equations of Motion

The basis for the proof of equivalence given in the next subsection is the vector form of the Euler equations of motion containing Lagrange-multiplier-type constraint terms. These equations are first stated and then derived.

For L rigid bodies and M vector constraint relations, the equations of motion are:

$$M_{\ell} \, \ddot{\vec{x}}^{\,\ell} = \sum_{m=1}^{M} \vec{f}_{m}^{\,\ell} + \vec{F}_{\ell} \qquad\qquad (A.32)$$

$$\ell = 1, \cdots L$$

$$\dot{\vec{H}}^{\,\ell} = \sum_{m=1}^{M} \vec{n}_{m}^{\,\ell} + \vec{N}_{\ell} \qquad\qquad (A.33)$$

$$\sum_{\ell=1}^{L} \left\{ A_{m}^{\ell} \cdot \vec{\omega}^{\,\ell} + B_{m}^{\ell} \cdot \ddot{\vec{x}}^{\,\ell} \right\} + \vec{D}_{m} = 0 \qquad\qquad (A.34)$$

$$m = 1, \cdots, M$$

$$\vec{f}_{m}^{\,\ell} = \vec{\lambda}_{m} \cdot B_{m}^{\ell} \qquad\qquad (A.35)$$

$$m = 1, \cdots, M$$

A-12

$$\vec{n}_m^{\ell} = \vec{\lambda}_m \cdot A_m^{\ell}$$

<div align="right">(A.36)</div>

where

$$\vec{e}_j^{\ell} \cdot \dot{\vec{H}}^{\ell} = \phi_j^{\ell} \dot{\omega}_j^{\ell} + \sum_{i=1}^{3} \sum_{k=1}^{3} \omega_i^{\ell} \omega_k^{\ell} \delta_{jki} \phi_i^{\ell}$$

<div align="right">(A.37)</div>

definitions follow:

M_ℓ mass of lth body

ϕ_i^ℓ moment of inertia of lth body about its ith principal axis

$\vec{F}_\ell$ net external force acting on lth body

$\vec{N}_\ell$ net external torque acting on lth body, about c.m. of lth body

$\vec{f}_m^\ell$ constraint force acting on lth body due to mth constraint

$\vec{n}_m^\ell$ constraint torque acting on lth body due to mth constraint

$\vec{H}^\ell$ angular momentum of lth body about its c.m.

$\vec{x}^\ell$ position vector of c.m. of lth body relative to origin of laboratory coordinate system

$\vec{\omega}^\ell$ angular velocity of lth body about its c.m.

A_m^ℓ tensor coefficient of $\vec{\omega}^\ell$ in mth constraint relation

B_m^ℓ tensor coefficient of $\dot{\vec{x}}^\ell$ in mth constraint relation

$\vec{D}_m$ coordinate-derivative-independent additive vector in mth constraint relation

$\vec{e}_j^\ell$ unit vector in direction of jth principal axis of lth body

$\hat{e}_j^o$ unit vector in direction of jth axis of laboratory coordinate system

δ_{ijk} alternating symbol equal to:

       0 if any two of the indices i,j,k are equal

       1 if ijk is an even permutation of 123

       -1 if ijk is an odd permutation of 123

ω_i^{ℓ} component of angular velocity of lth body about its c.m., in direction of ith principal axis of body

$\vec{\lambda}_m$ vector Lagrange multiplier for mth constraint

λ_{mk} $\vec{\lambda}_m \cdot \hat{e}_k^0 = $ Lagrange multiplier corresponding to kth component equation of mth vector constraint relation

χ_j^{ℓ} jth component of $\vec{\chi}^{\ell}$ in laboratory coordinate system

a_{mkj}^{ℓ} $\hat{e}_k^0 \cdot A_m^{\ell} \cdot \vec{e}_j^{\ell}$ coefficient of ω_j^{ℓ} in kth component equation of mth vector constraint relation

d_{mk} $\hat{e}_k^0 \cdot \vec{D}_m$ additive constant in kth component equation of mth vector constraint relation

b_{mkj}^{ℓ} $\hat{e}_k^0 \cdot B_m^{\ell} \cdot \hat{e}_j^0$ coefficient of $\dot{\chi}_j^{\ell}$ in kth component equation of mth vector constraint relation

The equations of motion have been displayed in the vector form because the constraint relations employed in the Calspan Model are inferred in vector form, and are more compact in the vector notation. Even more important, the vector forms allow flexibility in choosing optimal component representations. Component equations corresponding to the vector equations are derived in the following discussion.

Lagrange-multiplier-type constraint terms arise most naturally from the inclusion of constraint relations in Hamilton's Principle. However, the Euler equations of motion cannot be obtained directly by the application of Hamilton's Principle to a Lagrangian which is identified with the kinetic energy of the system.

One way in which this difficulty can be circumvented is to obtain the Euler equations including Lagrange-type constraint terms by direct transformation of the Lagrange equations of motion in terms of the Euler angles. This approach is employed here.

The starting point of the development is Lagrange's equations including generalized forces and holonomic constraints. These are (Ref. 11, page 42)

$$\frac{d}{dt} \cdot \frac{\partial \mathcal{L}}{\partial \dot{q}_k} - \frac{\partial \mathcal{L}}{\partial q_k} = \sum_{\ell=1}^{m} \lambda_\ell \, a_{\ell k} + Q_k$$
$$k = 1, \cdots, N$$
(A.38)

$$\sum_{k} a_{\ell k} \, \dot{q}_k + a_\ell = 0 \qquad \ell = 1, \cdots, m$$
(A.39)

where the q_k are generalized coordinates, the Q_k are generalized forces, Equations (A.39) are the constraint relations, and the λ_ℓ are Lagrange multipliers. In this formulation applied forces and constraints are included in the right side of (A.38) so the Lagrangian is given by

$$\mathcal{L}(q_1, \cdots, q_N, \dot{q}_1, \cdots \dot{q}_N) = T(q_1, \cdots, q_N, \dot{q}_1, \cdots \dot{q}_N)$$
(A.40)

where T denotes the total kinetic energy of the system expression in terms of the generalized coordinates q_j and coordinate derivatives $\dot{q}_j$.

The first step in the development is to particularize the relations in (A.38) and (A.39) to L rigid bodies with M_s holonomic constraints, and to the coordinates of interest. The coordinates for the lth body are the rectangular coordinates, X_i^ℓ, of the body c.m. in the laboratory frame, and the Euler angles $\theta^\ell, \phi^\ell, \psi^\ell$ defined on page 107 of Reference 11. As indicated by Goldstein, these coordinates are suitable for the Lagrangian formalism. For the sake of compactness of notation it proves convenient to employ the symbols θ_i^ℓ defined by

A-15

$$\left.\begin{array}{rcl} \bar{\theta}_1^{\ell} &=& \theta^{\ell} \\[2mm] \bar{\theta}_2^{\ell} &=& \phi^{\ell} \\[2mm] \bar{\theta}_3^{\ell} &=& \psi^{\ell} \end{array}\right\} \tag{A.41}$$

The Lagrange equations for the system may be expressed, in accord with (A.38) and (A.39) as

$$\frac{d}{dt}\frac{\partial \mathcal{L}}{\partial \dot{x}_i^{\ell}} - \frac{\partial \mathcal{L}}{\partial x_i^{\ell}} = \sum_{m=1}^{M_s} \lambda_m b_{m_i}^{\ell} + F_i^{\ell}$$
$$i=1,\cdots,3\,;\ \ell=1,\cdots,L \tag{A.42}$$

$$\frac{d}{dt}\frac{\partial \mathcal{L}}{\partial \dot{\bar{\theta}}_i^{\ell}} - \frac{\partial \mathcal{L}}{\partial \bar{\theta}_i^{\ell}} = \sum_{m=1}^{M_s} \lambda_m \bar{a}_{m_i}^{\ell} + \bar{N}_i^{\ell} \tag{A.43}$$

$$\sum_{\ell=1}^{L}\sum_{i=1}^{3}\left\{ \bar{a}_{m_i}^{\ell}\ \dot{\bar{\theta}}_i^{\ell} + b_{m_i}^{\ell}\ \dot{x}_i^{\ell}\right\} + d_m = 0$$
$$m=1,\cdots,M_s \tag{A.44}$$

In A.42 and A.43, F_i^{ℓ} and $\bar{N}_i^{\ell}$ denote the generalized forces. The holonomic constraints are expressed in A.44.

The kinetic energy of the system is given by:

$$T = \frac{1}{2}\sum_{\ell=1}^{L}\sum_{i=1}^{3}\left\{ \dot{\phi}_i^{\ell}\,(\omega_i^{\ell})^2 + M_{\ell}\,(\dot{x}_i^{\ell})^2\right\} \tag{A.45}$$

where the symbols ϕ_i^{ℓ}, M_{ℓ} and ω_i^{ℓ} are defined in the context of equation A.37. From Reference 11, page 134, and the symbol definitions in A.41,

$$\left.\begin{array}{rcl} \omega_1^{\ell} &=& \dot{\bar{\theta}}_1^{\ell}\cos\bar{\theta}_3^{\ell} + \dot{\bar{\theta}}_2^{\ell}\sin\bar{\theta}_1^{\ell}\sin\bar{\theta}_3^{\ell} \\[4mm] \omega_2^{\ell} &=& -\dot{\bar{\theta}}_1^{\ell}\sin\bar{\theta}_3^{\ell} + \dot{\bar{\theta}}_2^{\ell}\sin\bar{\theta}_1^{\ell}\cos\bar{\theta}_3^{\ell} \\[4mm] \omega_3^{\ell} &=& \dot{\bar{\theta}}_2^{\ell}\cos\bar{\theta}_1^{\ell} + \dot{\bar{\theta}}_3^{\ell} \end{array}\right\} \tag{A.46}$$

A-16

In order to obtain the Lagrangian of equations $A.42$ and $A.43$, it is only necessary to substitute for the ω_i^ℓ in A.45, employing A.46. It has been verified that this procedure yields the correct Lagrangian. The substitution is not necessary for the purposes of this development.

Employing the translation terms of $A.45$ equations $A.42$ become

$$M_\ell \; \ddot{x}_i^\ell = \sum_{m=1}^{M_s} \lambda_m \, b_{mi}^\ell + \hat{e}_i^{\,o} \cdot \vec{F}_\ell$$

$$i = 1, \cdots 3 \; ; \; \ell = 1, \cdots, L \quad (A.47)$$

where $\hat{e}_j^{\,o}$ and $\vec{F}_\ell$ are defined in the context of A.32.

The next step in the development is the reexpression of $A.43$ in the Newtonian form with Lagrange-type constraint terms. From page 52 of Ref. 11, the generalized force Q_j corresponding to an angle variable q_j such that dq_j corresponds to an infinitesimal rotation about an axis with direction $\hat{n}$ is given by

$$Q_j = \hat{n} \cdot \vec{N}$$

$$(A.48)$$

where $\vec{N}$ denotes the applied torque about the origin point from which q_j is measured. From page 107 of Ref. 11, $d\phi$ is an infinitesimal rotation about a space-fixed axis z, $d\theta$ is an infinitesimal rotation about the line of nodes, and $d\psi$ is an infinitesimal rotation about the body axis z'. So letting (in accord with the symbolism of A.41)

$\vec{\hat{e}}_1^\ell$ unit vector in direction of line of nodes for lth body

$\vec{\hat{e}}_2^\ell$ unit vector in direction of space-fixed axis z for lth body

$\vec{\hat{e}}_3^\ell$ unit vector in direction of body axis z' for lth body

it follows from A.48 that, in A.43

$$\vec{N}_i^{\,\ell} = \overline{\hat{e}}_i^{\,\ell} \cdot \vec{N}_\ell$$

<div align="right">(A.49)</div>

where $\vec{N}_\ell$ is defined in the context of A.33

As indicated on page 52 of Ref. 11, for an angle variable q_j of the type under consideration,

$$\frac{\partial T}{\partial \dot{q}_j} = \hat{n} \cdot \vec{L}$$

<div align="right">(A.50)</div>

where T denotes the kinetic energy and $\vec{L}$ denotes the body angular momentum about the origin point for measurement of q_j. Since in this development T expressed in terms of the q_j and $\dot{q}_j$ is the same as the Lagrangian, it is concluded that

$$\frac{\partial \mathcal{L}}{\partial \dot{\theta}_i^{\,\ell}} = \overline{\hat{e}}_i^{\,\ell} \cdot \vec{H}^\ell$$

<div align="right">(A.51)</div>

where $\vec{H}^\ell$ denotes the angular momentum of the 1th body about its c.m.

The forms of the left member and the last term on the right in A.43 are independent of the constraint terms. It follows that, in the absence of constraints,

$$\frac{d}{dt}\frac{\partial \mathcal{L}}{\partial \dot{\theta}^\ell} - \frac{\partial \mathcal{L}}{\partial \bar{\theta}_i^{\,\ell}} = \dot{N}_i^{\,\ell}$$

<div align="right">(A.52)</div>

or employing A.49 and A.51,

$$\frac{d}{dt}\left\{ \overline{\hat{e}}_i^{\,\ell} \cdot \vec{H}^\ell \right\} - \frac{\partial \mathcal{L}}{\partial \theta_i^{\,\ell}} = \overline{\hat{e}}_i^{\,\ell} \cdot \vec{N}_\ell$$

<div align="right">(A.53)</div>

But, in the absence of constraints,

$$\frac{d\vec{H}^\ell}{dt} = \vec{N}_\ell$$

and so,

$$\bar{\hat{e}}_i^\ell \cdot \frac{d\vec{H}^\ell}{dt} = \bar{\hat{e}}_i^\ell \cdot \vec{N}_\ell \tag{A.54}$$

The relations in A.53, A.54, and A.51 imply that

$$\frac{\partial \mathcal{L}}{\partial \theta_i^\ell} = \dot{\bar{\hat{e}}}_i^\ell \cdot \vec{H}^\ell \tag{A.55}$$

and

$$\frac{d}{dt} \frac{\partial \mathcal{L}}{\partial \dot{\theta}_i^\ell} - \frac{\partial \mathcal{L}}{\partial \theta_i^\ell} = \bar{\hat{e}}_i^\ell \cdot \frac{d\vec{H}^\ell}{dt} \tag{A.56}$$

The relations A.51, A.55 and A.56 have been verified by direct evaluations involving the Euler angles and the relations in A.46. This verification is a useful check on the correctness of the development.

Employing A.49 and A.56, A.43 may be reexpressed,

$$\bar{\hat{e}}_k^\ell \cdot \frac{d\vec{H}^\ell}{dt} = \sum_{m=1}^{M_s} \lambda_m \, \bar{a}_{mk}^\ell + \bar{\hat{e}}_k^\ell \cdot \vec{N}_\ell$$

$$k = 1, \ldots, 3 \; ; \; \ell = 1, \ldots, L \tag{A.57}$$

The relations in A.57 and A.44 will be transformed to obtain

$$\hat{e}_j^\ell \cdot \frac{d\vec{H}^\ell}{dt} = \sum_{m=1}^{M_s} \lambda_m \, a_{mj}^\ell + \hat{e}_j^\ell \cdot \vec{N}_\ell \tag{A.58}$$

$$j = 1, 2, 3 \; ; \; \ell = 1, \ldots, L$$

$$\sum_{\ell=1}^{L} \sum_{j=1}^{3} \left\{ a_{mj}^{\ell} \; \omega_j^{\ell} + b_{mj}^{\ell} \; \dot{x}_j^{\ell} \right\} \; + \; d_m = 0$$

(A.59)

where $\hat{e}_j^{\ell}$ denotes a unit vector in the direction of the jth principal axis of the 1th body.

To simplify the symbolism during transformation the superscript 1 will be dropped and restored later in the development. Equations A.57 and A.44 become

$$\bar{e}_k \cdot \frac{d\vec{H}}{dt} = \sum_{m=1}^{M} \lambda_m \; \bar{a}_{mk} + \bar{e}_k \cdot \vec{N}$$

(A.60)

$$\sum_{i=1}^{3} \left\{ \bar{a}_{mi} \; \theta_i + b_{mi} \; \dot{x}_i \right\} + dm = 0$$

(A.61)

where in A.61 the sum over 1 has been suppressed.

The transformations of A.60 and A.61 depend upon the transformations

$$\left(\theta_j \right) \longleftrightarrow \left(\omega_k \right)$$

(A.62)

$$\left(\bar{\hat{e}}_j \right) \longleftrightarrow \left(\hat{e}_k \right)$$

(A.63)

dropping the superscript 1 in A.46 and employing A.41 one obtains the transformation

$$\omega_k = \sum_j c_{kj} \; \theta_j$$

(A.64)

where

$$
C = \begin{pmatrix} \cos\psi & \sin\theta\sin\psi & 0 \\ -\sin\psi & \sin\theta\cos\psi & 0 \\ 0 & \cos\theta & 1 \end{pmatrix}
$$

(A.65)

The transform matrix C is nonorthogonal. The inverse of A.64 is

$$
\dot{\theta}_j = \sum_k C_{jk}^{-1} \omega_k
$$

(A.66)

where

$$
CC^{-1} = I
$$

(A.67)

and I denotes the identity matrix. The inverse C^{-1} is given by

$$
C^{-1} = \begin{pmatrix} \cos\psi & -\sin\psi & 0 \\ \dfrac{\sin\psi}{\sin\theta} & \dfrac{\cos\psi}{\sin\theta} & 0 \\ -\dfrac{\cos\theta\sin\psi}{\sin\theta} & -\dfrac{\cos\theta\cos\psi}{\sin\theta} & 1 \end{pmatrix}
$$

(A.68)

It will be observed that C^{-1} is singular when θ is an integral multiple of π. This point is discussed below.

To obtain the unit-vector transformation in (A.63), it is observed that the angular velocity, $\vec{\omega}$, is given by the relation

$$
\vec{\omega} = \sum_k \hat{e}_k \omega_k
$$

and by the relation,

$$
\vec{\omega} = \sum_j \bar{e}_j \dot{\theta}_j
$$

The latter expression is valid since independent angular velocities add like vectors.* Stated alternately, infinitesimal rotations can be represented by vectors, and independent infinitesimal rotations so represented can be added like vectors whether or not the rotations occur about orthogonal axes. Equating the two expressions for $\bar{\omega}$ yields

$$\sum_k \hat{e}_k \, \omega_k = \sum_j \bar{\hat{e}}_j \, \dot{\theta}_j$$

Substituting from A.64 and observing that the resulting relation must be valid for arbitrary values of θ_j , one obtains

$$\bar{\hat{e}}_j = \sum_k \tilde{c}_{jk} \, \hat{e}_k$$

(A.69)

where $\tilde{c}$ denotes the transpose of C. Since

$$(\tilde{c}^{-1}) = (\tilde{c})^{-1}$$

the inverse of A.69 is given by

$$\hat{e}_k = \sum_j \tilde{c}^{-1}_{kj} \, \bar{\hat{e}}_j$$

(A.70)

Now, it can be shown that the singularity of C^{-1} at $\theta = 0$ occurs because**

$$\bar{\hat{e}}_2 = \bar{\hat{e}}_3 \qquad \theta = 0$$

(A.71)

This degeneracy might cause difficulty in numerical integration of A.60 in some isolated cases.*** Such potential difficulty is not of concern in this develop-

---

*   Rigorously speaking, angular velocity is a psuedo vector. The distinction between pseudo vector and vector is not significant in this development.

**   Since the singularity of C^{-1} at $\theta = n\pi$ is similar to that at $\theta = 0$ we need consider only the latter singularity point.

***   The degeneracy at $\theta = 0$ must also be present in the corresponding Lagrange form of the Euler-angle-dependent equations from which A.60 was derived.

ment since the objective is the analytic derivation of the equations in A.58 and A.59, which are not affected by the degeneracy in A.71.

To treat the singularity of C^{-1} at $\theta = 0$ in the transformation in A.70 it is only necessary to perform the transformation for $\theta = \Delta\theta$ and then, in the result, pass to the limit as $\Delta\theta \to 0$. It is clear from A.70 that the limit exists and is well behaved. Consider the treatment of the singularity when and C^{-1} are functions of time, t. Suppose $\theta(t) = 0$ at t=t. In this case, one can employ A.70 to evaluate $\hat{e}_k$ at time t and then pass to the limit as $t \to t_o$ to obtain $\hat{e}_k$ at time t_o. If C^{-1} is a function of t but $\theta = 0$ always, one can again evaluate $\hat{e}_k$ for $\theta = \Delta\theta$ and then pass to the limit as $\Delta\theta \to 0$. The singularity at $\theta = 0$ in the transformation in A.67 can be handled by the same technique. With this understanding, the groundwork is complete for the transformations of A.60 and A.61.

Multiplying A.60 by C^{-1}_{kj} and summing over k yields

$$\left(\sum_k c^{-1}_{kj} \, \bar{\hat{e}}_k \right) \cdot \frac{d\vec{H}}{dt} = \sum_{m=1}^{M_s} \lambda_m \sum_k c^{-1}_{kj} \, \bar{a}_{mk} \tag{A.72}$$

$$+ \left(\sum_k c^{-1}_{kj} \, \bar{\hat{e}}_k \right) \cdot \vec{N}$$

Putting

$$a_{mj} = \sum_k c^{-1}_{kj} \, \bar{a}_{mk} \tag{A.73}$$

and employing A.70, A.72 reduces to

$$\hat{e}_j \cdot \frac{d\vec{H}}{dt} = \sum_{m=1}^{M_s} \lambda_m \, a_{mj} + \hat{e}_j \cdot \vec{N} \tag{A.74}$$

The inverse of A.73 is

$$\bar{a}_{mk} = \sum_j c_{jk} \, a_{mj} \tag{A.75}$$

A-23

Substituting (A.75) into (A.61) yields

$$\sum_{i=1}^{3} \left\{ \dot{\theta}_i \sum_{j=1}^{3} C_{ji} \, a_{mj} + b_{mi} \, \dot{x}_i \right\} + d_m = 0$$

Rearranging and employing (A.64) leads to the desired result

$$\sum_{j=1}^{3} \left\{ a_{mj} \, \omega_j + b_{mj} \, \dot{x}_j \right\} + d_m = 0 \tag{A.76}$$

Restoring the superscript 1 in (A.74) and (A.76), and the sum over 1 in (A.76) leads to the equations of motion in (A.58) and (A.59).

It has been shown that under the transformation

$$\omega_k^\ell = \sum_j C_{kj}^\ell \, \theta_j^\ell$$

$$a_{mj}^\ell = \sum_k C_{kj}^{-1\ell} \, \bar{a}_{mk}^\ell \tag{A.77}$$

where C_{kj}^ℓ is given by (A.46), the equations of motion in (A.57) and (A.44) imply the equations of motion in (A.58) and (A.59). Since it has been shown that, subject to the proper treatment of the singularity of C^{-1}, the inverse of the transformation in (A.77) exists, it is apparent that the equations of motion in (A.58) and (A.59) imply the equations of motion in (A.57) and (A.44), Thus the equations (A.58) and (A.59) are completely equivalent to the equations (A.57) and (A.44), and accordingly, to the Lagrange equations in (A.44) and (A.43). It is readily verified that equations (A.47), (A.58), and (A.59) are identical, except for notation, to the component equations corresponding to the vector equations (A.32)-(A.36).

The final step of the development is to express the left number of (A.58) in the Euler form. Put

or

$$\vec{H}^\ell = \oint^\ell \cdot \vec{\omega}^\ell$$

$$\tag{A.78}$$

$$\vec{H}^\ell = \sum_j \hat{e}_j^\ell \, \oint_j^\ell \, \omega_j^\ell$$

A-24

Differentiating (A.78) with respect to t leads to

$$\frac{d\vec{H}^\ell}{dt} = \sum_j \hat{e}_j^\ell \, \phi_j^\ell \, \dot{\omega}_j^\ell$$

$$+ \sum_j \dot{\hat{e}}_j^\ell \, \phi_j^\ell \, \omega_j^\ell \qquad\qquad (A.79)$$

now

$$\dot{\hat{e}}_j^\ell = \vec{\omega}^\ell \otimes \hat{e}_j^\ell$$

or

$$\dot{\hat{e}}_j^\ell = \sum_k \omega_k^\ell \, \hat{e}_k^\ell \otimes \hat{e}_j^\ell$$

The cross product may be expressed

$$\hat{e}_k^\ell \otimes \hat{e}_j^\ell = \sum_i \delta_{kji} \, \hat{e}_i$$

where δ_{kji} is the alternating symbol defined above.* Thus

$$\dot{\hat{e}}_j^\ell = \sum_k \sum_i \delta_{kji} \, \omega_k^\ell \, \hat{e}_i^\ell \qquad\qquad (A.80)$$

Since $\hat{e}_i^\ell \cdot \hat{e}_j^\ell = \delta_{ij}$ (A.80) and (A.79) lead to the relation

$$\hat{e}_j \cdot \frac{d\vec{H}^\ell}{dt} = \phi_j^\ell \, \dot{\omega}_j^\ell + \sum_{i=1}^{3} \sum_{k=1}^{3} \omega_i^\ell \, \omega_k^\ell \, \delta_{jki} \, \phi_i^\ell \qquad\qquad (A.81)$$

which is identical to equation (A.37). The development of the relations (A.32)-(A.37) is complete.

---

* The principal axis directions have been labelled so that $\hat{e}_1^\ell \otimes \hat{e}_2^\ell = \hat{e}_3^\ell$ This labelling is in accord with (A.46)

A.2.3   Equivalence Relations

As mentioned above, the purpose of this subsection is the formal demonstration of the equivalence of the Lagrange treatment of constraints to the treatment employed in the Calspan Crash-Simulation Model. No attempt is made here to independently derive the equations employed in the Calspan Model. Rather, these equations are inferred analytically from the Euler equations with Lagrange-type constraints, and then the equivalence of the two methods is proved.

The proof of equivalence hinges on the relations

$$\vec{f}_m^{\ell} = \vec{\lambda}_m \cdot B_m^{\ell} \tag{A.82}$$

$$\vec{n}_m^{\ell} = \vec{\lambda}_m \cdot A_m^{\ell} \qquad m = 1, \ldots M \tag{A.83}$$

$$\sum_{\ell=1}^{L} \left\{ A_m^{\ell} \cdot \vec{\omega}^{\ell} + B_m^{\ell} \cdot \dot{\vec{x}}^{\ell} \right\} + \vec{D}_m = 0 \tag{A.84}$$
$$m = 1, \ldots, M$$

which are the same as the relations (A.35), (A.36), (A.34) of the previous subsection. Following a discussion of the characteristics of the vector Lagrange multipliers, it is shown that the relations (A.82)-(A.84) imply the compatibility relations, which can be employed to convert the equations of motion from the Lagrange-multiplier form to the constraint-force from employed in the Calspan Model.

The constraint relations (see (A.84)) are expressed in the vector form since this is the form employed in the Calspan Model. However, the formalism is immediately applicable to scalar constraint equations (such as the torque-type constraint relation for the universal joint - see the subsection Examples.) To see how this is done, suppose the mth constraint relation is scalar. One

can then put

$$d_{m2} = d_{m3} = 0$$

$$a^{\ell}_{m2j} = a^{\ell}_{m3j} = b^{\ell}_{m2j} = b^{\ell}_{m3j} = 0 \qquad j = 1,\ldots,3 \tag{A.85}$$

and equations (A.82),(A.83), and (A.84) reduce to

$$\vec{f}^{\,\ell}_m = \lambda_{m1} \sum_{j=1}^{3} b^{\ell}_{m1j}\,\hat{e}^{\,o}_j$$

$$\vec{n}^{\,\ell}_m = \lambda_{m1} \sum_{j=1}^{3} a^{\ell}_{m1j}\,\hat{e}^{\,\ell}_j \left. \vphantom{\sum_{j=1}^{3}} \right\}$$

$$\sum_{j=1}^{3} \sum_{\ell=1}^{L} \left\{ a^{\ell}_{m1j}\,\vec{\omega}^{\,\ell}_j + b^{\ell}_{m1j}\,\dot{\vec{x}}^{\,\ell}_j \right\} + d_{m1} = 0 \tag{A.86}$$

When, for a particular value of m, the relations (A.85) are employed with
(A.82), (A.83), and (A.84), the solutions for λ_{m_2} and λ_{m_3} are totally am-
biguous. These ambiguities do not affect the solutions for $\vec{f}^{\,\ell}_m$, $\vec{n}^{\,\ell}_m$ and
other physical quantities of interest.

There are other cases in which certain ones of the Lagrange multi-
pliers cannot be uniquely determined. A case in point is the vector Lagrange
multiplier which corresponds to the torque-type constraint for the hinge joint
(see the subsection: Examples). The lack of uniqueness of the vector Lagrange
multipliers corresponding to some vector constraint relations is probably due
to the presence of redundant information in these relations. The removal of
such redundancies, while unnecessary, would probably usually be desirable in
applications based on the employment of Lagrange multipliers.* By contrast,
in the formulation employed in the Calspan Model, the removal of such redun-
dancies in the constraint relations is sometimes both unnecessary and undesirable.
There is a twofold reason for this circumstance. First, in the Calspan formu-
lation, the direct removal of redundancies in the constraint relations would

---

* The removal of redundancies in the constraint relations is not absolutely
  essential because ambiguities in values of the Lagrange multipliers do not
  result in ambiguities in the solution for physical quantities of interest.

sometimes result in added complexity in the formulation. Second, in this formulation, the constraint relations are supplemented by additional relations (the compatibility relations) which usually prevent the ambiguities in $\bar{f}_m^\ell$ and $\bar{n}_m^\ell$ which, in the Calspan formulation, would otherwise result from redundancies in the constraint relations.* Ambiguities in the values of the Lagrange multipliers have no effect whatever on the solution since the Lagrange multipliers are not employed in the Calspan formulation.

The foregoing discussion provides essential background information for the ensuing discussion on the relation between the Lagrange-multiplier dependent formulation and the formulation employed in the Calspan Model. In particular, in eliminating the Lagrange multipliers from the equations of motion, it cannot be assumed that the transform relations in (A.82) and (A.83) can be inverted to obtain unambiguous expressions for the vector Lagrange multipliers in terms of the quantities $\bar{n}_m^\ell$, $\bar{f}_m^\ell$, A_m^ℓ and B_m^ℓ. To determine how the Lagrange multipliers can be eliminated from the formulation, it is necessary to achieve an understanding of their ultimate role in the equations of motion.**

---

* Some types of redundancies (such as those resulting from the inadvertent employment of two distinct yet mathematically equivalent constraint relations) could not be offset by the compatibility relations. Such redundancies could result in ambiguities in the solutions for individual constraint-force and/or constraint-torque terms, but they could not affect the solutions for either the coordinate variables or the net constraint forces and torques.

** The content of the preceding two paragraphs can be better understood in retrospect, after reviewing the entire development of this section.

It will be recognized that the vector Lagrange multipliers, $\vec{\lambda}_m$, have no physical significance;* and further, in the entire formulation, they only appear in the relations in (A.82) and (A.83). Therefore, from the physical and mathematical standpoint, the only value of the Lagrange multipliers lies in what their <u>existence</u> in the relations (A.82) and (A.83) implies about the relationships between the quantities $\vec{F}_m^\ell$, $\vec{n}_m^\ell$, B_m^ℓ and A_m^ℓ . Accordingly, it is clear that the relations in (A.82) and (A.83) can be replaced by <u>any</u> <u>other</u> <u>relations</u> which are equivalent to (A.82) and (A.83) with regard to implications about the relationships between the quantities $\vec{F}_m^\ell$, $\vec{n}_m^\ell$, B_m^ℓ and A_m^ℓ and which imply nothing whatever except these relationships.

For reasons discussed below, the relations between the quantities $\vec{F}_m^\ell$, $\vec{n}_m^\ell$, B_m^ℓ and A_m^ℓ which are implied by (A.82) and (A.83) are called <u>compatibility</u> relations. As stated above, in the formulation employed in the Calspan Model, the Lagrange multipliers (and, therefore, the relations (A.82) and (A.83) are replaced by the compatibility relations. In this development, the nature of these relations will be inferred from the theory of equations. Two lemmas will be introduced, the first of which is:

<u>Lemma 1</u>

The equations

$$\left. \begin{array}{l} \vec{f}_m^\ell = \vec{\lambda}_m \cdot B_m^\ell \\[2ex] \vec{n}_m^\ell = \vec{\lambda}_m \cdot A_m^\ell \end{array} \right\} \quad \begin{array}{l} m = 1, \ldots, M \\[2ex] \ell = 1, \ldots, L \end{array} \qquad (A.87)$$

---

* Those instances in which one or more of the vector Lagrange multipliers are equal to constraint forces or torques are exceptions to this statement.

have at least one solution for the $\overline{\lambda}_m$ if and only if $\overline{n}_m^{\ell}$ and $\overline{f}_m^{\ell}$ satisfy the compatibility relations.

$$\sum_{\ell=1}^{L} \sum_{m=1}^{M} \left\{ \vec{G}_{\ell m}^{\,i} \cdot \vec{f}_m^{\,\ell} + \vec{C}_{\ell m}^{\,i} \cdot \vec{n}_m^{\,\ell} \right\} = 0 \qquad i = 1, \ldots, N-I$$

(A.88)

Where $\vec{G}_{\ell m}^{\,i}$ and $\vec{C}_{\ell m}^{\,i}$ are determinable functions of $A_{m'}^{\ell'}$ and $B_{m'}^{\ell'}$ $(\ell'=1,\ldots L; m'=1\ldots M)$, I is equal to the rank of the matrix of the N component equations corresponding to (A.87), and

$$N = 6LM$$

(A.89)

Except for the symbolism, this lemma is identical to a mathematical criterion which is proved in Reference 12, page 245. The compatibility relations in (A.88) are, except for notation, identical, to the <u>conditions of compatibility</u> stated in the reference. They are called conditions of compatibility since, if they are not satisfied, the system of equations in (A.88) has no solution or is incompatible. It is in keeping with the employment of the term <u>compatibility</u> in Reference 1, that the relations in (A.88) are termed <u>compatibility relations</u>.

The coefficients $\vec{G}_{\ell m}^{\,i}$ and $\vec{C}_{\ell m}^{\,i}$ in the compatibility relations can be evaluated from the determinant equations given on page 245 of Reference 11. However, in the examples given in the last subsection of this section, the compatibility relations are quickly obtained by analyses (or mathematical inferences) employing relations of the type in (A.87). As stated in the subsection <u>Methods</u>, the compatibility relations can be inferred directly from applications of Newton's third law and/or analyses of the constraint-force geometry. Prior to the analysis presented here they were always obtained by the latter means.

Though vector notation is employed in expressing the coefficients $\vec{G}_{\ell m}^{\,i}$ and $\vec{C}_{\ell m}^{\,i}$ in (A.88), these coefficients are not always vectors. In some cases they are (non-invariant) linear combinations of elements of tensors. In such cases,

certain ones of the compatibility relations in (A.88) can be combined to obtain invariant vector equations. In the examples in the last sub-section of this section, the compatibility relations are always expressed as invariant forms (that is, as invariant-scalar and vector equations.)

The satisfaction of the compatibility relations by the quantities $\vec{f}_m^\ell$ and $\vec{n}_m^\ell$ cannot be verified unless the values of these quantities are known. But the values of these quantities cannot be obtained until the equations of motion have been completely solved. For this reason, the compatibility relations must be regarded as constraints on the values of the quantities $\vec{f}_m^\ell$ and $\vec{n}_m^\ell$. As implied above, the compatability relations cannot introduce more information than that which is inherent in the relations (A.87), which they replace.

For the sake of tidiness and vigor of exposition, it is desirable, in the transition from the Lagrange-multiplier formulation to the formulation employed in the Calspan model, to replace the relations in (A.87) by mathematically-equivalent relations. Since it cannot be claimed that the compatibility relations in (A.88) are <u>completely</u> equivalent to the relations (A.87), a complete equivalence will be established through <u>Lemma 2</u>.

If the relations in (A.87) are solvable, they are mathematically equivalent to the compatibility relations (A.88) taken in conjunction with parametric expressions which express the general solutions of the relations (A.88) for the quantities .

In proving Lemma 2, it will be convenient to introduce the expression

$$\vec{\lambda}_m = \vec{\lambda}_m \left[(d_i) , (A_{m'}^{\ell'}) , (B_{m'}^{\ell'}) , (\vec{f}_{m'}^{\ell'}) , (\vec{n}_{m'}^{\ell'}) \right]$$

(A.90)

to represent the parametric form of solution of (4.114) for the $\vec{\lambda}_m$. In (A.90), ($A_{m'}^{\ell'}$), ($B_{m'}^{\ell'}$), ($f_{m'}^{\ell'}$), ($n_{m'}^{\ell'}$) denote sets for $\ell' = 1, \ldots L$; $m' = 1, \ldots M$ and (d_i) = an arbitrary - parameter set d_i , $i = 1, \ldots 3m-1$. The arbitrary value parameters, ϕ_i , express the arbitrariness in the solutions $\vec{x}_m$ of

A-31

the relations in (A.87). If the rank, I_{r}, of the matrix of the system (A.87) is equal to the total number of unknowns, 3M, (the M vectors, $\overline{x}_{m}$ have 3M components) there are no arbitrary parameters, d_i , and the vectors, $\overline{\lambda}_{m}$, are uniquely determined. If $3M > I_r$, there are $3M - I_r$ parameters d_i .

To prove <u>Lemma 2</u> it must be shown that, if the relations (A.87) are solvable, then the relations (A.87) imply and are implied by the compatibility relations (A.88) in conjunction with the solutions in (A.90).

The forward implication follows immediately from the discussion on page 245 of Reference 12.* The reverse implication follows, provided that subject to the satisfaction of the compatibility relations, the solution for the $\overline{\lambda}_{m}$, represented in (A.90), satisfies the equations (A.87). The discussion on page 245 of Reference 12 indicates not only steps which can be taken to obtain a general solution, but proves (again subject to the satisfaction of the compatibility relations) that the general solution so obtained does indeed satisfy the system of equations in (A.87). Thus, <u>Lemma 2</u> is valid.

With a simple proviso, the condition of solvability of the relations in (A.87) can be removed from the statement of Lemma 2. This proviso is in that it be understood that incompatibility in the relations (A.87) is equivalent to the failure of satisfaction of the compatibility relations. This proviso is, of course, just the statement of Lemma 1. With this proviso, it can be stated (without further qualification) that the relations in (A.87) are mathematically equivalent to the compatibility relations, (A.88) taken in conjunction with the expressions (A.90) for $\overline{\lambda}_{m}$.

---

* In Reference 12, arbitrariness in the solution for the unknowns is brought out by showing that $3M - I_r$ of the unknowns may have arbitrary values. Clearly, the assignment of arbitrary values to $3M - I_r$ unknowns is equivalent to the introduction of $3M - I_r$ arbitrary parameters, as in the representation in (A.90)

The transition from the Lagrange-multiplier-dependent formulation to the formulation employed in the Calspan Model is now obvious. In the former formulation, the relations in (A.87) are employed. To obtain the latter formulation, the relations in (A.87) are replaced by the relations in (A.88) in conjunction with the relations (A.87). It is clear that the compatibility relations (A.90) represent the result of eliminating the Lagrange mulitpliers from the equations of motion. Thus, in the Calspan formulation, the solutions for the physical quantities of interest can be obtained from the equations (A.32), (A.33), (A.34), and (A.88), and the expressions for $\bar{\lambda}_m$ in (A.90) are not needed. The exposition and proof of the mathematical equivalence of the Calspan formulation to the Lagrange multiplier-dependent formulation is now complete.

Since the constraints which are imposed by a simple joint involve only two rigid bodies, for each value of m in the constraint relations, A_m^ℓ and B_m^ℓ vanish for all but two values of 1. For the purposes of the analyses of joints given in the next subsection, it is desirable to identify each constraint relation in terms of the bodies involved. To this end, the subscript m in the quantities $\vec{f}_m^\ell$, $\bar{n}_m^\ell$, A_m^ℓ, B_m^ℓ can be interpreted, not as a simple subscript but as a triplet subscript:

$$m = (k, \ell, n)$$ (A.91)

In (A.91), k and 1 are labels of the interacting bodies and n denotes a particular constraint resulting from this interaction. For example,

$$(1,3,2)$$

means the second constraint relation resulting from the interaction (through a joint) of body 1 with body 3. Clearly (k,1,n) and (1,k,n) refer to the same constraint.

If m=(k,1,n), $\vec{f}_m^j$, $\vec{n}_m^j$, A_m^j, B_m^j all vanish unless k ≠ 1 and j is equal to k or 1. Thus, in the triplet notation, (A.82), (A.83), and (A.84) may be re-expressed:

A-33

$$\vec{A}_m^k \cdot \vec{\omega}^k + \vec{A}_m^{\ell} \cdot \vec{\omega}^{\ell} + \vec{B}_m^k \cdot \dot{\vec{x}}^k + \vec{B}_m^{\ell} \cdot \dot{\vec{x}}^{\ell} + \vec{D}_m = 0$$

$$\vec{f}_m^k = \vec{\lambda}_m \cdot \vec{B}_m^k \, , \qquad \vec{f}_m^{\ell} = \vec{\lambda}_m \cdot \vec{B}_m^{\ell}$$

$$\vec{n}_m^k = \vec{\lambda}_m \cdot \vec{A}_m^k \, , \qquad \vec{n}_m^{\ell} = \vec{\lambda}_m \cdot \vec{A}_m^{\ell}$$

$$m = (k, \ell, n) \tag{A.92}$$

Since a single joint can only transmit one net constraint force and one net constraint torque to a given body, there is, for a given joint, a maximum of two vector constraint relations. In the next subsection, the constraints are categorized as force-type and torque-type constraints.

A.2.4 Examples

In this subsection, the constraint relations corresponding to four simple joints are expressed. In each example, the compatibility relations are inferred, and the mathematical equivalence expressed in general in Lemma 1 and Lemma 2 is demonstrated. In the case of the hinge joint, it is shown that the compatibility relations offset the effect of the redundancy in the constraint relations.

The analyses depend only on the relations in (A.92). Since for each constraint only two rigid bodies are involved, there is no loss of generality in labeling our body by the index 1, and the other body by the index 2. The relations in (A.92) can then be re-expressed.

$$\vec{A}_n^1 \cdot \vec{\omega}^1 + \vec{B}_n^1 \cdot \dot{\vec{x}}^1 = - \vec{A}_n^2 \cdot \vec{\omega}^2 - \vec{B}_n^2 \cdot \dot{\vec{x}}^2 \tag{A.93}$$

$$\vec{f}_n' = \vec{\lambda}_n \cdot \mathcal{B}_n' \quad ; \quad \vec{f}_n^2 = \vec{\lambda}_n \cdot \mathcal{B}_n^2 \qquad\qquad (A.94)$$

$$\vec{n}_n' = \vec{\lambda}_n \cdot \mathcal{A}_n' \quad ; \quad \vec{n}_n^2 = \vec{\lambda}_n \cdot \mathcal{A}_n^2 \qquad\qquad (A.95)$$

where the subscript n can be identified with n in the definition of the triplet subscript m in (A.91). The additive vector, $\vec{D}_n$, has been deleted from the relation (A.93) since it is zero in the cases of interest.

There are, at most, two constraints corresponding to each joint. In the first type of constraint, which will be labeled n=1, the tensors $\mathcal{B}_n'$ and $\mathcal{B}_n^2$ are nonvanishing and they have inverses. Thus, the transforms in (A.94) can be inverted and the constraint torques can be expressed as linear functions of the constraint forces. This type of constraint (n=1) will be termed a force-type constraint.

In the second type of constraint (n=2) the constraint forces vanish. This type of constraint will be termed a torque-type constraint.

Every joint has exactly the same force-type constraint, and all joints except the ball joint have both force-type and torque-type constraints. For this reason, the ball joint is discussed first.

A.2.4.1   The Ball Joint

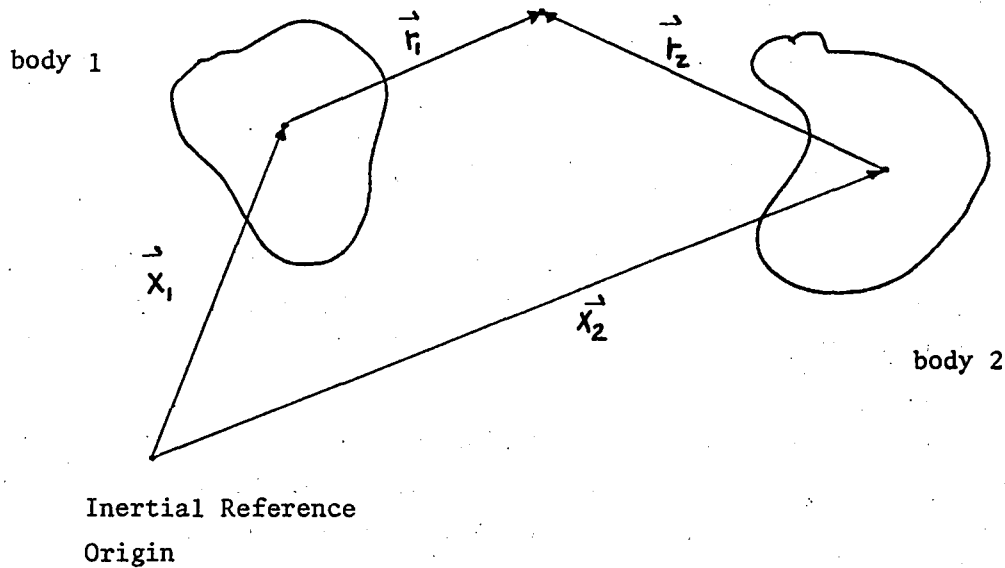The basic geometry of the rigid bodies and the joint is depicted in Figure A.2.

A-35

body 1

$\vec{r_1}$

$\vec{r_2}$

$\vec{X_1}$

$\vec{X_2}$

body 2

Inertial Reference
Origin

Figure A.2   BASIC RIGID BODY GEOMETRY

The vector $\vec{r_1}$ is the position vector of the joint relative to the c.m. of body 1 and the vector $\vec{r_2}$ is the position vector of the same joint relative to the c.m. of body 2. From the figure

$$\vec{x_1} + \vec{r_1} = \vec{x_2} + \vec{r_2}$$

(A.96)

Since the position of the joint is rigidly fixed relative to both bodies, it is clear that $|\vec{r_i}|$, ($\ell = 1, 2$), is constant, and the orientation of $\vec{r_\ell}$ ($\ell = 1, 2$) is completely determined by the orientation of body ℓ, ($\ell = 1, 2$). The orientation of ℓ ($\ell = 1, 2$) can be determined from the relation:

$$\hat{e}_j^o = \sum_i S_{ij}^\ell \hat{e}_i^\ell$$

(A.97)

Where the unit vectors $\hat{e}_j^o$ and $\hat{e}_j^\ell$ are defined in the content of equation (A.37) and S_{ij}^ℓ denotes a direction-cosine matrix. From (A.97)

A-36

$$\vec{r}_\ell \cdot \hat{e}_j^o = \sum_i s_{ij}^\ell \hat{e}_i^\ell \cdot \vec{r}_\ell \qquad\qquad \text{(A.98)}$$

Since $\vec{r}_\ell$ is rigid relative to body ℓ , its components, $\hat{e}_i^\ell \vec{r}_\ell$, in the body-fixed coordinate system are time-independent constants. Therefore, (A.98) may be employed to determine the components of $\vec{r}_\ell$ in the space-fixed coordinate system.

The transform (A.98) can be re-expressed in compact vector notation by introducing the vector $\vec{r}_\ell^o$ given by

$$\vec{r}_\ell^o = \sum_i \hat{e}_i^o \hat{e}_i^\ell \cdot \vec{r}_\ell \qquad\qquad \text{(A.99)}$$

Clearly, the vector $\vec{r}_\ell^o$ is constant. From (A.99)

$$\vec{r}_\ell^o \cdot \hat{e}_i^o = \vec{r}_\ell \cdot \hat{e}_i^\ell$$

substituting into (A.98)

whence
$$\vec{r}_\ell \cdot \hat{e}_j^o = \sum_i s_{ij}^\ell \hat{e}_i^o \cdot \vec{r}_\ell^o$$

$$\vec{r}_\ell = \tilde{S}^\ell \cdot \vec{r}_\ell^o \qquad\qquad \ell = 1, 2 \qquad \text{(A.100)}$$

Where $\tilde{S}^\ell$ denotes the transpose of the tensor S^ℓ given by

$$S_\ell = \sum_{i=1}^{3} \sum_{j=1}^{3} \hat{e}_i^o s_{ij}^\ell \hat{e}_j^o$$

From (A.100)

$$\dot{\vec{r}}_\ell = \vec{\omega}^\ell \otimes \vec{r}_\ell \qquad\qquad \text{(A.101)}$$

which may be re-expressed

$$\dot{\vec{r}}_{\ell} = -W^{\ell} \cdot \vec{r}_{\ell} \qquad (A.102)$$

where W^{ℓ} denotes the skew-symmetric tensor

$$W^{\ell} = -I \otimes \vec{\omega}^{\ell} \equiv -\vec{\omega}^{\ell} \otimes I \qquad (A.103)$$

and I denotes the identity tensor.

Differentiating (A.96) and employing (A.101) results in

$$\dot{\vec{x}}^{1} + \vec{\omega}^{1} \otimes \vec{r}_{1} = \dot{\vec{x}}^{2} + \vec{\omega}^{2} \otimes \vec{r}_{2} \qquad (A.104)$$

Equation (A.104) is, from the foregoing discussion, a force-type constraint relation. It represents the force-type constraint for all the joints discussed in this section.

Comparing (A.104) and (A.93), it is concluded that

$$B_{1}^{\prime} = B_{1}^{2} = I$$

$$A_{1}^{\prime} = -I \otimes \vec{r}_{1} ; \qquad A_{1}^{2} = I \otimes \vec{r}_{2}$$

Substituting into (A.94) and (A.95) and rearranging, results in

$$\left.\begin{array}{l} \vec{f}_{1}^{\prime} = \vec{\lambda}_{1} ; \qquad \vec{f}_{1}^{2} = -\vec{\lambda}_{1} \\[2mm] \vec{n}_{1}^{\prime} = \vec{r}_{1} \otimes \vec{\lambda}_{1} ; \quad \vec{n}_{1}^{2} = -\vec{r}_{2} \otimes \vec{\lambda}_{1} \end{array}\right\} \qquad (A.105)$$

The general solution for $\vec{\lambda}_{1}$ is clearly

$$\vec{\lambda}_{1} = \vec{f}_{1}^{\prime} \qquad (A.106)$$

A-38

The compatibility relations are obtained by eliminating $\vec{\lambda}_1$ from the equations (A.105):

$$\vec{f}_1^{\,\prime} + \vec{f}_1^{\,2} = 0$$

$$\vec{n}_1^{\,\prime} = \vec{r}_1 \otimes \vec{f}_1^{\,\prime} \;;\quad \vec{n}_1^{\,2} = \vec{r}_2 \otimes \vec{f}_1^{\,2} \qquad\qquad \right\}$$

(A.107)

Clearly, in accord with Lemma 2, (A.106) in conjunction with (A.107) implies and is implied by (A.105).

In the formulation of the Calspan model, there are four vector un-knowns, $\vec{f}_1^{\,\prime}$, $\vec{f}_1^{\,2}$, $\vec{n}_1^{\,\prime}$, $\vec{n}_1^{\,2}$, corresponding to the ball joint. Since the compata-bility relations, (4.134), in conjunction with the constraint relation, (A.104), constitute four vector equations, the number of unknowns. In the Lagrange-multi-plier formulation there is one constraint-induced unknown (namely $\vec{\lambda}_1$) and our corresponding constraint equation, (namely (A.104)). Again, the number of equations is equal to the number of unknowns.

The relation (A.96) is employed as an initial condition. In principle, the satisfaction of (A.104) would insure the satisfaction of (A.96) for all times t. However, it has been found that because of accumulated computer-round-off-errors, the employment of (A.104) in the computations does not insure the satisfaction of (A.96) for all t. For this reason, both (A.96) and (A.104) are employed in the computations, but not in a redundant manner. In particular, (A.104) is employed with (A.107) and the differential equations to solve for $\vec{x}^{\,\prime}$, $\vec{r}_1$ and $\vec{r}_2$. (A.96) is then employed to obtain $\vec{x}^{\,2}$. This procedure insures the satisfaction of (A.96) for all times, t. A parallel procedure is employed when there are more than two bodies and more than one joint.

Since the ball joint is completely flexible, it has no torque-type constraint.

A.2.4.2   The Locked Joint

    The locked joint is a joint that has seized or frozen so that it has
zero degrees of rotational freedom. It has several uses in the Calspan Model,
including the representation of a human joint which is locked due to muscle ex-
ertion.

    The force-type constraint relation for the locked joint is, as already
implied, the same as for the ball joint. Since the locked joint has no rotation-
al degrees of freedom, it forces the equality of the angular velocities of bodies
1 and 2. Therefore, the torque-type constraint for the locked joint may be ex-
pressed

$$\vec{\omega}^1 = \vec{\omega}^2$$

(A.108)

To verify that (A.108) and (A.104) adequately describe the locked joint, it is
observed that the rank of the system (A.108) and (A.104), when considered as an
equation in the unknowns $\vec{\omega}^2$ and $\vec{\dot{X}}^2$, is six. Thus, (A.108) and (A.104) re-
move all six degrees of freedom in the motion of body 2 relative to the coordi-
nate system of body 1. In other words, the two bodies behave as a single rigid
body.

    Comparing (A.108) and (A.93), it is concluded that

$$B_2' = B_2^2 = 0$$

$$A_2' = -A_2^2 = I$$

Thus, the constraint forces corresponding to (A.108) are zero, and (A.95) be-
comes:

$$\vec{n}_2'^1 = \vec{\lambda}_2 \quad ; \quad \vec{n}_2^2 = -\vec{\lambda}_2$$

(A.109)

Eliminating $\vec{\lambda}_2$ results in the compatibility relation

$$\vec{n}_2' + \vec{n}_2^2 = 0$$

(A.110)

There are, for the Calspan formulation, the two unknown constraint torques $\overline{n}_2'$ and $\overline{n}_2^2$. These can be eliminated from the equations of motion by employing (A.110) and (A.108).

A.2.4.3   The Hinge Joint

The hinge joint has a single pin, the orientation of which can be denoted by the unit vector. $\hat{h}_1$. Since the pin is rigidly oriented relative to body 1 and to body 2, it must rotate with each body. Therefore, in parallelism with the relations (A.100) and (A.99), one can put

$$
\left.\begin{array}{l}
\hat{h}_1 = \tilde{S}' \cdot \hat{h}_1^o \\[2mm]
\hat{h}_1 = \tilde{S}^2 \cdot h_2^o
\end{array}\right\} \tag{A.111}
$$

where

$$
\hat{h}_1^o = \sum_i \hat{e}_i^o \, \hat{e}_i^1 \cdot \hat{h}_1
$$

$$
\hat{h}_2^o = \sum_i \hat{e}_i^o \, \hat{e}_i^2 \cdot \hat{h}_1
$$

Clearly, $\hat{h}_1^o$ and $\hat{h}_2^o$ are constant vectors. The fundamental constraint is the satisfaction of (A.111). From the time derivatives of the relations m (A.111), one concludes

$$
\vec{\omega}' \otimes \hat{h}_1 = \vec{\omega}^2 \otimes \hat{h}_1 \tag{A.112}
$$

Equation (A.112) is the torque-type constraint relation for the hinge joint.

Comparing (A.112) and (A.93), it is concluded that

$$
B_2' = B_2^2 = 0 \; ; \;\; A_2^2 = -A_2' = I \otimes \hat{h}_1, \tag{A.113}
$$

and the expressions for the constraint torques in (A.95) become

$$\vec{n}_2' = -\vec{\lambda}_2 \otimes \hat{h}_1 \; ; \; \vec{n}_2^2 = \vec{\lambda}_2 \otimes \hat{h}_1$$

(A.114)

clearly, (A.114) implies

$$\left. \begin{array}{rcl} \vec{n}_2' + \vec{n}_2^2 &=& 0 \\ \vec{n}_2' \cdot \hat{h}_1 &=& 0 \end{array} \right\}$$

(A.115)

To obtain the solution for $\vec{\lambda}_2$, one can take the cross product of $\hat{h}_1$ and the second of the relations (A.114):

$$\hat{h}_1 \otimes \vec{n}_2^2 = \hat{h}_1 \otimes (\vec{\lambda}_2 \otimes \hat{h}_1)$$
$$= \vec{\lambda}_2 - \hat{h}_1 \cdot \vec{\lambda}_2 \, \hat{h}_1$$

or rearranging

$$\vec{\lambda}_2 = \hat{h}_1 \otimes \vec{n}_2^2 + \hat{h}_1 \cdot \vec{\lambda}_2 \, \hat{h}_1$$

(A.116)

But, (A.114) implies that $\vec{\lambda}_2$ is ambiguous to within an arbitrary multiple of $\hat{h}_1$. This fact and (A.116) lead to

$$\vec{\lambda}_2 = \hat{h}_1 \otimes \vec{n}_2^2 + a\hat{h}_1 \quad \text{(arbitrary a)}$$

(A.117)

as the general solution for $\hat{\lambda}_2$.

Substituting (A.117) into the second of the relations (A.114)

$$\vec{n}_2^2 = (\hat{h}_1 \otimes \vec{n}_2^2 + a\hat{h}_1) \otimes \hat{h}_1$$

$$= \vec{n}_2^2 - \hat{h}_1 \cdot \vec{n}_2^2 \, \hat{h}_1$$

which reduces to an identity by virtue of the compatibility relations (A.115). Thus, (A.115) in conjunction with (A.117), imply (A.114)

This example is the first in which the solution for $\vec{\lambda}$ is ambiguous. The ambiguity results from redundancy in the constraint relation (A.112).

This relation only constrains $(\vec{\omega}_1 - \vec{\omega}_2)$ to be paralled to $\hat{h}_1$, so the rank of the matrix for the relation is <u>two</u>. On the other hand, the relation corresponds to <u>three</u> component equations and $\overline{\lambda}_2$ has <u>three</u> components. In the Lagrange-multiplier formulation, the ambiguity in $\overline{\lambda}_2$ could be removed by an additional constraint such as

$$\vec{\lambda}_2 \cdot \hat{h}_1 = 0 .$$

which can be satisfied within the arbitrariness of the solution in (A.117).

Turning to a consideration of the formulation in the Calspan Model, there are two vector unknowns, $\overrightarrow{h'_2}$ and $\overrightarrow{h_2}^2$, which result from the torque-type constraint. But the rank of the matrix of the system composed of the constraint relation (A.112) in conjunction with the compatability relations (A.115) is <u>six</u>. This rank is the same as the rank of two non-redundant vector equations. Therefore, the equations of motion can be solved without ambiguity.

A.2.4.4 <u>The Universal Joint</u>

The double-trunion universal joint has two hinge pins, of which the axis of one is rigidly oriented relative to body 1, and the axis of the other is rigidly oriented relative to body 2. The only rotational constraint in the joint is that the two hinge pins are always perpendicular. This constraint can be expressed by the relation

$$\hat{h}_1 \cdot \hat{h}_2 = 0 \tag{A.118}$$

where $\hat{h}_\ell$ is a unit vector in the direction of the pin which is rigidly oriented relative to body ℓ, $(\ell = 1, 2)$.

Relations similar to (A.111) can be introduced to express the orientations of $\hat{h}_1$ and $\hat{h}_2$. Differentiating (A.118) with respect to t results in

$$\hat{h}_1 \otimes \hat{h}_2 \cdot \vec{\omega}^1 = \hat{h}_1 \otimes \hat{h}_2 \cdot \vec{\omega}^2 \tag{A.119}$$

which is a scalar constraint relation. It is equivalent to the vector constraint relation

$$\hat{e}_1^o \, \hat{h}_1 \otimes \hat{h}_2 \cdot \vec{\omega}^1 = \hat{e}_1^o \, \hat{h}_1 \otimes \hat{h}_2 \cdot \vec{\omega}^2 \tag{A.120}$$

Comparing (A.120) and (A.93), it is concluded that

$$\beta_2^1 = \beta_2^2 = 0$$
$$A_2^1 = -A_2^2 = \hat{e}_1^o \, \hat{h}_1 \otimes \hat{h}_2$$

so (A.93) becomes

$$\vec{n}_2^1 = \vec{n}_2^2 = \vec{\lambda}_2 \cdot \hat{e}_1^o \, \hat{h}_1 \otimes \hat{h}_2 \tag{A.121}$$

If $\vec{\lambda}_2 \cdot \hat{e}_1^o$ is replaced by the scalar Lagrange multiplier λ_{21} , the relations (A.121) are identical to those that would be obtained from the approach which is formalized in (A.85) and (A.86). It is of academic interest that the vector $\vec{\lambda}_2$ may be retained and the ambiguity removed by the supplementary relation

$$\vec{\lambda}_2 \otimes \hat{e}_1^o = 0 \tag{A.122}$$

which restricts $\vec{\lambda}_2$ within the range of the general solution of (A.121) for $\vec{\lambda}_2$. Since (A.122) has a rank of two and (A.119) has a rank of one, these two relations do indeed remove ambiguities in $\vec{\lambda}_2$ in the solution of the equations of motion.

The equations (A.121) imply the compatibility relations.

$$\left. \begin{array}{l} \vec{n}_2^1 + \vec{n}_2^2 = 0 \\[2mm] \vec{n}_2^1 \times (\hat{h}_1 \times \hat{h}_2) = 0 \end{array} \right\} \tag{A.123}$$

The general solution to (A.121) for $\vec{\lambda}_2$ is

$$\vec{\lambda}_2 = \frac{\vec{n}_2^1 \cdot (\hat{h}_1 \otimes \hat{h}_2) \, \vec{e}_1^o}{\left| \hat{h}_1 \otimes \hat{h}_2 \right|^2} + \vec{a} \otimes \hat{e}_1^o \tag{A.124}$$

where a is arbitrary. To prove this, (A.124) is substituted into (A.121). The
resulting relation

$$\vec{n_2}' = \left[\frac{\vec{n_2}' \cdot (\hat{h_1} \otimes \hat{h_2})}{|\hat{h_1} \otimes \hat{h_2}|^2} \right] (\hat{h_1} \otimes \hat{h_2})$$

is implied by (A.123). Thus (A.124) and (A.123) imply (A.121). It will be ob-
served that the expression (A.124) can be simplified since, from (A.118),

$$|\hat{h_1} \otimes \hat{h_2}| = 1$$

In the Calspan formulation, the torque-type constraint in (A.119) leads
to two unknown constraint torques, $\vec{n_2}'$ and $\vec{n_2}^2$. Since (A.119) has a rank of one,
and the total rank of the relations (A.123) is five, the equations of motion can
be solved unambiguously.

A-45